Quantifying and Modeling the Influence of Forest on the Magnitude and Duration of Mountain Snow Storage in the Pacific Northwest, USA

Susan E. Dickerson-Lange

A dissertation

submitted in partial fulfillment of the

requirements for the degree of

Doctor of Philosophy

University of Washington

2016

Reading Committee:

Jessica D. Lundquist (Chair)

Rolf F. Gersonde

Bart Nijssen

Program Authorized to Offer Degree:

Department of Civil and Environmental Engineering

University of Washington

Abstract

Quantifying and Modeling the Influence of Forest on the Magnitude and Duration of Mountain Snow Storage in the Pacific Northwest, USA

Susan E. Dickerson-Lange

Chair of the Supervisory Committee:

Associate Professor Jessica D. Lundquist
Department of Civil and Environmental Engineering

Forests strongly influence the amount and duration mountain snow storage because forest cover modifies both snow accumulation and ablation processes. Quantifying and predicting forest effects on snow processes and snow storage is critical for understanding the effects of forest change on snow storage, and subsequent impacts on downstream water resources. However, both the magnitude and direction of forest modifications of individual snow processes vary with climate, topography, and forest characteristics. Accurate prediction of the net effects of forest change on mountain snow storage, particularly in a warming climate, depends on accurately representing the spatiotemporal variability of forest-snow interactions.

With a goal to better understand forest-snow processes in the maritime snow zone, we collected snow observations over four winters within diverse forest types in western Washington, USA. We utilize these new observations to quantify forest effects on snow duration, as well as to assess the robustness of remote methods to observe snow-covered area within a forest. We find

that mean snow duration is 8 days longer in forest gaps than in forested plots, but that snow duration in thinned forest and dense forest are indistinguishable at the 1600 m^2 plot-scale. We additionally show that time-lapse cameras and spatially distributed ground temperature sensors are both robust methods for observing snow duration, and make suggestions about the optimal spatial density of snow observations within forests. The entire four-year dataset and related metadata are extensively described, and are now publicly available for potential use in numerous modeling applications.

To expand our focus on forest-snow interactions to the Pacific Northwest, USA, regional-scale, we collaborate with other research institutions and engage citizen scientists. Regional synthesis and analysis of snow depth and duration at 12 out of 14 paired open-forest locations show that differential snow duration ranges from synchronous, to snow lasting up to 13 weeks longer in the open. The differences in snow duration are attributed to forest effects on snow accumulation, with larger differences between snow accumulation rates than between ablation rates in the open and forested sites through the duration of the forest snowpack. In 2 out of the 14 locations, differential snow duration is 2-5 weeks longer in the forest. These 2 sites are subject to hourly average wind speeds ranging up to 8 and 17 m s^{-1}. Therefore, longer snow duration in the forest likely results from a combination of enhanced deposition of snow and reduced snow loss from canopy interception in the forested sites. These findings suggest that a regional framework to understand forest effects on snow storage in the maritime to maritime-continental transitional climate across the Pacific Northwest must account for high interception efficiencies in warmer climates as well a high winds due to topographic exposure and climate.

Lastly, we assess the influence of forest structural characteristics on snow storage in western Washington by linking lidar-derived forest canopy metrics to snow depth and snow

duration. By using a matrix decomposition method to collapse the variance of spatially distributed observations of snow depth onto a few dominant modes, we show that the top two modes represent forest effects on snow accumulation and ablation, respectively. Furthermore, gridded metrics of canopy cover and height that quantify the canopy directly overhead, rather than to the south, correlate equally strongly (r^2 of up to 0.74) with the spatial coefficients that scale both of these modes. This finding suggests that the role of forests in shading the snowpack from sunlight is diminished at this site. Furthermore, multivariate analysis of physiographic predictors of snow duration across a range of elevations and years quantifies the important role of canopy characteristics in controlling snow duration. At the study site in western Washington, the binary simplification of considering forested versus open locations is supported by evidence for a stepped response, in which snow duration shifts from longer to shorter around values of 60-70% canopy cover. Collectively, the findings demonstrate that forest effects on snow accumulation dominate the overall influence of forest on snow storage in the Pacific Northwest, USA, resulting in larger magnitude and longer duration snow storage in canopy gaps, except in locations subject to high wind speeds.

Dedication

To my family, near and far, for their steadfast support and encouragement.

Acknowledgements

I would like to thank the numerous individuals and institutions that have supported and contributed to this body of work. I have benefited tremendously from your generosity, ideas, and support. First and foremost to my advisor, Dr. Jessica Lundquist, who has provided invaluable mentorship and a seemingly endless supply of excellent ideas. My dissertation committee has contributed guidance and encouragement to the research process. Dr. Jim Lutz and Dr. Rolf Gersonde personally collected data and contributed useful suggestions to numerous proposals and manuscripts. Dr. Bart Nijssen consulted on model representations of forest-snow processes and provided early encouragement for publishing a paper on our citizen science efforts. Dr. Joe Cook taught me everything I know about water resources economics and served as the Graduate School representative on my dissertation committee.

Many, many individuals helped with the collection and analysis of data in the Cedar River Municipal Watershed and across the Pacific Northwest. Dr. Van Kane processed the Cedar River lidar data and consulted on multivariate data analysis. Dr. Nic Wayand collected data at Snoqualmie Pass and served as the chief trail-finder for our excursions into eastern Cascades data collection. Mark Raleigh provided iButton and data processing support. Field efforts were supported by a cast of several dozen, but particular thanks are due to the sustained, rigorous efforts of Kael Martin, Teddy Thorson, Adam Massmann. Seattle Public Utilities provided access to the Cedar River Municipal Watershed and Scott Pattee at National Resource Conservation Service provided logistical support for data collection at SNOTEL sites.

Synthesis work across the Pacific Northwest was only possible via the generosity of our collaborators at Oregon State University and University of Idaho. In particular, Dr. Anne Nolin and Travis Roth provided data and local expertise for western Oregon. Dr. Tim Link and Dr. Jason Hubbart did the same for central and northern Idaho. Dr. Karla Eitel and Leslie Dorsey at the University of Idaho's McCall Outdoor Science School provided enormous enthusiasm and support to make our collaborative citizen science effort a success.

I personally benefited from conversations, mentoring, and collaborations with my colleagues across the University of Washington and beyond. Steve Malloch helped link this work to relevant, local applications. Dr. Paul Sampson (and his statistical consulting team of graduate students) contributed to data analysis and interpretation. I enjoyed and learned a lot from working with Dr. Mark Wigmosta and the technical advisory group of the Upper Columbia Salmon Recovery Board. Dr. Brian Collins and Dr. Juliet Crider provided mentorship from an earth sciences perspective. I thank the entire Mountain Hydrology Research Group as well as colleagues from across the Civil Engineering Hydrology and Hydraulics group for encouragement, constructive feedback, and friendship, particularly Brian Henn, Nic Wayand, Karl Lapo, Nicoleta Cristea, Ryan Currier, Ronda Strauch, Christina Bandaragoda, Sai Nudurupati, Chris Frans, Julie Vano, Joe Hamman, and Liz Clark.

Finally, I am grateful for the financial support for all of these research efforts that was provided by the National Science Foundation, the Northwest Climate Science Center, the Center for Transformative Environmental Monitoring Programs, the National Center for Airborne Laser

Mapping, the University of Washington Ronald and Mary Nece Endowed Fellowship**,** the American Water Resources Association (WA chapter), and the American Water Works Association (PNW chapter).

Published Material

At the time of writing, three of the following chapters have been published in peer-reviewed journals, and I would like to acknowledge John Wiley and Sons, publisher of *Water Resources Research,* for granting permission to reproduce two of the articles in this dissertation. The third article was published by the *Journal of Science Communication*, which is an open access journal, and permission to reproduce is included under a Creative Commons 4.0 by-nc-nd license.

The citations for published material are:

Dickerson-Lange SE, Lutz JA, Martin KA, Raleigh MS, Gersonde R, Lundquist JD. 2015. Evaluating observational methods to quantify snow duration under diverse forest canopies. *Water Resources Research* 15 (2): 1203–1224 DOI: 10.1002/2014WR015744

Dickerson-Lange SE, Lutz JA, Gersonde R, Martin KA, Forsyth JE, Lundquist JD. 2015. Observations of distributed snow depth and snow duration within diverse forest structures in a maritime mountain watershed. *Water Resources Research* 51 (11): 9353–9366 DOI: 10.1002/2015WR017873

Dickerson-Lange SE, Eitel KB, Dorsey L, Link TE, Lundquist JD. 2016. Engaging citizen scientists to observe patterns of snow cover across the Pacific Northwest. Journal of Science Communication 15(01) (A01)

Chapter 6 is currently in review at *Hydrological Processes.*

The citation for the manuscript in review is:

Dickerson-Lange SE, Gersonde RF, Hubbart JA, Link TE, Nolin AW, Perry GH, Roth TR, Wayand NE, Lundquist JD. 2016. Snow disappearance timing in warm winter climates is dominated by forest effects on snow accumulation. *Hydrological Processes* In Review

Table of Contents

List of Figures

List of Tables

Chapter 1. Forests and Mountain Snow Storage in the Pacific Northwest, USA

1.1 Introduction

Coniferous forests cover much of the seasonal snow zone in the Pacific Northwest (PNW), USA, and strongly influence hydrological processes by modifying water and energy fluxes at a range of spatial and temporal scales. Therefore, forest change due to management activities or natural disturbance affects the amount and duration of snow storage in a watershed [*Hedstrom and Pomeroy*, 1998; *Storck et al.*, 2002; *Musselman et al.*, 2008; *Molotch et al.*, 2009; *Lundquist et al.*, 2013], with a cascade of impacts on soil moisture availability [*Veatch et al.*, 2009; *Harpold et al.*, 2015b], phenology [*Ford et al.*, 2013], tree line migration [*Geddes et al.*, 2005], soil-atmosphere exchanges of gases [*Groffman et al.*, 2006] and energy [*Cherkauer and Lettenmaier*, 1999], water availability during flood events [*Marks et al.*, 1998; *Wayand et al.*, 2015b], the timing and magnitude of spring and summer streamflow [*Wilm and Dunford*, 1948; *Bosch and Hewlett*, 1982; *Jones*, 2004; *Lyon et al.*, 2008], and stream temperature [*Moore et al.*, 2006; *Gravelle and Link*, 2007]. Understanding and predicting the difference in the magnitude of peak snow storage and the timing in snow disappearance as a function of forest cover (or lack thereof) in response to changing climate and forest conditions are therefore critical for quantifying and projecting hydrological and ecological impacts at the local and watershed scale (Figure 1.1).

As a result, many studies have addressed the effects of timber harvest, silvicultural practices, and forest disturbance on snow processes [*Golding and Swanson*, 1986; *Murray and Buttle*, 2003; *Winkler et al.*, 2005; *Jost et al.*, 2007] and water yield [*Rothacher*, 1970; *Bosch and Hewlett*, 1982; *Stednick*, 1996]. However, although the key influence of forests, and forest

change, on snow processes has been widely observed, the net effect of forests on snow storage across the landscape varies with forest characteristics like canopy density and stand age [*Kittredge*, 1953; *Jost et al.*, 2007], topographic position [*Strasser et al.*, 2011; *Ellis et al.*, 2013], latitude [*Musselman et al.*, 2008; *Harpold et al.*, 2015b], and climate [*Lundquist et al.*, 2013]. As a result, predicting or modeling the net effects of forest on snow depends on the integration of multiple forest-snow processes, and is an on-going research challenge that has widely been noted as a critical hydrological knowledge gap [*Essery et al.*, 2009; *Rutter et al.*, 2009; *Varhola and Coops*, 2013].

Understanding forest-snow-climate interactions is particularly important in the heavily forested PNW. Snow storage in the headwaters of the Columbia River basin and the coastal drainages, such as the Skagit and Snoqualmie basins, directly contributes to the suitability of stream habitat for endangered salmonids, hydropower generation for the PNW and beyond, and agricultural and municipal water supply. Furthermore, the PNW is an ideal local laboratory to assess forest-snow-climate relations, with extensive and diverse forest types, extensive seasonal snow storage, and both maritime and continental climates. Active forest management programs in the PNW include timber harvest, silvicultural thinning, and prescribed burns [*Richards et al.*, 2012; *Wigmosta et al.*, 2015]. Extensive logging has resulted in widespread 2nd growth forest composed of densely packed stands of even-age trees [*Kane et al.*, 2010b, 2011]. Policy tools such as the Northwest Forest Plan and Habitat Conservation Plans driven by compliance with the Endangered Species Act have prompted some public land management agencies, such as Seattle Public Utilities (SPU) to implement management strategies to accelerate the development of complex terrestrial habitat [*Seattle*, 2000]. In particular, variable density thinning and gap-cutting are used to support the conversion of dense 2nd growth forests with homogeneous canopy cover

to the more complex canopy structures and stem distributions of old growth forests [*Richards et al.*, 2012].

Forest harvest activities are additionally overprinted by large swaths of forest land burned by wildfire [*Westerling*, 2006; *Barbero et al.*, 2015] or defoliated by insects [*Welch et al.*, 2015]. Accounting for forest change effects on snow processes will become even more important under changing climate conditions because climate change is likely to simultaneously increase forest disturbances [*Wimberly and Liu*, 2014] and reduce snow storage [*Mote et al.*, 2005; *Adam et al.*, 2009; *Elsner et al.*, 2010].

This dissertation focuses on quantifying and modeling forest influences on snow in the mountain watersheds of the PNW. In particular, this research seeks to better understand the spatiotemporal variability of forest effects on individual snow processes as well as integrated quantities such as snow depth and snow duration. The overarching goal of this body of work is to ultimately enhance prediction skill for conceptual, empirical, and process-based models such that we can better anticipate the combined effects of forest change and climate change on mountain snow storage and downstream water resources. A brief overview of the relevant literature on forest-climate-snow interactions is presented in chapter 2, and chapter 3 focuses on methods for collecting snow observations within diverse forest types. The operational snow networks are designed to capture maximum snow accumulation in locations where there are no trees, and there is a relative paucity of snow data from within forests. As such, chapter 4 details the forest, snow, and meteorological observations that we collected over four winters in the Cedar River Municipal Watershed, in western Washington, and represents an effort to make this rich dataset both publicly available and usable by other interested researchers. Our findings in the Cedar River Municipal Watershed led to a global synthesis of forest-snow studies [*Lundquist et al.*,

2013], and ultimately to a PNW-focused study of where and why snow lasts longer in the forest versus the open. To address this question in a regional context, we sought to collect and gather forest snow data from across the PNW. This goal resulted in a 4-year citizen science campaign that is described in chapter 5, and in collaborative analysis with researchers at Oregon State University and the University of Idaho, which is detailed in chapter 6. The PNW forest-snow synthesis presented in chapter 6 elucidates the dominant components of forest-snow interactions that contribute to the amount and duration of mountain snow storage, but necessarily simplifies the landcover comparison into binary categories of forest or open. Lastly, chapter 7 addresses the important role of forest structure on snow processes by analyzing spatially distributed snow observations from the Cedar River Municipal Watershed in conjunction with lidar-derived forest and topographic predictor variables.

1.2 Figures

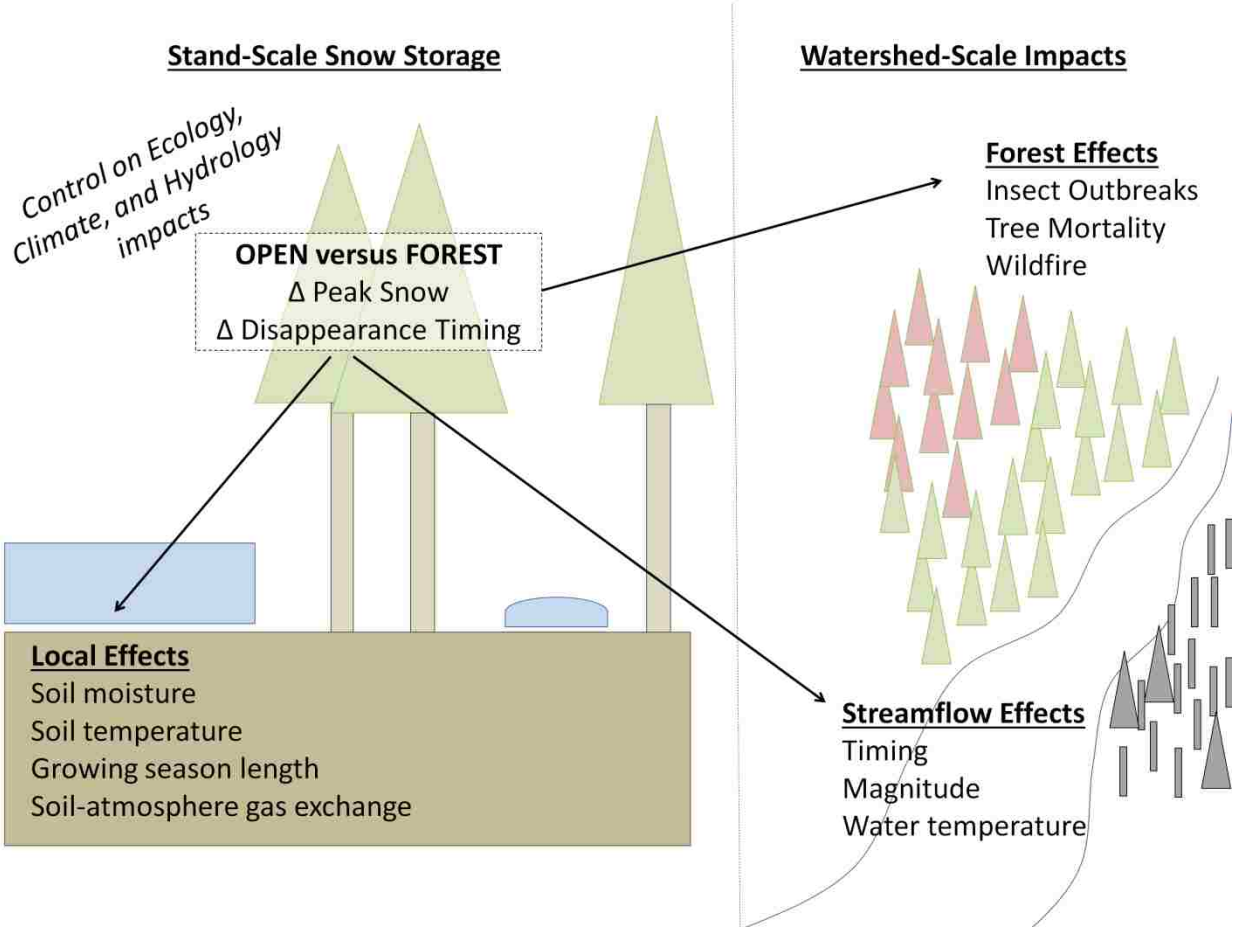

Figure 1.1 Illustration of local, forest, and streamflow effects of differences in snow storage amount (Δ Peak Snow) and duration (Δ Disappearance Timing) between forests and open areas.

Chapter 2. Background: forest modifications of snow processes

Forests affect under-canopy snow accumulation via canopy snow interception and storage. Since snow that is stored in the forest canopy is subject to higher rates of loss due to sublimation [*Pomeroy et al.*, 1998b, 2002; *Molotch et al.*, 2007] and melt [*Storck et al.*, 2002], interception typically results in reduced under-canopy snowpack relative to open areas [*Storck et al.*, 2002; *Winkler et al.*, 2005; *Molotch et al.*, 2009; *Veatch et al.*, 2009; *Moeser et al.*, 2015; *Revuelto et al.*, 2015]. Snow accumulation is also modified by the attenuation of wind by surrounding forest cover, which leads to redistribution of snow from exposed to sheltered areas [*Winstral and Marks*, 2002, 2014; *Essery and Pomeroy*, 2004b; *Trujillo et al.*, 2009], or locally enhanced deposition within forests or at forest edges where the trees effectively act as a snow fence [*Miller*, 1964; *Tabler*, 1975; *Hiemstra et al.*, 2002; *Geddes et al.*, 2005].

Forest cover modifies ablation processes by enhancing or diminishing radiative inputs and diminishing turbulent heat transfer due to reduced wind speeds. The forest canopy reduces the magnitude of incoming solar radiation [*Link et al.*, 2004; *Sicart et al.*, 2004; *Lawler and Link*, 2011; *Musselman et al.*, 2013, 2015], but can also increase net solar radiation via leaves and needles that reduce under canopy snow albedo [*Hardy et al.*, 2000; *Pugh and Small*, 2012]. Forest cover can contribute enhanced longwave radiation to under canopy snowpack from the relative warmth of tree temperatures as compared with the atmosphere [*Essery et al.*, 2008; *Lawler and Link*, 2011], and from enhanced warming of tree stems and leaves from penetration of solar radiation into the forest [*Pomeroy et al.*, 2009]. Finally, turbulent energy exchanges within forest are typically reduced relative to open areas due to reduced wind speeds [*Chen et al.*, 1993; *Marks et al.*, 1998].

In a global synthesis of observations of snow disappearance timing from forest and open study plots, [*Lundquist et al.*, 2013] documented the range of overall forest effects on snow retention, and demonstrated that winter climate is a first-order predictor for whether the net effect of forest is to delay [*Gelfan et al.*, 2004; *Thyer et al.*, 2004; *Burles and Boon*, 2011] or accelerate [*Storck*, 2000; *Bales et al.*, 2011; *Dickerson-Lange et al.*, 2015a] snow disappearance timing relative to an open area. In particular, in locations with warmer winter climates (greater than -1 °C), snow persisted up to two weeks longer in the open after snow disappeared in the forest, while in colder winter climates (below -6 °C) snow persisted up to two weeks longer in the forest. Snow disappearance timing was approximately synchronous (i.e., ± 3 days) in locations where DJF temperature ranged from -6 to -1 °C. A key implication of this winter temperature-based framework is that air temperature plays a primary role in influencing the processes by which forests modify snow accumulation and ablation.

Average winter air temperature affects the magnitude of the forest's impact on each individual snow process, contributing to locally modified rates of snow accumulation and ablation. Snow interception rates, which reflect the efficiency with which the forest canopy captures and stores snow, are typically higher in warmer climates [*Shidei et al.*, 1952; *Miller*, 1964; *Storck et al.*, 2002; *Martin et al.*, 2013; *Friesen et al.*, 2015]. Interception efficiencies have been observed to range from 30-60% in colder climates [*Schmidt*, 1991; *Schmidt and Gluns*, 1991; *Hedstrom and Pomeroy*, 1998], and from 50 to 80% in warmer climates [*Storck et al.*, 2002; *Martin et al.*, 2013]. The differences have been primarily attributed to the higher cohesion of snow at warmer temperatures [*Shidei et al.*, 1952; *Kobayashi*, 1987; *Pfister and Schneebeli*, 1999]. Temperature also influences the role of forest in ablation processes via controlling the magnitude of incoming longwave radiation and influencing the relative contribution of

shortwave radiation to the energy balance. Since longwave radiation is a function of temperature to the 4th power (i.e., the Stefan-Boltzman law), trees that are approximately the same temperature as the surface air temperature contribute much more downwelling longwave radiation to a snowpack that the surrounding open area, where downwelling longwave radiation is diminished due to the lower temperature and emissivity of the upper atmosphere. This difference in longwave radiation can result in enhanced mid-winter melt (i.e., before peak snow accumulation), leading to earlier snow disappearance under the forests in warmer winter climates [*Lundquist et al.*, 2013].

Average winter air temperature indirectly impacts solar radiation at the surface by affecting the timing of when a snowpack becomes isothermal through longwave and sensible heat fluxes. This timing, in turn, influences the relative importance of forest cover for shading the snowpack. At warmer sites, whether low elevation or situated in a warmer climate, ablation may take place early in the season while solar zenith angles are relatively low, which diminishes the importance of shading effect of forest cover on ablation rates [*Sicart et al.*, 2004; *Lundquist et al.*, 2013; *Musselman et al.*, 2015]. Conversely, the role of the forest in reducing incoming solar radiation may be enhanced at colder sites that still have snow when solar angles are high [*Musselman et al.*, 2008; *Molotch et al.*, 2009; *Veatch et al.*, 2009; *Harpold et al.*, 2015b].

Thus, both previous synthesis work and process understanding of forest-snow interaction provide compelling evidence that winter climate is a key influence on differential snow disappearance timing between forests and open areas. However, documented exceptions to this framework exist and are driven by local meteorological and canopy conditions. For example, [*Lundquist et al.*, 2013] reported that snow disappearance timing in the relatively warm winter climate of the Spanish Pyrenees (average winter temperature of 2.2 °C based on gridded climate

data, see Table 1 and Figure 2a of [*Lundquist et al.*, 2013]) was observed to be synchronous [*López-Moreno and Latron*, 2008], whereas a temperature-based framework suggests that snow would persist longer in the open. However, the locale is subject to very high wind events, which were highlighted at a nearby site in the analysis of repeat terrestrial laser scanner snow surveys [*Revuelto et al.*, 2015]. Thus, wind redistribution of snow to the forest or wind-driven preferential accumulation in forests may contribute to enhanced snow accumulation and longer snow persistence within forests despite warm winter temperatures.

Previous investigations have also shown that both the density and structure of the forest stands [*Kittredge*, 1953; *Varhola et al.*, 2010a; *Musselman et al.*, 2012] and the size and distribution of openings [*Lawler and Link*, 2011; *Ellis et al.*, 2013; *Seyednasrollah and Kumar*, 2014; *Broxton et al.*, 2015; *Moeser et al.*, 2015] influence the ways in which the presence of forest modifies snow processes. Both canopy density and tree stem (i.e., trunk) density have been shown to affect under-canopy snow accumulation and ablation processes [*Gary and Troendle*, 1982; *Davis et al.*, 1997; *Link et al.*, 2004; *Woods et al.*, 2006; *Jost et al.*, 2007; *Veatch et al.*, 2009; *Seyednasrollah et al.*, 2013]. High resolution modeling [*Broxton et al.*, 2015] as well as spatially distributed observations of snow [*Veatch et al.*, 2009; *Harpold et al.*, 2015b; *Moeser et al.*, 2015] and radiative fluxes [*Lawler and Link*, 2011; *Musselman et al.*, 2015] have demonstrated the dependence of snow accumulation and ablation processes on proximity and direction to a canopy edge.

Chapter 3. Evaluating observational methods to quantify snow duration under diverse forest canopies

Susan E. Dickerson-Lange[1,5], James A. Lutz[2], Kael A. Martin[1], Mark S. Raleigh[3], Rolf Gersonde[4], and Jessica D. Lundquist[1]

[1]Civil and Environmental Engineering, University of Washington, Seattle, Washington, USA
[2]Wildland Resources Department, Utah State University, Logan, Utah, USA
[3]National Center for Atmospheric Research, Boulder, Colorado, USA
[4]Seattle Public Utilities, Seattle, Washington, USA

Note: This chapter has been published in its current form as an article in Water Resources Research [*Dickerson-Lange et al.*, 2015a]; the only differences are in section, figure, and table numbering, and in the casing of lidar, which has been updated to reflect current consensus [*Deering and Stoker*, 2014]. It is used here by permission of John Wiley and Sons.

3.1 Abstract

Forests cover almost 40% of the seasonally snow-covered regions in North America. However, operational snow networks are located primarily in forest clearings, and optical remote sensing cannot see through tree canopies to detect forest snowpack. Due to the complex influence of the forest on snowpack duration, ground observations in forests are essential. We therefore consider the effectiveness of different strategies to observe snow-covered area under forests. At our study location in the Pacific Northwest, we simultaneously deployed fiber-optic cable, stand-alone ground temperature sensors, and time-lapse digital cameras in three diverse forest treatments: control second-growth forest, thinned forest, and forest gaps (one tree height in diameter). We derived fractional snow-covered area and snow duration metrics from the co-located instruments to assess optimal spatial resolution and sampling configuration, and snow duration differences between forest treatments. The fiber-optic cable and the cameras indicated that mean snow duration was 8 days longer in the gap plots than in the control plots ($p < 0.001$). We conducted Monte Carlo experiments for observing mean snow duration in a 40 m forest plot, and found the 95% confidence interval was ± 5 days for 10 m spacing between instruments and ± 3 days for 6 m spacing. We further tested the representativeness of sampling one plot per treatment group by observing snow duration across replicated forest plots at the same elevation, and at a set of forest plots 250 m higher. Relative relationships between snow duration in the forest treatments are consistent between replicated plots, elevation, and two winters of data.

3.2 Introduction

The duration of the seasonal snowpack that develops and melts each year in mountain watersheds is a key influence on runoff, soil moisture, surface-atmosphere energy fluxes, and ground temperature. Observations of snow-covered area in mountain watersheds are assimilated into land surface models (e.g.[*Rodell and Houser*, 2004; *Clark et al.*, 2006]), used to validate snow models (e.g.[*Parajka et al.*, 2012]), and incorporated in investigations related to terrestrial habitat and phenology (e.g., [*Ford et al.*, 2013]). Both snow-covered area observed commonly via remote sensing (e.g., the Moderate Resolution Imaging Spectroradiometer (MODIS)), and point observations of snow water equivalent (SWE) from snow telemetry instrument networks (e.g., Natural Resources Conservation Service Snow Telemetry stations (NRCS SNOTEL)) are used to assess how the snowpack and snow processes vary across the landscape, but each provides incomplete snow information. Snow cover characterizes extent, but not magnitude of the amount of water stored on the landscape, and point SWE measurements provide magnitude information at a subset of locations. Furthermore, both snow cover and SWE data are typically sparse or estimated within forests due to the blocking of the optical sensors (e.g., MODIS) or a lack of operational data collection in forests (e.g., SNOTEL stations).

Deriving or estimating snow magnitude (i.e., SWE) or snow cover from the other of the two variables is possible by combining observed snow cover with a distributed modeling approach (e.g., [*Yatheendradas et al.*, 2012; *Guan et al.*, 2013]), interpolating point values of snow water equivalent (SWE) to gridded products (e.g., [*Fassnacht et al.*, 2003; *Rice et al.*, 2011]), and applying snow depletion curves that describe the empirical relationship between snow magnitude and snow cover (e.g., [*Liston*, 2004; *Luce and Tarboton*, 2004; *Clark et al.*, 2011]). However, accurate estimation of both SWE and snow-covered area in forested watersheds is problematic

(e.g., [*Meromy et al.*, 2013; *Raleigh et al.*, 2013]). With forests extending over approximately 40% of the seasonally snow-covered zone in North America [*Klein et al.*, 1998], improvements in accurate quantification of both snow magnitude and snow cover within forests is crucial. We focus on snow cover, which reflects the net effect of the variability in snow processes across the landscape, is a key variable in hydrological, ecological, and atmospheric processes, and has a direct relationship to quantifying SWE.

Snow duration varies in space and time across forested watersheds due to the complex influence of the forest on snow accumulation, redistribution, and ablation processes (e.g., [*Varhola et al.*, 2010a]). The spatial distribution of snow duration, or snow-covered area, is the result of the spatial distribution of snow depth [*Luce et al.*, 1998; *Anderton et al.*, 2004] and spatially varying melt and sublimation rates [*Lawler and Link*, 2011; *Musselman et al.*, 2012], all of which are influenced by the presence and characteristics of vegetation. Thus, it is difficult to extrapolate snow observations made in clearings to adjacent forests [*Rice and Bales*, 2010; *Yatheendradas et al.*, 2012; *Meromy et al.*, 2013].

Remote sensing delivers gridded characterization of snow cover, but trees limit the viewable snow on the ground. Snow coverage under the canopy is therefore estimated from the percentage of snow cover in open areas (e.g., [*Durand et al.*, 2008]). The assumption that snow-covered area within forests is proportional to snow-covered area within the open (i.e., the viewable gap fraction) is particularly problematic because the magnitude and direction of forest effects on snowpack depends on forest characteristics (e.g., [*Winkler et al.*, 2005; *Burles and Boon*, 2011]), climate (e.g., [*Lundquist et al.*, 2013], and topographic position (e.g., [*Strasser et al.*, 2011; *Ellis et al.*, 2013]), so the relationship between snow-covered area in the open versus in the forest, as well as between different forest types, should also be expected to vary. For example, Raleigh et

al. [2013] found that the fractional snow-covered area across a range of forest densities was underestimated by 9 to 37% by optical remote sensing techniques as compared to spatially-distributed ground-based observations in the Sierra Nevada. Repeat airborne lidar (light detection and ranging) has the capability to detect snow cover and depth accurately under forests (e.g.,[*Deems et al.*, 2013]), but this technology has only recently been considered for operational purposes, and it is not yet clear how the high costs compare to the potential benefits of improved snow information.

Ground-based observational methods are therefore necessary within forests to quantify the duration of snow cover, which varies in space and time. Distributed point observations that are sufficiently dense and representatively positioned are critical for accurately scaling-up to quantify time-varying snow-covered area at the scale of a grid element of interest, such as a Landsat pixel, a model grid cell, or a forest stand. Ground observations, however, can be difficult and expensive to obtain. Limited resources and rugged conditions motivate using the optimal strategy to maximize the likelihood of successfully collecting representative data. Stand-alone instruments are ideal because data collection does not depend on winter road access and trained personnel to visit the sites at the desired frequency. Many options for ground-based detection of areal snow cover exist, including self-recording ground temperature sensors (e.g., [*Lundquist and Lott*, 2008], fiber-optic cable (e.g.,[*Tyler et al.*, 2008]), and time-lapse photography (e.g., [*Parajka et al.*, 2012]) but each strategy has a unique set of advantages and disadvantages. Thus, in order to guide the collection of snow duration observations in forests, we test observational strategies to determine which instruments, sampling configurations, and plot selection are optimal in terms of accuracy, representativeness, cost, and ease.

Quantification of the spatial variability in snow duration under different forest types has applications for predicting the magnitude and timing of streamflow, modeling energy and water fluxes, and explaining ecological patterns. Increased heterogeneity in snow duration is associated with melting extending to later in the season, providing contributions to spring and summer streamflow [*Luce et al.*, 1999; *Essery and Pomeroy*, 2004a; *Lundquist et al.*, 2005; *Clark et al.*, 2011]. Areal snow coverage is an important parameterization in land surface models because the presence of snow modifies the exchange of energy between the land and atmosphere via the increased albedo of snow [*Liston*, 1995; *Slater et al.*, 2001], and snow-covered area can be used to derive snow water equivalent (SWE) [*Liston*, 1999, 2004; *Luce et al.*, 1999; *Faria et al.*, 2000; *Essery and Pomeroy*, 2004a]. From an ecological standpoint, local snow duration influences the length of the growing season and the availability of soil moisture for plant communities [*Lutz et al.*, 2010; *Ford et al.*, 2013]. Snow also insulates the ground surface, protecting soils and plants from extreme temperatures [*Brown and DeGaetano*, 2011], and affects soil-atmosphere fluxes of nitrous oxide (N_2O) and other trace gases [*Groffman et al.*, 2006].

Since the forest influences both snow accumulation (reduced snow depth [*Hedstrom and Pomeroy*, 1998; *Pomeroy et al.*, 1998b; *Storck et al.*, 2002; *Martin et al.*, 2013]) and snow ablation (reduced or enhanced melting [*Essery et al.*, 2008; *Ellis et al.*, 2011; *Lawler and Link*, 2011; *Mahat and Tarboton*, 2012]), and snow duration is the net result of accumulation and ablation, variability in snow duration can be diminished or amplified relative to the variability observed in snow depth, depending on whether the presence of forest delays [*Molotch et al.*, 2009] or enhances [*Lundquist et al.*, 2013] ablation processes. Local weather patterns can also diminish or amplify forest influences on snow melt processes. For example, rain-on-snow events

can temporarily enhance snowmelt rates in open areas as compared with forests [*Marks et al.*, 1998].

Mountain landscapes are covered by a mosaic of forest stands, each with a unique history of natural disturbance and management actions [*Kane et al.*, 2010b, 2011]. However, spatially-distributed snow duration in forests is rarely directly observed, and, in particular, diverse forest types are underrepresented. Many useful investigations have measured snow depth and duration in forest plots via repeat manual snow course observations (e.g., [*Koivusalo and Kokkonen*, 2002]), ultrasonic snow depth sensors (e.g., [*Bales et al.*, 2011]), and time-lapse cameras (e.g., [*Garvelmann et al.*, 2013]), or snow duration only using ground temperature measurements (e.g., [*Raleigh et al.*, 2013]). Fewer studies have observed snow cover in a range of forest types, including deciduous and coniferous stands (e.g., [*Pohl et al.*, 2014]), different coniferous species and canopy densities (e.g., [*Kittredge*, 1953]), stands disturbed by fire (e.g., [*Burles and Boon*, 2011]) or insects (e.g., [*Varhola et al.*, 2010b]) regenerating stands following timber harvest (e.g., [*Winkler et al.*, 2005]), and stands subject to thinning in various patterns and densities (e.g., [*Storck et al.*, 2002]).

The purpose of this study is to determine optimal strategies for observing spatially distributed snow duration in a range of diverse forest treatments. Since forests have complex influences on snow, quantifying the evolution of snow-covered area in a representative range of forests types is critical to hydrological and ecological investigations, and there is currently no feasible substitute for ground observations given common financial constraints. By co-locating multiple instruments at three intensive 40 × 40 m study plots previously subjected to different silvicultural treatments, and by replicating study plots in a single study area and at a higher elevation study area, we consider the following key questions: How does each instrument

characterize differences in snow duration between forest treatments? What sampling density at the plot-scale is optimal to detect differences in snow duration and avoid redundant sampling? How representative is snow duration observed at one plot of snow duration at other plots subject to the same forest treatment, both within the same elevation band and in a different elevation band?

In section 2 we introduce the study location, observational strategies, and methods used to infer snow presence from observations. We compare snow duration results between methods and between replicated experimental plots in section 3, and additionally present results from Monte Carlo experiments to further explore the optimal sampling density and configuration. In section 4 we discuss applications of our findings, and the unique perspective of each method and its influence on our results. We conclude by making recommendations for future field campaigns.

3.3 Methods

3.3.1 Study sites

We deployed stand-alone instrumentation to observe snow duration in diverse forest types over two winters in the Cedar River Municipal Watershed (47° 20’ N, 121° 32’ W), located approximately 50 km east of Seattle, Washington, USA (Figure 3.1a). The protected municipal watershed is located on the western slope of the Cascade Range. Within a 10 km^2 area in the upper watershed, we collected data at two study sites (Bear Creek and Mount Gardner) at different elevations (640 m and 890 m, respectively). Both sites encompass multiple study plots approximately 1600 m^2 in area, which were previously subjected to two silvicultural manipulations: thinning and gap creation. These forest management strategies are used by Seattle Public Utilities in dense, second-growth forests with homogeneous canopy to facilitate the recovery of ecosystem functions, such as habitat for species that depend on late-successional forests [*Richards et al.*, 2012].

The Cedar River Watershed has a maritime climate, with cool winter temperatures that fluctuate around the freezing point and heavy winter precipitation. Mean January minimum and maximum temperatures are -3.3°C and 3.5°C, respectively, at the lower elevation Bear Creek study site, and are -3.6°C and 1.4°C at the higher elevation Mount Gardner study site (based on 1971-2000 climate normals derived from PRISM [*Daly et al.*, 2008]). Mean annual precipitation is 2,490 mm surrounding the lower site and 2,690 mm surrounding the upper site (also from PRISM [*Daly et al.*, 2008]); annual snow accumulation varies from 0 to 800 mm of SWE.

Bear Creek is the most comprehensively sampled study site, and comprises a 400 m × 80 m domain (Figure 3.1b) of approximately 70 year old evergreen forest [*Sprugel et al.*, 2009; *Lutz et al.*, 2012]. The second-growth forest is dominated by western hemlock (*Tsuga heterophylla)* and

Douglas-fir (*Pseudotsuga menziesii),* with some western redcedar (*Thuja plicata),* Pacific silver fir (*Abies amabilis)* and noble fir *(Abies procera),* and an overall stem density of ~1500 stems ha^{-1} (see *Sprugel et al.*, [2009] for details). The study site includes fifteen 40 m × 40 m experimental plots, including five each of control forest, thinned forest, and gap plots. The five control forest plots are covered by untreated second-growth forest with an average of 68.4 m^2 of basal area (i.e., sum of the cross-sectional stem area at 1.4 m height) per hectare (see Table 3.1 for lidar-derived canopy cover metrics). In the thinned plots approximately 30% of the basal area was removed from the entire plot, with the largest trees retained (basal area of 46.3 $m^2\,ha^{-1}$). In the gap plots a circular gap with a diameter of 20 m, equal to approximately one tree height, was cut into the middle of the plot, resulting in zero canopy cover over about 20% of the plot. Three of the Bear Creek study plots, a control plot and one representing each forest treatment, were designated as intensive study plots (hereafter, "intensive plots"; shaded on Figure 3.1b). The remaining 12 plots at Bear Creek were designated as "additional plots".

The Mount Gardner site provides a higher elevation comparison to the Bear Creek site (elevation difference of 250 m), and consists of three 40 m × 40 m study plots: a control forest plot, a thinned plot, and a gap in which the NRCS Mount Gardner SNOTEL site (#898) is co-located (hereafter "higher elevation plots"; Figure 3.1c). Despite the modest elevation difference between Mount Gardner and Bear Creek, snow coverage at the higher site tends to be more temporally and spatially continuous; the higher site was included to characterize snow processes in comparable forest treatments above the intermittent snow zone. The second-growth evergreen forest at the Mount Gardner site includes Pacific silver fir as the dominant species, with some western hemlock, Douglas-fir, and western redcedar. Stand density in the control plot is ~ 2900 stems ha^{-1} and 78.7 $m^2\,ha^{-1}$ basal area. Basal area in the thinned plot density is 45.8 $m^2\,ha^{-1}$.

3.3.2 Data Collection & Processing

Our observational strategy included replicated measurements at variable spatial and temporal resolutions at the Bear Creek site to test observational methods and sampling configurations (water year (WY) 2011 only), and replicated forest treatments at Bear Creek and Mount Gardner to test the representativeness of a set of forest plots (WY 2011 and 2012). At each study plot we collected time series of ground temperature data using either a grid of individual ground temperature sensors deployed slightly below the ground surface, or a fiber-optic cable (FOC) deployed on top of the ground surface (Table 3.1). From the ground temperature data we inferred daily snow presence/absence based on the diurnal temperature cycle. At the three intensive plots at Bear Creek in WY 2011 we simultaneously collected snow presence data using both types of ground temperature instruments and time-lapse cameras to detect snow presence visually.

We derived a time series of daily snow presence/absence at each sample point for each observational method. Each instrument has a different support (i.e., the area over which the observation is integrated [*Blöschl*, 1999]), discussed below. However, for the purpose of using point data to represent snow duration variability at the scale of a forest plot, we generalize all of our instruments as collecting point-scale data, as distinguished from the plot-scale. To assess spatially distributed snow duration we used the point observations to compute plot-scale metrics: 1) the evolution of fractional snow-covered area (fSCA) through time, and 2) distributions of snow duration metrics, including the number of days of snow cover during a given period of time (relative snow-covered days, RSCD, which is intended to be a relative metric between plots during the same snow season), and the snow disappearance date (SDD). These metrics reflect the net effect of the magnitude of snow accumulation combined with the rate of snow ablation on

snow duration at a point, and the distribution of the metrics characterizes the spatial variability of snow duration at the plot-scale.

In addition to the snow presence data discussed in detail below, we collected meteorological, canopy, and snow depth observations to support our analyses and provide context. We measured air temperature at the intensive gap and control plots, and at a clearing located 2 km from Bear Creek at an elevation of 730 m (Clearing Met on Figure 3.1a). Due to discontinuous air temperature data collection at the two intensive plots and close agreement between air temperature recorded at the study plots and the nearby Clearing Meteorological Station, we used air temperature at the Clearing Meteorological Station in our analyses. We acquired airborne lidar on 31 August and 1 September 2012 (i.e., leaf on), with an average return density of 7.5/m^2 over the study area, from which we derived 5 m gridded canopy cover. Canopy cover was defined as the proportion of returns from canopy (>2 m above the ground model) compared to the total number of returns, and relates to the vertical projection of canopy crowns upon the ground surface [*Jennings et al.*, 1999]. To characterize plot-scale canopy cover, we present the mean and standard deviations of the gridded data over individual study plots in Table 3.1. Additionally, prior to the start of the snow season in WY 2011, we measured canopy closure with a GRS densiometer (Geographic Resource Solutions, Arcata, California) at 0.5 m intervals directly above the FOC transect, discussed below. Canopy closure relates to the sky hemisphere that is obscured by vegetation when viewed from a single observation point. We used a nearest neighbor algorithm to take the 5 m average of canopy closure for every 1 m along the FOC. Lastly, we collected snow depth observations via approximately bi-weekly manual snow course transects at each of our intensive plots; mean snow depth was calculated from two perpendicular 20 m transects consisting of 20 evenly spaced measurements.

3.3.2.1 Ground Temperature Observations & Snow Presence

Snow presence/absence data at point locations were derived from ground temperature data collected via two types of instruments: self-recording ground temperature sensors and a fiber-optic cable (FOC). Ground surface temperature measurements are a reliable way to determine when and where snow is present [*Lundquist and Lott*, 2008; *Lyon et al.*, 2008; *Tyler et al.*, 2008; *Raleigh et al.*, 2013]. When the diurnal fluctuation of ground surface temperature is damped (due to the insulating properties of snow) relative to nearby air temperature, we infer that the surface is snow-covered. When surface temperature and air temperature fluctuate by similar amounts, we infer that the ground surface is snow-free.

We deployed grids of 9-10 individual ground temperature sensors (Maxim DS 1922L thermochrons, hereafter "iButtons") per study plot at a spacing of 10 m for the full duration of the snow season in both WY 2011 and 2012 at Bear Creek and at Mount Gardner. The iButtons were wrapped in self-sealing plastic and buried 1-2 cm below the ground surface, where they recorded hourly near-surface temperature to an accuracy of 0.5 °C; the diameter (i.e., support) of an individual instrument is 1.5 cm. All iButtons were validated before and after usage via ice bath and ambient air temperature tests. Using the hourly temperature data, we inferred daily snow cover using two criteria: a maximum temperature less than 2 °C and a maximum diurnal temperature range less than 1.5 °C (see Figure 2 in Raleigh et al. [2013] for illustration). Due to instrument failure, however, as few as 5 per plot in WY 2011, and as few as 7 per plot in WY 2012 (indicated in Figure 3.1b and c), recorded continuous data during the ablation season.

A 900 m FOC (BRUsens Temperature +85 °C; Brugg Cable International, Bragg, Switzerland) was deployed in WY 2011 to collect ground temperature, integrated over every 1 m along the cable at 30 minute temporal resolution; data from 800 m of the FOC that transected the

experimental plots were retained for analysis. A Sensornet Oryx distributed temperature sensing (DTS) system (Sensornet, Elstree, United Kingdom) was installed in an equipment trailer and used to generate light pulses and measure the corresponding reflected spectra. The Oryx compares the ratio of anti-Stokes photons (higher frequency, shorter wavelength) and Stokes photons (lower frequency, longer wavelength) that are absorbed and reemitted as the light pulse comes into contact with the cable wall [*Tyler et al.*, 2009]. The ratio of anti-Stokes photons to Stokes photons follows a Boltzmann distribution proportional to the ambient temperature surrounding the FOC [*Selker et al.*, 2006; *Tyler et al.*, 2008, 2009; *Lutz et al.*, 2012]. Deployment specifics are described further in Lutz et al. [2012].

We measured ground temperature using the FOC during the snowmelt period from 17 March 2011, when the entire study area was snow-covered, to 25 May 2011, when the entire area was snow free (70 days). Since the FOC was deployed on the snow-free ground surface rather than underground, we used co-located time-lapse cameras to visually compare snow presence with the diurnal temperature range observed at two 10 m stretches of FOC, one in the intensive gap plot and one in the intensive control plot. We found that the diurnal temperature range fluctuated up to 2.0°C even when completely covered by snow, and was sensitive to sunny days (Figure 3.2). Therefore, to account for its position on top of the ground, rather than below the ground, we used slightly different criteria to determine snow presence, including an additional criterion of maximum daily air temperature recorded at the nearby Clearing Meteorological Station to dynamically determine the temperature thresholds. On days when maximum air temperature was less than or equal to 12.0 °C, we used a maximum temperature of 2.5 °C and a maximum diurnal range of 2.0°C to infer snow presence, whereas when the maximum daily air

temperature was greater than 12.0 °C we used 3.0 and 2.5 °C, respectively (see supplemental material for more details and sensitivity testing).

Due to power disruptions caused by snow accumulating on the solar panels and preventing battery recharge, cloudy conditions that diminished battery recharge, and insufficient battery capacity, FOC data were collected for approximately 2/3 of the sampling times. Power disruptions followed a diurnal cycle, and we collected a minimum of one datum per day (in the afternoon) at all sampling locations, with the exception of four missing periods longer than one day. Since many of these disruptions occurred due to snowfall, which were periods during which snow disappearance was unlikely to occur, the missing FOC data had a minimal effect on our ability to represent daily snow presence (see supplemental material for more details). For days on which the last day of continuous snow cover occurred before a missing day, we assumed that snow disappeared on the next day of data collection (Figure 3.2b). In these cases, the ground temperature clearly indicates snow presence on the day before the data gap, and snow absence on the day following the data gap. This assumption recognizes that snow was most likely to disappear after a missing period if the cause of the data gap was snowfall; however, in some cases data were missing due to cloudy conditions. Sensitivity testing of this assumption yielded negligible differences in distributions of snow metrics.

3.3.2.2 Time-Lapse Cameras & Snow Presence

We deployed time-lapse digital cameras to identify snow presence at the three Bear Creek intensive plots, where iButtons and the FOC were also deployed in WY 2011. Each digital camera was encased in a weather-resistant box and mounted 2 m high on a tree trunk, with the field of view including roughly one fifth of the plot. Multiple photos were taken each day in order to capture a range of weather and light conditions. Daily images were chosen for analysis

on the basis of consistent light (i.e., daytime, few shadows) and a clear view (i.e., no falling snow, minimal condensation on the lens). Photos were cropped during analysis to exclude the view of adjacent plots from analysis (Figure 3.3a).

We used semi-automated image analysis to determine the spatial extent of the ground surface (i.e., removing tree trunks that obscured the field of view from analysis), and then classified snow presence/absence for each pixel via a threshold brightness approach (Figure 3.3b). We used a MATLAB tool (graythresh.m) that implements Otsu's method for determining the optimal threshold for converting an image to binary, by choosing a group cutoff to maximize the ratio of between group variance to within group variance [*Otsu*, 1979]. Due to the brightness of the forest floor (e.g., some woody debris), snow cover was overestimated in many of the images with sparse snow cover; in these cases, we manually selected a threshold that resulted in the closest match between the visual image and the binary image.

Before calculating fSCA or extracting snow duration metrics, we aggregated the photo into equal-area boxes, each of which represents approximately 0.08 m^2 on the ground (Figure 3.3c). Since each pixel covers a different amount of ground area, resulting in a different support for the observation depending on position within the photo, we adjusted the number of pixels included in each aggregated box according to their respective representative areas. To determine the number of pixels needed to achieve equal area boxes, we estimated the distance on the ground captured in each pixel as a function of distance from the camera, using known values for the height, focal length, and view angle of the camera, and making the simplifying assumption that the ground surface was horizontal. We classified snow as present/absent for each box on each day from the percentage of snow-covered pixels (>50%), and then treated each box as a point location for quantifying snow duration.

3.3.2.3 Quantifying Snow Duration

From the time series of snow presence, we computed the time-evolution of fSCA at the spatial scale of a plot, and snow duration metrics at the scale of a point sample. Daily fSCA quantifies snow duration through time for each plot, and is calculated for each day based on the ratio of data points at a plot that indicate snow presence to the total number of data points at that plot. Thus, although thinking of this ratio as an area provides physical relevance, we are strictly describing the ratio of snow presence within each configuration of sensors, including a partial grid (iButtons), a transect (FOC), and a sub-area (photos). The spatial resolution of the fSCA metric therefore varies with the sensor type.

We additionally compute two snow duration metrics for each sampling location (e.g., one iButton) to summarize overall snow duration for the season. We then quantify the differences across observational methods and across forest treatments by first comparing metrics from co-located instruments and then the distributions of values derived from the three instruments located at the same plot. The first metric, the relative number of snow-covered days (RSCD), represents snow duration at a single point and allows for snow cover to be intermittent. To compare snow duration for the period during which the three instrument types at the intensive plots were all collecting data (WY 2011), we computed the RSCD as the number of days of snow cover during the period of FOC data collection and omitted days of missing FOC data. For both years at Mount Gardner and for WY 2012 at Bear Creek, we computed the number of days of snow cover since peak snow depth at Bear Creek (determined from the snow courses). The choice of starting date for this metric is arbitrary, since it is intended for comparison of different plots during the same snow season, rather than for comparison between years.

Our second metric, snow disappearance date (SDD), is the last day of any snow presence (e.g., snow is present in the morning, but absent by the afternoon) at a single location (e.g., Figure 3.2a). The SDD is an ecologically relevant metric for growing season length and ground temperature (e.g.,[*Ford et al.*, 2013]), but the intermittent nature of seasonal snow cover in the Cedar River watershed has a strong influence on this method of quantifying snow duration. Periods of mid-winter melt and late season snowfall contribute to multiple occurrences of snow appearance and disappearance, especially at the lower elevation Bear Creek site. This episodic accumulation and disappearance of a spring snowfall results in a "final" SDD that is synchronous across many locations, and these event-driven SDD metrics can be independent of the net effects of the forest on snow duration. For example, at locations where snow disappears early in the ablation season, the accumulation and subsequent disappearance of late season snowfall will result in the same SDD value at these locations despite each location having variable snow disappearance timing prior to final snowfall. Thus, we consider both the number of snow-covered days (RSCD) as well as final snow disappearance date (SDD) to robustly quantify snow duration.

In order to characterize plot-scale snow duration, the metrics were computed for every sample location for the ground temperature sensors. Since the cameras have a much higher spatial resolution, we computed snow duration metrics for the equal-area, aggregated sample locations (Figure 3.3c). Previous investigations have derived spatially-distributed snow metrics from the camera's field of view by analyzing snow depth [*Parajka et al.*, 2012], snow albedo and canopy interception [*Garvelmann et al.*, 2013], or fractional snow-covered area [*Ide and Oguma*, 2013] at discrete locations in the photograph. Kerr et al. [2013] assessed the spatial pattern of snow disappearance by resampling time-lapse photos and identifying SDD for each aggregated

domain. We build on this approach to resample the entire domain of each photo and extract SDD and RSCD values, allowing for a direct comparison to the empirical distributions derived from the iButtons and the FOC.

3.4 Results

3.4.1 Comparing Observational Strategies: Point Comparison

In a direct comparison of the time series of snow presence/absence observed by co-located instruments, the iButton and cameras agree very closely, whereas the FOC indicates less continuous snow duration and earlier snow disappearance. We utilized four locations in which the marker for an iButton was clearly visible within the field of view of the camera (Figure 3.4a), and compared the time series of snow presence at those locations derived from the iButton and the camera. We found that the two methods matched very closely, with SDD and RSCD values that were within +/- 1 day.

Similarly, we compared the FOC with co-located iButtons at six locations (three of which were also visible in time-lapse photos, e.g., Figure 3.4a), assessing the agreement between the time series of ground temperature (Figure 3.4b) and of snow presence (Figure 3.4c). In all locations the FOC observed a larger diurnal temperature range during times when the iButton (and camera for three locations) indicated that snow was present, generally resulting in an early bias in snow disappearance and a low bias in the RSCD relative to the other methods. At two locations the SDDs derived from the iButton and the FOC were identical, whereas at the other four locations the FOC observed an SDD that was 1-5 days earlier than the iButton (e.g., the FOC SDD is one day earlier than the iButton SDD in Figure 3.4b and c). The RSCD observed by the FOC was biased low relative to the iButtons at four locations, where the iButtons recorded 3-9 more snow covered days than the FOC for the same observational period. At two locations the FOC observed 2-6 more snow covered days.

3.4.2 Comparing Observational Strategies: Fractional Snow-covered Area

The three observational strategies for capturing the evolution of fSCA through time agree closely on the overall shape and timing of snow duration at each of the three intensive plots (Figure 3.4d-f). All three methods consistently indicate that snow duration is longer at the intensive gap plot (Figure 3.4d) relative to the thinned and control plots (Figure 3.4e and f), and that snow disappears and then reappears in late April over some portion of the area at all three plots. Results from the iButtons are affected by their sparser spatial coverage: the iButtons underestimate snow coverage at the gap relative to the FOC and camera, dropping to 40% fSCA in late April and early May when the other sensors indicate 50-70% snow coverage. Since the iButtons agree closely with the cameras on point-scale snow presence, the difference is attributable to the sample density. With only 5 functioning iButtons at the gap, this translates to 2 out of 5 sensors indicating snow presence, whereas fSCA derived from the other instruments is based on more than 40 sample locations. However, fSCA derived from the finer spatial resolution FOC and camera also disagree at times; fSCA from the camera is lower than fSCA from the FOC during most of April at all three plots.

Visual comparison of the time series of fSCA with the camera images provides an independent check on the consistency of the different methods. During the early portion of the ablation season, in the middle two weeks of April, the FOC shows slightly higher fSCA by missing localized snow disappearance around trees (i.e., tree wells) at all three intensive plots. Note that this tendency toward higher fSCA due to the spatial coverage of the FOC is in the opposite direction of the point-scale tendency toward detection of early snow disappearance (i.e., underestimation of fSCA), which emphasizes the separate contribution of point-scale and plot-scale uncertainties. The dense spatial coverage of the camera captures, and possibly

overemphasizes, the subtle effect of snow disappearance gradually extending outward from tree trunks. Since the warmest tree trunks in the gap are likely located on the north side of the gap due to the heating by direct solar radiation, the north-facing camera may underestimate fSCA in the gap plot by sampling only that portion of the gap. Thus, the true plot-scale value likely lies in between the FOC and the camera.

3.4.3 Comparing Observational Strategies: Distributions of Snow Duration Metrics

The overall spatial variability in snow duration at each intensive plot is represented by the distributions of snow metrics (Figure 3.5a and b). Snow duration was longer at the gap plot relative to the control and thinned plots (also illustrated in the time series of fSCA in Figure 3.4d-f). However, the values of the metrics, and the quartiles and range of the distributions of metrics, extracted from each of the three observational strategies are different even at the same plots.

At the intensive gap plot, the median value for RSCD quantified by the FOC and the camera is the same, whereas the median RSCD observed by the iButtons is 10 days shorter (Figure 3.5a). As discussed in section 3.4.2, this key difference in the distribution of snow duration metrics at the plot-scale is related to sampling density and placement. With a sample size of 5 iButtons at the gap, median snow duration (as quantified by RSCD) is highly influenced by one iButton that was deployed next to a tree trunk and consequently observed very early snow disappearance. The maximum values (i.e., longest snow duration) of the distributions are within 1 day of each other for the FOC and iButtons, but the maximum derived from the camera is 4 days longer. The three methods conflict most in terms of quantifying the minimum snow duration, with the

camera showing the longest tail on the earlier end of the distribution, extending toward low snow duration values.

Data from the intensive thinned plot also illustrate disagreement between methods, particularly in median values. The iButtons observed the longest median snow duration, with a median RSCD value of 32 days, whereas the camera recorded the shortest, with a value of 22 days. The median FOC value is 28 days, which falls between the other two methods. The three methods agree most closely at the control plot; the median RSCD values are within one day for all instruments. However, similar to the comparison at the gap and thinned plots, the range of values recorded by the camera is larger than the ranges observed by the FOC and iButtons.

Comparisons of final SDD values recorded by the different instruments at the same forest treatments yield similar results as the comparisons of RSCD (Figure 3.5b). However, the SDD is approximately synchronous at the control and thinned plots due to late season snowfall, where snow accumulated on bare ground and then disappeared again the next day. The resulting distributions of SDD values at these plots are therefore much tighter. In contrast, the distribution of SDD for the gap plot is unaffected by the snowfall event since the snow cover was continuous over much of the plot both prior to and after the one-day event.

Another perspective for comparing these methods at the plot-scale is to consider how each instrument captured the difference in median snow duration between the three forest treatments. Results from the FOC and cameras indicate that median (mean) snow duration is 8-10 (8) days longer in the gap plot as compared with the control, and 14-20 (12-16) days longer in the gap as compared to the thinned plot; the iButtons detect a median (mean) difference of only 1 (1) day in RSCD between the gap and control plots. All three measurement types indicate that snow duration at the control and thinned plots is similar. The mean differences between the gap and

non-gap plots that were detected by the FOC and camera are statistically significant when tested via an analysis of variance (ANOVA) after sub-sampling to account for spatial dependence (see further details on spatial autocorrelation below, and see supplemental materials for details on statistical testing). In contrast, the RSCD values observed by the iButtons are statistically indistinguishable between all three plots. The comparison between the observational strategies at the intensive plots suggests that the methods characterize snow duration differently based on the method by which they detect snow presence, and their spatial resolution and placement.

3.4.4 Representing Forest Types: Replicated Experimental Plots at Bear Creek

Observational strategies aside, we further consider results from the additional plots at Bear Creek (as opposed to the intensive plots only), all of which were transected by the FOC (Figure 3.1b), to test the representativeness of a single set of intensive plots to characterize snow duration in a forest treatment (e.g., both the intensive gap plot and the additional gap plots). Within both natural and managed forests, canopy characteristics are spatially heterogeneous even in a single forest type. Thus, the representativeness of a given experimental plot is critical to extrapolating snow duration from one plot to a forest type present across the landscape.

Distributions of RSCD observed via the FOC at all plots (i.e., the intensive and additional plots subject to the same silvicultural treatment) compared with the intensive plots tend to have a larger overall range, but with median and interquartile range values within 3 days or less of each other for RSCD (Figure 3.5c). Boxplots of canopy closure distributions for all plots of the same treatment and the intensive plots only indicate that intensive plots are representative of their treatment groups, with small deviations from the overall distributions of canopy closure (Figure 3.5d). The difference in mean snow duration for all gap plots and non-gap plots is much greater

than within-treatment group variability and is statistically distinguishable (1-way ANOVA on plot means: $F = 11.3$, $\alpha = 0.05$, $p < 0.005$; Tukey Honestly Significant Difference (HSD): $p < 0.005$ for gap-control and gap-thinned). Mean snow duration in the control and thinned plots is not statistically distinguishable by treatment.

3.4.5 Representing Forest Types: Different Elevations and Years

At the Bear Creek site, results from replicated experimental plots indicate that sampling snow duration at one plot in each treatment group captures the overall relationship between gap and non-gap forest treatments. To assess the relationship between snow duration in different forest treatments at different elevations, we used snow presence data derived from grids of iButtons over two winters at the Bear Creek and Mount Gardner sites. The comparison includes the three intensive plots at Bear Creek and the higher elevation gap, thinned, and control plots at Mount Gardner. The inability of a small number of iButtons to detect a significant difference in plot-averaged snow duration between intensive plots at Bear Creek in WY 2011 highlights the challenge in robustly characterizing the distribution of snow duration from a sparse network of instruments. However, despite the low number of sensors at Bear Creek in WY 2011, the shape of the curve for the evolution of fSCA and the final snow disappearance are closely represented (Figure 3.4d-f). Furthermore, more working sensors at Bear Creek during WY 2012 (8-10 per plot), and at Mount Gardner during both water years (6-9 per plot) yielded slightly higher sample sizes and statistically distinguishable differences in some cases (see Table 3.7). We therefore present the comparison of fSCA at our two study sites over two years, with the caveats that these instruments grids do not provide full spatial coverage nor are they capturing substantial interannual variability in snow accumulation.

At both sites, the time series of snow accumulation and the evolution of fSCA were similar between the two years of data collection, but there are important differences between the different elevation sites (Figure 3.6). Final snow disappearance was 13-15 days later at the gap plots than in the non-gap plots at both Bear Creek and Mount Gardner. However, the relative timing of the onset of snow disappearance at different forest treatments, and the relative impact of mid-winter melt events on snow cover differed substantially. At Bear Creek, snow began to disappear from the gap plot before the control plot, but then lasted longer in the gap plot (Figure 3.6c and d). As a result, both plots reached 50% snow-covered area at approximately the same time and the snow that persisted in the gap plot was discontinuous (i.e., < 50% fSCA). In contrast, the beginning of ablation at the Mount Gardner gap plot is synchronous with or later than the onset of snow disappearance at the Mount Gardner control and thinned plots (Figure 3.6e and f). Thus, since fSCA depletion starts later at the gap relative to the other plots, snow cover at the Mount Gardner gap is still almost continuous when the control and thinned plots reach 50% snow-covered area.

The comparison of fSCA between Bear Creek and Mount Gardner additionally indicates that mid-winter melt events are enhanced at the control plots at both elevations, but that the difference between the control and the other forest treatments is amplified at lower elevations, where snow accumulation is lower overall. For example, during a mid-winter melt event in January 2012, the fSCA at the Bear Creek control plot drops from 100 to 0%, while the higher elevation Mount Gardner control plot drops only to 50% fSCA (Figure 3.6d and f).

3.4.6 Spatial Patterns of Snow Metrics & Autocorrelation

Snow duration varies spatially across each of the plots, and RSCD data across the FOC transects suggests that snow duration is influenced by canopy closure (Figure 3.7). Therefore, the spatial sampling density and positioning of the different instruments are likely to influence the distribution of snow duration values observed at the plot. Semi-variograms of RSCD from the 1-m FOC data show increasing variance with distance across the experimental plots, indicating that snow duration is spatially autocorrelated within the treatment types (Figure 3.7c). Maximum variance (i.e., the sill on the semi-variogram) in snow duration occurs at the control and thinned plots at a distance of approximately 4-8 m (i.e., the range on the semi-variogram). Reaching the maximum variance suggests that all sample locations separated by at least that much distance are subject to equal random variability, whereas sample locations that are closer will reflect the same local influences. Variance continuously increases across the gap plots, up to the maximum lag distance of 20 m, which is indicative of a plot-scale spatial trend related to the gap size in addition to local autocorrelation effects (see supplemental material).

To determine an optimal minimum spatial sampling resolution we extended the Monte Carlo approach of Lundquist and Lott [2008], who estimated the number of samples necessary to approximate the true mean and variance of a distribution. The previous investigation drew from a lognormal distribution because the distribution of pre-melt SWE has been commonly approximated as lognormal (e.g., [*Essery and Pomeroy*, 2004a]). However, our observations of snow duration at these plots are not distributed lognormally, which is illustrated by the symmetrical positioning of the 25^{th} and 75^{th} percentiles around the median and is particularly evident in the FOC data (Figure 3.5). We therefore built empirical 95% confidence limits for distance to the true value of mean RSCD by repeatedly drawing a given number of samples

without replacement from the observed distribution (as derived from the FOC) for each treatment type. We tested the effect of randomly sampling from the distribution (i.e., randomly taking 4 samples from a treatment group, regardless of location) versus sampling at a fixed spacing (i.e., taking 4 samples spaced 10 m apart to evenly cover the entire 40 m transect across the experimental plot).

We found that 10 sensors per forest treatment are needed to minimize the range of the 95% confidence interval to ± 5 days around the mean RSCD in the case of random sampling, but that the number of samples can be reduced (3-4 sensors) to achieve the same confidence interval in the fixed spacing approach (Figure 3.8). By spacing sample locations evenly, the sampling design minimizes the effect of spatial autocorrelation and therefore is more effective than more randomly-distributed samples in representing the mean snow duration. For all plots, an even sample spacing of 10 m (i.e., 4 samples per 40 m transect) characterizes the true mean to within ± 5 days, whereas an even spacing of 6 m (i.e., 7 samples) brings the confidence interval to ± 3 days.

To extend our analysis to representing variability in all directions rather than along a linear transect, we repeated the experiment by sampling from the camera images using a random and a fixed-grid spacing approach (not shown). The results indicated that a grid of 6-8 sample points is sufficient to represent the field of view of the camera, but the results were sensitive to the treatment type, and to the spatial orientation of the grid spacing. For example, as previously discussed, the camera deployed in the intensive gap plot includes in its view a portion of the gap and a portion of south-facing trees, which we would expect to heat up due to direct sunlight and thus enhance local melting [*Pomeroy et al.*, 2009]. Configuring a 3 × 2 sampling grid (i.e., 6 samples) to have 3 samples across the maximum gradient (e.g. from gap to surrounding forest, or

vertically in the photo in Figure 3.1b) versus across the minimum gradient (e.g., through the middle of the gap, not entering the forest) strongly influenced the mean. We therefore recommend considering the direction of maximum gradient from canopy data and plot orientation (e.g., location, aspect), in addition to the extent of process variability, and orienting grids of ground sensors and cameras to sample the maximum range of variability.

3.5 Discussion

3.5.1 Applications

The two-week difference in final snow disappearance between the gap plot and non-gap plots observed in the Cedar River watershed is on par with the greatest differences observed worldwide [*Lundquist et al.*, 2013]. Numerous investigations across the world have noted a difference of more than one week in final snow disappearance between forested and open sites, but the direction of the difference varies, with snow persisting longer under the forest in Alberta, Canada [*Burles and Boon*, 2011], Northwest Russia [*Gelfan et al.*, 2004], Japan [*Rutter et al.*, 2009], and Finland [*Koivusalo and Kokkonen*, 2002], and snow persisting over a week longer in the open in southwestern Oregon [*Storck et al.*, 2002].

The observed differences in how forest cover influences both the magnitude and direction of snow duration highlights the necessity of observations to quantify snow cover in both forested and open areas. Snow cover observed in open areas (i.e., the viewable gap fraction (VGF)) via remote sensing is commonly used to extrapolate snow cover under the forest canopy, but relies on the critical assumption that fSCA in the open represents fSCA under the forest canopy [*Durand et al.*, 2008; *Liu et al.*, 2008; *Xin et al.*, 2012]. Applying this assumption to the Cedar River watershed data presented here, snow-covered area in the forest would be over-estimated for at least two weeks based on the difference between final snow disappearance in the gap and control plots. Field campaigns to quantify the evolution of fSCA in representative forest plots could be used locally to improve methods of extrapolating from the visible snow cover in the open, to the hidden snow cover under the forest.

Improving model representation of snow processes in forested watersheds is another key application of quantifying spatially distributed snow duration. Previous investigations have

demonstrated shortcomings in accurately modeling snow accumulation and ablation within forests (e.g., [*Rutter et al.*, 2009; *Du et al.*, 2013; *Martin et al.*, 2013]). Many recent steps toward improving model representation of snow processes in forested watersheds focus on explictly characterizing the structure and density of the forest. These efforts include representing forest gaps [*Ellis et al.*, 2013], modeling time-varying canopy transmissivity [*Musselman et al.*, 2012, 2013], and estimating spatially-distributed forest metrics from lidar [*Varhola et al.*, 2012; *Varhola and Coops*, 2013]. Key challenges remain in learning which forest metrics to measure and implement in a modeling framework, because these metrics vary widely in resolution, methodology, and interpretation [*Fiala et al.*, 2006; *Korhonen et al.*, 2006; *Pueschel et al.*, 2012]. For example, at these study sites, mean canopy cover values derived from lidar (Table 3.1) are quite different than mean canopy closure values along the FOC transet (Figure 3.5d), which is to be expected based on different view angles. Whereas canopy closure relates well to the below canopy light environment, canopy cover is better suited to estimate interception through canopies [*Jennings et al.*, 1999]. Further work is needed to determine which forest metrics would best support model representation of the observed impacts of forest type on snow duration.

Since the observational strategies presented here were tested in a study location in which forest cover plays a key role in snow duration, we assert that the guidelines discussed below are a robust starting point for planning a field campaign at any site in which forest is a key influence on snow duration. However, in locations in which snow duration variability may be dominated by wind, aspect, or other local influences, increased sampling density is advised.

3.5.2 Sampling Snow Duration in Forest Plots: Representativeness

To use distributed ground observations to characterize snow duration in diverse forest treatments, sampling density at the plot-scale must be sufficient to represent the plot, and the number and locations of experimental plots must be sufficient to represent the forest type present across the landscape. Clark et al. [2011] previously found that a resolution of 5 m is necessary to resolve snow heterogeneity at the hillslope scale, where the dominant influences are vegetation, avalanching, and wind. At our protected, flat study sites, the pattern of spatial autocorrelation indicates that the 1 m sampling density of the FOC is subject to spatial redundancy. To maximize sampling efficiency, sample locations should be at least 4 m apart (i.e., the lag distance to the plateau of variance at the control plot (Figure 3.7c)) and the results from the Monte Carlo experiments suggest an optimal sample spacing of 6 m (Figure 3.8). Since the point-scale comparison of the iButtons to the camera indicate similar detection of snow presence, and grids of iButtons successfully detected a plot-scale difference in other cases, we conclude that the failure of the iButtons to detect a significant plot-scale difference between the gap and non-gap plots in WY 2011was due to the small population of point samples. Thus, plot-scale differences in snow duration (and the evolution of fSCA through the ablation season) could be accurately represented by increasing the sampling density of iButtons (or an equivalent sensor).

Detection of snow presence/absence by the FOC differs from the other two instruments due to its deployment position and support. The positioning of the FOC on top of the ground, rather than under the ground as in the case of an iButton, results in a larger diurnal temperature range even when the cameras indicate that the section of FOC is snow-covered. Additionally, the extent of the FOC observation is integrated over 1 m, which also contributes to differing results between instruments at the same sample locations.

The spatial configuration of each instrument, along with the sampling density, further contributes to the representativeness of each method. Each instrument was deployed in a typical configuration (e.g., the FOC as a linear transect), although each also has a varying degree of flexibility in spatial placement. Whereas the high sampling density of the FOC and camera exceed the optimal sample resolution indicated by the Monte Carlo experiments, both instruments have the potential to misrepresent plot-scale snow duration depending on the location and direction of the FOC transect and the camera. In contrast, grids of iButtons can be deployed to cover the entire plot, but spacing of the sensors determines representativeness.

In concept, the FOC and iButtons provide an evenly-distributed sample of snow duration across the entire plot, though in practice, sensor failure among the iButtons could result in spatial bias. We were fortunate that the five surviving iButtons in the gap during WY 2011 were evenly distributed across the plot, with one sensor in the middle of the gap, two in the gap near the edge, and two in the adjacent forest. Even so, high variability of canopy characteristics and ground conditions result in spatially heterogeneous snow duration that even a fully-distributed network will likely miss. For example, the placement of a single iButton very close to a tree in the intensive gap plot resulted in observation of a low snow duration location that was missed by the FOC transect (Figure 3.5a and b). In addition, variability is likely a function of direction across the plot, particularly in the gap and thinned plots, where gaps and small openings are not evenly distributed (Figure 3.7b). A sufficiently dense grid of ground sensors deployed to characterize anisotropic variance may therefore be preferred over a linear transect.

The higher resolution camera data captured observations of localized processes that the ground temperature instruments missed, such as gradual melting extending outward around trees, but the cameras are subject to bias due to positioning and perspective. Although the spacing of

camera samples is small, the extent is limited to the field of view, and an extent that is below the scale of process variability can result in a trend in the data [*Blöschl*, 1999]. For this reason, the extent and the direction of the camera are particularly influential where there is a clear spatial trend to snow duration. For example, at a gap plot, snow duration observations will differ between a camera facing the south side of a gap versus the north side; Golding and Swanson [1986] found 40-50% lower SWE on the northern side than the southern side of gaps. Similarly, snow duration observations at the thinned plot will depend on whether the camera is facing a section with a more open canopy versus a section with more closed canopy. This limitation could be overcome by representative placement, and particularly by deploying multiple cameras to sample across the entire plot. Consideration of the azimuth of the camera (i.e., facing North) during installation would aid in minimizing bias due to directional effects on snow duration (e.g., shading from sunlight) and could contribute to improved image processing (e.g., minimizing shadows).

The perspective of the camera is also unique compared to the ground sensors. The FOC and iButtons detect snow presence from below, sensing only temperature variations, which help to infer whether snow is on top of the sensor or not. In contrast, the camera detects snow from above, and the quantification of snow cover is influenced by the oblique view of the heterogeneous ground surface. When snow melts, logs on the ground that were previously covered are revealed, which leads to detection of reduced fSCA even when snow may still cover the ground around, behind, or under portions of the log (e.g., Figure 3.3, see log across the middle of the field of view and the impact on RSCD metrics).

3.5.3 Representing Snow Duration in a Forested Watershed: How Many Plots?

The relationship between snow duration in the gap and non-gap forest treatments was clearly defined by one set of plots at Bear Creek and Mount Gardner, but more variable forest types may require additional plots. In particular, the lack of a detectable plot-scale treatment response between the control and thinned plots indicates that the effect of forest thinning (30% basal area removal) on snow duration is either too small to be detected, or there is no difference between the control and thinned plots despite the reduced stem density. The high spatial density of samples and numerous replicated plots support a process-based explanation: snow duration is similar at these particular control and thinned plots.

For a hypothetical case in which thinning produces a sufficiently sparse canopy to have a detectable treatment effect on snow duration, more samples are advisable simply to account for increased canopy heterogeneity. Snow duration at the intensive thinned plot shows the largest deviation from the distribution of snow duration for the thinned treatment group as a whole, including the intensive and additional plots (Figure 3.5c). Whereas the gap plots have a wide total range of canopy closure (Figure 3.5d), the thinned plots have high variation in short distances, with small gaps and openings that are likely to contribute to variability in snow accumulation and ablation (Figure 3.7a and b). Woods et al. [2006] previously found that snow accumulation in a lodgepole pine forest in Montana was three times more variable in a plot thinned using a shelterwood method (i.e., clusters of trees remain) than a plot that was evenly thinned. Thus, although snow duration was indistinguishable between the control and thinned plots in this study, results at other thinned plots may vary widely depending on silvicultural methods. Further consideration to replicate sampling plots for heterogeneous forest types should be extended to other types of diverse canopy structures, including old growth stands and forests

subject to multiple episodes of thinning through time, due to proven difficulty in predicting snow duration in these forest types (e.g., [*Du et al.*, 2013]).

Although we observed consistency in the relationship between forest treatments at different elevations and over two years, sampling representative forest plots at different elevations is advised in some applications. For our study area, the two sites have different snow duration characteristics due to climate. The lower elevation Bear Creek site experiences intermittent snow cover, where multiple episodes of snow appearance and disappearance occur, whereas continuous snow cover is more common at the higher elevation Mount Gardner site. For applications in which the intermittency may be more important, such as quantifying land surface albedo or determining light conditions for undergrowth, sampling in both of these snow regimes would be critical.

Sampling across multiple years is also important. We found similar relationships between treatment groups through our two years of data collection, but both years had similarly high snowfall. Weather conditions will influence the offset in snow duration between plots, and the variability within a single plot. Snow duration at the gap plots was the most variable of the three treatment groups, with a standard deviation typically 1 to 3 times higher than the nearby control plot. During WY 2011, however, the standard deviation of snow duration (the number of snow-covered days since peak snow depth) was within 2 days at all three higher elevation plots at Mount Gardner. The substantial spring snowfall evened out snow duration variability by augmenting locations where snowpack was thin. Extended snow duration in these locations that otherwise would have disappeared earlier resulted in lower than typical variability in the gap plot.

3.5.4 Practical Considerations

The deployment of multiple instruments resulted in field-tested insight into the feasibility of these observational strategies in environments with limited access, wet conditions, and varied forest cover. The high spatial resolution snow observations from the FOC are invaluable for dense, regularly-spaced observations of snow presence. However, utilization of the FOC posed some challenges. In particular, deployment was physically difficult and required a strong field team to carry a heavy spool of cable over 1 km of uneven, forested terrain (See Figure 8 in [*Lutz et al.*, 2012]). Despite their best efforts, the resulting placement of the cable included short stretches that were suspended over a hollow or draped over large woody debris, where the FOC did not represent ground conditions (see supplemental material). The high expense of purchasing the FOC equipment was avoided by using loaned equipment from the Center for Transformative Environmental Monitoring Programs (CTEMPS, see acknowledgements). However, utilizing the FOC required substantial in-person intervention to achieve semi-continuous operation of the instrument; for example, during our 70-day deployment during WY 2011, we made weekly or more-frequent trips to our study location after snowfall events to replace batteries and clear snow off the solar panel. Despite this effort, approximately 1/3 of the time steps were missing, frequently following a diurnal cycle in which data were collected only during daylight hours when solar power was available. The investment of time and money to deploy and operate the FOC successfully yielded dense ground temperature data over 800 m, covering multiple experimental plots.

In contrast, both iButtons and time-lapse cameras are easy to deploy and relatively inexpensive, but they are also subject to problems with data continuity. In most cases, these issues could be resolved by learning from experience, with better waterproofing of the sensors

and by using improved cameras that last longer on a single set of batteries. In addition, the operational independence of the iButtons and cameras poses advantages and disadvantages. One key advantage of stand-alone instruments is that if one fails, data from only one sampling location is lost. Conversely, the networked nature of a continuous cable is such that a power outage or damage to one part of the cable results in data gaps across the entire FOC. An additional consideration for using stand-alone instruments in analyses is that particular care must be taken to complete accurate geolocation and record-keeping in the field in order to confidently compare results between years and to other spatially distributed datasets. Table 3.2 in the supplemental material further summarizes the advantages and disadvantages of each method, and provides details about instruments and recommendations for future deployments.

3.6 Conclusion

Ground observations of snow coverage in diverse forest types are required for numerous applications across disciplines, because operational snow networks are located in clearings, and remote sensing techniques have limited accuracy for detecting snow on the ground in forests. Furthermore, manual snow courses are typically too infrequent to characterize variability in snow duration. However, limitations on time and money for field campaigns are a ubiquitous challenge. By comparing the ability of multiple instruments to detect snow presence, and investigating optimal sample spacing to represent heterogeneous snow duration at the scale of a grid element, we address practical considerations for optimal field campaigns.

Our results support the deployment of inexpensive remote instruments such as time-lapse cameras and self-recording ground temperature sensors. Based on Monte Carlo experiments drawing from the high spatial resolution FOC ground temperature data and camera data, the optimal sampling spacing for stand-along ground temperature sensors is 6-10 m in second-growth forest and partially open forest plots (i.e., with gaps). Experience with the cameras and analysis of the Monte Carlo experiments suggest that a minimum of two cameras, facing different directions, are needed to address anisotropic variance in snow duration.

More dense sampling and more replicated plots may be needed in diverse canopy and ground conditions, such as those found in old growth stands and 2nd growth forest subject to multiple thinning events. Sampling multiple plots at different elevation bands, and particularly straddling the intermittent and continuous snow zones, is advised for applications in which the intermittency of snow cover is critical.

3.7 Acknowledgements

Primary support for this project was provided by the National Science Foundation (NSF), CBET-0931780. Lidar data collection and processing was provided by the National Center for Airborne Laser Mapping (http://ncalm.cive.uh.edu/) via a seed grant to S. Dickerson-Lange, and Van Kane generously provided additional processing and analysis. M. Raleigh was supported by a postdoctoral fellowship in the Advanced Study Program at the National Center for Atmospheric Research (sponsored by the NSF). We thank John Selker and Scott Tyler for providing the fiber-optic measurement equipment, cable, and considerable technical advice, and the Center for Transformative Environmental Monitoring Programs (http://www.ctemps.org) for supplying the distributed temperature sensing system. We are grateful to Seattle Public Utilities for allowing watershed access and providing equipment and to Michelle Ma for photographs of the Mount Gardner site. We especially thank the many people who assisted with instrument deployment and field data collection including Jenna Forsyth, Nic Wayand, Courtney Moore, Shara Feld, Sam Barr, Mathieu Marineau, Chris Lyles, Steve Burges, and many others. The manuscript benefited from critical review by Associate Editor Noah Molotch, three anonymous reviewers, and the UW Mountain Hydrology Research Group. The data described herein are publically available via the University of Washington (http://depts.washington.edu/mtnhydr/data/cedar.shtml; ground temperature and snow duration data) and NSF Open Topography (http://www.opentopography.org/; Lidar data).

3.8 Tables

Table 3.1 Study sites and plots therein, with snow duration data collected at each location indicated by water year. Mean and standard deviation (SD) of canopy cover over each plot or groups of plots were computed from a gridded ratio of the number of airborne lidar returns from above 2 m height to the total number of returns for each 5 m pixel.

Site	Elev. (m)	Plot(s)	Snow Presence Data					
			Fiber Optic Cable		iButtons		Time Lapse Camera	
			2011	2012	2011	2012	2011	2012
Bear Creek	640	1 intensive control plot	x		x	x	x	
		4 additional control plots	x					
		1 intensive thinned plot	x		x	x	x	
		4 additional thinned plots	x					
		1 intensive gap plot	x		x	x	x	
		4 additional gap plots	x					
Mount Gardner	890	1 control plot			x	x		
		1 thin plot			x	x		
		1 gap plot (snotel site)			x	x		

3.9 Figures

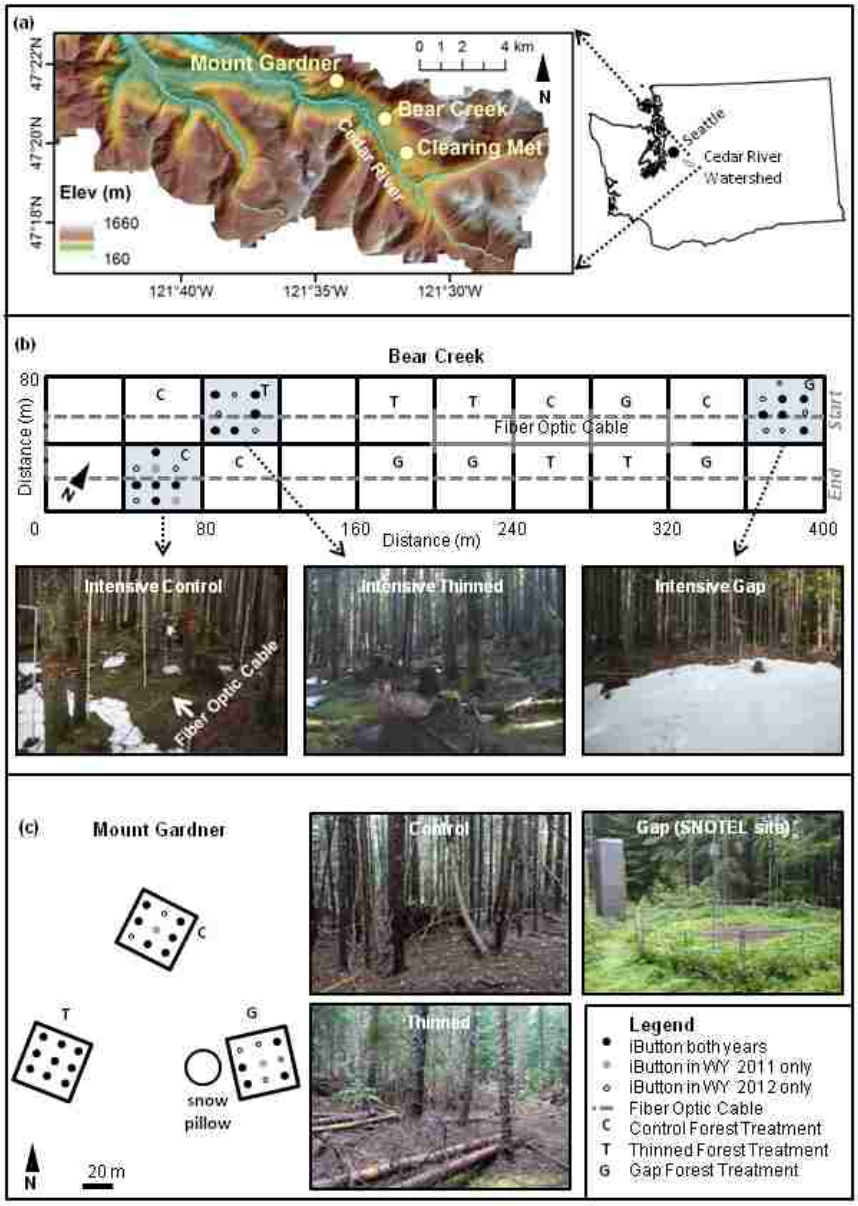

Figure 3.1 a) Hillshade map of the upper Cedar River Municipal Watershed, with study sites indicated, and outline of Washington State (USA) showing location of the watershed. b) Layout of Bear Creek site, showing the path of the fiber-optic cable transect across 20 experimental plots with the start (0 m) and end (800 m) points of data collection indicated, (the 40 m turn-around on the western side of the site was excluded from analysis); and the locations of iButtons (dots) at the three intensive plots. Synchronous time-lapse photos of the three intensive plots (shaded on the map) are shown for 4 May 2011, near the end of the snowmelt period. c) Layout of Mount Gardner site, and photos of the three higher elevation plots taken in the summer.

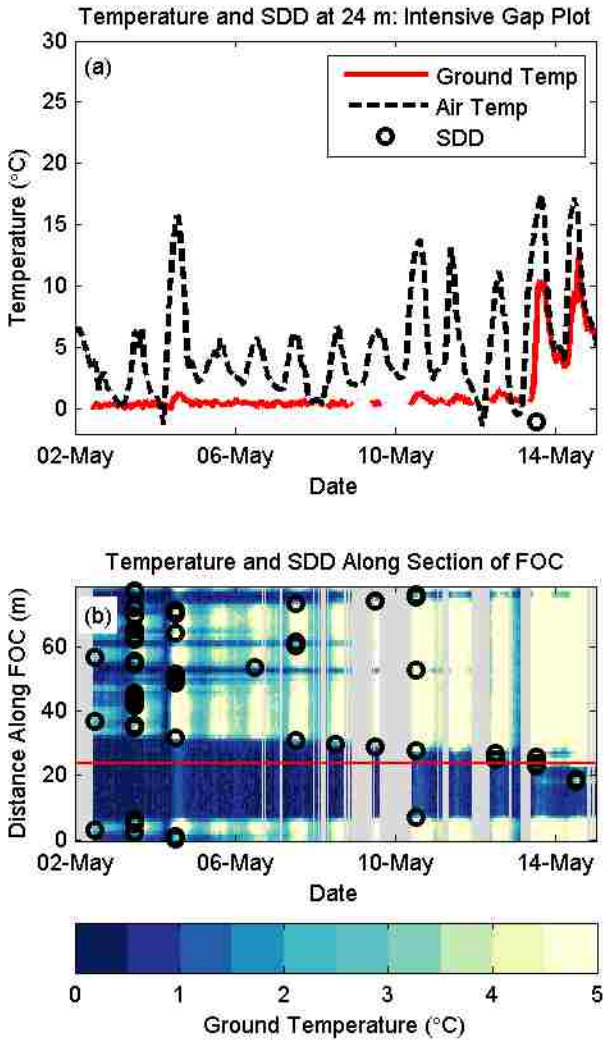

Figure 3.2 a) Thirty-minute ground temperature from 2 May through 15 May 2011 measured at 24 m on the fiber-optic cable (FOC), which is near the middle of the intensive gap plot. Hourly air temperature from the nearby Clearing Meteorological Station is shown for comparison. The snow disappearance date (SDD) is indicated by a black circle for 13 May, when the diurnal variation in ground temperature indicates that the location became snow free. b) Ground temperature for same time period along an 80 m section of the FOC (combining 80 time series of data like the one shown in (a)), transecting a gap plot (0-40 m distance) and a control plot (40-80 m distance). Note that the temperature color bar is truncated to show detail within 5 °C above the melting point. The SDD at every 1 m is derived from the temperature record and is indicated by a black circle. Vertical gray stripes are periods of missing data. Red line indicates location of the ground temperature time series shown in (a).

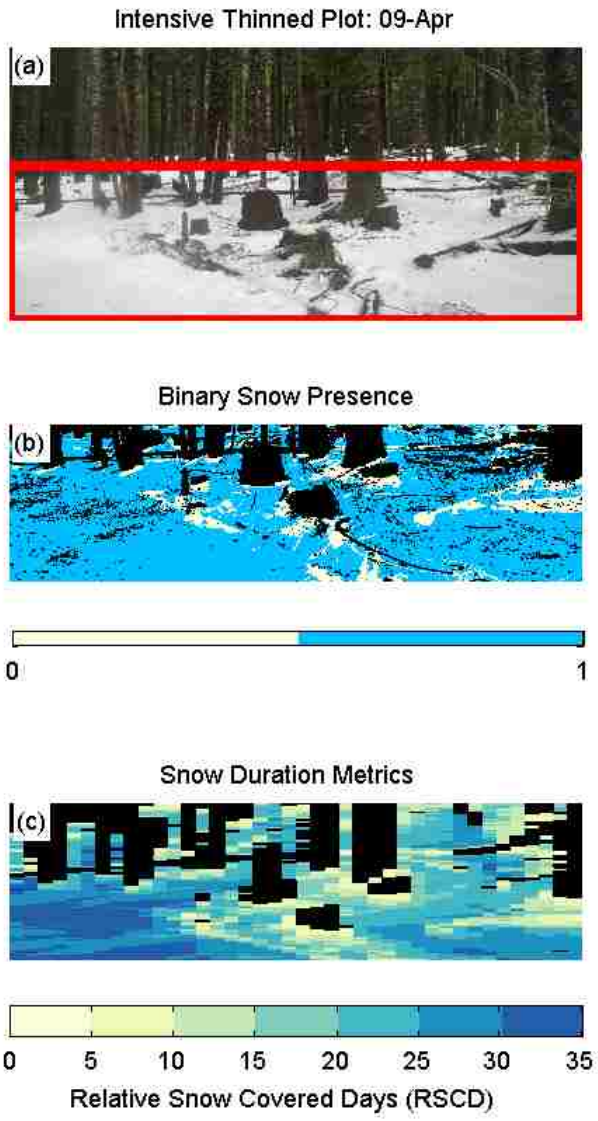

Figure 3.3 a) Time-lapse photo of the intensive thinned plot on 9 April 2011, with analysis area indicated by the red box. b) Photo converted to binary snow presence (blue) or absence (yellow). c) Relative snow-covered days (RSCD) since 17 March 2011, determined from snow presence in aggregated regions of equal ground area. Note that the vertical dimensions of (b) and (c) vary due to the pixel aggregation method, and black areas in (b) and (c) were excluded from analysis.

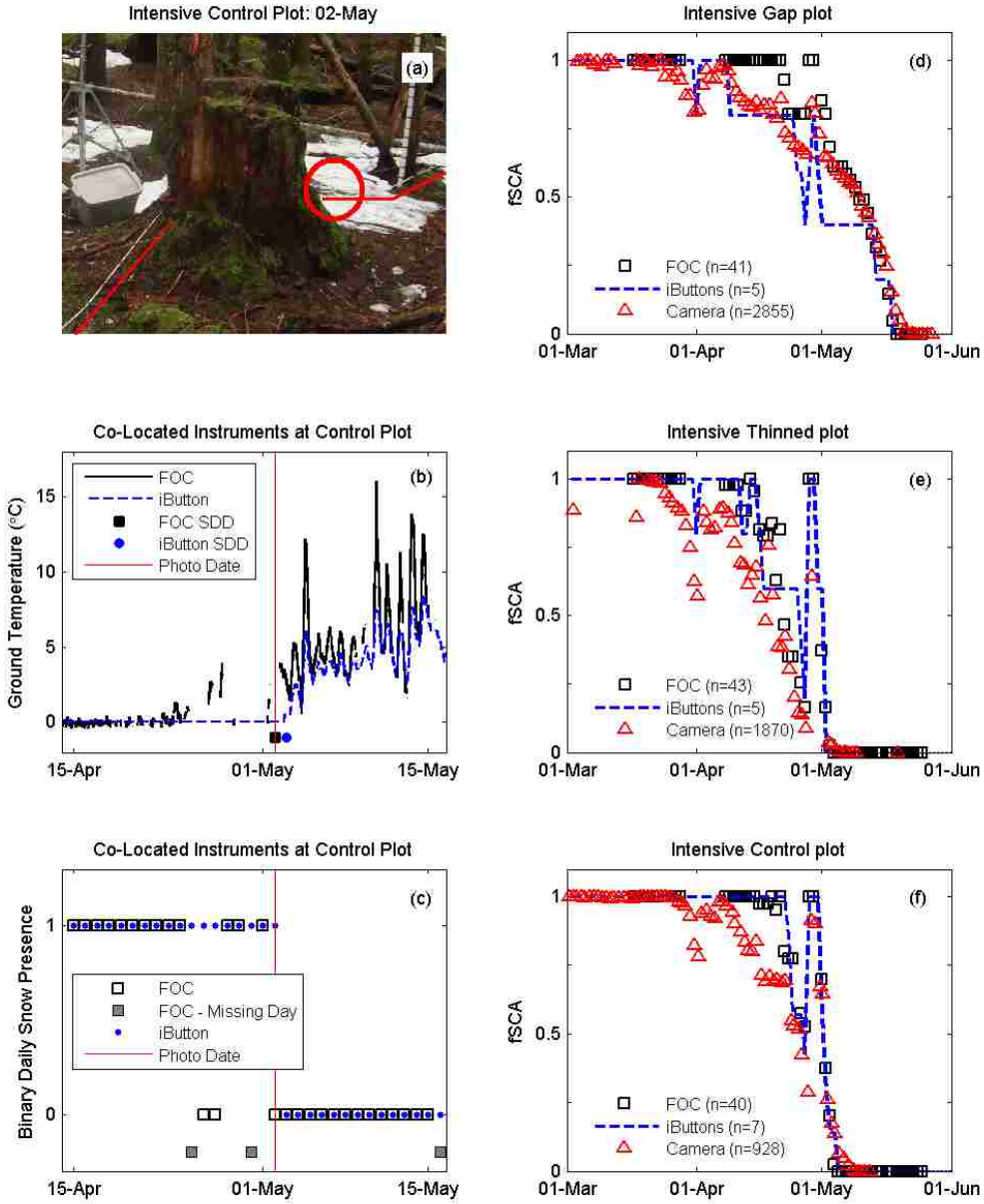

Figure 3.4 Comparison of instruments at the point-scale (a-c) and at the plot-scale (d-f). (a) Photo of a portion of the intensive control plot on 2 May 2011, with the location of the fiber optic cable (FOC) indicated by red lines, and the location of an iButton indicated by a red circle. (b) Comparison of one month of ground temperature data observed by the co-located section of FOC and iButton shown in (a), and (c) snow presence derived from both instruments (date of photo shown in (a) is indicated by a vertical red line in (b) and (c)). Data from all of the point locations measured from a fiber optic cable (FOC) transect, a grid of iButtons, and a single time-lapse camera in each 40 × 40 m plot are combined to compute plot-scale fractional snow-covered area (fSCA) through WY 2011 at the (d) intensive gap plot, (e) intensive thinned plot, and (f) intensive control plot at Bear Creek. The number of sample points used in the computation of fSCA for each plot and method is shown in each legend.

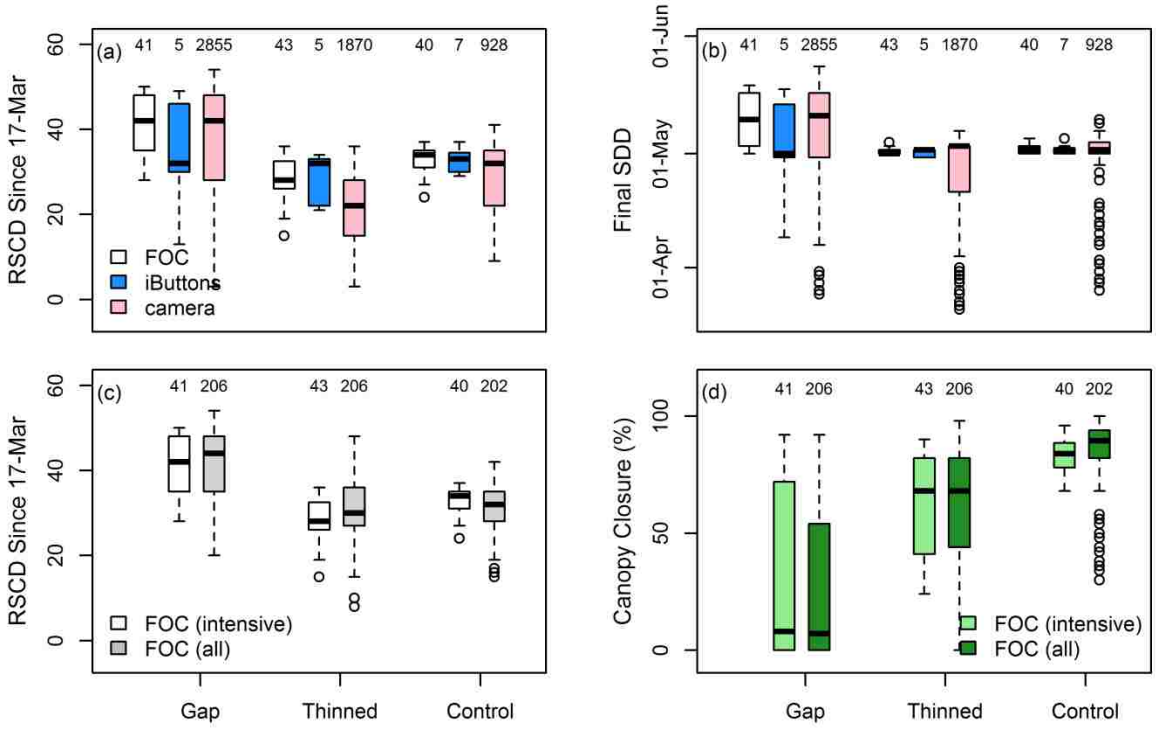

Figure 3.5 a) Boxplots showing distributions of the relative number of snow-covered days (RSCD) since 17 March 2011, calculated from (left to right for each forest treatment): the 40 m fiber-optic cable (FOC) transect, the iButton grid, and the time-lapse camera in each intensive plot. The median of each distribution is indicated by the heavy line; boxes extend to the 25th and 75th percentiles, whiskers to remaining data points within 1.5x the interquartile range, and dots to outliers. b) Distributions of WY 2011 snow disappearance dates (SDD), with groupings as in (a). c) Distributions of RSCD, calculated from the 40 m FOC transect that runs through each intensive plot (also shown in (a)) and all plots transected by 800 m of FOC, including all five plots (1 intensive + 4 additional) in each treatment group. d) Distributions of 5 m canopy closure values along the FOC with groupings as in (c). Numbers above boxes are the number of data points represented by each boxplot.

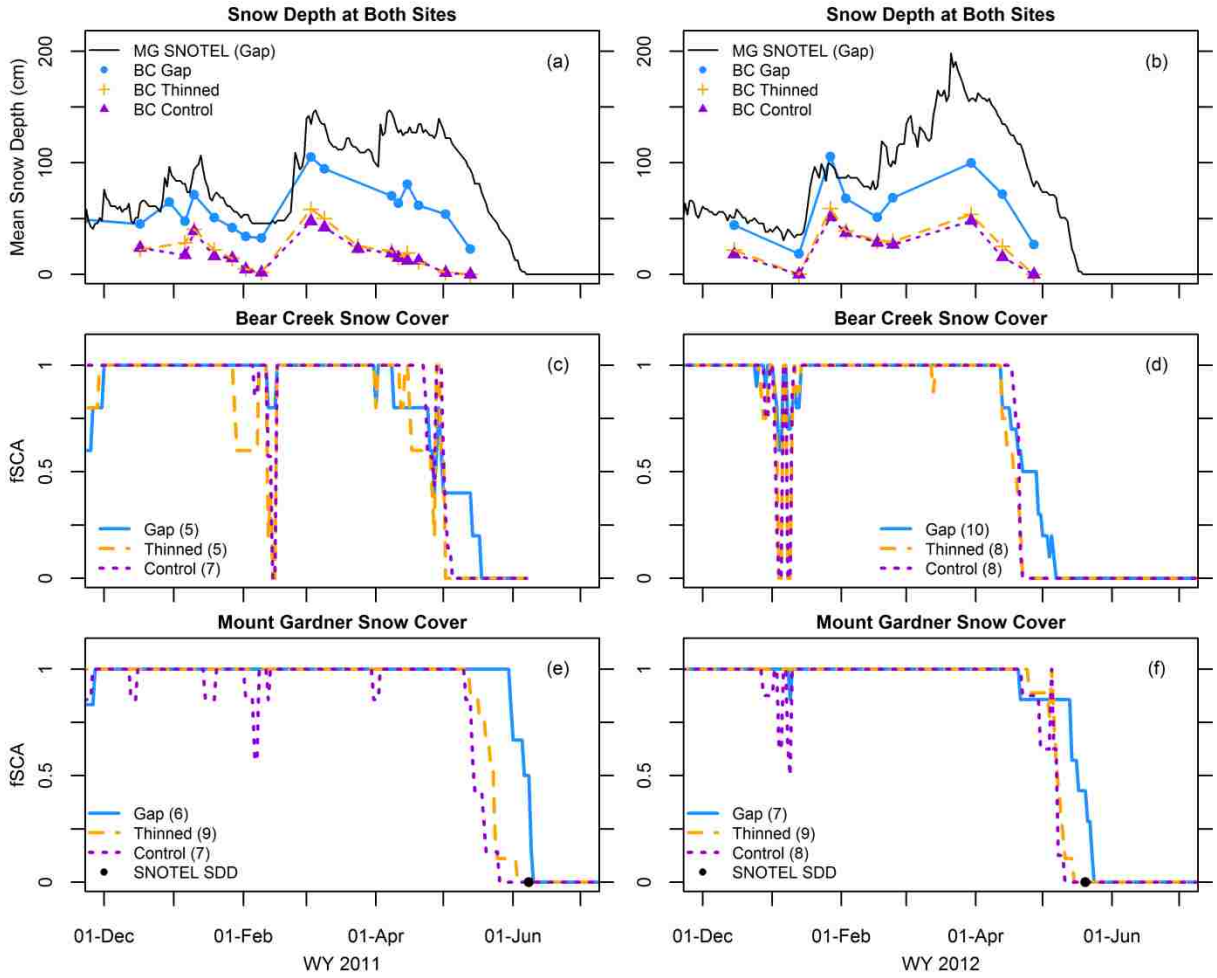

Figure 3.6 Mean snow depth at Bear Creek (BC) and Mount Gardner (MG) (a-b) and fractional snow-covered area (fSCA), calculated as the fraction of iButtons at each plot that indicate snow presence, through time at Bear Creek ((c) and (d)) and Mount Gardner ((e) and (f)) for WY 2011 and 2012. The number of instruments included in the calculation of fSCA is noted in parenthesis. The SDD recorded by the snow pillow at the Mount Gardner SNOTEL (co-located with the Mount Gardner gap plot) is shown in (e) and (f) for comparison. See Table 3.4 for exact snow disappearance dates (fSCA = 0 when maximum SDD is reached).

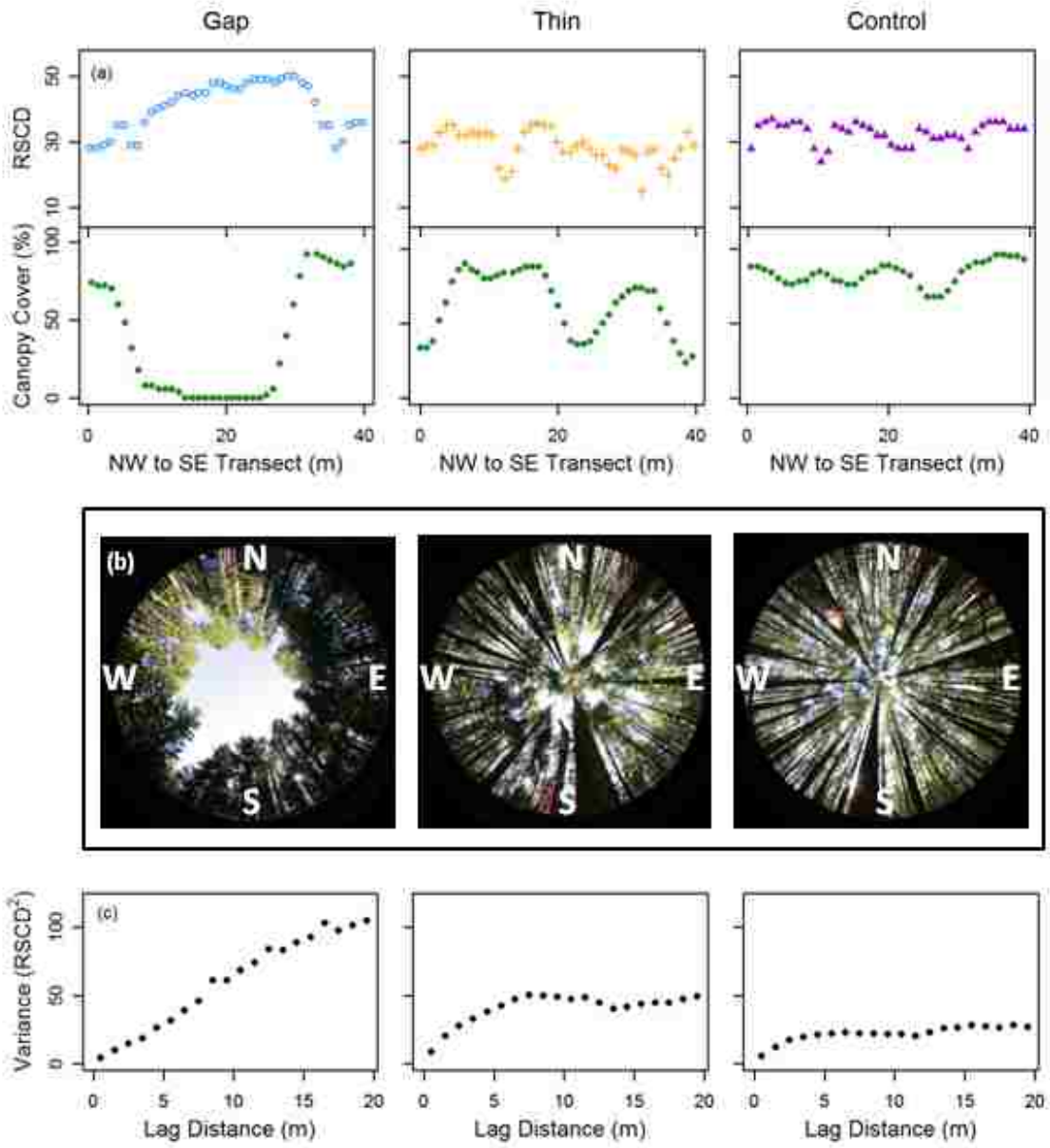

Figure 3.7 a) Relative number of snow-covered days (RSCD) since 17 March 2011 recorded by the FOC transect across the three intensive plots, and percent canopy closure. All transects are approximately NW to SE. b) Hemispherical photos from the center of each plot. c) Semi-variograms of RSCD for all plots transected by the FOC (including the intensive and additional plots). Note that lag distance is the distance separating each pair of samples, rather than a linear distance along the FOC.

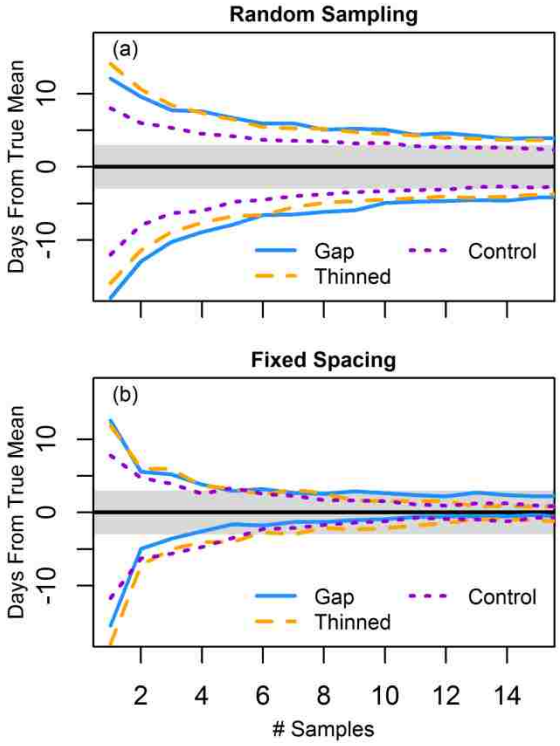

Figure 3.8 Results from Monte Carlo experiments for RSCD from WY 2011 snow presence data at Bear Creek. a) A given number of samples were randomly drawn without replacement 1000 times from the distribution of FOC data for each forest treatment (including intensive and additional plots), and the results were used to build empirical 95% confidence limits around the true mean. Gray shading indicates ± 3 days around the true mean. b) Same approach as in (a), but the starting sample location was chosen at random, but then additional samples were drawn at a constant spacing from the same plot.

3.10 Supporting Information

3.10.1 Introduction

The supporting information provides additional details related to data collection and analyses of the snow duration data presented in the main text. In particular, we address practical considerations of instruments used to detect snow presence, operation of the fiber optic cable (FOC) and subsequent data processing, additional snow duration metrics, statistical hypothesis testing, and the spatial autocorrelation of the data.

3.10.2 Deploying Stand-Alone Remote Instruments

Each instrument has its own unique set of advantages and disadvantages. In addition to the comparison of observational effectiveness described in the text, we have found that particular instruments are more or less rugged in design. A synopsis of key observations, and details on manufacturers and current pricing are presented in Table 3.2. Protection from water seepage into the instrument and longevity of the power source are the two critical operational issues for both the iButtons and the cameras. Our experience with these instruments in the field has also led to the development of sampling protocols, below. Note that the Cedar River watershed is subject to a maritime climate, with very wet conditions common during the non-summer months and relatively warm winter temperatures; thus, our recommendations are based on experience in this environment, and may be less applicable in drier or colder climates.

3.10.2.1 Self-recording Ground Temperature Sensors

We have seen numerous iButton failures from battery shorting due to water. Although some co-authors of this paper have successfully deployed iButtons wrapped in Glad Press ‘N Seal self-sealing plastic in somewhat drier climates (e.g., the Sierra Nevada of California, the Front Range

of Colorado), we find that the maritime climate is too wet to ensure continuous operation. We therefore recommend using temperature sensors for which waterproof shells are a standard component (e.g., Onset Hobo Pendants) or purchasing them as an accessory (e.g., iButton Capsule). Encapsulating each instrument in a water balloon before deployment is an inexpensive idea that we have recently encountered but we do not have the field experience to comment on this strategy. We find that battery longevity of the iButtons is generally good, and that storing hourly data for 10-11 months is comfortably accommodated provided that care is taken with programming (e.g., disable roll-over).

In addition to choosing a rugged instrument, we suggest the following deployment protocols:

- Validate iButton accuracy prior to and after deployment by measuring sub-hourly temperature in an ice bath (stirring frequently to ensure well-mixed water), and air temperature (in a location not subject to temperature gradients or sudden changes in temperature). Check both the absolute values observed by each instrument compared to the expected values (e.g., 0 °C) and the resolution of the instrument (e.g., ±0.5 °C), as well as the relative performance of each instrument compared to the standard deviation of the population. Instruments with suspect performance should be noted and re-tested, either to determine whether to deploy (prior to a field season) or to flag the data as possibly suspect (subsequent to field deployment).
- Take care with programming to ensure the rollover option (i.e., over-writing data when storage becomes full) is disabled, and that the sampling interval is consistent with the data storage capacity and length of deployment. For example, an 8-bit iButton thermochron measuring to a resolution of 0.5 °C will store approximately 11 months of hourly temperature data, whereas an 8-bit iButton hygrochron will store only 5.5 months of hourly temperature and relative humidity data. We do not recommend hygrochrons for detecting snow presence, as snow presence can be inferred from temperature alone and because soil saturation conditions can damage the humidity sensor.
- Record the ID number of field number of each instrument and its precise location during deployment, and check again during retrieval that the deployment map matches the instruments retrieved in the field. Once the iButton has been retrieved there is no way to reconstruct where it was deployed.
- In our limited-access location in the Cedar River Watershed, we used the same positioning stakes every year. We suggest pre-determining a consistent spatial

deployment (distance and azimuth) relative to georeferenced locations, e.g., 20 cm north of the position stake, for multi-year deployments to allow for comparison to high resolution spatial data such as lidar.

- In a public access location where marking the locations may invite curiosity, the position of each instruments needs to be recorded (e.g., via GPS) for retrieval and for analysis. A metal washer taped to the iButton fob is helpful when using a metal detector to aid instrument retrieval. For this method, we recommend first scanning the target installation area with a metal detector to ensure that there are no other metallic objects in the soil, as these will complicate identification of the sensor's location upon retrieval.

3.10.2.2 Time-Lapse Cameras

Battery longevity and memory capacity were the most persistent issues with our time-lapse cameras. In WY 2011 and 2012 we deployed a custom combination of an off-the-shelf digital camera wired to a time-lapse mechanism, all powered by 3.6V lithium ion batteries and housed in a waterproof case. Continuous operation of these cameras depended on regular replacement of the batteries and memory cards, and even then, we had limited success with collecting images in WY 2012. Since that time, inexpensive time-lapse hunting cameras have become available, which are ruggedly packaged. In our limited usage of these new cameras we have found mixed success with AA battery longevity (even switching from alkaline to lithium batteries), but are optimistic about newer models that accommodate six C-cells and about add-on solar panels that are available (e.g., Wingscapes TimelapseCam with Wingscapes PowerPanel). We expect these will reduce the odds of complete power failure through the winter, though there may be intermittent outages after snow storms.

We make the following suggestions for deployment of time-lapse cameras:

- Measure the height, angle relative to vertical and azimuth of the camera.
- Use an SD card reader and laptop computer in the field to take test photographs in order to ensure that the field of view is as expected.
- Place multiple, clear markers over georeferenced points within the field of view to allow for orthorectification of image.

3.10.3 Fiber-Optic Cable

3.10.3.1 FOC Deployment

Deployment of over 900 m of FOC across uneven terrain was physically challenging (see Figure 3.8 and description of deployment in Lutz et al.[2012]) and posed issues with the representativeness of some sampling locations (Figure 3.9). During processing (see below), locations that were never snow covered during the data collection period (when there were multiple snowfall events) were excluded from analysis. These locations were likely suspended above the ground, since their temperature record mimics the observed air temperature.

3.10.3.2 FOC Operation

Continuous operation of the FOC was affected by power because the instrument sends a pulse of light at every sampling interval. As a side note, operation was also affected by a bear biting through the cable, but power was the more persistent, if less exciting, issue (Figure 3.10). Thus, since we lacked a power source at our remote location, we used a 12 volt battery in combination with a solar panel to recharge the battery (Figure 3.11). However, the majority of complete days of missing data are attributable to snowfall events, during which time there was low light and snow sitting on the solar panel. To minimize the effect of these events on data collection, the day after snowfall ended we visited the field site to switch out the battery and brush snow off of the panel. Low power resulted in a diurnal cycle to data collection, in which samples were only taken during daylight hours (Figure 3.12).

3.10.3.3 FOC Data Processing

The temporally discontinuous data contributes to uncertainty in inferring snow presence and snow disappearance date. Previous work on inferring snow presence from ground temperature has relied upon the damped diurnal temperature range as an indicator of snow cover. Whereas

we, too, utilize the diurnal range for inferring snow presence on both the iButtons and the FOC, the number and temporal spread of data points collected by the FOC is problematic. During days in which data were only collected during daylight hours (e.g., 27 April through 1 May, shown in Figure 3.12), we lack enough information to determine the true diurnal temperature range. However, we proceeded with inferring daily snow presence using the criteria of a maximum temperature threshold and a maximum diurnal range, designating snow absence for each day when one or both thresholds were exceeded. We justify this method based on two reasons: the timing of successful data collection, and sensitivity testing on the temperature thresholds. First, the FOC collected data at times that were likely to be near the daily maximum (i.e., the middle of the day during the sunniest conditions). If any of the sub-hourly temperature values exceeded the maximum temperature threshold for that day, then snow was inferred to be absent. In the case when temperature was below the threshold and there were only a few data points, it is possible that the daily maximum temperature was higher than we observed; however, the timing of data collection makes this case unlikely. Furthermore, we tested the sensitivity of our derived snow presence data to the temperature criteria, but increasing and decreasing both thresholds by 0.5 and 1 °C. By plotting fSCA with the upper and lower bounds represented by reprocessing the temperature data using different criteria, we see how sensitive our snow duration metrics are to these processing decisions (Figure 3.13). The bounds on fSCA are fairly small through time when reprocessed using ± 0.5 °C for temperature thresholds; the maximum difference is about 20% during the ablation season, with little to no difference during much of the time series. Results of sensitivity testing using ± 1.0 °C led to unreasonable results (e.g., 0% fSCA in mid-March, when all evidence points to nearly complete snow coverage), leading us to conclude that the criteria we used are physically realistic.

One additional source of uncertainty in our processing of the FOC data is the designation of SDD during periods when full days of data were missing. As stated in the main text, if snow was present at a location before a missing day, and the location failed the criteria for daily snow presence after the missing period, then the first day after the missing period was designated as the SDD. This assumption is based on the likelihood that the missing period was due to snowfall, during which time snow disappearance is unlikely. However, we tested the sensitivity of our distributions of SDD to this assumption by recalculating the distribution based on the opposite assumption: that snow disappeared the first day that the FOC was not working. We find differences of 0-1 days in the median SDD for each forest treatment (Figure 3.14).

3.10.4 Snow Duration Metrics

We present the quantiles of RSCD and SDD values presented in Figure 4 of the main text in Table 3.3 and Table 3.4.

3.10.4.1 Length of Ablation Season

For both Bear Creek and Mount Gardner in WY 2011, we further quantified snow duration in the different treatment plots by using a snow covered days approach. This comparison used data from the iButtons only, all of which continuously logged hourly temperature data through the snow season. We designated the last day of peak snow depth (from bi-weekly manual snow course measurements) as the starting day for calculating snow covered days in order to quantify the length of the ablation season (LAS) for comparison between forest treatments and study sites. However, the utility of this metric is in comparing snow duration at different plots from the same year. The length of ablation lacks year-to-year comparability in the intermittent snow zone

because accumulation and ablation cannot be neatly divided into only two periods; instead, in both years, there were two snow depth peaks of similar magnitude separated by a period of ablation.

The resulting distributions of LAS values are simply another way to look at the data presented in Figure 3.6 in the main text, which shows the evolution of fSCA as a function of forest treatment at the different sites during the two years. Distributions of LAS illustrate that there is more overall difference between the gap and non-gap plots at Mount Gardner than at Bear Creek, but that the relative relationship between forest treatments is similar at each site and each year (Table S4 and Figure 3.15).

3.10.4.2 Additional SDD Data

We present SDD values from grids of iButtons at Bear Creek and Mount Gardner in WY 2011 and 2012 in Table 3.6 and Figure 3.16. Comparisons of snow duration in the main text are based on RSCD values due to the event-driven nature of SDD in the intermittent snow zone; however, final SDD is a key metric in numerous applications.

3.10.5 Statistical Testing

To assess the magnitude of treatment effect detected by each instrument we used a statistical hypothesis testing approach. We compared the RSCD by forest treatment for the FOC, iButtons, and Cameras using a 1-way analysis of variance (ANOVA), followed by Tukey's Honestly Significant Difference (HSD) for the tests in which the null hypothesis could be rejected. Since only the FOC observed snow presence at multiple plots, we tested all of the data at the sample level without accounting for plot-level variance. Statistical testing on the plot means of the FOC data is presented in the main text.

Prior to testing the sample-level data we accounted for spatial autocorrelation by sub-sampling the FOC and camera data. In other words, we used only a subset of the data, from locations that were physically spread by 4 m or more, to meet the assumption of independent samples required by hypothesis testing. The results from each test are presented in Table 3.7.

3.10.6 Autocorrelation and Spatial Trends

The analysis of autocorrelation of snow metrics across each plot reveals a spatial trend in the gap plots: variance increases up to a lag distance of 20 m (which is the maximum lag distance under consideration when considering relationships between pairs of observations across a 40 m transect; see Figure 3.7). We hypothesized that the increasing variance was the results of a spatial trend related to the size of the gaps. The maximum variance is reached at a distance of 20 m since the diameters of the gaps are approximately 20 m. At a distance of 20 m, two sample locations are likely to be positioned so that one in the forest and one is in the open, whereas the likelihood of both samples being either in the open or under the forest increases with diminishing distance between the samples.

To test this hypothesis, we assessed autocorrelation between points located within the same treatment group across the entire site, utilizing their position in X-Y space to extend the analysis to longer lag distances (Figure 3.17). The semi-variogram for each treatment across the entire site confirms the hypothesis of a spatial trend in which variance within gap plots is maximized at a distance of 20 m between pairs of points (Figure 3.17a). Also notable is the increase in variance at a lag distance of 40 m across all treatments types, which we attribute to the differences between plots of the same treatment type. Since the 40 × 40 m forest plot served as our unit of analysis, the extension of autocorrelation analysis to the entire site raises some

questions about the suitability of a group of randomly placed treatment plots for spatial analysis. The peak in variance at 40 m illustrates the discontinuous response of snow duration in adjacent treatment plots.

To separate the spatial relationship in snow duration due to the spatial trend across gap plots and the spatial autocorrelation of proximal measurements, we then de-trended the observations across each gap plot and assessed autocorrelation of the residuals. Based on the observation that snow duration across the gap plots resembled a parabolic form, we fit a 3rd order polynomial function to each plot and computed the residuals from the fitted function (Figure 3.18). We then computed the semi-variogram on the residuals as a function of position (Figure 3.19, utilizing their position in X-Y space, as in Figure 3.17). The resulting semi-variogram shows a peak and subsequent plateau in variance (i.e., the sill of the semi-variogram) at a lag distance of 6 m, which is similar to the range found for the thinned plots (Figure 3.6).

The results of this analysis confirm that a spatial trend is clearly the large-scale control on snow duration variability in the gap plots, but that there's additional spatial auto-correlation that affects the local similarly of samples. From a practical standpoint this is useful for quantifying snow presence in regularly spaced canopy openings: to quantify the range of variability a sensor in the middle of the gap and in the forest are sufficient, whereas to fully characterize the variability without redundancy a spacing of approximately 6 m is recommended.

3.11 Supporting Tables

Table 3.2 Summary of advantages and disadvantages for each method for observing snow duration.

Instrument	Advantages	Disadvantages	Example Brands & Costs
Fiber Optic Cable	• High spatial and temporal resolution • Single instrument deployment for large spatial coverage	• Cumbersome to deploy in forest • Placement can diminish representativeness (e.g., hanging over logs, in depressions) • Missing data due to power disruptions when solar panel is blocked or experiences low light conditions	• BRUsens Temperature +85 °C cable and Sensornet Oryx distributed temperature sensing (DTS) system
Ground Temperature Sensors	• Easiest to deploy of the three methods • Inexpensive	• Higher spatial resolution requires more instruments • Disturbance can diminish representativeness (e.g., being dug up by animals)	• Maxim DS1922L thermochrons (iButtons), $52[a]/iButton for 1-24 iButons, with waterproof iButton Capsule, $25/each (DS9107) • Onset Hobo Pendants, $ 59[b]/instrument for 1-9 instruments (UA-001-64)
Time Lapse Cameras	• Easy to deploy, depending on the average winter snow depth • One deployment covers a much larger area than a single ground temperature sensor • Highest spatial resolution (but distortion must be accounted for in some situations) • Visual assessment of conditions allows method for ground-truth of snow cover quantification	• Missing data due to battery or camera failure, although improvement likely with add-on solar panel. Multiple cameras recommended for back-up. • Positioning can diminish representativeness, requiring multiple cameras. • Perspective of cameras seeing tree trunks and logs may underestimate snow on the ground. • Environmental conditions affect detection of snow presence (e.g., precipitation, condensation, shadows, and branches entering the field of view).	• Wingscapes TimelapseCam, $99, with Wingscapes PowerPanel, $64

[a] Cost varies by quantity ordered. Requires reader, e.g., Blue Dot Receptor, USB and Serial Port (DS1402D-DR8), $12
[b] Cost varies by quantity ordered. Requires reader and software, e.g., Optic USB Base Station for Pendant (BASE-U-1), $70, and HOBOware Pro (BHW-PRO-CD), $99

Table 3.3 Quantiles of RSCD metrics, plotted in Figure 3.5 of the main text.

Bear Creek WY 2011		RSCD since 17-March					
Treatment	**Method**	**Min**	**Q25**	**Median**	**Mean**	**Q75**	**Max**
gap	FOC (all)	20	35	44	41	48	54
thinned	FOC (all)	8	27	30	31	36	48
control	FOC (all)	15	28	32	31	35	42
gap	FOC (intensive)	28	35	42	41	48	50
thinned	FOC (intensive)	15	26	28	28	33	36
control	FOC (intensive)	24	31	34	33	35	37
gap	iButtons	13	30	32	34	46	49
thinned	iButtons	21	22	32	28	33	34
control	iButtons	29	30	33	33	35	37
gap	camera	3	28	42	37	48	54
thinned	camera	3	15	22	21	28	36
control	camera	9	22	32	29	35	41

Table 3.4 Quantiles of SDD metrics, plotted in Figure 3.5 of the main text.

Bear Creek WY 2011		Snow Disappearance Date (SDD)					
Treatment	**Method**	**Min**	**Q25**	**Median**	**Mean**	**Q75**	**Max**
gap	FOC (all)	1-May	3-May	12-May	10-May	17-May	23-May
thinned	FOC (all)	29-Apr	1-May	1-May	3-May	3-May	17-May
control	FOC (all)	1-May	1-May	2-May	2-May	3-May	10-May
gap	FOC (intensive)	1-May	3-May	10-May	9-May	17-May	19-May
thinned	FOC (intensive)	1-May	1-May	1-May	1-May	2-May	4-May
control	FOC (intensive)	1-May	1-May	2-May	2-May	3-May	5-May
gap	iButtons	9-Apr	30-Apr	1-May	2-May	14-May	18-May
thinned	iButtons	30-Apr	30-Apr	2-May	1-May	2-May	2-May
control	iButtons	1-May	1-May	2-May	2-May	2-May	5-May
gap	camera	25-Mar	30-Apr	11-May	7-May	17-May	24-May
thinned	camera	21-Mar	21-Apr	3-May	27-Apr	3-May	7-May
control	camera	26-Mar	1-May	2-May	1-May	4-May	10-May

Table 3.5 Quantiles of LAS metrics, plotted in Figure 3.15. BC = Bear Creek, MG = Mount Gardner.

			Length of Ablation Season (LAS)					
Site	**WY**	**Treatment**	**Min**	**Q25**	**Median**	**Mean**	**Q75**	**Max**
BC	2011	gap	36	55	57	59	72	76
BC	2011	thinned	45	45	58	53	59	60
BC	2011	control	54	55	59	58	61	63
BC	2012	gap	14	19	27	26	32	38
BC	2012	thinned	14	16	20	19	22	23
BC	2012	control	19	22	22	22	22	23
MG	2011	gap	89	91	97	95	98	99
MG	2011	thinned	71	78	82	81	82	92
MG	2011	control	69	71	72	75	78	84
MG	2012	gap	22	45	48	46	53	55
MG	2012	thinned	27	38	39	39	41	46
MG	2012	control	24	32	39	36	39	42

Table 3.6 Quantiles of SDD metrics, plotted in Figure 3.16. BC = Bear Creek, MG = Mount Gardner.

			Snow Disappearance Date (SDD)					
Site	**WY**	**Treatment**	**Min**	**Q25**	**Median**	**Mean**	**Q75**	**Max**
BC	2011	gap	9-Apr	30-Apr	1-May	2-May	14-May	18-May
BC	2011	thinned	30-Apr	30-Apr	2-May	1-May	2-May	2-May
BC	2011	control	1-May	1-May	2-May	2-May	2-May	5-May
BC	2012	gap	13-Apr	17-Apr	25-Apr	24-Apr	30-Apr	7-May
BC	2012	thinned	13-Apr	14-Apr	19-Apr	18-Apr	21-Apr	22-Apr
BC	2012	control	18-Apr	20-Apr	21-Apr	20-Apr	21-Apr	22-Apr
MG	2011	gap	31-May	2-Jun	7-Jun	5-Jun	9-Jun	10-Jun
MG	2011	thinned	13-May	20-May	24-May	22-May	24-May	3-Jun
MG	2011	control	11-May	14-May	15-May	17-May	19-May	26-May
MG	2012	gap	21-Apr	14-May	17-May	14-May	22-May	24-May
MG	2012	thinned	6-May	7-May	8-May	8-May	10-May	15-May
MG	2012	control	6-May	6-May	8-May	7-May	8-May	11-May

Table 3.7 Results from sample-level hypothesis testing regarding the forest treatment effect on snow duration observed by each instrument.

Site	Year	Method	F	p ANOVA: All Treatments	p Tukey HSD: Gap vs. Non-Gap	Notes
BC	2011	FOC (all)	35.45	< 0.001	< 0.001	Tested all data points, sub-sampled at 4 m spacing
BC	2011	FOC (all)	11.29	< 0.005	< 0.005	Tested plot means, n=5 for each treatment
BC	2011	FOC (intensive)	12.75	< 0.001	<0.05 (gap vs. control), <0.001 (gap vs. thinned)	Tested data points at intensive plot only, sub-sampled at 4 m spacing
BC	2011	camera	10.14	< 0.001	<0.05 (gap vs. control), <0.001 (gap vs. thinned)	Tested data points, sub-sampled at even spacing for 10 total data points (for equivalent number of samples at the sub-sampled FOC)
BC	2011	iButtons	0.52	0.605	n/a	Tested all data points
BC	2012	iButtons	2.85	0.079	n/a	Tested all data points
MG	2011	iButtons	24.45	< 0.001	< 0.001	Tested all data points
MG	2012	iButtons	3.44	0.051	n/a	Tested all data points

3.12 Supporting Figures

Figure 3.9 Photograph of the fiber-optic cable draped over a large stump, resulting in temperature observations that represents the stump or the adjacent air space rather than the ground temperature.

Figure 3.10 Photograph of bear damage to the fiber-optic cable.

Figure 3.11 Photograph of the equipment trailer and solar panel used to power and operate the FOC. View is toward the southwest, with the Bear Creek intensive gap plot in the forest shown in the background. Partway through the deployment, the trailer was moved further away from the trees in an attempt to reduce the time during which the solar panel was shaded each day.

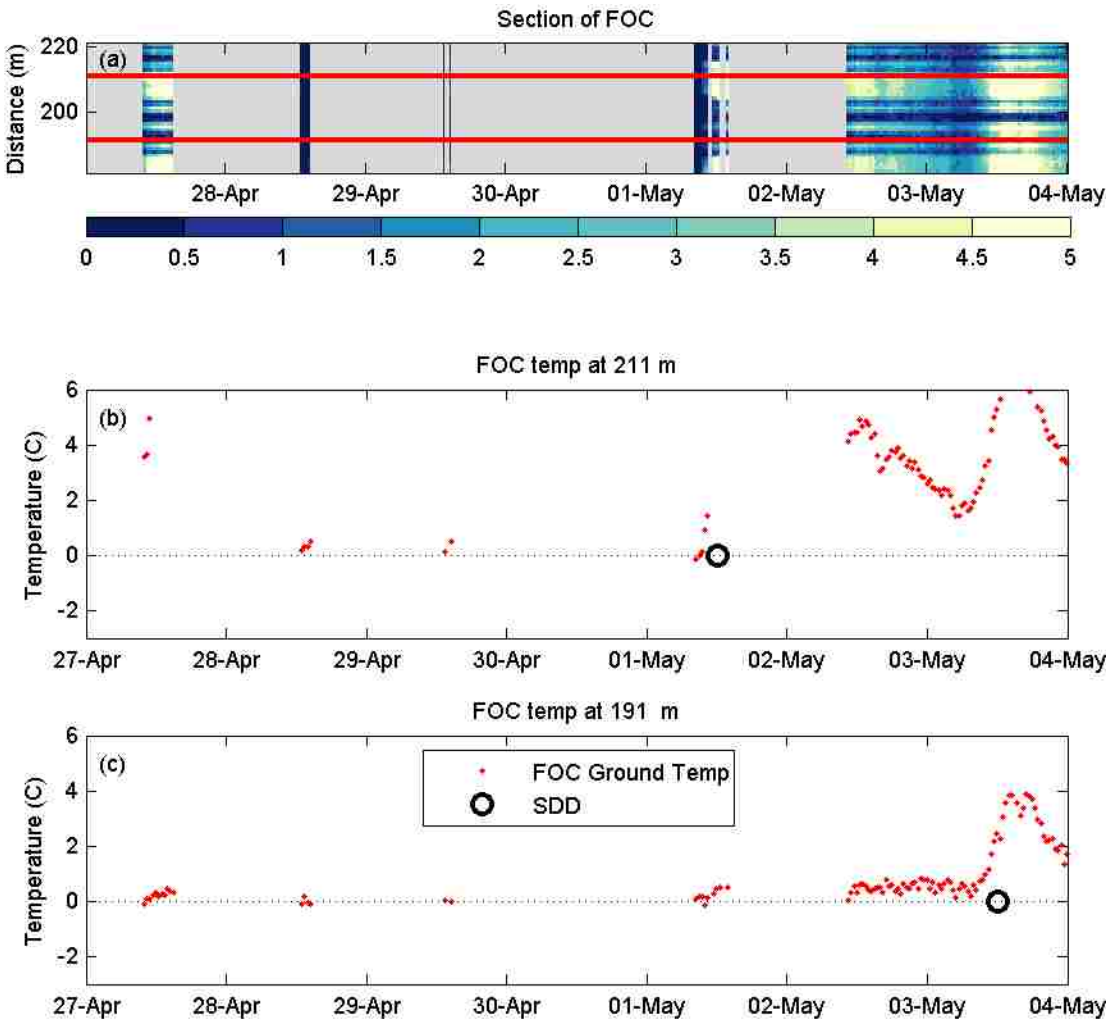

Figure 3.12 Data continuity of ground temperature observed by the FOC during one week in WY 2011 at Bear Creek. (a) Temperature along a 40 m stretch of the FOC, with the two sample locations shown in (b) and (c) indicated as red lines. (b) Ground temperature through time at one sampling location (211 m, located in a thinned plot), and (c) at a second sampling location (191 m, located in a thinned plot). Note that 30 April is the only day with completely missing data (due to >10 cm of snowfall) during this time period. Date ticks indicate 0000 hrs (i.e., midnight) of each day.

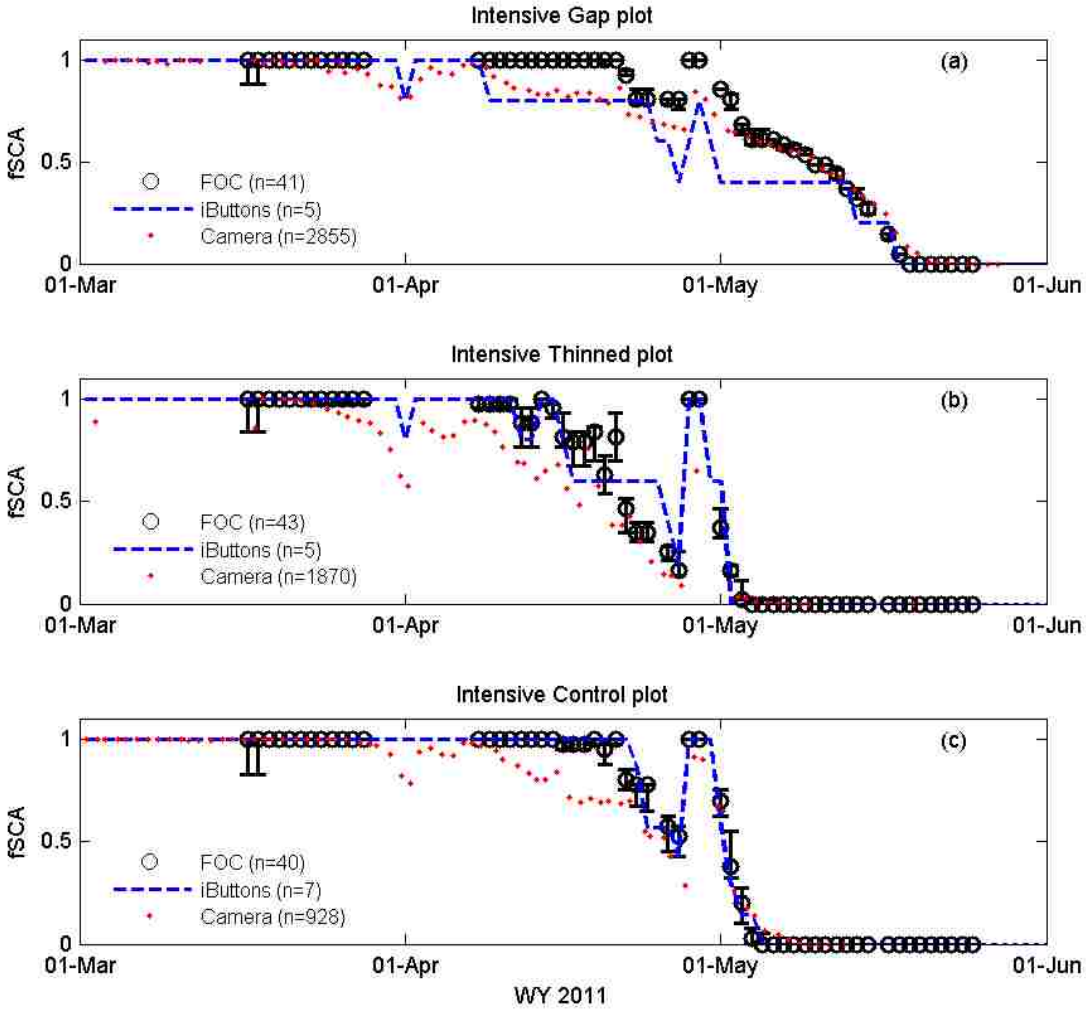

Figure 3.13 Fractional snow covered area (fSCA) through time during WY 2011 at the (a) intensive gap plot, (b) intensive thinned plot, and (c) intensive control plot at Bear Creek, as measured from a fiber optic cable (FOC) transect, a grid of iButtons, and a single time lapse camera. Bars on the FOC data represent the sensitivity of the values to temperature thresholds used when deriving snow presence from the time series of ground temperature. Upper and lower limits of the bars are determined from re-processing the ground temperature data using ± 0.5 °C on the thresholds for maximum temperature and the maximum diurnal temperature range.

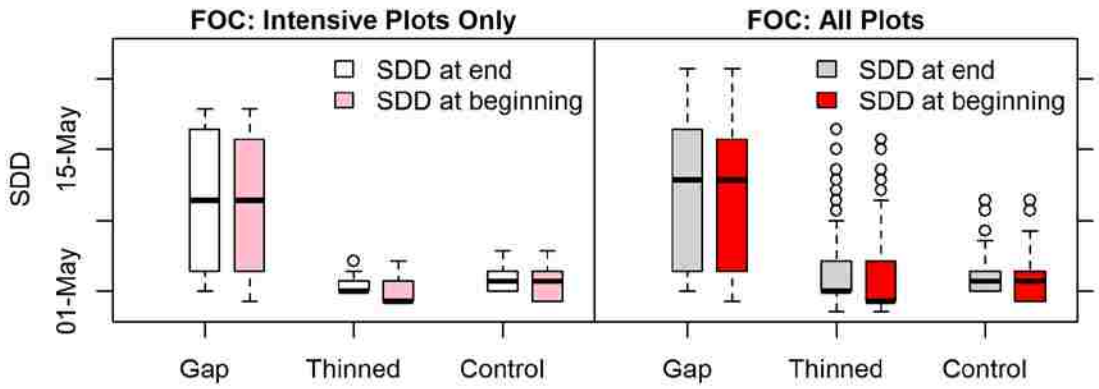

Figure 3.14 Distributions of snow disappearance date (SDD) at Bear Creek for each forest treatment for (a) the intensive plots only, and for (b) all of the experimental plots transected by the FOC (5 plots per forest treatment). The two distributions shown for each forest treatment in (a) and (b) are based on SDD values derived using the assumption stated in the main text, that SDD occurred at the end of a missing period of data, and the opposite assumption of SDD occurring at the beginning of a missing period of data.

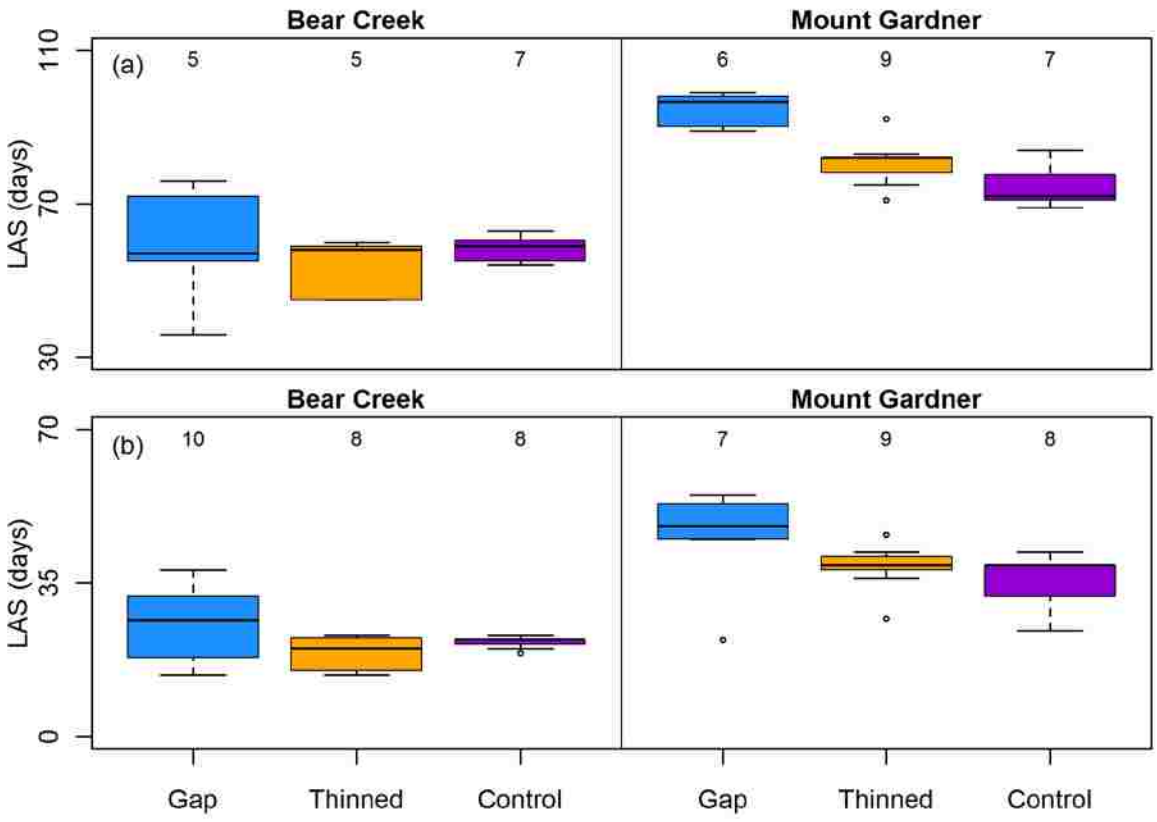

Figure 3.15 Boxplots of the length of ablation season (LAS, the number of snow covered days since peak snow depth, note different scale for each year) derived from grids of iButtons at Bear Creek and Mount Gardner for (a) WY 2011 and (b) 2012. Number shown above each boxplot is the number of working sensors for that plot and year.

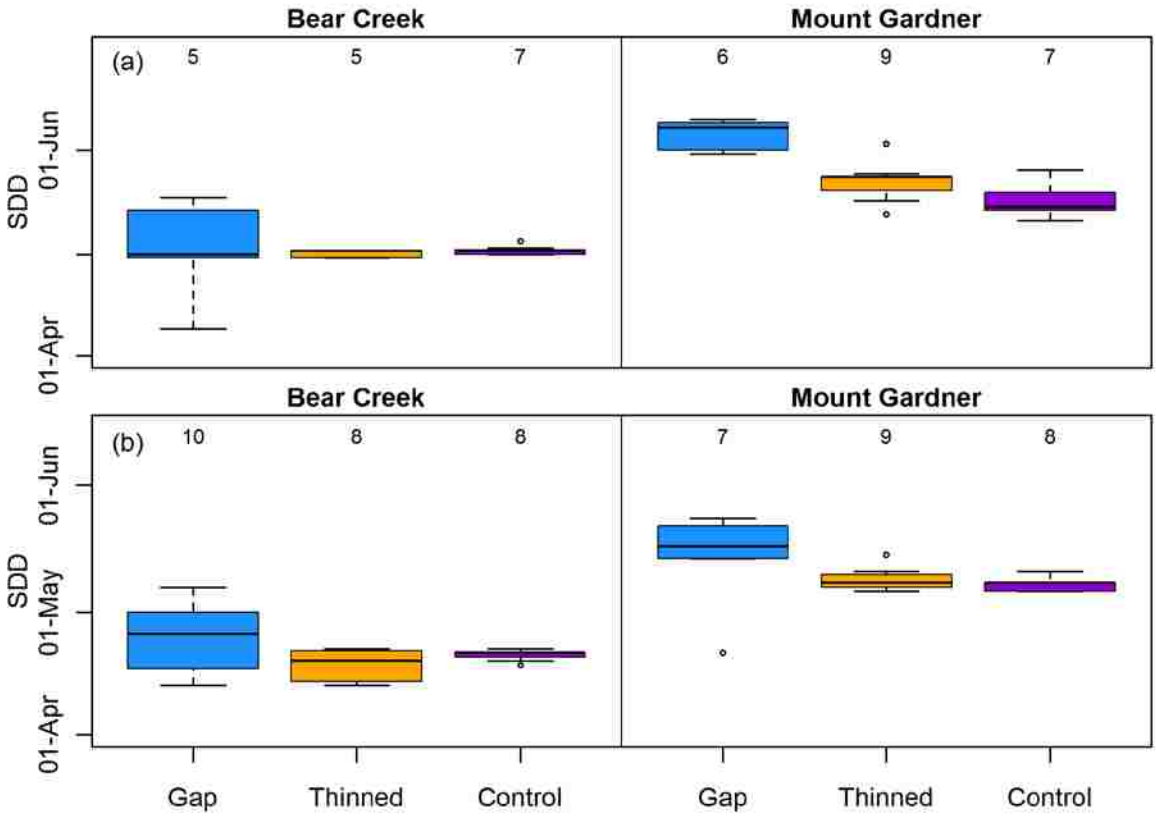

Figure 3.16 Boxplots of SDD derived from grids of iButtons at Bear Creek and Mount Gardner for (a) WY 2011 and (b) 2012. Number shown above each boxplot is the number of working sensors for that plot and year.

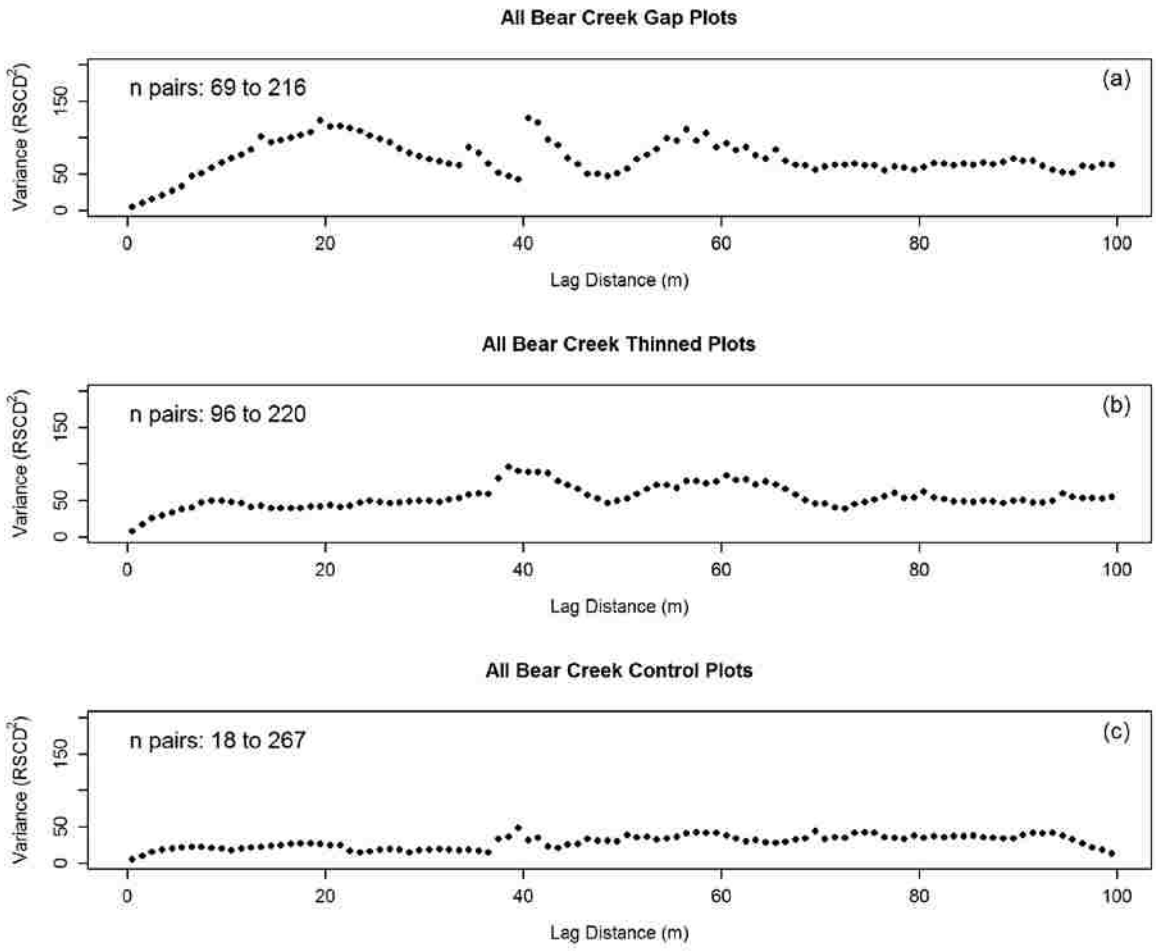

Figure 3.17 Semi-variograms of RSCD for all five plots in each forest treatment group. This analysis utilizes the position of each point measurement in X-Y space, without regard to its membership in a particular plot, thus, extending the analysis over longer lag distances.

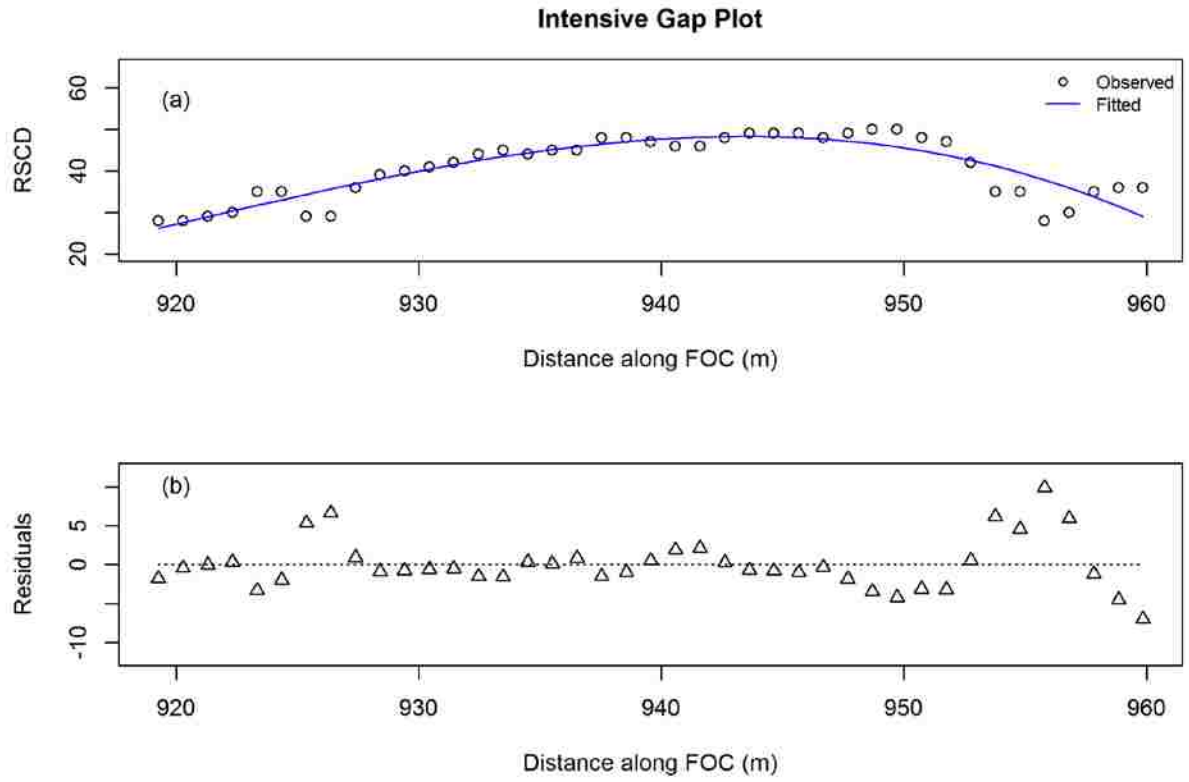

Figure 3.18 Example of fitting a 3rd order polynomial to RSCD as a function of distance along the FOC for one of the gap plots (a), and the residuals from the fitted function (b).

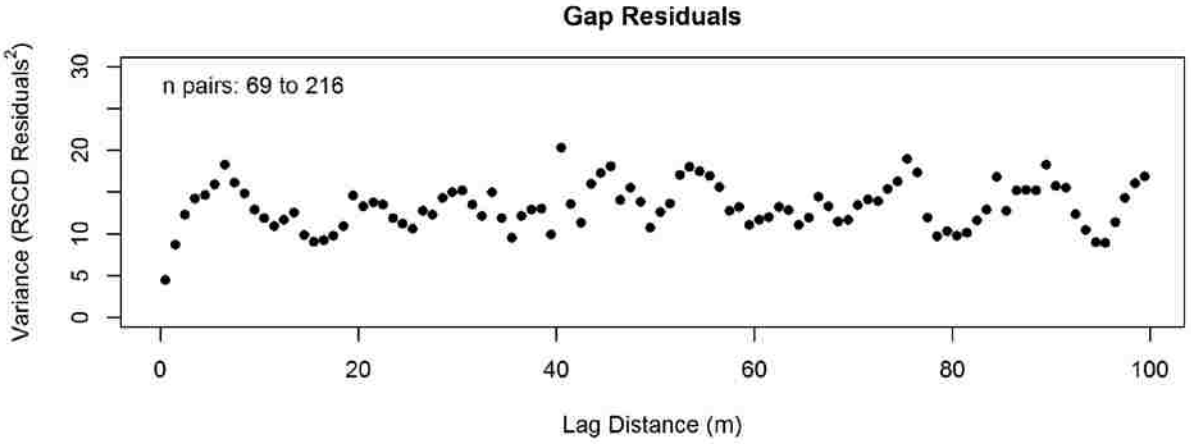

Figure 3.19 Semi-variogram of the residuals of RSCD at all five of the Bear Creek gap plots after fitting RSCD as a function of distance across each plot to a 3rd order polynomial function. Note that variance peaks (i.e., the sill is reached) at a lag distance of approximately 6 m.

Chapter 4. Observations of distributed snow depth and snow duration within diverse forest structures in a maritime mountain watershed

Susan E. Dickerson-Lange[1,5], James A. Lutz[2], Rolf Gersonde[3], Kael A. Martin[1], Jenna E. Forsyth[4], and Jessica D. Lundquist[1]

[1]Civil and Environmental Engineering, University of Washington, Seattle, Washington, USA
[2]Wildland Resources Department, Utah State University, Logan, Utah, USA
[3]Seattle Public Utilities, Seattle, Washington, USA
[4]School of Earth Sciences, Stanford University, California, USA

Note: This chapter has been published in its current form as an article in Water Resources Research [*Dickerson-Lange et al.*, 2015b]; the only differences are in section, figure, and table numbering, and in the casing of lidar, which has been updated to reflect current consensus [*Deering and Stoker*, 2014]. It is used here by permission of John Wiley and Sons.

4.1 Abstract

Spatially distributed snow depth and snow duration data were collected over two to four snow seasons during water years 2011-2014 in experimental forest plots within the Cedar River Municipal Watershed, 50 km east of Seattle, Washington, USA. These 40 × 40 m forest plots, situated on the western slope of the Cascade Range, include un-thinned second-growth coniferous forests, variable density thinned forests, forest gaps in which a 20 m diameter (approximately equivalent to one tree height) gap was cut in the middle of each plot, and old-growth forest.

Together, this publicly available dataset includes snow depth and density observations from manual snow surveys, distributed snow duration observations from ground temperature sensors and time-lapse cameras, meteorological data collected at two open locations and three forested locations, and forest canopy data from airborne light detection and ranging (lidar) data and hemispherical photographs. These co-located snow, meteorological, and forest data have the potential to improve understanding of forest influences on snow processes, and provide a unique model-testing dataset for hydrological analyses in a forested, maritime watershed. We present empirical snow depletion curves within forests to illustrate an application of these data to improve sub-grid representation of snow cover in distributed modeling.

4.2 Introduction

The forests that cover mountain watersheds influence snow accumulation and ablation processes as a function of climate (e.g., [*Lundquist et al.*, 2013]), topographic position (e.g., [*Ellis et al.*, 2013]), and forest characteristics such as stand composition and density (e.g., [*Kittredge*, 1953]). Snow depth and duration within forested watersheds are therefore difficult to accurately model (e.g., [*Rutter et al.*, 2009]) or estimate from sparse point observations of snow depth (e.g., [*Meromy et al.*, 2013]) or from remotely-sensed detection of snow cover in open areas (e.g., [*Raleigh et al.*, 2013]). As a result, distributed observations are critical for improving process understanding and for model development and testing of snow process representation within forests.

We present a dataset of snow depth, snow water equivalent (SWE), and snow duration observations, and related meteorological and forest data, collected within a forest-snow regime that is both under-sampled and is an extreme case in the range of observed forest influences on snow processes. The study site is situated in a maritime climate zone and subject to heavy winter precipitation and relatively warm winter temperatures that fluctuate around 0 °C. The observed influence of the forest on snow processes in this location is an end point in the published range. Both canopy snow interception efficiency (83%, [*Martin et al.*, 2013]), and the difference in snow disappearance timing between forested and open locations (14 days later in the open, [*Lundquist et al.*, 2013]) are of the largest magnitude observed worldwide. Furthermore, the net effect of forest cover on snow duration is in the opposite direction than more well-studied continental sites where snow frequently persists longer within forests (e.g., [*Gelfan et al.*, 2004; *Winkler et al.*, 2005; *Rutter et al.*, 2009]).

Whereas several high quality snow datasets are publicly available (e.g.,[*Reba et al.*, 2011; *Morin et al.*, 2012; *Landry et al.*, 2014]), the few that include snow observations within forests are situated in colder, continental climates (e.g., the Cold Land Processes Field Experiment (CLPX) [*Elder and Cline*, 2003; *Elder et al.*, 2009]), or are situated at lower latitudes and subject to clearer skies and higher solar elevations during the ablation season [e.g., the Sierra and Jemez Critical Zone Observatories (CZO; http://criticalzone.org/)]. The notable exception is the HJ Andrews Experimental Forest in western Oregon at which variable frequency snow stake observations capture differences in peak snow depth between paired open and forested sites (http://andrewsforest.oregonstate.edu/data/). The warm, wet winter climate conditions represented at the Cedar River Municipal Watershed are also observed in other maritime snow zones worldwide (e.g., northern Europe and Japan [*Sturm et al.*, 1995]), and have been previously shown to result in high snow accumulation (e.g., the world record of observed snow accumulation at Mount Baker, 29 m in water year (WY) 1999 [*Mass*, 2008]), high canopy interception efficiency [*Storck et al.*, 2002; *Martin et al.*, 2013], and mid-winter melt events that can be enhanced [*Lundquist et al.*, 2013] or diminished [*Marks et al.*, 1998] due to forest cover. Since individual components of the under-forest snowpack mass and energy balance are partially controlled by winter climate (e.g., canopy snow interception efficiency is commonly formulated as a function of temperature [*Hedstrom and Pomeroy*, 1998]), testing of snow model representations and process understanding in a warmer climate may become critical for accurate hydrologic predictions under projected climate warming [*Cristea et al.*, 2014].

In addition to the unique climate-forest-snow interactions represented in this dataset, these observations were collected within a range of forest types in order to better characterize the relations between snow processes and forest structural characteristics. Since much of the

seasonally snow-covered landscape is also covered by a mosaic of forest stands that reflect a history of timber harvesting, silvicultural activities, and natural disturbance [*Kane et al.*, 2010b, 2011], improved quantification of snow processes within diverse forest types are needed. Spatially distributed snow observations within forests have the potential to support enhanced understanding of the relationship between forest characteristics and snow processes [*Molotch et al.*, 2009; *Musselman et al.*, 2012; *Lundquist et al.*, 2013], testing and validation of hydrologic model representation in forests [*Whitaker et al.*, 2003; *Du et al.*, 2013; *Martin et al.*, 2013], and the comparison of empirical results to theoretical snow depletion curves [*Liston*, 2004; *Luce and Tarboton*, 2004; *Clark et al.*, 2011]. Furthermore, co-located forest observations (i.e., lidar and hemispherical photographs) additionally provide testing data for the implementation of forest metrics in models [*Varhola et al.*, 2012].

We therefore present field observations collected over four winters (WY 2011 – 2014) within the upper Cedar River Watershed to provide data for empirical analyses and model testing focused on forest influences on snow processes. We describe the study site in section 4.3, provide an overview of the data in section 4.4, and briefly discuss empirical snow depletion curves as an example application of these data in section 4.5.

4.3 Site Description

Snow and meteorological data were collected in the Cedar River Municipal Watershed (47° 20' N, 121° 32' W), which is a protected watershed located on the western slope of the Cascade range, approximately 50 km to the east of Seattle, Washington USA (Figure 4.1). Within a 60 km^2 area in the upper watershed, we collected data at six study sites ranging in elevation from 620 m to 1165 m. Each site encompassed one or more study plots approximately 1600 m^2 in area (i.e., 40 m × 40 m), which were designated based on forest type or silvicultural treatment (Table 4.1; Figure 4.2). Mean January minimum and maximum temperatures are -2.4°C and 4.0°C (based on 1981-2010 climate normals derived from PRISM [*Daly et al.*, 2008; *PRISM Climate Group*, 2012]), respectively, at the warmest study site (Bear Creek), and are -3.2°C and 1.7°C at the coldest study site (Tinkham Creek). Mean annual precipitation is 2570 mm at Bear Creek and 2710 mm at Tinkham Creek (again based on 1981-2010 climate normals [*Daly et al.*, 2008; *PRISM Climate Group*, 2012]); annual peak SWE ranged from 300 to 1500 mm at the three co-located National Resource Conservation Service snow telemetry (NRCS SNOTEL) sites during the study period.

Coniferous forest covers approximately 95% of the upper watershed above Chester Morse Reservoir, and includes stands of naturally regenerated second-growth forest, second-growth forest subject to silvicultural thinning or gap creation, old-growth forest, and clearings, each of which is represented by one or more study plots (Table 4.1; Figure 4.2). The watershed is managed both for municipal water supply and ecological functions, and silvicultural thinning and gap creation are used to facilitate the recovery of ecosystem functions in second-growth forests with dense, homogeneous canopies [*Richards et al.*, 2012]. Two study sites, Bear Creek and Mount Gardner, include one or more plots that represent unmanipulated (control) second-growth

forest, thinned forest, and a forest plot with a canopy gap cut in the middle. The four other sites, including City Cabin, Clearing Meteorology (Met), Tinkham Creek, and Rex River, encompass one or two experimental forest plots. Mount Gardner, Tinkham Creek and Rex River are additionally co-located with SNOTEL stations (#898, #899 and #911, respectively).

Two to four snow seasons of snow duration observations were collected at each study plot, with two years of manual snow surveys, and up to four years of meteorological data collected at a

subset of plots (

Site	Field Metrics[2]				LiDAR Metrics		
	Approximate Stem Density (stems hectare^{-1})	Mean Basal Area (m^2 hectare^{-1})	Mean Diameter at 1.4 m (cm)	Mean Tree Height (m)	% Canopy Cover		Canopy Height[3] (m)
					Mean	SD	Mean
Bear Creek (BC)	1018	80	28	38	92	3	34
	Metrics at additional control plots are similar to intensive control plot, but were not measured				88	12	31
	541	62	36	37	78	13	33
	Metrics at additional thinned plots are similar to intensive thinned plot, but were not measured				76	19	31
	Center of gap plots are clear of trees; refer to control plot metrics for surrounding forest metrics for gap plots				72	30	30
					71	29	30
	Metrics at additional forest plots are similar to intensive control plot, but were not measured				90	8	34
Clearing Met (CM)	0	NA	NA	NA	NA[4]	NA	NA
City Cabin (CC)	302	99	38-71	41-54	87	7	39
Mount Gardner (MG)	1370	60	23	25	94	4	22
	890	41	26	28	73	14	22
	Gap portion of plot is clear of trees; refer to control plot metrics for surrounding forest metrics for gap plot				73	31	22
	380	96	42-76	40-50	95	3	38
Tinkham Creek (TC)	891	55	36	31	90	12	23
	318	14	25	20	46	23	14
Rex River (RR)	320	20	27	15	32	18	10

1. Plot code, refers to the position within the Bear Creek site, with the southwest plot designated as Row 1 Column 1 (R1C01). 2. Forest metrics are based on manual measurements of stem density and diameter, and field estimates of basal area and tree height 3. Mean of the 5m gridded 95th percentile canopy height over the 40 x 40 m plot. 4. The Clearing plot was not treated as a 40 x 40 m plot that included all land cover within, but, rather, all data collection took place within the clearing, which renders the plot-scale canopy metrics irrelevant.

Table 4.2). Hourly air temperature data from transects of temperature sensors deployed in trees were collected over portions of WY 2012 through 2014 to characterize terrain effects on air temperature in the rain-snow transition zone. Within the upper basin, there are three SNOTEL stations which are adjacent to study plots, a fourth SNOTEL station (Meadow Pass, #897), and four USGS stream gages, which together provide public access to hourly meteorological, snow, and streamflow data.

As a critical water and ecological resource to the region, the protected Cedar River Municipal Watershed has a long history of use a field research site. Most relevant to the data presented herein, [*Dickerson-Lange et al.*, 2015a] previously analyzed snow duration data at Bear Creek and Mount Gardner in WY 2011 and 2012, [*Martin et al.*, 2013] completed an investigation quantifying canopy snow interception during WY 2012 at Bear Creek, and [*Sprugel et al.*, 2009] and [*Lutz et al.*, 2012] provide details on tree location mapping and ecological investigations at Bear Creek. The correspondence of ground measurements and remotely sensed lidar data in the watershed is given in [*Kane et al.*, 2010a]. A list of citations to decades of ecological and hydrological studies is provided with the dataset.

4.4 Data Description

4.4.1 Data Availability and Metadata

The data described herein are publicly available. Snow and meteorological data are archived at the University of Washington (http://hdl.handle.net/1773/33268) and FOC data are additionally archived at the Consortium of Universities for the Advancement of Hydrologic Science, Inc. (CUAHSI) Water Data Center (https://dx.doi.org/10.4211/his-data-cedarriverforestsnow). Airborne lidar data are available through Open Topography (http://www.opentopography.org/). Location metadata provide attributes of each data collection location, including site name, plot type (forest type or treatment), and geolocation. Coordinates are based on GPS points collected with handheld instruments or on interpolation between georeferenced points. Metadata provided with each dataset additionally include details on the instrumentation used to collect data, the manufacture-provided or estimated accuracy, and post-processing or quality control procedures.

4.4.2 Meteorological Data

Meteorological data, including temperature, relative humidity, wind speed, wind direction, incoming solar radiation, and photosynthetically active radiation were collected in various combinations at all study sites and at two additional transects through the upper watershed, with sensors mounted to towers and tripods, and sensors hanging in trees. Precipitation data are available from the three co-located SNOTEL stations.

4.4.2.1 Meteorological Stations

Five stations recorded hourly meteorological data, each with a variable length of operation. Two meteorological stations provide semi-continuous observations, with one located in a

clearing (Clearing Met) and one located in an old-growth forest (City Cabin) (Figure 4.1). The Clearing Met site captured the most continuous data stream, with 3% of time steps missing in four years (with the exception of the wind direction sensor, which only functioned correctly for 20% of time steps). The time series recorded at City Cabin has 4% of time steps missing until datalogger malfunction in May 2013. Additional stations at the Bear Creek intensive control and gap plots, and Mount Gardner control plot provide shorter records of observations. The intensive plots are designated as such because of the high concentration of different observations (see Figure 4.2d and [*Dickerson-Lange et al.*, 2015a]).

Each of the meteorological stations included a temperature and humidity sensor with a radiation shield and an unheated wind speed sensor installed approximately 2.5 m above ground level. At Clearing Met and City Cabin, photosynthetically active radiation (PAR) was observed, and at Clearing Met incoming solar radiation and wind direction were additionally observed. Data were generally logged every 1 minute and aggregated to hourly values (Campbell Scientific CR10X). Observations have undergone basic quality control, including checks for missing or repeated time steps and reasonable values, with flags indicating changes made. Pyranometers and wind sensors were unheated and thus subject to error when covered by snow or ice [*Malek*, 2008]. Time-lapse photographs (described below) are archived with the dataset and provide a view of the Clearing Met and City Cabin stations that could be used to check for field issues.

Additional, proximal meteorological forcing data were observed beginning in WY 1989 at the Snoqualmie Pass Meteorological Station, located 5 km from the northeastern edge of the Cedar River watershed [*Wayand et al.*, 2015a]. The dataset includes standard meteorological variables in addition to 4-stream radiation and quantification of turbulent fluxes during WY 2013 onward.

4.4.2.2 Sensors in Trees

For some plots without a meteorological tower, we deployed one or more self-recording temperature sensors (Maxim DS 1922L thermochrons, hereafter "iButtons"), or temperature and relative humidity sensors (Maxim DS 1923, hygrochrons, hereafter "hygrochrons") within trees to collect hourly (iButtons) or 2-hourly (hygrochrons) observations (

Site	Field Metrics[2]				LiDAR Metrics		
	Approximate Stem Density (stems hectare^{-1})	Mean Basal Area (m^2 hectare^{-1})	Mean Diameter at 1.4 m (cm)	Mean Tree Height (m)	% Canopy Cover		Canopy Height[3] (m)
					Mean	SD	Mean
Bear Creek (BC)	1018	80	28	38	92	3	34
	Metrics at additional control plots are similar to intensive control plot, but were not measured				88	12	31
	541	62	36	37	78	13	33
	Metrics at additional thinned plots are similar to intensive thinned plot, but were not measured				76	19	31
					72	30	30
	Center of gap plots are clear of trees; refer to control plot metrics for surrounding forest metrics for gap plots				71	29	30
	Metrics at additional forest plots are similar to intensive control plot, but were not measured				90	8	34
Clearing Met (CM)	0	NA	NA	NA	NA[4]	NA	NA
City Cabin (CC)	302	99	38-71	41-54	87	7	39
Mount Gardner (MG)	1370	60	23	25	94	4	22
	890	41	26	28	73	14	22
	Gap portion of plot is clear of trees; refer to control plot metrics for surrounding forest metrics for gap plot				73	31	22
	380	96	42-76	40-50	95	3	38
Tinkham Creek (TC)	891	55	36	31	90	12	23
	318	14	25	20	46	23	14
Rex River (RR)	320	20	27	15	32	18	10

1. Plot code, refers to the position within the Bear Creek site, with the southwest plot designated as Row 1 Column 1 (R1C01). 2. Forest metrics are based on manual measurements of stem density and diameter, and field estimates of basal area and tree height 3. Mean of the 5m gridded 95th percentile canopy height over the 40 x 40 m plot. 4. The Clearing plot was not treated as a 40 x 40 m plot that included all land cover within, but, rather, all data collection took place within the clearing, which renders the plot-scale canopy metrics irrelevant.

Table 4.2). We additionally deployed an east-west and a north-south transect of iButtons and hygrochrons covering approximately 13 km at a 1 km spacing to further characterize the spatial and temporal variability of temperature and relative humidity across complex terrain (Figure 4.1). For example, the mean January air temperature ranges from -0.8 to 1.4 in WY 2012 and from 1.1 to 4.0 °C in WY 2014 along these transects.

We used funnels with holes drilled in them as radiation shields and positioned strings over tree branches to raise instruments to the desired heights. At three plots, we deployed 2-3 sensors at

different heights (

Site	Field Metrics[2]				LiDAR Metrics		
	Approximate Stem Density (stems hectare^{-1})	Mean Basal Area (m^2 hectare^{-1})	Mean Diameter at 1.4 m (cm)	Mean Tree Height (m)	% Canopy Cover		Canopy Height[3] (m)
					Mean	SD	Mean
Bear Creek (BC)	1018	80	28	38	92	3	34
	Metrics at additional control plots are similar to intensive control plot, but were not measured				88	12	31
	541	62	36	37	78	13	33
	Metrics at additional thinned plots are similar to intensive thinned plot, but were not measured				76	19	31
					72	30	30
	Center of gap plots are clear of trees; refer to control plot metrics for surrounding forest metrics for gap plots				71	29	30
	Metrics at additional forest plots are similar to intensive control plot, but were not measured				90	8	34
Clearing Met (CM)	0	NA	NA	NA	NA[4]	NA	NA
City Cabin (CC)	302	99	38-71	41-54	87	7	39
Mount Gardner (MG)	1370	60	23	25	94	4	22
	890	41	26	28	73	14	22
	Gap portion of plot is clear of trees; refer to control plot metrics for surrounding forest metrics for gap plot				73	31	22
	380	96	42-76	40-50	95	3	38
Tinkham Creek (TC)	891	55	36	31	90	12	23
	318	14	25	20	46	23	14
Rex River (RR)	320	20	27	15	32	18	10

1. Plot code, refers to the position within the Bear Creek site, with the southwest plot designated as Row 1 Column 1 (R1C01). 2. Forest metrics are based on manual measurements of stem density and diameter, and field estimates of basal area and tree height 3. Mean of the 5m gridded 95th percentile canopy height over the 40 x 40 m plot. 4. The Clearing plot was not treated as a 40 x 40 m plot that included all land cover within, but, rather, all data collection took place within the clearing, which renders the plot-scale canopy metrics irrelevant.

Table 4.2). At locations along the north-south transect, sensors were hung in trees on the south and north side of the tree at approximately 3 m above ground. Sensors on the east-west transect were hung on the north side of trees at 4 m above ground. Whereas the manufacturer-stated accuracy is ±0.5 °C for the temperature sensors, [*Lundquist and Huggett*, 2010] showed that sensors deployed in dense stands of trees are subject to a positive bias relative to a shielded sensor of up to 0.8 and 0.4 °C in daily maximum and mean temperature, respectively. Most sensors were subject to substantial shading from adjacent trees.

4.4.3 Snow Depth & Density

For the duration of continuous snowpack in WY 2011 and 2012, we performed manual snow surveys in select study plots, and from WY 2011 through 2014 we collected hourly snow depth

observations at Clearing Met with an acoustic snow depth sensor (

Site	Field Metrics[2]				LiDAR Metrics		
	Approximate Stem Density (stems hectare^{-1})	Mean Basal Area (m^2 hectare^{-1})	Mean Diameter at 1.4 m (cm)	Mean Tree Height (m)	% Canopy Cover		Canopy Height[3] (m)
					Mean	SD	Mean
Bear Creek (BC)	1018	80	28	38	92	3	34
	Metrics at additional control plots are similar to intensive control plot, but were not measured				88	12	31
	541	62	36	37	78	13	33
	Metrics at additional thinned plots are similar to intensive thinned plot, but were not measured				76	19	31
	Center of gap plots are clear of trees; refer to control plot metrics for surrounding forest metrics for gap plots				72	30	30
					71	29	30
	Metrics at additional forest plots are similar to intensive control plot, but were not measured				90	8	34
Clearing Met (CM)	0	NA	NA	NA	NA[4]	NA	NA
City Cabin (CC)	302	99	38-71	41-54	87	7	39
Mount Gardner (MG)	1370	60	23	25	94	4	22
	890	41	26	28	73	14	22
	Gap portion of plot is clear of trees; refer to control plot metrics for surrounding forest metrics for gap plot				73	31	22
	380	96	42-76	40-50	95	3	38
Tinkham Creek (TC)	891	55	36	31	90	12	23
	318	14	25	20	46	23	14
Rex River (RR)	320	20	27	15	32	18	10

1. Plot code, refers to the position within the Bear Creek site, with the southwest plot designated as Row 1 Column 1 (R1C01). 2. Forest metrics are based on manual measurements of stem density and diameter, and field estimates of basal area and tree height 3. Mean of the 5m gridded 95th percentile canopy height over the 40 x 40 m plot. 4. The Clearing plot was not treated as a 40 x 40 m plot that included all land cover within, but, rather, all data collection took place within the clearing, which renders the plot-scale canopy metrics irrelevant.

Table 4.2). Snow surveys, including snow depth transects and snow courses, were performed approximately bi-weekly, with more frequent surveys during the melt season, but the number of plots that were surveyed varied by field day. Snow depth was measured manually to the nearest 1 cm with an avalanche depth probe at 20 locations across each of two 20-35 m long, perpendicular transects of the study plots; at Clearing Met only one transect was completed. At five study plots, snow depth and SWE were measured in three locations using a federal snow sampler, and snow density was computed.

4.4.4 Snow Duration

We observed spatially distributed snow duration via three instruments: grids of individual iButtons (see above) that were shallowly buried in the ground, a 900 m linear transect of fiber-optic cable (FOC; BRUsens Temperature +85 °C; Brugg Cable International, Bragg, Switzerland) that was deployed on the ground surface, and time-lapse cameras mounted in trees. The FOC was paired with a Sensornet Oryx distributed temperature sensing (DTS) system (Sensornet, Elstree, United Kingdom), in order to generate laser light pulses and measure the corresponding reflected spectra, from which ambient temperature around the FOC is determined through the principle of Raman scattering [*Raman and Krishnan*, 1928; *Selker et al.*, 2006; *Tyler et al.*, 2009; *Lutz et al.*, 2012]. For the iButtons and FOC, we inferred daily snow presence from hourly or sub-hourly ground temperature [*Lundquist and Lott*, 2008; *Lyon et al.*, 2008; *Tyler et al.*, 2008; *Raleigh et al.*, 2013]. Rugged, time-lapse hunting cameras were mounted on trees and collected one or more images per day. Each image records a view of a portion of the plot, including 1-3 depth measurement poles. Thus, snow presence across the image can be quantified (e.g.,[*Dickerson-Lange et al.*, 2015a]) in addition to point snow depth.

The iButtons and FOC were used to derive a time series of snow presence for the support of the sensor (i.e., the area or length over which the instrument integrates an observation [*Blöschl*, 1999]), which was subsequently used to calculate snow duration metrics (e.g., snow disappearance date) at the point-scale, and to use the distribution of snow duration metrics at the plot-scale to characterize snow duration variability. Both the support and the spatial configuration of the instruments varied, resulting in differences between characterization of both point-scale and plot-scale snow duration. The FOC observed ground temperature integrated over every 1 m along the length of the cable and the iButtons were deployed in grids covering each plot. Spacing between iButton locations was designed to be either 5 or 10 m, but sensor failures resulted in larger spacing in some locations and years. Methods and a comparison of strategies to detect snow duration are discussed further in [*Dickerson-Lange et al.*, 2015a]. In total, snow duration data include the sub-daily raw ground temperature data from which snow presence was derived, the daily time series of snow presence/absence derived from each temperature instrument, related snow duration metrics, and daily time-lapse photographs.

4.4.5 Forest Canopy Characteristics

The forest canopy at each site is represented by a combination of airborne lidar data, manually measured forest metrics, and hemispherical photographs. Lidar data were collected over all of the study locations by the National Center for Airborne Laser Mapping (NCALM, see acknowledgements). The survey was performed with an Optech Gemini on 31 August and 1 September 2012 (i.e., leaf on), with an average pulse density of 7.5 m^{-2} and up to 4 returns per pulse. The mean and standard deviation of 5 m gridded canopy cover values derived from lidar

(i.e., the ratio of the number of returns from >2 m above the ground model to the total number of returns for the pixel), and mean canopy height over the study locations are provided in Table 4.1.

Prior to the start of the snow season in WY 2011, we measured canopy closure with a densiometer (Geographic Resource Solutions, Arcata, California) at 0.5 m intervals directly above the fiber-optic cable (FOC) transect, discussed above (see also Figures 5d and 7a of [*Dickerson-Lange et al.*, 2015a]). We used a nearest neighbor algorithm to take the 5 m average of canopy closure for every 1 m along the FOC. To further characterize the canopy, we took hemispherical photographs over select iButton and FOC locations, and under radiation instruments. The camera was leveled and oriented with the top toward north and five exposures were collected per location.

4.5 Example Application: Snow Depletion Curves

Accurate quantification of the spatial distribution of snow depth, SWE, and snow duration is critical for hydrological and ecological investigations. Since direct observations of both snowpack magnitude and extent are sparse, the relationship between distributed snow depth and snow cover is commonly used to estimate one quantity from the other [*Liston*, 1999, 2004; *Luce et al.*, 1999; *Faria et al.*, 2000; *Essery and Pomeroy*, 2004a]. In particular, snow depletion curves are used to parameterize fractional snow-covered area across a grid element as a function of snow depth and snow depth variability at peak values [*Luce et al.*, 1999; *Luce and Tarboton*, 2004; *Clark et al.*, 2011].

Whereas previous work to implement snow depletion curves in models relies on general categories of snow variability based on climate and land cover type [*Liston*, 2004], a potential application of this dataset is fitting snow depletion curves to observed data in order to parameterize the relationship for different forest treatments or test theoretical representations [*Pomeroy et al.*, 1998a]. In particular, the types of forest treatments in which we collected snow data span large portions of the Cedar River watershed. Therefore, estimating the relationship between snow depth and snow cover based on representative field data could support distributed modeling efforts across this landscape of distinct blocks of managed forest stands (e.g.,Figure 4.2).

Observations illustrate the differing relationship between snow depth and snow covered area, calculated from distributed measurements of snow duration, in three forest treatments (Figure 4.3). At the control plots, where the mean coefficient of variation (CV, the ratio of the standard deviation to the mean) of snow depth at peak depth is low (0.13), snow cover remains relatively continuous during ablation, and rapidly drops off when snow depth drops below 25%

of maximum snow depth. In contrast, at both the thinned and gap plots, the spatial variability of snow depth is higher (i.e., indicated by higher mean CV values, 0.16 and 0.22, respectively) and snow covered area begins to decrease when snow depth reaches 25-50% of maximum.

4.6 Conclusion

The dataset presented here quantifies snow metrics across experimental forest plots in a climate regime that has previously been shown to be an end point in the observed spectrum of forest influence on snow processes. These field observations include distributed snow magnitude and snow duration, and meteorological data collected over multiple years. In addition to the empirical snow depletion curves discussed above, potential applications of these data include assessing relations between canopy metrics and snow depth and duration, testing model representations of forest-snow processes, and assessing spatial and temporal variability in meteorological forcing data in different forest types. Furthermore, since the influence of forest on snow processes varies with climate, these data could provide a testing platform for modeling the hydrologic effect of a warmer winter climate in forested, mountain watersheds.

4.7 Acknowledgements

Primary support for data collection and analysis was provided by the National Science Foundation (NSF), CBET-0931780, and support for data archiving was provided by the Department of the Interior Northwest Climate Science Center (NW CSC) through a Cooperative Agreement GS297A from the United States Geological Survey (USGS). Lidar data collection and processing was provided by the National Center for Airborne Laser Mapping (NCALM, http://ncalm.cive.uh.edu/) via a seed grant to S. Dickerson-Lange, and Van Kane generously provided additional processing and analysis. We are grateful to Seattle Public Utilities for allowing watershed access and providing field equipment. We thank John Selker and Scott Tyler for providing the fiber-optic measurement equipment, cable, and considerable technical advice, and the Center for Transformative Environmental Monitoring Programs (http://www.ctemps.org) for supplying the distributed temperature sensing system. We especially thank the many people who assisted with field data collection, in particular Sam Barr, Teddy Thorson, and Adam Massmann. All data described herein are publicly available via the University of Washington (http://hdl.handle.net/1773/33268), the CUAHSI Water Data Center (https://dx.doi.org/10.4211/his-data-cedarriverforestsnow) and NSF Open Topography (http://www.opentopography.org/).

4.8 Tables

Table 4.1 Description of the location and forest characteristics at each study site and plot. Note that the table is split into two parts. The reader is referred to the published citation for a more legible version of this table.

Site	Elev. Range (m)	Site Description	Plot(s)	Plot Code(s)[1]	Plot Description (i.e., silvicultural treatment or forest type)
Bear Creek (BC)	620-640	A 400 m × 80 m domain of approximately 70 year old second-growth forest, dominated by western hemlock (*Tsuga heterophylla*) and Douglas-fir (*Pseudotsuga menziesii*), with some western redcedar (*Thuja plicata*), and Pacific silver fir (*Abies amabilis*) and noble fir (*Abies procera*). See [Spriegel et al., 2009; Lutz et al., 2012] for additional site details.	1 intensive control plot	R1C02	The control plots consist of untreated second-growth forest
			4 additional control plots	R1C03, R2C02, R2C07, R2C09	
			1 intensive thinned plot	R2C03	Approximately 30% of the basal area (i.e., sum of the cross-sectional stem area at 1.4 m height) was removed from each thinned plot with the largest trees retained.
			4 additional thinned plots	R1C07, R1C08, R2C05, R2C06	
			1 intensive gap plot	R2C10	The gap plots include a circular gap with a diameter of 20 m, equal to approximately one tree height, that was cut into the middle of the plot, and the surrounding second-growth forest.
			4 additional gap plots	R1C05, R1C06, R1C09, R2C08	
			5 additional forest plots	R1C01, R2C01, R1C04, R2C04, R1C10	The forest plots consist of untreated second-growth forest, and were excluded from random designation of control, thinned, or gap treatment due to higher pre-treatment heterogeneity (described in [Lutz et al. 2012]).
Clearing Met (CM)	740 - 745	An approximately 30 m diameter clearing at which two meteorological towers were installed in WY 2011. Data collection in this location took place only within the confines of the clearing and did not include the surrounding forest.	1 clearing plot	NA	see site description
City Cabin (CC)	775 - 780	A single study plot with approximately 300 year old western hemlock, Douglas-fir, and western redcedar. The stand is characterized by a relatively homogeneous canopy and sparse undergrowth for a stand of its age and location.	1 old-growth plot	NA	see site description
Mount Gardner (MG)	860-900	Four study plots, with three clustered within 100 m of the SNOTEL site, and one old-growth plot 600 m to the west. The second-growth forest at the Mount Gardner site is approximately 48 years old and includes Pacific silver fir as the dominant species, with some western hemlock, Douglas-fir, and western redcedar. The Mount Gardner old-growth plot is located in a 280 year old Douglas-fir and western hemlock stand.	1 control plot	NA	The control plot consists of untreated second-growth forest with little to no undergrowth present.
			1 thinned plot	NA	Approximately 30% of the basal area (i.e., sum of the cross-sectional stem area at 1.4 m height) was removed from the thinned plot, with the largest trees retained.
			1 gap plot (SNOTEL site)	NA	An oblong gap approximately 30 m x 20 m in size and the surrounding second-growth forest. The snow pillow is located just to the northwest of the plot.
			1 old-growth plot	NA	The plot consists of untreated old-growth forest, with a southern aspect on a 20° slope.
Tinkham Creek (TC)	910 - 930	Two study plots within 50 m of the SNOTEL site.	1 control plot	NA	The control plot is located adjacent to the SNOTEL site, and adjacent to a small, ephemeral tributary to Tinkham Creek. The forest is 58 years old, has a closed canopy, and consists of Pacific silver fir, western hemlock, and Douglas-fir, with very little undergrowth.
			1 thinned plot (multiple thinnings)	NA	The thinned plot, which has been subject to multiple episodes of thinning, is located 60 m uphill from the control plot, with an eastern aspect on a 20° slope. The forest composition is similar to the nearby control plot, but with a more open canopy and a dense understory, dominated by wild blueberry (*Vaccinium alaskaense* and *V. ovalifolium*).
Rex River (RR)	1160 - 1165	One thinned plot located in a flat terrace adjacent to the SNOTEL site on the northwest-facing side of the headwater basin of the Rex River. The forest has an open canopy and consists of 47 year old Pacific silver fir and dense understory of huckleberry (*Vaccinium membranaceum*) and blueberry (*V. alaskaense*).	1 thinned plot (multiple thinnings)	NA	see site description

Site	Field Metrics[2]				LiDAR Metrics		
	Approximate Stem Density (stems hectare^{-1})	Mean Basal Area (m^2 hectare^{-1})	Mean Diameter at 1.4 m (cm)	Mean Tree Height (m)	% Canopy Cover		Canopy Height[3] (m)
					Mean	SD	Mean
Bear Creek (BC)	1018	80	28	38	92	3	34
	Metrics at additional control plots are similar to intensive control plot, but were not measured				88	12	31
	541	62	36	37	78	13	33
	Metrics at additional thinned plots are similar to intensive thinned plot, but were not measured				76	19	31
	Center of gap plots are clear of trees; refer to control plot metrics for surrounding forest metrics for gap plots				72	30	30
					71	29	30
	Metrics at additional forest plots are similar to intensive control plot, but were not measured				90	8	34
Clearing Met (CM)	0	NA	NA	NA	NA[4]	NA	NA
City Cabin (CC)	302	99	38-71	41-54	87	7	39
Mount Gardner (MG)	1370	60	23	25	94	4	22
	890	41	26	28	73	14	22
	Gap portion of plot is clear of trees; refer to control plot metrics for surrounding forest metrics for gap plot				73	31	22
	380	96	42-76	40-50	95	3	38
Tinkham Creek (TC)	891	55	36	31	90	12	23
	318	14	25	20	46	23	14
Rex River (RR)	320	20	27	15	32	18	10

1. Plot code, refers to the position within the Bear Creek site, with the southwest plot designated as Row 1 Column 1 (R1C01). 2. Forest metrics are based on manual measurements of stem density and diameter, and field estimates of basal area and tree height 3. Mean of the 5m gridded 95th percentile canopy height over the 40 x 40 m plot. 4. The Clearing plot was not treated as a 40 x 40 m plot that included all land cover within, but, rather, all data collection took place within the clearing, which renders the plot-scale canopy metrics irrelevant.

Table 4.2 Overview of which observations were collected at each plot over four winters of data collection. Note that the table is split into two parts. The reader is referred to the published citation for a more legible version of this table.

Site	Co-located SNOTEL station number	Plot(s)	Snow Magnitude			
			Snow Depth	Snow Course	Snow Depth	Snow Course
			2011		2012	
Bear Creek (BC)	none	1 intensive control plot	x	x	x	x
		4 additional control plots	x		x	
		1 intensive thinned plot	x	x	x	x
		4 additional thinned plots	x		x	
		1 intensive gap plot	x	x	x	x
		4 additional gap plots	x		x	
		5 additional forest plots				
Clearing Met (CM)	none	1 clearing plot	x	x	x	x
City Cabin (CC)	none	1 old-growth plot	x	x	x	x
Mount Gardner (MG)	898	1 control plot 1 thinned plot 1 gap plot (SNOTEL site) 1 old-growth plot				
Tinkham Creek (TC)	899	1 control plot 1 thinned plot (multiple thinnings)				
Rex River (RR)	911	1 thinned plot (multiple thinnings)				

Site	Snow Duration and Snow Cover									Meteorologic Data[2]				
	Fiber Optic Cable	Ground iButtons				Time-Lapse Camera[1]				Met Station (Water years of operation)	Sensors in Trees (Number of sensors at different heights)			
	2011	2011	2012	2013	2014	2011	2012	2013	2014	2011-2014	2011	2012	2013	2014
Bear Creek (BC)	x	x	x	x	x	M	P	P		T, RH, WS (2011-2013)				
	x													
	x	x	x	x	x	M								
	x													
	x	x	x	x	x	M	P	P		T, RH, WS (2011-2012)		T/RH (2)	T/RH (3)	T (3)
	x													
	x													
Clearing Met (CM)						M	P	P		T, RH, WS, WD, SR, PAR, SD (2011-2014)				
City Cabin (CC)				x	x	M	P	A		T, RH, WS, PAR (2011-2013)			T/RH (2)	T/RH (1)
Mount Gardner (MG)		x	x	x	x			P		T, RH, WS (2011-2012)				
		x	x	x	x				A		T/RH (2)	T/RH (2)	T/RH (1)	T (1)
		x	x											
				x	x			P					T/RH (1)	T/RH (1)
Tinkham Creek (TC)				x	x									T/RH (1)
				x	x			P	A				T/RH (1)	T/RH (1)
Rex River (RR)				x	x			P						

1. The operation of time lapse cameras varied from continuous to intermittent, therefore the continuity is classified as follows: A = all, covers entire snow season with daily resolution. M = most, covers entire snow season (including disappearance) with some gaps. P = partial, camera failed before final snow disappearance. 2. Meterological observations included: T = air temperature. RH = relative humidity. WS = wind speed. WD = wind direction. SR = incoming solar radiation. PAR = incoming photosynthetically active radiation. SD = snow depth.

4.9 Figures

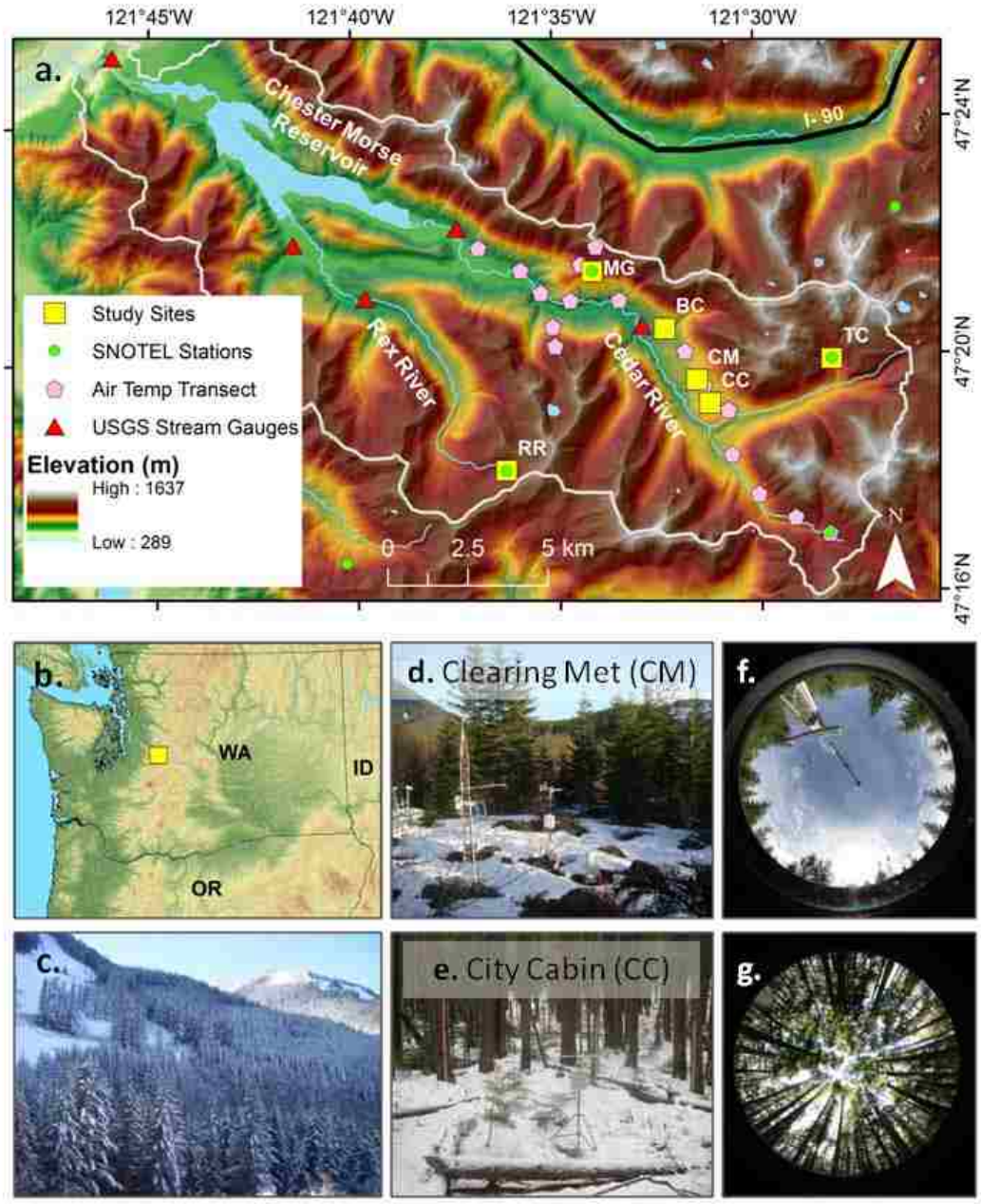

Figure 4.1 Map of the upper Cedar River Municipal Watershed (a), with locations of point observations indicated, and location of the watershed shown in regional context (b). Photograph of the north-facing side of the Cedar River valley taken near Mount Gardner (MG) shows typical combination of forest cover interspersed with talus fields (c). Photographs at Clearing Met (d and f) and City Cabin (e and g) show meteorological stations, and hemispherical photographs taken from below the respective pyranometers show the overlying canopy.

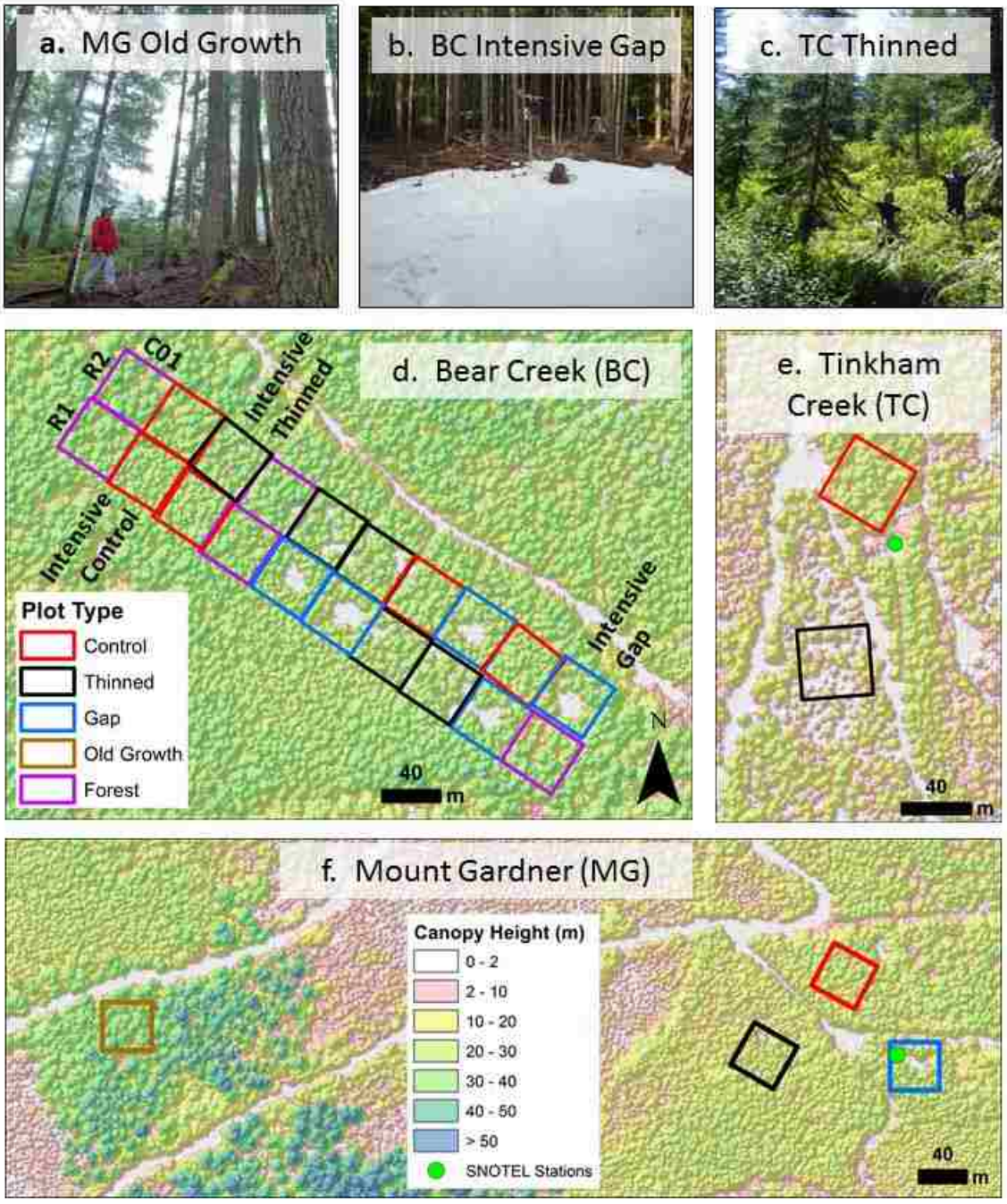

Figure 4.2 Photographs and lidar-derived canopy height (overlaid on canopy surface model) showing examples of forest plots. The Mount Gardner (MG) old-growth plot (a) is shown in context of canopy height and location relative to the other MG plots (f). The Bear Creek (BC) intensive gap plot (b) is one of five gap plots at BC (d), where each forest treatment is replicated at five experimental plots; rows 1 and 2 (R1 and R2) and column 1 (C01) are indicated for distinguishing BC plots by plot code. The Tinkham Creek (TC) thinned plot (c) represents a sparse forest canopy at the higher elevation TC site (e).

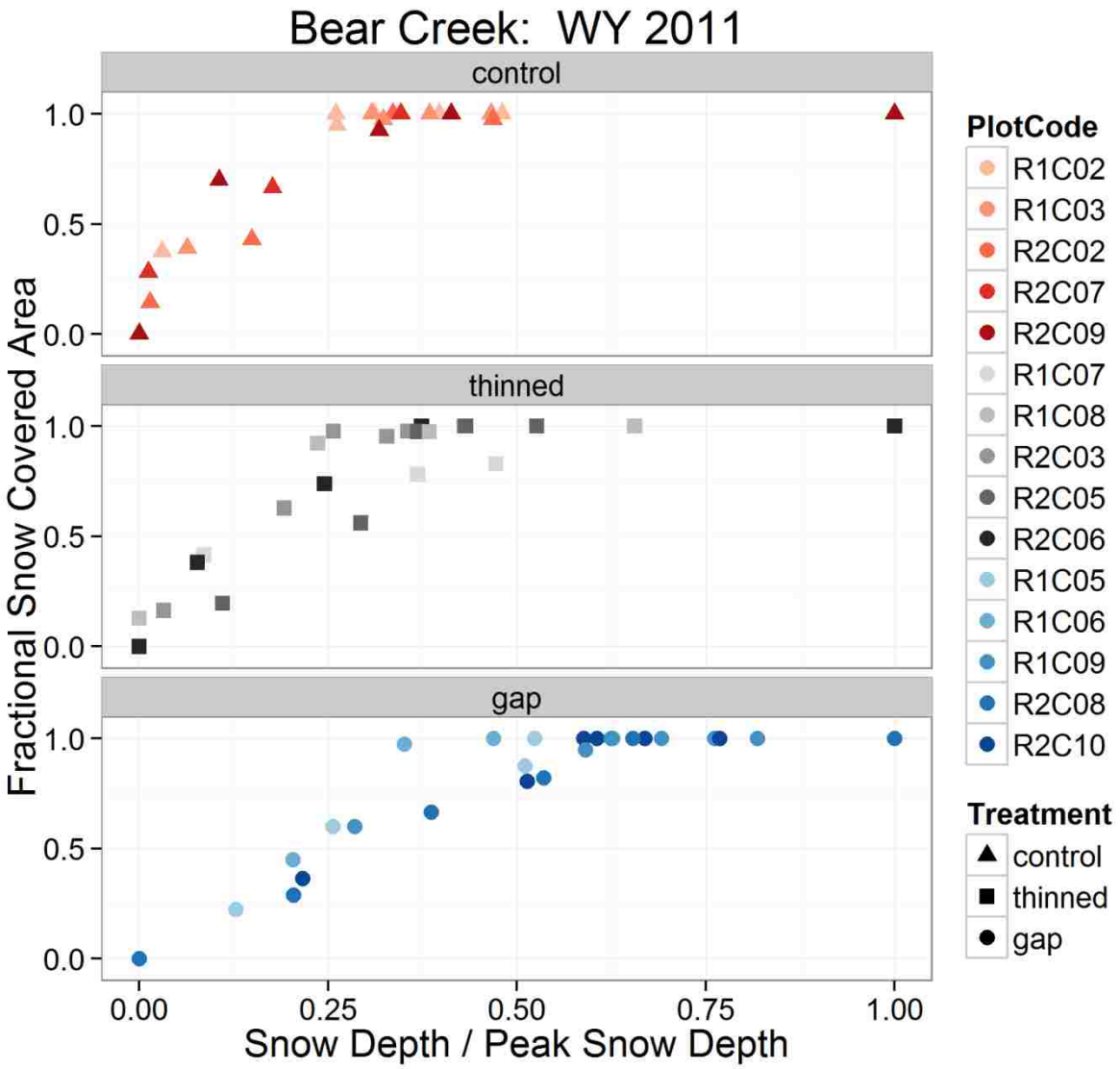

Figure 4.3 Fractional snow covered area as a function of snow depth (relative to the maximum snow depth) for each plot, at all of the BC experimental plots in WY 2011. The data are grouped by forest treatment, including five control plots (a), five thinned plots (b) and five gap plots (c), with the gradations in color indicating the individual plot (i.e., plot code, see Table 4.1 and Figure 4.2d). Snow depth is the mean of bi-weekly manual snow depth transects at each plot, and fractional snow covered area was derived from ground temperature observed by fiber-optic cable (n≈40 at each plot) for the same day that snow depth was measured.

Chapter 5. Challenges and successes in engaging citizen scientists to observe snow cover: From public engagement to an educational collaboration

Susan E. Dickerson-Lange[1,4], Karla Bradley Eitel[2], Leslie Dorsey[2], Timothy E. Link[3], and Jessica D. Lundquist[1]

[1]Civil and Environmental Engineering, University of Washington, Seattle, Washington, USA
[2] McCall Outdoor Science School, College of Natural Resources, University of Idaho, McCall, Idaho, USA
[3]Department of Forest, Rangeland, and Fire Sciences, University of Idaho, Moscow, Idaho, USA

Note: This chapter has been published in its current form as an article in the Journal of Science Communication [*Dickerson-Lange et al.*, 2016a]; the only differences are in section, figure, and table numbering.

5.1 Abstract

Whereas the evolution of snow cover across forested mountain watersheds is difficult to predict or model accurately, the presence or absence of snow cover is easily observable, and these observations contribute to improved snow models. We engaged citizen scientists to collect observations of the timing of distributed snow disappearance over three snow seasons across the Pacific Northwest, USA. The primary goal of the project was to build a more spatially robust dataset documenting the influence of forest cover on the timing of snow disappearance, and public outreach was a secondary goal. Each year's effort utilized a different strategy, building on the lessons of the previous year. We began by soliciting our professional networks to contribute observations via electronic or paper forms, moved to a public outreach effort to collect geotagged photographs, and finally settled on close collaboration with an outdoor science school that was well-positioned to collect the needed data. Whereas the outreach efforts garnered abundant enthusiasm and publicity, the resulting datasets were sparse. In contrast, direct collaboration with an outdoor science school that was already sending students to make weekly snow observations proved fruitful in both data collection and educational outreach. From a data collection standpoint, the shift to an educational collaboration was successful because it essentially traded wide spatial coverage combined with sparse temporal coverage for dense temporal coverage at a single, but important, location. From a public engagement standpoint, the partnership allowed for more intensive participation by more people and enhanced the science curriculum at the collaborating school.

5.2 Context

The spatial pattern of snow cover across a forested mountain watershed is easily observed by outdoor enthusiasts who readily make note of snow disappearance patterns at a range of scales when they avoid skiing into tree well, change a hiking route after encountering a snow field, or capture a photograph of patchy snow across a valley. Whereas these patterns are obvious to an observer, reproducing such a pattern via a computer model is an ongoing research challenge[*Essery et al.*, 2009]. Hydrologic models attempt to incorporate the physical influences of forest cover on snow processes, but are limited by approximations of physical processes that are based on site-specific field data that may lack transferability to different climates and forests[*Clark et al.*, 2015]. In particular, observational data documenting snow cover patterns, which represent the spatial variability of the timing of snow disappearance, in forested mountain watersheds are needed because the net effect of forest cover on snow can be to delay or accelerate the date of snow disappearance relative to open areas[*Lundquist et al.*, 2013]. Subsequently, the timing of snow disappearance influences soil moisture availability, streamflow amount, and stream temperature during the dry summer season in the mountains of the American West[*Lundquist et al.*, 2005; *Ford et al.*, 2013]. By capitalizing on the presence of hikers, skiers, snowmobilers and others who are often in "the right place at the right time" to observe snow cover patterns, a citizen science approach has the potential to yield critical data to further understanding of snow processes and to test watershed models.

Improved estimates of the effect of forest management actions, such as thinning or clear-cutting, on the timing of snow disappearance are relevant to land managers who consider multiple objectives when making decisions, including forest resilience to insect outbreaks, aquatic ecosystem health, fire fuels management, and adaptation to climate change. Previous

work has supported the creation of forest gaps as a way to retain snow on the landscape [*Dickerson-Lange et al.*, 2015a] and thus shift the timing of peak spring streamflows to later in the year (i.e., due to later snowmelt[*Ellis et al.*, 2013]) to the benefit of late season water supply and ecosystem health. However, this management strategy is likely to have the intended effect only within a specific set of conditions. The magnitude and direction of forest influences on snow processes, such as snow accumulation and melt, depends on winter climate[*Lundquist et al.*, 2013], topographic position such as north- versus south-facing slopes[*Ellis et al.*, 2013], and forest composition and density[*Kittredge*, 1953].

Thus, in order to support an ongoing effort to develop management-relevant maps of where forest is likely to delay versus accelerate snow disappearance in the Pacific Northwest, USA, additional field data documenting the differential timing of snow disappearance between forested and non-forested areas are needed. Unfortunately, such observational data are limited in both temporal and spatial coverage because field campaigns are expensive, time-consuming, and hindered by access issues[*Elder and Cline*, 2003]. Furthermore, satellite methods to detect snow cover are uncertain within forests because the tree canopies obscure the ground surface conditions[*Raleigh et al.*, 2013]. Therefore, even after incorporating field data from a network of collaborating institutions across the region into this project there are still critical data gaps in parts of the region, including eastern Washington, eastern Oregon, and central Idaho, each of which has unique climate and forest conditions (Figure 5.1a).

Since the beautiful mountain landscapes that attract outdoor enthusiasts are home to the same locations in which additional forest-snow observations are needed, engaging the people who already recreate there in collecting data seems ideal. Furthermore, with a particular interest in the snowmelt season (i.e., spring and summer), skiers who are seeking spring snow and hikers

who are seeking snow-free routes are well-positioned to collect data at the optimal time to capture differential timing of snow disappearance across forested and open areas.

This model of opportunistic citizen science has previously proven successful in locations that people are motivated to visit, such as to see the wildflowers bloom on Mount Rainier each summer[*Wilson et al.*, 2015]. Many successful citizen science projects leverage large numbers of observations to develop robust spatial or temporal resolution, and to reduce the uncertainty associated with amateur data collectors. For example, one million bird observations are submitted from around the world each month as part of the bird observation programs implemented by the Cornell Lab of Ornithology[*Bonney et al.*, 2009]. The utilization of citizens to collect large numbers of data points is typically associated with minimal training, and this strategy has been described as utilizing citizens as sensors[*Haklay*, 2013] or as crowdsourcing in a framework of the possible levels of engagement of citizen scientists (hereafter "level 1").

In the same model[*Haklay*, 2013], the next level of participation (hereafter, "level 2") involves more training in order to develop interpretation skills, relying on participants to complete some basic interpretation while collecting data. The data collected by citizens who are participating in a level 2 project are likely to be higher quality, but since data collection involves more training and therefore is more time and energy-intensive, a level 2 project is also likely to engage fewer people. Many successful school-based citizen science programs occur at this level, in which teachers provide instruction, a framework for participation, and assistance in making decisions about when and where to collect data[*Rock and Lauten*, 1996; *Eick et al.*, 2008]. Such programs have been shown to generate high quality data[*Lawless and Rock*, 1998; *Galloway et al.*, 2006; *Peckenham and Peckenham*, 2014] in addition to improving educational outcomes[*Bingaman and Eitel*, 2010; *Schon et al.*, 2014].

Although citizen science arguably has its roots in ecology in general[*Silvertown*, 2009], and surveys in particular, many previous efforts have successfully incorporated citizen science in hydrology[*Buytaert et al.*, 2014]. These investigations have focused primarily on water quality[*Peckenham and Peckenham*, 2014] or water quantity in the form of precipitation[*CoCoRaHS*, 2015] or streamflow[*Lowry and Fienen*, 2013]. Previous snow hydrology investigations to formally utilize citizen scientists are limited, as far as we are aware, to a snow study that involves tweeting point snow depth values (http://scistarter.com/project/205-SnowTweets?tab=project, accessed 14 May 2015) but citizen observations of snow presence and conditions are certainly included in backcountry snow reports utilized by the recreation community (e.g., http://www.wta.org/go-hiking/trip-reports, accessed 14 May 2015) and on social media.

In addition to providing a method to collect spatially distributed data, citizen science has been shown to have key benefits for public engagement. Projects have yielded positive social benefits by enhancing community collaboration[*Borden et al.*, 2007], increasing participation in locally-relevant environmental issues[*Cooper et al.*, 2007], and guiding development of land management strategies[*Rosenberg et al.*, 2003]. Bonney *et al.*[*Bonney et al.*, 2014] further predict that increased implementation of citizen science holds potential for strengthening the relationship between scientific efforts and society. Since the ongoing forest-snow investigation described here has potential management applications, communication with land managers and public stakeholders is a key project goal, and a citizen science approach provides an avenue to engage the public in addition to collecting data. Thus, in March 2012, we moved forward with enthusiasm for the idea but few analogous models for utilizing citizen science to observe snow cover and develop a more spatially robust dataset for the Pacific Northwest.

5.3 Objective & Methods

Motivated by the clear congruence between our data needs, public outreach goals, and the already-occurring citizen forays into the mountains, we began a citizen science project three years ago to document the timing of snow disappearance across the mountains of the Pacific Northwest. The project was initiated by a team of two university researchers at the University of Washington, and evolved into collaboration between three universities and a K-12 outdoor science school. We detail our citizen science effort from the perspective of both researchers and educators, using the writing voice of the research institutions but including co-authors from both sides of the educational collaboration.

The project evolved substantially each year as we incorporated lessons from the successes and failures of the previous year. This citizen science effort was motivated first and foremost by a critical need for more distributed data across the greater Pacific Northwest region, rather than as a study of citizen science itself. Thus, evaluation efforts focused on quantifying the usable data received each year in an effort to understand what was working for meeting our scientific goals. To consider the success of the project in terms of public outreach, we informally assessed the experience of participants through written comments included in data submission and follow-up email communications and made adjustments accordingly.

Whereas the first two years were effective in increasing engagement with public stakeholders, the participation model that we utilized did not ultimately match our primary data needs. We therefore re-assessed the requirements for usable data and shifted our focus from public engagement to collaboration with an outdoor science school on the third year, effectively trading spatial coverage for usable temporal resolution. This tradeoff between breadth and depth has been previous identified as a potential difficulty facing researchers who delve into citizen

science[*Riesch et al.*, 2013]. However, we found that the decision to change our focus from widespread participation to a single site was a turning point in the overall success of the project and a model from which the project could again expand in spatial scope. We therefore present the relevant experiences and lessons from three years of citizen science, with a particular emphasis on the evolution of the project from public outreach to educational collaboration.

5.4 Results

5.4.1 Year One and Two: The Evolution of a Citizen Science Effort

We originally envisioned the citizen science project as a crowdsourcing effort[*Howe*, 2006; *Haklay*, 2013] in which numerous participants, who were in the mountains during the spring and summer for other purposes (e.g. recreation), would document observations of the differential timing in snow disappearance between forested and open areas. In essence, we needed comparisons of snow presence between forested areas and meadows or clearings that would allow us to determine 1) where snow lasted longer in the forest versus an equivalent open area (or vice versa), and 2) how long the snow persisted in the forest after disappearing from the clearing (or vice versa).

In year one, we contacted our personal networks to solicit "beta testing" from people we knew who were likely to be in the mountains during the melt season, including researchers, a national park scientist, and mountaineers. We developed a questionnaire to record time and location details, relative snow presence, and opportunities for additional observations and feedback. We provided basic instructions in email communications and two formats for responding: an on-line Google form and a paper form. We received 12 electronic responses and 2 paper responses, from which we extracted five data points for the investigation.

Two key issues arose from the data. First, the location and physical data associated with each response were not always adequate; for example, a trail rather than a precise location would be given because the hiker either did not have a Global Positioning System (GPS) or had a GPS but did not have a convenient way to record their position. Second, the responses did not always contain the direct comparison between forest and open areas that we were interested in; for example, one response described the snow conditions above tree line. We additionally observed

that we lacked both spatial and temporal resolution in the year one dataset, but we attributed our sparse dataset to the "soft" roll-out in year one.

Feedback from the participants communicated a general sense of enthusiasm for the scope of the project, but also reflected some of the same data issues. Participants commented that they thought they understood what observations to collect in the field, but then were unsure when it came time to fill out the form upon their return. The most complete observations came from a participant who routinely makes multi-day treks in the mountains and specifically requested that we provide a paper form that could be used to make notes while in the field. Our assessment from our year one experience was that we needed to streamline the data collection and submission process, to provide more explicit instructions, and to recruit more participants.

Thus, we began year two with a change in focus from recording written observations to collecting geotagged photographs, improved educational materials, and an effort to recruit many more participants to generate more data in both time and space. The advantage of geotagged photographs is that the metadata embedded in the photograph includes the key information, including date and time, latitude and longitude, and elevation, and they are easy to take with a smartphone or GPS-enabled camera[*Wilson et al.*, 2015]. We updated our website and written materials with education related to the project and re-tooled directions to describe 1) how to take a geotagged photograph, 2) what to take the photos of, and 3) how to submit the photos. We created a 2-minute YouTube video describing the project and how to participate (https://www.youtube.com/watch?v=JEmIV9vOXZ4). With the infrastructure in place, we reached out to the community via calls and emails to hiking organizations, emails to university and research groups, blog posts, presentations at conferences and professional meetings, and the personal networks of the research team. We embedded a Google Earth map into the project

website to display observations as they were submitted next to our model predictions for the region. Judging from the abundant enthusiasm that we encountered, we prepared ourselves for numerous submissions and declared the public outreach goal of the project to be a success.

However, from the standpoint of usable data, the 28 photo submissions from 9 individuals that we received were less than we had hoped for, and the usability of the observations documented in photographs was highly variable. Participants in year two included hikers, mountaineers, and scientists doing other field research, and they provided positive feedback that they enjoyed contributing to the investigation. However, the range in the field of view of the photographs created challenges for data analysis, with submissions that ranged from landscape shots to photographs documenting local snowmelt features such as tree wells. With landscape shots, the geolocation of the photograph (i.e., the coordinates of the camera position) does not match the geolocation of the observation, nor indicate the topographic position of the subject (i.e., a north-facing versus south-facing slope). With close-up shots, the spatial context of the observations is not apparent, so drawing a conclusion about snow presence within a forest becomes difficult when looking at only a few trees.

5.4.2 Reflection: More data points or more engagement?

At the end of year two we substantially reconsidered our strategy and ultimately redesigned the project. To date, the observations that we had received were too sparse in both time and space to provide a meaningful way to bracket the difference in the timing of snow disappearance between the forest and the open. At best, photographs from a single location could tell us whether snow persisted longer in the forest or in the open, but could not indicate the absolute difference in timing, which is critical to our investigation. We realized that even without issues

of data quality, we would need many, many more observations for the approach of collecting geotagged photographs to be successful.

Upon reflection, we discovered a mismatch between the level of engagement and the numbers of participants that we needed for the dataset that we originally envisioned. We realized that our vision of participation fell between two common levels of citizen science engagement [*Haklay,* 2013]. We wanted participants to function at level 2 and make an informed decision about where to observe a fair comparison between snowpack in the forest and open and about the spatial scale at which to document that comparison. At the same time, we fundamentally needed a lot of data to bracket differential snowmelt timing over such a large region, which calls for a level 1 approach. Since the design of our project fell in between the two levels, the program did not successfully engage participants at either level. On one hand, our training resources and participation guidelines were not fully utilized by those who did participate which resulted in unusable data. Simultaneously, the extensive directions probably acted as a barrier to achieve widespread participation by making the process too complicated.

Additionally, a level 1 approach is perhaps most feasible when the subject of data collection is inherently interesting or photogenic, as in the case of birds or wildflowers. Snowy landscapes are frequently photographed, but close range views of melting snow have less general appeal. We briefly considered mining public repositories of photographs for the observations and locations of interest as previously tested for monitoring wildflower phenology on Mount Rainier[*Wilson et al.*, 2015]. However, we ruled this option out because the spatial scale of landscape photographs would limit our data quality, and the approach lacks a meaningful public outreach component. We were left with a choice to make: focus on expanding participation in a simplified public project or focus in on training volunteers who would commit to making repeat

observations in specific locations. Around the time that we were considering how to move forward, we became aware of the University of Idaho College of Natural Resources' McCall Outdoor Science School (MOSS), and quickly realized that a direct collaboration with an education program located in a region where we needed data could be a solution to meet both our data needs and our goal to involve public stakeholders. Thus, we shifted our focus from a public outreach to a collaboration, in which we would trade spatial coverage for informed participation and high temporal resolution via repeat observations.

5.4.3 Year Three: Collaboration with MOSS

From our first conversation it became apparent that a partnership between the research institutions and the MOSS would be mutually beneficial. MOSS is a residential outdoor science school serving more than 2500 students each year in week-long inquiry-based, place-based experiential science programs. Each week throughout the school year, groups of approximately 60-80 5^{th} – 8^{th} grade students from a variety of locations throughout Idaho, Oregon, and Washington travel to MOSS to spend a week attending school in the outdoors. Their instructors are graduate students enrolled in a graduate residency in environmental education through the University of Idaho's College of Natural Resources. The winter curriculum at MOSS focuses on snowpack dynamics, hydrology, winter ecology and energy balances, so the citizen science project was a natural complement to the existing curriculum. MOSS instructors lead field groups of 8-12 students into snow-covered, forested field sites on a weekly basis to collect snow data, resulting in groups who are well-positioned to constrain the timing of snow disappearance to a weekly temporal resolution.

The structured, educational data collection program implemented at MOSS is atypical from the standpoint of a traditional citizen science project in which volunteer citizens participate on an ad hoc basis. However, the program also very clearly fits the model for best practices related to involving citizens in scientific research that was developed by the Cornell Lab of Ornithology, which has famously led large-scale successful citizen science projects such as Project Feederwatch and the Great Backyard Bird Count[*Bonney et al.*, 2009]. The Cornell citizen science framework served as a guide for developing the collaboration and provides guidance for reflection on successes and possible improvements. For our experience, the first steps in the framework were already complete by the time we initiated the collaboration, including choosing a scientific question and forming the collaborative team.

The key step that was essential to complete together was to adjust and test protocols and materials for implementation in the MOSS program. This step was initiated via conversations about the nature of the data collection needs and the MOSS program, with both the research team and the MOSS team trying to understand how one would most easily and beneficially fit into the other. Since the MOSS program already includes instructor-led field excursions and field data recording on tablet computers, we decided to 1) standardize the locations which each instructor would visit each week so as to collect repeat observations in the same place, 2) design protocols to include taking photographs to record observations (Figure 5.1b), and 3) build a web-based form for data entry of estimated snow cover (Figure 5.1c). The research team provided initial protocols and drafts of web forms, with iterative feedback from the MOSS team as to the fit for their curriculum and logistics. The MOSS team was responsible for site selection and training of graduate students, with feedback and contributions from the research team via a video seminar.

By incorporating two forms of data collection in the protocols, including photographs and field-based estimates, we met the dual goals of collecting quality data and providing students a means by which to see their contribution to the project. The fraction of snow-covered area in each cardinal direction was estimated for the forested and open portions of each site, entered into the web form while in the field, and then automatically averaged and displayed as a time series plot (Figure 5.1c). As a subjective estimate, these numbers could then be validated via quantitative image analysis.

Although the program seemed to be a perfect fit in many ways, the implementation into the MOSS curriculum was not without challenges. Each graduate instructor was responsible for visiting their site every other week, ideally with their students, but this did not always happen. Reaching a fixed site via snowshoes during field instruction was occasionally limited by students' physical abilities and stamina, as well as bad weather. Future integration of the data collection into instructor training will help to define it as an integral part of the educational experience rather than an additional task. Other challenges were encountered during the key step of recruiting participants for a citizen science program; in this case recruitment was easy since the data collection was integrated into the overall educational program. However, we suspect that the fact that participation was not entirely voluntary did occasionally result in a lack of motivation on the part of the instructors. Based on informal conversations with instructors we determined that their level of commitment varied between those who were motivated by the educational opportunity of collecting data relevant to a research investigation, to those with lower interest due to difficulty getting to the site, lack of understanding of the importance of the work, or lack of understanding how to incorporate the data collection into the rest of the field curriculum. For the future we would implement face-to-face meetings between the research team

and the graduate instructors to instill a sense of why the research matters. Although such a meeting is not possible with the student groups, we are also considering making an introductory movie or meeting with students each week via video-conferencing technology.

From the perspective of MOSS, the citizen science program provides a promising way in which to connect educational activities to scientific practice. In addition to content exploration, the MOSS curriculum focuses on engaging students in the process of doing science, so partnering with research projects provides a way for students to connect with real scientists, and to see their data contribute to an on-going investigation. Previous studies have demonstrated that citizen science provides a platform on which science process skills can be practiced[*Trumbull et al.*, 2000], and that participants show an increased support for science, scientific literacy, and sense of connection to the environment[*Conrad and Hilchey*, 2011]. Future iterations of this project at MOSS could include a formal evaluation of the participation experience of both students and graduate instructors in order to measure any or all of these learning outcomes and enhance our understanding of how to improve the program.

From a research perspective, we drastically limited the spatial scope of our citizen science project by abandoning our dispersed approach and partnering with MOSS for improved temporal data resolution. However, there are three key scientific reasons that this partnership proved more successful than previous years: 1) the data collected by students and instructors conformed to standardized protocols and were therefore high quality, 2) repeat observations through time were collected at a scientifically relevant time step, and 3) observations at the MOSS field site fill a spatial data gap for the project. For all of these reasons the MOSS dataset is being incorporated into the regional investigation, and represents important field data from a geographic and

climatic data gap. As the only data from central Idaho, these observations record forest-snow interactions that are specific to a colder, continental/maritime climate regime.

5.5 Conclusion

Overall, two key lessons arose from our three year experience with citizen science: 1) the data collection needed for the investigation needs to align with the strengths of the citizen science approach, and 2) the level of participation needed from the audience needs to align with both the regular activities and interests of the audience and the type of data being collected. For us, the first lesson was built into our approach when we recognized that this would be an ideal citizen science project. We are investigating processes that are difficult to model but straightforward to observe for someone who is in the right place at the right time. Thus, from the beginning we recognized that the data needed for this investigation would align well with a citizen science approach.

The second lesson was learned via the successes and failures over three years. In scaling up from year one to year two we focused on expanding participation in order to develop a spatially and temporally dense dataset. However, the flaw in this approach was that the level of engagement was mismatched with the numbers needed to achieve the desired dataset. Whereas we needed participants to collect data in an informed and thoughtful way, we also needed a large quantity of data that would be more readily achievable by engaging a large number of participants. Thus, we chose to compromise broad spatial coverage for quality data and changed our focus from engaging the public to engaging an organization that makes repeat trips to the same locations. We gave up the desired spatial resolution but achieved the temporal resolution and structured data collection that resulted in a usable dataset.

Through trial and error, we better defined the parameters for the collection of usable data, and we recognized that we either needed orders of magnitude more data in order to filter out the unusable data, or we needed our participants to follow specific instructions. We therefore honed

in on the style of citizen science that resulted in success for the partnership and success for the investigation. In connecting with MOSS, we partnered with an organization that was already collecting similar data and that was seeking ways to make educational data collection more meaningful for students via connection with a research effort. Furthermore, the pilot program with MOSS has the potential to be replicated with other schools or organizations that are already making repeat visits to locations of interest throughout the snow season. Possible future partners include outdoor education centers located in mountainous or snowy regions, as well as organized recreational groups, such as snowmobiling clubs that make repeat trips along certain trails. In addition to the potential application of the approach described herein to other distributed snow studies, any scientific project to employ a citizen science for collecting distributed data may benefit from consideration of a spatially targeted approach.

In conclusion, our three year journey with citizen science resulted in meaningful connections with a wide range of interested individuals and organizations. In addition to the benefits of communicating current research to the public and supporting the educational goals of MOSS, the effort resulted in a temporally consistent dataset that filled a single spatial data gap in our regional analysis of forest influences on the timing of snow disappearance.

5.6 Acknowledgements

Primary support for the citizen science projects was provided by the National Science Foundation, CBET-0931780, and the Department of the Interior Northwest Climate Science Center (NW CSC) through Cooperative Agreement GS297A from the United States Geological Survey (USGS). The contents of this manuscript are solely the responsibility of the authors and do not necessarily represent the views of the NW CSC or the USGS. We are grateful to the many organizations and individuals that supported this effort each year, especially the instructors and students at the McCall Outdoor Science School, the Mountaineers, Anne Nolin, JoAnna Wendel, and Dave Tucker.

5.7 Figures

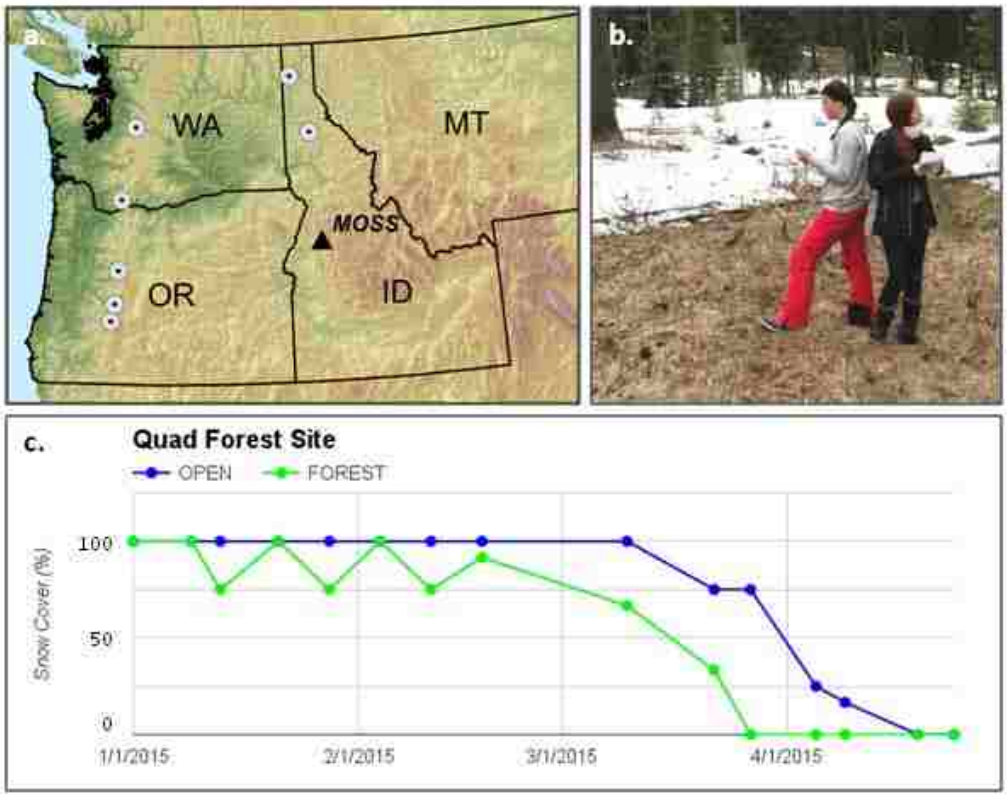

Figure 5.1 Map of the Pacific Northwest showing collaborating field sites (gray dots) and McCall Outdoor Science School (MOSS, black triangle) (a). Photograph of MOSS students estimating snow cover in different directions (b). Example graph of average snow cover in open and forested areas at Quad Forest, one of the MOSS field sites. Graphs for each site were updated in real-time on a website that was linked to the online form for data collection (c).

Chapter 6. Snow disappearance timing in warm winter climates is dominated by forest effects on snow accumulation

Susan E. Dickerson-Lange[1,6], Rolf F. Gersonde[2], Jason A. Hubbart[3], Timothy E. Link[4], Anne W. Nolin[5], Gwyneth H. Perry[1], Travis R. Roth[5], Nicholas E. Wayand[1], and Jessica D. Lundquist[1]

[1]Civil and Environmental Engineering, University of Washington, Seattle, Washington, USA
[2] Seattle Public Utilities, Seattle, Washington, USA
[3]University of West Virginia, Morgantown, West Virginia, USA
[4]College of Natural Resources, University of Idaho, Moscow, Idaho, USA
[5]College of Earth, Ocean, and Atmospheric Sciences, Oregon State University, Corvallis, Oregon, USA

Note: This chapter is under review at *Hydrological Processes*.

6.1 Abstract

Forests modify snow processes and affect snow water storage as well as snow disappearance timing. However, forest influences on snow accumulation and ablation vary with climate and topography, and are therefore subject to substantial temporal and spatial variability. We utilize multiple years of snow observations from across the Pacific Northwest, USA, to assess forest-snow interactions in the relatively warm winter conditions characteristic of maritime and transitional maritime-continental climates. We (1) quantify the difference in snow magnitude and disappearance timing between forests and open areas and (2) assess how forest modifications of snow accumulation and ablation combine to determine whether snow disappears later in the forest or in the open.

We find that snow disappearance timing at 12 (out of 14) sites ranges from synchronous in the forest and open, to snow persisting up to 13 weeks longer in the open relative to a forested area. By analyzing accumulation and ablation rates up to the day when snow first disappears from the forest, we find that the difference between accumulation rates in the open and forest is larger than the difference between ablation rates. Thus, canopy snow interception and subsequent loss, rather than ablation, sets up longer snow duration in the open. However, at two windy sites (hourly average wind speeds ranging up to 8 and 17 m/s) differential snow disappearance timing is reversed: snow persists 2-5 weeks longer in the forest. At these sites, accumulation rates in the forest and open are similar, and longer snow retention in the forest appears to be controlled by preferential snow deposition. While ablation rates are higher in the open, the difference between ablation rates in the forest and open is approximately equivalent to the difference at less-windy sites. These findings suggest that improved quantification of forest effects on snow accumulation

processes are needed to accurately predict the effect of forest canopy change via harvest or natural disturbance on snow water resources.

6.2 Introduction

The forests that cover much of the seasonal snow zone in the Pacific Northwest (PNW), USA, modify snow accumulation [*Shidei et al.*, 1952; *Miller*, 1964; *Hedstrom and Pomeroy*, 1998; *Hiemstra et al.*, 2002; *Storck et al.*, 2002; *Moeser et al.*, 2015] and ablation processes [*Marks et al.*, 1998; *Hardy et al.*, 2000; *Link et al.*, 2004; *Molotch et al.*, 2009; *Pomeroy et al.*, 2009; *Veatch et al.*, 2009; *Lawler and Link*, 2011; *Reba et al.*, 2012; *Gleason et al.*, 2013; *Musselman et al.*, 2015], with a variable impact on the amount of snow that is stored and the timing of snowmelt across the landscape. The net effect of forest-snow interactions is manifest in spatial patterns of snow cover near the end of the ablation season, and specifically in the difference in snow disappearance timing between forests and open areas. However, predicting the overall effect of forest cover on snow retention (i.e., the timing of snow disappearance) is complex because both the amount and direction of forest influence on individual snow processes change with climate [*Hedstrom and Pomeroy*, 1998; *Storck et al.*, 2002; *Lundquist et al.*, 2013; *Martin et al.*, 2013], topographic position [*Strasser et al.*, 2011; *Ellis et al.*, 2013], latitude [*Musselman et al.*, 2008; *Harpold et al.*, 2015b], and forest characteristics [*Kittredge*, 1953; *Jost et al.*, 2007; *Veatch et al.*, 2009; *Varhola et al.*, 2010a]. The net effect of forest cover on snow retention therefore depends on the integration of multiple forest-snow processes, each of which varies spatially and temporally.

Prediction of where and how forest cover will accelerate versus delay snow disappearance timing has valuable forest management applications, particularly in regions of extensive forest cover and intensive timber harvest such as the PNW [*Spies and Franklin*, 1991]. In particular, snow retention is linked to the timing of peak soil moisture [*Molotch et al.*, 2009; *Veatch et al.*, 2009; *Harpold et al.*, 2015b] and the onset of soil moisture depletion [*Flint et al.*, 2008], the

timing of spring and summer streamflow [*Whitaker et al.*, 2003; *Lundquist et al.*, 2005; *Lyon et al.*, 2008], stream temperatures [*Langan et al.*, 2001; *Gravelle and Link*, 2007; *Leach and Moore*, 2014], and wildfire risk [*Westerling*, 2006]. However, an improved understanding of how different forest-snow processes combine to contribute to snow disappearance timing is needed before applying empirical models [*Winkler et al.*, 2005; *Jost et al.*, 2007; *Varhola et al.*, 2010a; *Lundquist et al.*, 2013], or physically-based hydrologic models [*Ellis et al.*, 2013; *Du et al.*, 2016] to management practices.

Lundquist *et al.* (2013) suggested that average winter temperature is a first-order predictor of differential snow disappearance timing, and found that snow storage duration is longer in the open as compared to the forest for two locations in the PNW. However, local influences such as high winds [*Revuelto et al.*, 2015] and cold-air pooling [*Whitaker and Sugiyama*, 2005] have been shown to affect differential snow disappearance timing, and point to the need for region-specific investigations that sample a range of climatic and topographic conditions.

We therefore draw upon observational snow data from forest-open comparisons across a climate gradient in order to assess what conditions lead to longer retention of snow in forested or open areas. Previous investigations have demonstrated that the density and structure of forest stands [*Kittredge*, 1953; *Varhola et al.*, 2010a; *Musselman et al.*, 2012; *Seyednasrollah and Kumar*, 2014; *Broxton et al.*, 2015; *Moeser et al.*, 2015] influence the ways in which forest cover modifies snow processes. However, representing and predicting where and when forests will accelerate versus delay snow disappearance timing is an ongoing research challenge even for a simplified comparison of forest versus open [*Rutter et al.*, 2009; *Lundquist et al.*, 2013]. Thus, in order to advance a regional understanding of forest effects on snow storage we assess binary categories of forest cover (i.e., forested and open) and note the importance of continued

investigation into canopy structure effects on snow processes as such analysis is beyond the scope of this paper.

The field sites encompass forest-open comparisons within a relatively warm winter climate regime, where average winter (December-January-February (DJF)) temperatures range from -5 to 2 °C [*PRISM Climate Group*, 2012](Figure 6.1). Thus, we hypothesize differences in snow disappearance timing ranging from synchronous at the colder sites (< -1 °C) to snow lasting longer in the open at the warmer sites (> -1 °C), based on values proposed by Lundquist *et al.(*2013). Observational studies of the forest effects on snow processes in this region are sparse relative to more numerous studies in colder, continental climates. However, the maritime PNW represents an observational endpoint for forest effects on snow disappearance timing: two sites included in the Lundquist *et al.(* 2013) synthesis recorded the largest acceleration of snow disappearance in forests seen worldwide, with snow lasting two weeks longer in the open as compared to the forest [*Storck et al.*, 2002; *Dickerson-Lange et al.*, 2015a].

An improved understanding of forest-snow dynamics in warmer climates is therefore essential for assessing potential combined effects of forest change and climate change. For example, under warmer winter climate conditions, or in anomalously warm years, forest-snow interactions in colder, continental locations could shift to become more similar to the forest influences observed in warmer sites today. We therefore present analyses from forest-snow field studies from across the PNW in order to test the relation between winter temperature and differential snow disappearance timing between open and forested areas, and to assess the relative contribution of forest influences on snow accumulation and ablation.

6.3 Study Locations

The PNW, represented by Washington (WA), Oregon (OR), and Idaho (ID), USA (Figure 6.1a), depends on mountain snow storage to augment summer dry season water resources [*Hamlet and Lettenmaier*, 1999; *Nolin and Daly*, 2006; *Adam et al.*, 2009]. The west side of the north-south trending Cascade Range is characterized by a maritime climate and maritime snow regime [*Sturm et al.*, 1995], with typically large amounts of winter precipitation and temperatures that fluctuate around the freezing point (Figure 6.1a). The region east of the Cascade Range is colder and drier, with a transitional maritime-continental climate, and a mix of snow regime classes, including maritime (warm, deep snowpack), alpine (intermediate snowpack), and prairie (thin, cold snowpack) snow classes [*Sturm et al.*, 1995].

Snow and meteorological observations were collected over a range of water years (WY) by three research institutions and by citizen scientists to characterize forest effects on snow processes across the region. Each study location includes one or more paired forest and open area in which to compare snow observations (Table 6.1). A subset of annotated aerial images (Figure 6.1) demonstrate the range of forest canopy densities and data collection strategies, which included paired manual snow courses, snow pits, and automated sensors. Fourteen total study sites cover the western slopes and crest of the Cascade Range in WA and OR, and central and northern ID. Site and data collection details are provided in Table 6.1 and section 6.11, and in the references provided. Where available, forest metrics are given to illustrate the range of forest canopy densities that constitute “open” or “forest” classifications, but explicit consideration of forest structure is outside the scope of this investigation.

6.4 Methods

6.4.1 Annual and Long-Term Average Air Temperature

To assess the climatic context of the snow observations, we used a gridded dataset to compute mean air temperature values for the year of snow observations and all the years of record. Gridded data rather than *in situ* observations were used because of the availability of a much longer temperature record. We extracted 4-km gridded monthly mean temperature for the period 1981–2015, provided by PRISM [*Daly et al.*, 2008], for the grid cells enclosing the study sites. We then computed mean DJF temperature for every water year on record, and compared the value for the year of snow observations to the 34-year distribution of values.

6.4.2 Snow Metrics

To compute snow metrics we used a combination of point values from snow depth sensors and fixed snow measurement poles, and spatially distributed values from snow depth transects and grids of ground temperature sensors. Distributed observations were spatially aggregated to median snow depth values for each forest or open area. For all metrics and analyses we used snow depth rather than SWE to quantify snow magnitude because of the availability of snow depth data at all field sites, the robustness of manual snow depth observations at low snow values, and the uncertainty related to snow density differences between forest and open. We demonstrate and discuss the robustness of the results to utilizing depth versus SWE in the supporting information.

Summary metrics derived from each time series of snow depth include the magnitude of peak snow depth and the snow disappearance date (SDD). For sites at which both distributed and point observations were collected (Table 6.1), summary metrics were based on distributed data in

order to represent spatial snow heterogeneity within the forest or open area. Peak snow magnitude represents the end of the accumulation season, and was taken as the local maxima on the latest date on which peak snow depth values were observed. The SDD represents the first day when snow depth was zero (or in the case of distributed observations, when over half of the snow depth measurements are zero).

The SDD was generally extrapolated from the preceding values. For acoustic snow depth sensors, the extrapolation was performed in order to reduce the effects of increasing uncertainty as the snow surface becomes uneven or patchy [*Ryan et al.*, 2008]. For manual snow observations, the extrapolation was applied to account for the weekly to bi-weekly temporal resolution of data collection. Since a manual observation of zero snow only indicates that the SDD occurred sometime between two dates, the elapsed time between manual measurements can artificially delay the SDD. Thus, the SDD was linearly extrapolated from the slope of the two values previous to the day on which zero snow was observed. Sensitivity analyses at a subset of sites demonstrated that this approach reduces the absolute error relative to using the observed SDD by an average of 2, 5, or 9 days for a 1, 2, or 3 week temporal resolution (supporting information).

For the distributed snow duration datasets (Cedar River, Table 6.1) we inferred SDD from each ground temperature sensor and aggregated to the plot-scale by determining the day on which >50% of the sensors in a plot indicated that snow had disappeared [*Dickerson-Lange et al.*, 2015a]. Similarly, at one site in ID (MOSS, Table 6.1), SDD at each field location was determined as the day when fractional snow covered area dropped below 0.5.

We compared snow observations between the forest and open area by computing the ratio of peak snow depth and the differential snow disappearance timing. For all sites, the paired forest-

open locations are topographically similar and are typically adjacent. The ratio of peak snow depth is the peak snow depth in the open divided by peak snow depth in the forest. Differential snow disappearance timing quantifies the difference in SDD, in days, between open and forest plots. The difference is represented as ΔSDD (after [*Lundquist et al.*, 2013], but note the switch in sign to be consistent with the additional metrics presented herein), which is defined here as:

$$\Delta SDD = SDD_{open} - SDD_{forest}$$

A positive ΔSDD indicates the number of days that snow persists longer in the open after snow has disappeared in the adjacent forest. Conversely, a negative ΔSDD is the number of days that snow persists longer in the forest relative to the open.

6.4.3 Cumulative Gain and Loss Analysis

Where available, we utilized sub-daily snow depth values to assess cumulative gain (i.e., accumulation and redistribution) versus loss (i.e., compaction, melt, and sublimation) through time to distinguish the relative importance of forest effects on snow accumulation versus ablation. We aggregated to daily median snow depth values in order to reduce noise associated with snow depth sensors [*Ryan et al.*, 2008]. Since we estimated the precision of visually reading snow depth poles from time-lapse images as 5 cm, we rounded both the forest and open data streams to the nearest 5 cm for comparisons that utilized data from time-lapse cameras (Figure 6.2a). The mismatch between a pole that is read to the nearest 5 cm and an acoustic snow depth sensor with an accuracy of ±2cm has the potential to substantially affect results when summing differences through time.

When snow was present at both the forest and open area, we computed the change in depth for each day and at each sensor (i.e., $\Delta depth_{forest}$ and $\Delta depth_{open}$), and then summed daily gain

and loss through time (Figure 6.2b). Days for which data were missing or snow depth was zero (i.e., measured as <1 cm) at either the forest or open were excluded. We treated all positive Δdepth values as gain, and all negative Δdepth values as loss. This approach does not account for sub-daily fluctuations in depth, snow compaction (i.e., settling and metamorphism), or spatial variation in snow density. Thus, although we used the change in daily depth as a proxy for snow accumulation or ablation, we were strictly computing changes in height. Sensitivity analyses that account for time-varying density and snow compaction demonstrate that the general results presented in section 6.5 are insensitive to these simplifications (supporting information).

After computing time series of cumulative gain and loss, we extracted the values from the paired plots at the time of peak snow depth and at the time when snow at one of the plots disappeared (i.e., the first SDD). To approximate the influence of forest on snow accumulation and ablation rates, we summarized the findings by taking the difference between cumulative gain/loss at the paired open and forest plots at the timing of peak snow and snow disappearance. As such, we present these difference metrics for cumulative gain as:

$$\Delta \sum Gain_{peak} = \sum Gain_{peak_{open}} - \sum Gain_{peak_{forest}}$$

for the difference at the timing of peak snow, and as

$$\Delta \sum Gain_{SDD} = \sum Gain_{SDD_{open}} - \sum Gain_{SDD_{forest}}$$

for the difference at the timing of the SDD at the first plot, with the similar equations for cumulative loss. Figure 6.2 presents an annotated example of this analysis.

6.5 Results

6.5.1 Winter Temperature and Differential Snow Disappearance Timing

Climatological winter temperature, extracted from PRISM for each site, indicates that mean DJF temperature at most of the WA and OR sites is above or very close to -1 °C, while mean DJF temperature at all of the ID sites falls between -6 and -1 °C (Figure 6.3a). DJF temperature for the years of snow observations (i.e., red circles on Figure 6.3a) indicate that the climatic context for these snow observations range from a colder-than-average year (e.g., WY 2008 at UIEF, ID), to the warmest year on record (e.g., WY 2015 at MOSS, ID).

We find that differential snow disappearance timing generally follows the hypothesized temperature-based thresholds, with snow lasting 0-4 weeks longer in the open across the western WA and OR sites (Figure 6.3b; values provided in Table 6.2). At one site, during the anomalously low snow year of WY 2015, snow lasts 93 days longer in the open relative to the forest (Olallie on Figure 6.7; point removed from Figure 6.3b for readability). One notable exception to snow lasting longer in the open at the WA and OR sites is Hogg Pass (Table 6.1), at the crest of the Cascades in western OR, where snow lasted 15-29 days longer in the forest relative to the open. Differential snow disappearance timing at the colder ID sites ranges from approximately synchronous (i.e., ΔSDD = -1) to snow lasting 9 days longer in the open, with the exception of one comparison in which snow lasted 44 days longer in the forest. The ΔSDD values of -1 and 0 observed at Mica Creek in northern ID (Table 6.1), contrast with the general conclusion of [*Hubbart et al.*, 2015] who showed that snow lasts 3 weeks longer in the open as compared to the forest (i.e., ΔSDD = 21) in an aggregated analysis that did not explicitly account for topographic position and related preferential deposition.

The ratio of peak snow accumulation in the open to the forest at the WA and OR sites is consistently high, ranging from 1.4 to 3.5 at all sites except Hogg Pass, OR, with a median ratio of 2.2 (Figure 6.3c). Ratios at Hogg Pass are below 1 (i.e., more snow in the forest than in the open). There are fewer data points for the colder sites in ID, but the ratio ranges from 0.9 to 2.9 with a median of 1.9.

6.5.2 Forest Effects on Snow Gain versus Loss

Analysis of daily snow depth observations indicates higher rates of snow gain and snow loss in the open as compared to the forest. This result is consistent with previous synthesis work by Varhola *et al.(* 2010) on the relation between forest presence and snow accumulation and ablation. Figure 6.4 illustrates three examples of cumulative gain and loss analysis, and at each site there is consistently more cumulative gain and loss in the open as compared to the forest (i.e., the blue and green lines in Figure 6.4). Cumulative gain and loss analysis at all sites (not shown) is summarized by extracting ΔΣGain and ΔΣLoss (i.e., the distance between the blue and green lines in Figure 6.4d-4f) at the timing of peak snow depth and at the first SDD. The consistent result that rates of snow gain and loss are higher in the open at all sites is illustrated by positive values for both ΔΣGain and ΔΣLoss, where both metrics are computed as values at the open site minus values at the forest site (Figure 6.5a and b).

Furthermore, the comparison of cumulative gain and loss demonstrates that forest effects on snow accumulation effectively set up differential snow disappearance timing at these sites. When snow is present at both the open and the forest, there is more difference between open and forest sites in gain than in loss. This is illustrated by ΔΣGain values that are consistently higher than ΔΣLoss, and therefore plot below the 1:1 line at the time peak snow depth is reached (Figure

6.5a) as well as at the timing of first SDD (Figure 6.5b). By the time snow first disappears from either the open or forest, ΔΣGain is still larger than ΔΣLoss at all sites except Hogg Pass (i.e., all but one data point fall below the 1:1 line in Figure 6.5b). The difference between ΔΣGain and ΔΣLoss at the first SDD is a proxy for the amount of snow that remains in either the forest or open area when snow has disappeared from the other. This difference is therefore a predictor of how long snow will persist and the resulting differential snow disappearance timing (Figure 6.5c).

One exception is observed at Hogg Pass, where ΔΣGain is lower than ΔΣLoss (i.e., it plots above the 1:1 line) at the timing of peak snow depth and at the first SDD. This exception is further illustrated by the time series of snow depth at Hogg Pass, where values in the open and forest track very closely (Figure 6.4c) and, consequently, there are small differences between cumulative gain and loss, with slightly more cumulative loss than gain (Figure 6.4f).

6.5.3 Wind Effects

Assessment of local meteorological conditions for the two sites where snow lasts longer in the forest (Figure 6.3b) illustrates cases in which wind is a key influence on forest-snow interactions. Hogg Pass is both topographically exposed in a mountain pass, and the open location consists of mostly standing dead trees (Figure 6.1e, Figure 6.6e). Thus, observed wind speeds are high, with average hourly values that range from 0–17 m/s, and a mean hourly value of 4 m/s during winter and spring at the Hogg Pass open meteorological station (Figure 6.6d). In contrast, average hourly wind speed ranges from 0–3 m/s at a nearby lower elevation open site (McK Mid, OR; Table 6.1), which is less exposed topographically and has sparse vegetation cover (Figure 6.1d, Figure 6.6b and c). Similarly, one of the open locations at UIEF, ID (the

"open reference" sensor, Table 6.1), recorded average hourly wind speeds of 1–8 m/s, and a mean hourly value of 2 m/s during February through May (Figure 6.6g) during the study period as compared to 0–2 m/s at all of the other forest and forest gap sensors (not shown). The UIEF open reference sensor is located on an exposed hilltop in the Palouse region of the interior Pacific Northwest, which is a region that is known to be subject to high winds during storm events. In summary, at both of these sites the higher observed winds in conjunction with the peak snow ratio and ΔSDD metrics suggest that wind influences on forest-snow processes control the differential snow disappearance timing.

6.6 Discussion

6.6.1 Forest effects on accumulation drive differential snow duration in PNW

Observations from these sites provide evidence that forest modification of snow accumulation processes is the dominant factor in determining differential snow disappearance timing between forested and open areas in the PNW. Two cases of differential snow disappearance timing were observed, both of which result from forest modification of accumulation processes. In the most common case, the presence of forest results in snow accumulation that is substantially reduced beneath the canopy. Reduced under-canopy snow accumulation subsequently sets up snow disappearance timing that ranges from synchronous to longer snow duration in the open. In the second case, which is particular to two windy sites, forest cover results in enhanced snow accumulation. The net result is longer snow duration in the forest relative to the open areas.

Effectively, the two cases reflect the role of the forest when snow is falling: does the presence of trees reduce or enhance the accumulation of under-canopy snowpack? We discuss the specifics of each case below.

6.6.1.1 Case One: Reduced accumulation in forest

Twelve of the fourteen forest-open comparisons fall into the first category, in which diminished snow accumulation in the forest drives synchronous to longer snow persistence in the open (Figure 6.3b). At these sites, more snow accumulates in the open relative to the forest, illustrated by ratios of open-to-forest peak snow depth that range from 1.2 to 3.5 (Figure 6.3c). Previous work has demonstrated that canopy snow interception efficiency and storage capacity are larger where and when temperature is higher [*Kobayashi*, 1987; *Friesen et al.*, 2015]. These results corroborate previous observations of higher canopy snow interception efficiency values in

maritime versus continental climates (i.e., 30–50% in continental climates [*Hedstrom and Pomeroy*, 1998] and up to 60–80% in maritime climates [*Andreadis et al.*, 2009; *Martin et al.*, 2013]).

Beyond supporting previous findings, the results from cumulative gain and loss analysis provide strong evidence that canopy snow interception is the driving process that sets up differential snow disappearance timing in the PNW. The ΔΣGain values extracted from snow depth are larger than the ΔΣLoss values at all of these sites at the time of first SDD (Figure 6.5b), suggesting that difference in snow magnitude at the time when snow disappears from the forest is initiated by differences in snow accumulation rates. Reduced accumulation within the forest establishes the direction of differential snow disappearance timing, in that snow disappearance timing will range from synchronous to snow lasting longer in the open. Even though cumulative loss in the open is consistently higher than in the forest, diminished rates of loss in the forest are not sufficient to balance out the diminished snow accumulation. After snow disappearance occurs in the forest, the number of days of snow duration difference results from the amount of snow remaining in the open divided by the rate of loss in the open (Figure 6.5c).

6.6.1.2 Case Two: Enhanced accumulation in forest

In the second case, forest effects on accumulation set up the opposite snow retention pattern at sites subject to high wind. Observations from Hogg Pass and the UIEF open reference site indicate that approximately the same amount of snow accumulates in the forest as in the open (Figure 6.3c), that snow persists longer in the forest (Figure 6.3b), and that wind speeds are higher than other, nearby open sites (Figure 6.6). Ablation rates at Hogg Pass are similar to values from the other, less windy sites, however, snow accumulation is almost equivalent between forest and open, resulting in a ΔΣGain value that is lower than all other sites (Figure

6.5a and b). This suggests that accumulation processes that differ from the majority of sites drive the longer snow retention in the forest, rather than greatly enhanced ablation rates in the open. We speculate that the equivalent accumulation in the forest and open at this site is driven by preferential snow deposition (and thus accumulation) in the forest due to the transition to slower wind speeds [*Hiemstra et al.*, 2002; *Geddes et al.*, 2005] and possibly from the contribution of canopy-intercepted snow to the under-canopy snowpack due to wind unloading [*Roesch et al.*, 2001]. Qiu *et al.(*2011) previously found that high winds during storm events in the Palouse region (i.e., where the UIEF site is located) result in large spatial heterogeneity in snow accumulation, with less snow on ridge tops relative to more sheltered locations. Redistribution of snow from the open to forested area after a storm event ends is less likely due to relatively warm winter temperatures that support high snow cohesion [*Li and Pomeroy*, 1997].

6.6.2 Winter climate and forest-snow processes

Setting aside the sites where wind is the dominant factor, these results generally support categories of differential snow disappearance timing delineated by DJF temperature [*Lundquist et al.*, 2013]. Specifically, in locations with warmer winter temperatures such as those investigated herein, differential snow disappearance timing ranges from synchronous, to snow persisting longer in the open relative to the forest. These sites and observation years reflect a relatively narrow range of DJF temperatures (Figure 6.3a), and there is substantial interannual variability in both snow metrics and DJF temperature at individual sites (e.g., McK Mid on Figure 6.3). Thus, the observations do not display a robust correlation with DJF temperatures (Figure 6.3b).

The finding that snow duration is generally longer in the open at these sites suggests that climate-mediated forest-snow processes contribute substantially to overall forest-snow interactions. In addition to rates of canopy interception, discussed above, winter climate also influences the under-canopy energy balance and resulting ablation rates. Warmer air temperatures can directly result in increased ablation rates in forests due to enhanced under-canopy longwave radiation [*Essery et al.*, 2008; *Lundquist et al.*, 2013; *Cristea et al.*, 2014]. However, we find temperature-influenced enhancement of under-canopy snowmelt to be a second-order effect relative to reduced under-canopy snow accumulation. Lundquist *et al.*(2013) presented an example from western OR in which snow accumulation before the first SDD was greater in the open, but cumulative loss was actually greater in the forest due to mid-winter melt events driven by enhanced longwave radiation. In contrast, all of the sites in this study show higher ablation rates in the open, and accumulation processes, rather than enhanced ablation in the forest, appear to set up the difference in snow disappearance date.

Additionally, many studies have established that forest cover can substantially reduce ablation rates via shading the snowpack from solar radiation [*Sicart et al.*, 2004; *Musselman et al.*, 2008, 2012; *Ellis et al.*, 2011], but climate can have an indirect effect on the magnitude of the contrast between ablation rates in the open and in the forest. For example, colder air temperatures contribute to a later ablation season, when forest shading is more important because solar elevation angles are higher [*Sicart et al.*, 2004; *Musselman et al.*, 2015]). High atmospheric transmissivity (i.e., more clear-sky days) later in the ablation season can also enhance the importance of forest shading [*Seyednasrollah and Kumar*, 2014]. In the PNW, synchronous snow disappearance timing at the colder, sunnier ID sites likely results from the combination of

lower canopy snow interception relative to the warmer sites (Figure 6.3c) and diminished ablation rates in the forest that compensate for reduced accumulation in the forest.

6.6.3 Implications for Future Work

The finding that forest effects on accumulation processes drive differential snow disappearance timing has important implications for future investigations of forest-snow processes. Many studies have focused on quantifying the effect of forests on modifying the below-canopy energy balance (e.g., [*Davis et al.*, 1997; *Essery et al.*, 2008; *Ellis et al.*, 2011; *Musselman et al.*, 2013]), which is particularly relevant to forest-snow processes in colder climates and higher latitude locations. However, at the PNW sites considered here, forest modifications of accumulation processes dominate. Although many studies have documented the difference in snow accumulation under forest canopy as compared to the open, much work remains in quantifying tree-scale and stand-scale canopy snow interception and storage [*Friesen et al.*, 2015]. For example, Clark *et al.*(2015) demonstrated that two commonly used parameterizations of canopy snow interception in hydrologic models exhibit opposite dependencies on air temperature: canopy snow interception capacity increases with air temperature in one [*Andreadis et al.*, 2009] while decreasing with air temperature in the other [*Hedstrom and Pomeroy*, 1998]. Additional work quantifying canopy interception processes is needed in light of the importance of accurately representing snowpack in the PNW, and potentially in other forested, snowy regions that are subject to a warming climate.

The role of forest in snow accumulation processes must also be considered in the context of wind, which varies greatly over complex terrain and affects patterns of snow deposition and energetics. The findings of this investigation, as well as previous investigations [*Gary*, 1974;

Hiemstra et al., 2002; *Geddes et al.*, 2005; *Fortin et al.*, 2015], demonstrate that forests can act to enhance snow deposition and retention, with implications for snow storage across the landscape. Improved modeling of forest-snow processes in this region requires consideration of where wind attenuation at the edge or within forests may dominate over other forest-snow interactions. Existing methods to map winds on complex terrain include statistical (e.g., [*Winstral and Marks*, 2002]), statistical-dynamic (e.g., [*Liston and Elder*, 2006]), or completely dynamic (e.g.,[*Mott et al.*, 2014]) approaches that account for some combination of local topography (slope and curvature), wind speed, and direction. While many high-resolution wind models are computationally impractical to run over larger domains [*Mott et al.*, 2014], recent developments in physical-statistical modeling (e.g.,[*Liston et al.*, 2016]) show promise for representing wind-related deposition and redistribution with relatively little computational cost.

Lastly, the compilation of forest-snow sites presented here represents a diverse cross-section of topography and climate in the region, but there are substantial observational data gaps in forest-snow studies in the PNW. Specifically, observations are needed from locations where conditions during snowmelt are sunnier, and therefore forest shading is likely to be more important, such as on the eastern slopes of the Cascade Range. In addition, data from the coldest parts of the region, such as the North Cascades or the Sawtooth Mountains would be helpful for understanding the climate dependency of forest-snow processes in the region.

6.7 Conclusions

Snow observations from WA, OR, and ID were analyzed to determine the difference in snow accumulation magnitude and snow disappearance timing between forests and open areas, and to assess the relative contribution of forest-modulated accumulation versus ablation to snow storage and duration. We find that snow disappearance timing ranges from approximately synchronous, to snow lasting several weeks longer in the open as compared to the adjacent forest, except where wind speeds are high. Excluding the windy sites, differences in snow accumulation between the forest and open area result from canopy snow interception and subsequent loss, which sets up differential snow disappearance timing. Where similar amounts of snow accumulate under the forest and in the open, snow disappearance timing is close to synchronous. Where substantially more snow accumulates in the open, the deeper snow takes longer to melt, and the time lag between SDD in the forest to SDD in the open is longer. At wind-affected sites, differential snow duration is in the opposite direction, with snow persisting 2–5 weeks longer in the forests. We attribute the differential snow disappearance timing primarily to forest effects on snow deposition and retention in the windy environments, rather than enhanced ablation rates. These findings provide a regional framework for understanding the range of forest and forest-change effects on snow retention across the landscape.

This study focused on PNW sites with fairly warm winters, but these findings have broad implications for improving prediction of the effects of forest change on snow retention. The forest-snow community has made great advances in improving model representations of the below-canopy and within-gap energy balance, but the results presented here suggest that even greater model improvements could be obtained by focusing on snow accumulation processes associated with forest conditions. These findings are applicable not only to practitioners working

in warmer forested snow regimes but also to scientists trying to predict global impacts of climatic change. Forest-snow processes important today in the PNW may be critically important in any forest worldwide in a winter with similarly warm temperatures.

6.8 Acknowledgements

Primary support for this project was provided by the Department of the Interior Northwest Climate Science Center (NW CSC) through Cooperative Agreement GS297A from the United States Geological Survey (USGS). Collection of previously unpublished data includes support from the National Science Foundation (NSF) for the Snoqualmie Pass forest data (EAR-1215771) and the Oregon data (EAR-1039192), and from USDA CSREES NRI (2003-35102-13675 and 2006-35102-17689), NSF (CBET- 0854553), and USFS (#03-JV-11222065-068 and #04-D6-11010000-037) for the Idaho data. We thank the many researchers and technicians who participated in field campaigns at all of the study sites. We are additionally grateful to the land agencies who granted access and the staff who provided expertise in choosing sites for these snow-forest studies, including Seattle Public Utilities, the Potlach Corporation, the U.S. Forest Service, Scott Pattee, and Cheryl Freisen. We thank Karla Bradley Eitel, Leslie Dorsey, and the students and instructors at the McCall Outdoor Science School who helped to fill a key data gap. The manuscript benefited from critical review by the UW Mountain Hydrology Research Group. All data described herein are publically available via the USGS Science Base archive (http://dx.doi.org/10.5066/F70C4SW3).

6.9 Tables

Table 6.1 Locations and attributes of field sites included in this analysis, including the types of data collected, the timeframe over which data were collected and indications of which data were used in the derivation of summary metrics (e.g., the peak snow ratio).

					Analyses			**Land cover**	
Location (Lat/Lon)	**Site Name(s)**	**Elev (m)**	**Type(s) of data used in analysis**	**Water Years**	*Peak Ratio*	*ΔSDD*	*Cumulative*	*Open*	*Forest*
Cedar River, WA (47.3° N, 121.5° W)	Cedar Low (Bear Creek)	640	Snow depth from 20 m perpendicular manual transects (n=40 for each plot) in 5 open and 5 gap plots	2011 - 2012	D	D		20 m diameter, circular gap; data from gap and surrounding forest	2nd-growth, closed canopy, CC=88, H=31
	Cedar Low (City Cabin and Clearing Met)	780	Snow depth from time-lapse photos at City Cabin (forest) and snow depth sensor at nearby Clearing Met (open)	2011, 2013	P	P	P	Met Station in 30 m diameter gap	Old-growth, closed canopy, CC=87, H=39
	Mount Gardner	890	Snow duration from grid of iButtons (forest) and snow depth sensor (open)	2011 - 2014		D		Forest gap, SNOTEL (#898)	2nd-growth, closed canopy, CC=94, H=22
	Tinkham Creek	910	Snow duration from grid of iButtons (forest) and acoustic snow depth sensor (open)	2013 - 2014		D		Forest gap, SNOTEL (#899)	2nd-growth, closed canopy, CC=90, H=23
Cascade Crest, WA (47.4° N, 121.4° W)	Snoqualmie	910	Snow depth from time-lapse photos (forest) and acoustic sensor (open)	2015	P	P	P	Met Station in 30 m diameter gap	2nd-growth, closed canopy, ND

	Olallie	1180	Snow depth from time-lapse photos (forest) and acoustic sensor (open)	2015	P	P	P	Meadow, SNOTEL (#672)	2nd-growth, closed canopy, ND
McKenzie River, OR (44.4° N, 122.0° W)	McK Low	1110	Snow depth from 500 m manual transects (n=50) and acoustic sensors from both	2012 - 2014	D	D	P	Regenerating clear-cut, SVF=0.70, H=8	Old-growth, closed canopy, SVF=0.10, H=30
	McK Mid	1350	Snow depth from 500 m manual transects (n=50) and acoustic sensors from both	2012 - 2014	D	D	P	Regenerating clear-cut, SVF=0.44, H=12	Old-growth, closed canopy, SVF=0.10, H=21
	Hogg Pass	1480	Snow depth from 500 m manual transects (n=50) from both	2012 - 2014	D	D		Standing burned stems, SVF=0.88, H=10	Sparse, beetle-impacted forest, SVF=0.35, H=14
			Acoustic sensors from both	2014			P		
Middle Fork Willamette, OR (43.6° N, 121.1° W)	MFW Low	1200	Snow depth from 500 m manual transects (n=50) and acoustic sensors from both	2012 - 2013	D	D	P	Regenerating clear-cut, SVF=0.18, H=15	Closed canopy, SVF=0.08, H=26
	MFW Mid	1350	Snow depth from acoustic sensors from both	2012 - 2013	P	P	P	Regenerating clear-cut, H=10	Closed canopy, H=36
Mica Creek, ID (47.2° N, 116.3° W)	Mica Creek	1420	Snow depth from acoustic sensors from both	2004			P	Regenerating clear-cut, CC=0.03, H=2	Second-growth, closed canopy, CC=0.82, H=28
			Snow depth from 20 m manual transects (n=20)	2006	D	D	P		

			and acoustic sensors					
UIEF, ID (46.9° N, 116.7° W)	UIEF Lawler Gap	880	Snow depth from acoustic sensors, starting at peak snow depth	2008	P	P	40 m long elliptical gap and clear-cut "open reference" location	ND
McCall Outdoor Science School, ID (44.9° N, 116.1° W)	MOSS	1540	Snow depth from bi-weekly snow pits (n=10) and snow duration from snow cover estimates	2015	D	D	ND	ND

D = Distributed snow observations

P = Point snow observations

CC = Mean Canopy Cover from lidar (%); H = Mean Tree Height (m); SVF = Mean sky view fraction from hemispherical photographs

ND = Qualitative assessment of canopy only; no canopy data available

6.10 Figures

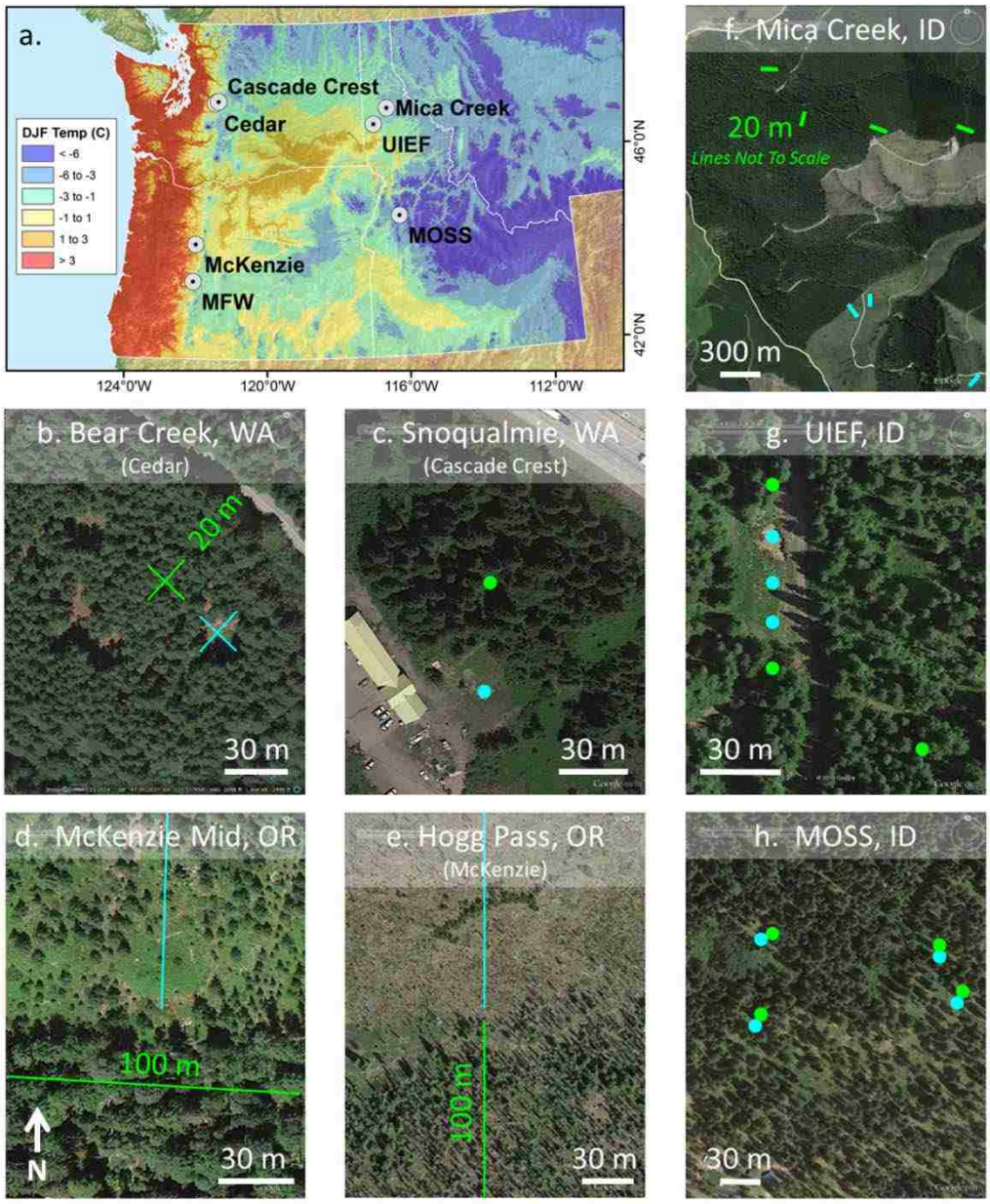

Figure 6.1 (a) Map of the PNW, showing field locations and (b-h, see Table 6.1 for site details) aerial photographs showing forested and open areas from representative snow observation sites. Approximate locations of snow depth transects are shown as green (forest) and blue (open) lines, with the length of the forest transect that is visible in the photograph indicated in green type. Approximate point observation locations are shown as green and blue dots. Photographs courtesy of Google Earth Imagery, © 2016 Google, with the following additional data sources: (b,c,f,g) Landsat and (d,e) Landsat, LDEO-Columbia, NSF, and NOAA.

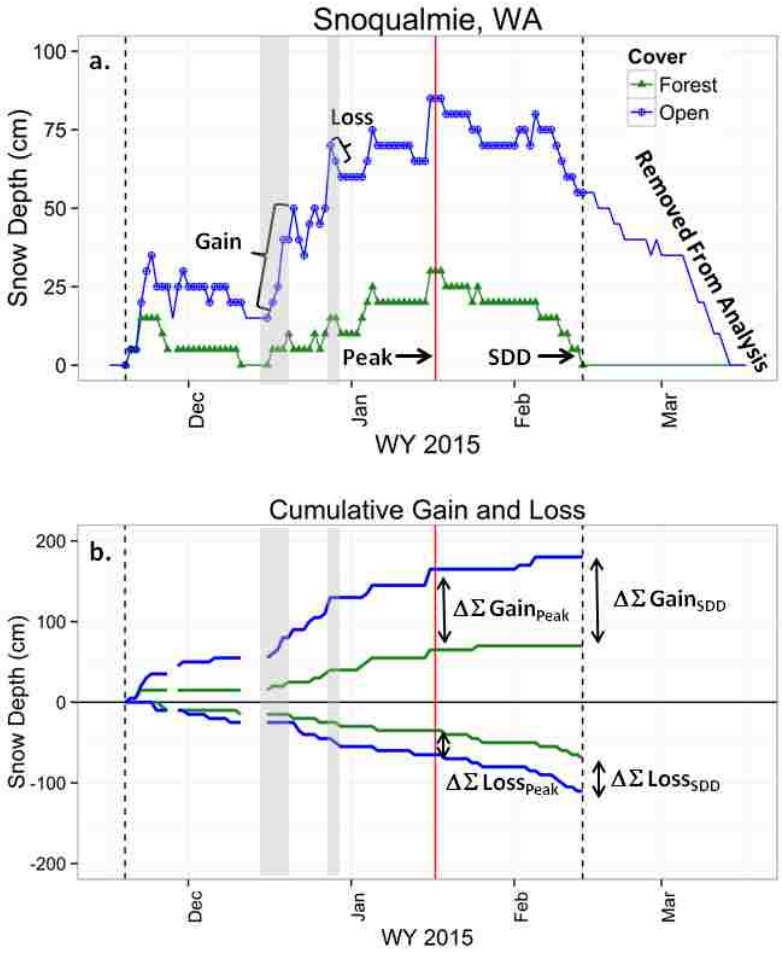

Figure 6.2 Annotated cumulative depth analysis, showing (a) the time series of daily median snow depth in the open (blue) and forest (green) at the Snoqualmie, WA site (see Figure 6.1c). Snow depth is rounded to 5 cm, which is the estimated precision of visually reading the snow depth pole from time-lapse images in the forest. (b) The time series of cumulative gain and loss derived from positive and negative changes in daily snow depth. Gray bars illustrate a period of gain and a period of loss at the open site in (a), which is refected in the time series of cumulative values in (b). ΔΣGain and ΔΣLoss metrics at the timing of peak snow depth (i.e., Peak in (a)) and at first snow disappearance (i.e., SDD in (a)) are annoated as the distance between the traces of cumulative values in the open and forest in (b).

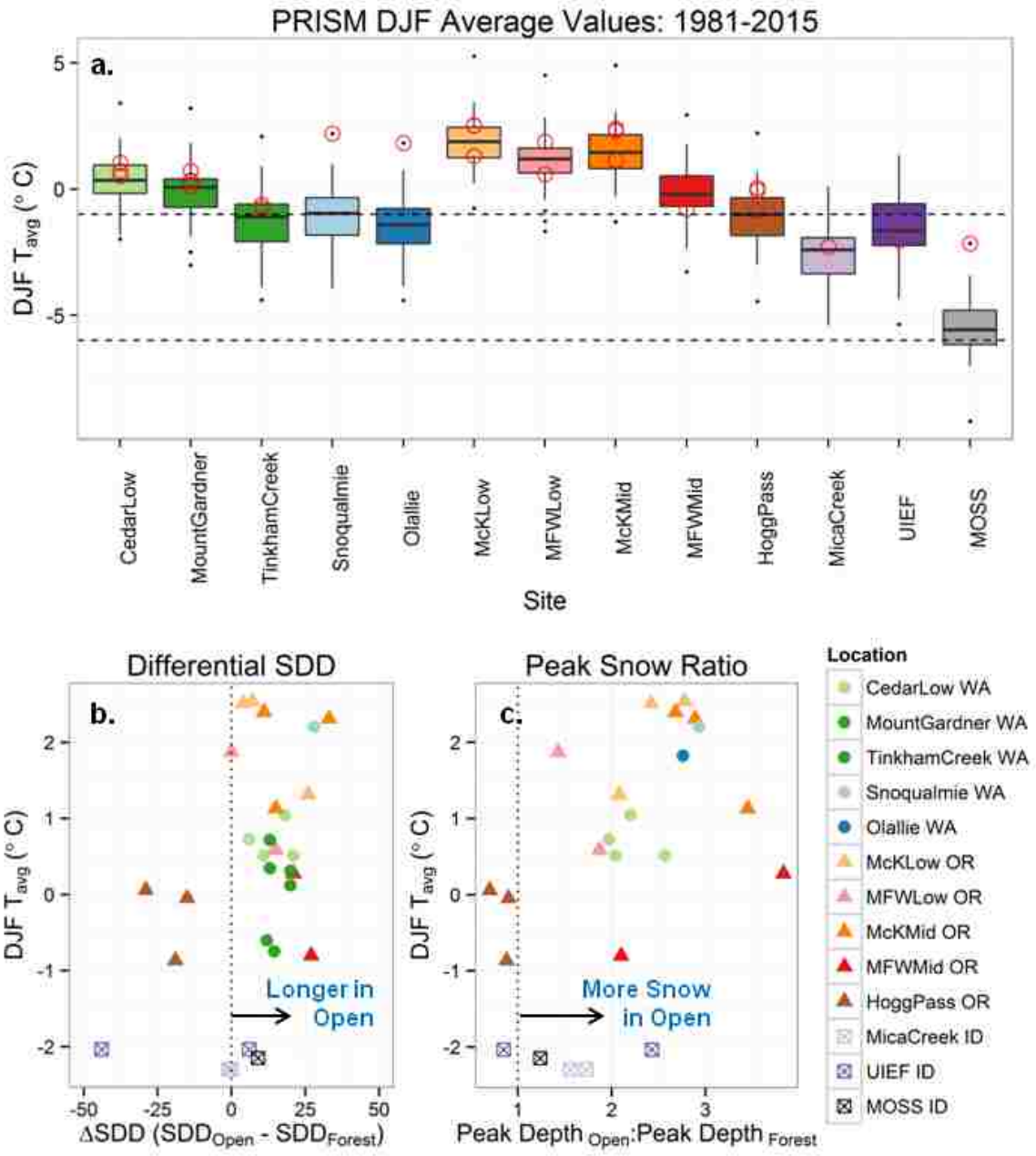

Figure 6.3 (a) Boxplots of December, January, February (DJF) average air temperature extracted for each field site from PRISM 4 km gridded monthly average values for WY 1982-2015. The values for the years of snow observations at each site are indicated with a red circle. The dashed lines at -1 and -6 ° C indicate previously proposed temperature thresholds for differential snow disappearance timing [Lundquist et al., 2013]. (b) Differential snow disappearance timing (ΔSDD) and (c) the ratio of peak snow depth in the open to the forest versus 4 km DJF average air temperature for the year of snow observations at each site (i.e., the red circles in (a)). An outlier ΔSDD value of 96 days observed at Olallie has been removed from (b) for readability (see Figure 6.7).

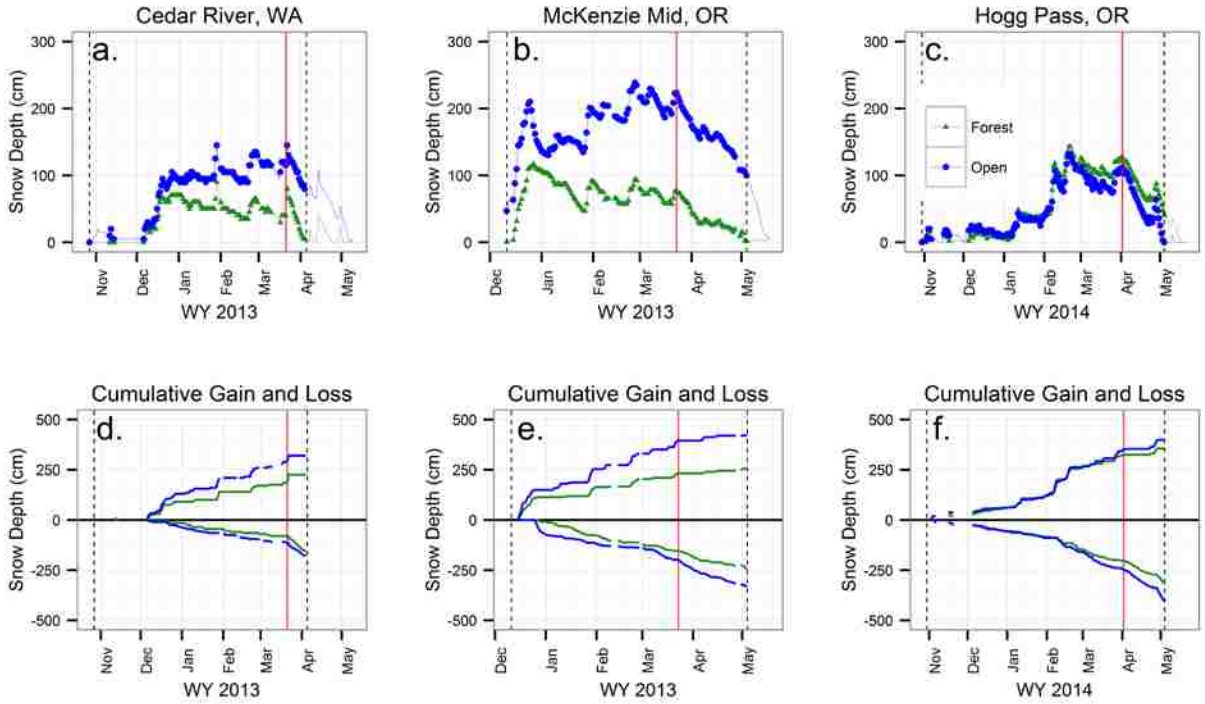

Figure 6.4 Examples of cumulative gain and loss analysis from three sites, including (a-c) time series of snow depth in the open (blue) and forest (green), and (d-f) time series of cumulative gain and loss. Temporal bounds on analysis are indicated as vertical black lines and the timing of peak snow magnitude indicated as a vertical red line (see Figure 6.2 for annotations). Analysis for WY 2013 at (d) Cedar River and (e) McKenzie Mid, where the difference in cumulative gain is larger than the difference in cumulative loss at both peak snow and first SDD, is typical of all the sites and years analyzed, with the exception of (f) Hogg Pass in WY 2014.

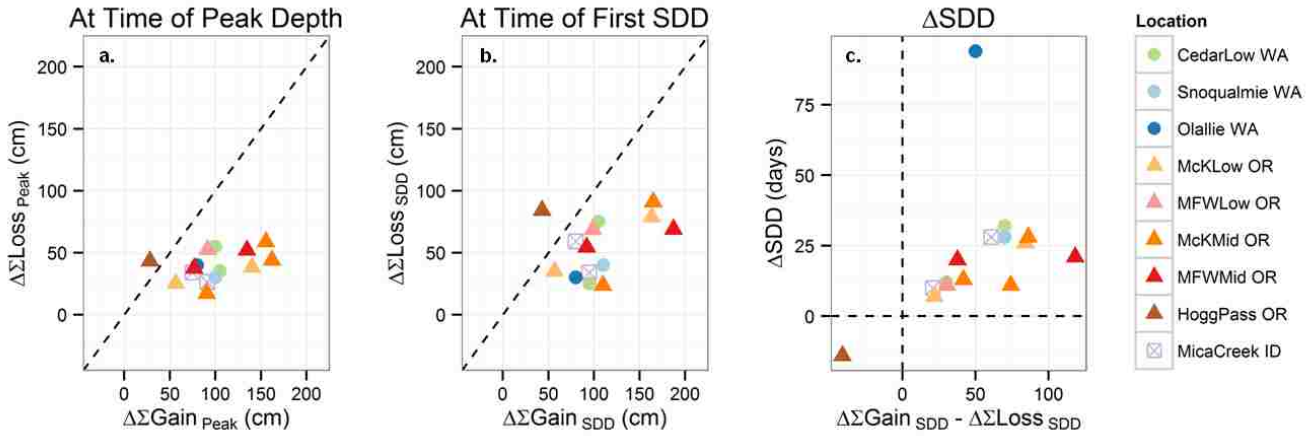

Figure 6.5 (a) ΔΣGain (i.e., cumulative gain in the open minus cumulative gain in the forest) versus ΔΣLoss at the time of peak snow depth (vertical red dotted lines in Figure 6.3) and (b) at the first SDD, which is the end of the shared snow period (vertical black dotted lines in Figure 6.3). (c) ΔSDD as a function of the difference in ΔΣGain and ΔΣLoss when snow disappears at the first site (i.e., a proxy for the amount of snow left at first SDD). Dashed lines in (c) indicate zero values.

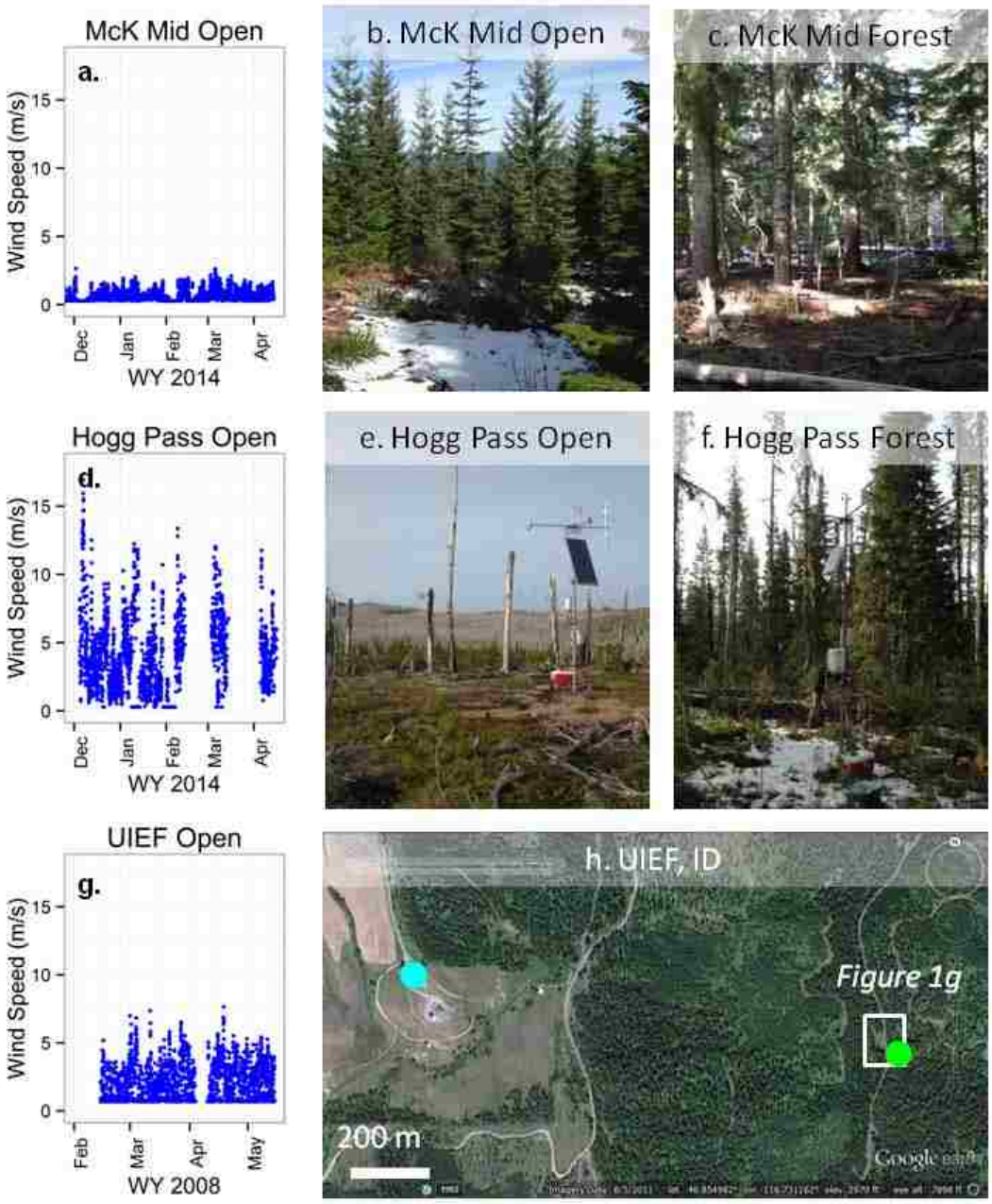

Figure 6.6 Wind and forest characteristics at (a-c) McK Mid, (d-f) Hogg Pass, and (g-h) UIEF sites. (a, d, g) Average hourly wind speeds (m/s) observed at the open meteorological stations show the wind conditions at each site, and (b, c, e, f) field illustrate differing types of forest and open locations. (h) 2011 aerial view shows the position and land cover characteristics of the open reference (blue dot) and forest reference (green dot) sensors, and the domain of Figure 6.1g is also noted for comparison. See Figure 6.1d and e for aerial views of McK Mid and Hogg Pass. Aerial photograph courtesy of Google Earth Imagery, © 2016 Digital Globe.

6.11 Appendix 1. Site Details

6.11.1 Cedar River Watershed, western Washington

Snow and meteorological data were collected in the Cedar River Municipal Watershed, located on the western slopes of the Cascade Range, approximately 50 km east of Seattle, WA (Figure 6.1b). These data were collected over WY 2011–2014 at four sites spanning an elevation range of 640–910 m, and are described in Dickerson-Lange *et al.*(2015a). Distributed snow depth data were collected bi-weekly via 20-m manual transects at one site (Bear Creek). Following the methods for observing snow depth via time-lapse cameras that were assessed by Parajka *et al.* *(*2012), point snow depth data were determined from digital images of fixed measurement poles in the forest (City Cabin), and compared to snow depth data collected with an acoustic sensor in the nearby open site (Clearing Met). For the purposes of this study, forest-open comparisons at Bear Creek and City Cabin/Clearing Met are lumped as Cedar Low due to their proximity.

At two additional sites (Mount Gardner and Tinkham Creek), snow duration in a forest plot was inferred from distributed observations of ground temperature [*Dickerson-Lange et al.*, 2015a] and compared with snow duration extracted from the adjacent National Resource Conservation Service Snow Telemetry (SNOTEL) depth sensor observations (i.e., the open comparison).

6.11.2 Cascade Crest, western Washington

Point observations of snow depth were collected at two locations during WY 2015 at the crest of the Cascade Range, 70 km east of Seattle, Washington. One location, Snoqualmie (elevation 920 m), is situated at Snoqualmie Pass, and encompasses a 30-m diameter forest gap and a second-growth coniferous forest study plot adjacent to the gap (Figure 6.1c). Daily manual

snow board measurements were collected in the gap, and automated, sub-hourly snow depth and meteorological measurements were collected in the gap [*Wayand et al.*, 2015a] and adjacent forest. Sub-daily time-lapse photographs of snow measurement poles were also collected in the forest and validated against the snow depth sensor.

The Olallie site (elevation 1180 m) is just east of the Cascade crest, and co-located with the Olallie Meadows SNOTEL (# 672), which is situated in a meadow. Time-lapse cameras and snow measurement poles were deployed in the gap around the SNOTEL station, and in the adjacent forest, approximately 60 m to the southeast. Snow depth from the time-lapse photographs in the meadow was validated via close agreement with the SNOTEL acoustic snow depth sensor. At both Olallie and Snoqualmie, the photograph-derived forest time series was compared with manual or automated snow depth data from the gaps to comprise forest-open comparisons.

6.11.3 McKenzie River and Middle Fork Willamette Watersheds, western Oregon

Snow and meteorological data were collected over WY 2012–2014 from five paired forest-open sites chosen to span a broad elevation range (1110–1480 m) [*Sproles et al.*, 2013; *OSU*, 2016]. Three study sites were located in the upper McKenzie (McK) River watershed, approximately 100 km east of Corvallis, OR on the western slope of the Cascade Range (Figure 6.1d and e). Two additional sites were located in the Middle Fork Willamette (MFW) watershed, located to the south of the McKenzie. The highest site, Hogg Pass (Figure 6.1e), is located approximately 500 m from the Hogg Pass SNOTEL (#526).

Distributed snow depth and snow water equivalent (SWE) observations were collected via monthly manual snow courses along 1000 m transects from 1 November through 1 April and bi-

weekly thereafter. Meteorological stations were deployed at some sites and years to record sub-hourly snow depth and meteorological variables from both the forest and the open (Table 6.1).

6.11.4 Mica Creek Watershed, northern Idaho

Snow magnitude and meteorological data were collected over WY 2004 and 2006 at the Mica Creek Experimental Watershed in northern ID, approximately 25 km southeast of St. Maries, ID. Observations were collected in second-growth coniferous forest and clear-cut blocks (Figure 6.1f), and are described in detail by Hubbart *et al.*(2015). During WY 2004 and 2006, two meteorological stations that recorded 30-minute point values of snow depth were deployed in the forest and in the clear-cut. Distributed snow depth and SWE data were collected approximately weekly from February through May during WY 2006 via 4 manual transects per forest or open.

The topographic positions of the meteorological stations and snow courses represent a relatively small elevation range (i.e., 1380-1460 m), but include diverse aspect positions. We aggregated the data by forest or open, and by aspect into topographically equivalent comparisons of the north-facing and non-north facing snow courses, based on a pattern of preferential snow deposition on north-facing slopes, and compared the aggregated clear-cut (i.e., open) and forest transects. Additional information about the history and physiography is given in Hubbart *et al.(*2007) and Gravelle and Link (2007).

6.11.5 UIEF Lawler Landing, north-central Idaho

Within the Flat Creek Unit of the University of Idaho Experimental Forest (UIEF) near Moscow, ID, snow depth data were collected at seven locations across the Lawler Landing site (elevation 880 m) from February to May of WY 2008 [*Carson*, 2010]. A 70 m north-south

oriented transect of 5 snow depth sensors was deployed to record sub-daily snow depth, with co-located meteorological instruments. The sensors traversed a 40 m long elliptical forest gap and the adjacent forest in both directions (Figure 6.1g). The locations were the same as those used previously to quantify how shortwave and longwave radiation vary across a forest gap [*Lawler and Link*, 2011]. Two additional snow depth sensors and meteorological stations were deployed at "interior forest reference" and "open reference" sites, situated 80 m southeast and 1200 m west, respectively, from the main transect. Whereas the forest reference site was similar to the surrounding forest, the open reference site was much more exposed than the forest gap. Thus, we aggregated the data to two forest-open comparisons: one between the two reference sites and one between the sensors in gap and in the surrounding forest.

6.11.6 McCall Outdoor Science School (MOSS), central Idaho

Students and instructors at the University of Idaho McCall Outdoor Science School (MOSS) in McCall, ID participated in a citizen science campaign designed for this project, detailed in Dickerson-Lange *et al.(*2016). Weekly to monthly field observations of snow cover were collected at 6 field sites within Ponderosa State Park (elevation 1540 m), adjacent to Payette Lake, during WY 2015 (Figure 6.1h). Students documented snow cover within forested versus open areas at each site via photographs and estimates of the continuity of snow cover. Additionally, snow depth and density were measured via snow pits in the forest and the open. All observations were collected within a relatively flat, 1 km^2 area, and metrics were aggregated to median values for one forest-open comparison. Checks on estimates of snow covered area as compared to photographs, and previous work utilizing citizen science [*Lawless and Rock*, 1998;

Galloway et al., 2006; *Peckenham and Peckenham*, 2014] demonstrated that amateurs are capable of collecting high quality data.

6.12 Supporting Information

Supporting information is provided to further describe data, methods, and sensitivity testing referenced in the main text. In particular, Table 6.2 presents values and metadata for snow metrics presented in Figure 6.3. Figure 6.7 replicates Figure 6.3b, but with the outlier included. Finally, analyses and discussion that support the methods described in section 6.4 are presented.

6.12.1 Sensitivity of results to methods

We performed a series of sensitivity tests to assess the effect of methodology on the robustness of results.

6.12.1.1 Extrapolating SDD from Manual Snow Observations

For comparisons of ΔSDD we utilized distributed observations where available in order to fairly represent the spatial heterogeneity of snow. However, many of these distribution observations were manually collected, and therefore the temporal resolution ranges from 1 to 3 weeks. The SDD derived from manual observations is subject to temporal uncertainty related to the elapsed time between field visits. Thus, we used linear extrapolation to improve estimates of SDD (described in section 6.4.2 in the main text). We tested the robustness of the extrapolation approach for a subset of sites by analyzing daily snow depth data from acoustic sensors and manually identifying the true SDD. We then resampled the data at varying temporal resolutions to mimic the frequency of manual observations. From the sparser subset of observations we identified the observed SDD (i.e., the first day on which snow depth was < 1 cm) and extrapolated the SDD from the two observations previous to the observed SDD. We used the extrapolated SDD in cases for which it occurred before the observed SDD; otherwise, we used the observed SDD.

We utilized a Monte Carlo approach over numerous starting points and sampling frequencies to assess the absolute error, in days from the true SDD, for the extrapolation approach as compared to the manually observed SDD. We found that the extrapolation approach was almost always closer to the true SDD, with a reduction in the absolute error relative to using the observed SDD by an average of 2, 5, or 9 days for a 1, 2, or 3 week temporal resolution (Figure 6.8).

6.12.1.2 Utilizing observations of snow depth versus SWE

Snow depth is widely used to quantify the magnitude of the snowpack. However, accumulation and ablation processes affect the mass of the snowpack, or SWE, which is a function of both depth and density. We used snow depth as a measure of snow magnitude, rather than SWE, because of the availability of data, the number of repeated observations, and the uncertainty related to how snow density varies with land cover. Furthermore, we ignored compaction by using snow depth as an indicator of snow magnitude. The reasons for and sensitivity tests related to these choices are detailed below.

For distributed manual observations, which were utilized for computing ΔSDD metrics, we used observations from snow depth transects even where SWE was also observed. The snow depth transects at all of these sites included approximately 10 times more samples than the co-located snow course (i.e., SWE transect). Since SWE observations are known to be more uncertain at lower snow values [*Work et al.*, 1965], we used snow depth observations for the extraction of snow metrics.

Previous work established that snow density is less spatially variable than snow depth [*Elder et al.*, 1998; *Sturm et al.*, 2010; *López-Moreno et al.*, 2013], which supports the use of snow depth as a proxy for SWE. However, studies that have explicitly compared snow density

observed in the forest to the open have found that snow density is 1-8% higher in the open (1-5%,[*Griffin*, 1918]; approximately 8% [*Veatch et al.*, 2009]) and that snow density is negatively correlated with forest cover [*Molotch and Bales*, 2005]. Thus, we repeated cumulative gain and loss analysis on estimated daily SWE at select sites by using three approaches to quantify density: (1) linearly interpolating between snow course observations of density for forest and open (aggregated by land cover to median values for each day of observations), (2) linearly interpolating between snow course observations of median density (aggregated to a single median value for each day of observations), and (3) choosing the most extreme differences in density that were observed in the forest and the open and applying them as constant density values to snow depth. For the first two cases, we applied a time-varying density value based on the observations. In the third case, we chose the end member density differences between land cover types observed on the same day, including one case for which snow density in the open was observed to be larger than in the forest and vice versa. We then applied those values to the entire time series of observations from the appropriate cover class. Results from applying different methods of calculating SWE from depth and then using SWE as input to cumulative gain and loss analysis are similar to the results presented in section 6.5. The values for $\Delta\Sigma$Gain and $\Delta\Sigma$Loss metrics vary somewhat with the method used, but the general relation that $\Delta\Sigma$Gain is larger than $\Delta\Sigma$Loss is robust.

Lastly, we considered the potential effect of ignoring snowpack settling and metamorphism in cumulative gain and loss analysis. By ignoring vertical shortening (hereafter "shortening") due to settling and metamorphism, cumulative gain would be underestimated because when snow shortening occurs the depth of the snowpack is less than accumulated snow depth [*U.S. Army Corps of Engineers*, 1956]. Subsequently, cumulative loss would be underestimated because the

accumulated snow depth is underestimated. However, loss could also be overestimated because shortening during periods of loss results in a negative change in depth and is therefore counted as loss even if there is no change in snow mass.

We tested the effect of these over- and under-estimates by applying a linearly changing multiplication factor to adjust the depth of the snowpack for shortening, based on previous findings comparing the depth of the snowpack to cumulative snow depth measured with a snow board [*U.S. Army Corps of Engineers*, 1956] (See Plate 8-1). The USACE factor ranged from 1 at the start of the accumulation season, when there is no shortening effect, to 1.5 at peak accumulation and onward, when the depth of the snowpack is smaller than the depth of accumulated snow. We applied this factor to the snow depth data from the open and forest independently and then repeated cumulative gain and loss analysis. The results confirmed that the pattern illustrated in Figure 5 is robust.

6.13 Supporting Tables

Table 6.2 Snow metrics for each site, including ratios of peak snow depth and ΔSDD, and notes of how each value was determined from the dataset. Figure 6.3 in the main text and Figure 6.7 are based on these values.

Site	Water Year	Peak Snow Depth (cm)		Snow Disappearance Day (Julian)		Comparison Metrics		Notes
		Open	*Forest*	*Open*	*Forest*	*Peak Ratio*	*ΔSDD*	
Hogg Pass	2012	229	254	148	163	0.9	-15	Extrapolated from median snow course value
Hogg Pass	2013	179.5	203.5	122	141	0.9	-19	Extrapolated from median snow course value
Hogg Pass	2014	105	151	112	141	0.7	-29	Extrapolated from median snow course value
McK Low	2012	138	57	126	122	2.4	4	Extrapolated from median snow course value
McK Low	2013	133	64	122	96	2.1	26	Extrapolated from median snow course value
McK Low	2014	64	23	72	65	2.8	7	Used sensors for snow metrics due to only 3 days of manual observations. Note that sensors follow median snow course depth for the 3 days of distributed observations.
McK Mid	2012	260	90	155	122	2.9	33	Extrapolated from median snow course value
McK Mid	2013	195	56.5	137	122	3.5	15	Extrapolated from median snow course value
McK Mid	2014	67	25	115	104	2.7	11	Extrapolated from median snow course value
MFW Low	2012	50	35	104	104	1.4	0	Extrapolated from median snow course value
MFW Low	2013	95.5	51	106	91	1.9	15	Extrapolated from median snow course value for forest; extrapolated from sensor for open because median snow course follows sensor, and accumulation event on 15 April prolongs snow cover in open; thus, this is a more conservative estimate for the ΔSDD calculation
MFW Mid	2012	161	42	138	117	3.8	21	Used sensors; no snow course at this site. Took SDD as inflection point for open site, where the sensor reaches minimum value near 6 cm.
MFW Mid	2013	168	80	136	109	2.1	27	Used sensors; no snow course at this site

UIEF Lawler Landing	2008	34	40	65	109	0.9	-44	Open and forest "reference stations" (Met 6 and Met 7); used smoothed depth; used 16 February as the day of peak depth because first day that all sensors were functioning, actual peak depth was likely before this date.
UIEF Lawler Landing	2008	96	39.5	118	112	2.4	6	Mean of two forest stations adjacent to gap; median of 3 gap stations; used smoothed depth; used 16 February as the day of peak depth because first day that all sensors were functioning
Mica Creek	2006	173	100	132	132	1.7	0	North-facing depth transects; used observed SDD (extrapolation would have resulted in a value later than the observed SDD)
Mica Creek	2006	109	70	117	118	1.6	-1	Non-north-facing depth transects (3 in open, 3 in forest); extrapolated from median snow course value
MOSS	2015	62	50	90	81	1.2	9	Aggregate by week and by forest cover; used week 5 as timing of peak depth
Olallie	2015	69	25	122	29	2.8	93	Forest cameras (mean of 2) versus snotel depth; Forest SDD ignores late March accumulation event
Snoqualmie	2015	82	28	75	47	2.9	28	Forest cameras (mean of 2) versus snow depth sensor in gap
Cedar Low (City Cabin and Clearing Met)	2011	113	44	139	128	2.6	11	Forest cameras (mean of 3) at City Cabin old growth versus snow depth sensor at Clearing Met
Cedar Low (City Cabin and Clearing Met)	2013	128	65	130	124	2.0	6	Forest camera (1) at City Cabin old growth versus snow depth sensor at Clearing Met
Cedar Low (Bear Creek)	2011	102	50	143	122	2.0	21	Extrapolated from median snow course depth, median of all control values and of all gap values for Bear Creek; Peak values are from later peak
Cedar Low (Bear Creek)	2012	108	49	129	111	2.2	18	Extrapolated from median snow course depth, median of all control values and of all gap values for Bear Creek; Peak values are from later peak
Mount Gardner	2011			157	137		20	Open SDD from snow depth sensor; Forest SDD as median of iButton grid; No depth observations

Mount Gardner	2012	142	129	13	Open SDD from snow depth sensor; Forest SDD as median of iButton grid; No depth observations
Mount Gardner	2013	136	123	13	Open SDD from snow depth sensor; Forest SDD as median of iButton grid; No depth observations
Mount Gardner	2014	122	102	20	Open SDD from snow depth sensor; Forest SDD as median of iButton grid; No depth observations
Tinkham Creek	2013	162	150	12	Open SDD from snow depth sensor; Forest SDD as median of iButton grid; No depth observations
Tinkham Creek	2014	146	131.5	14.5	Open SDD from snow depth sensor; Forest SDD as median of iButton grid; No depth observations

6.14 Supporting Figures

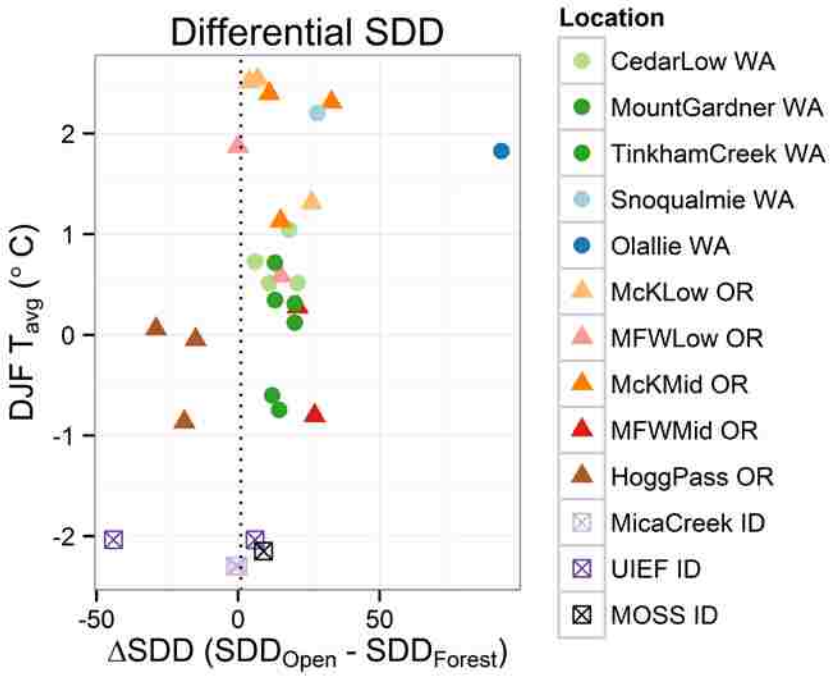

Figure 6.7 This is the same plot as shown in Figure 6.3b, but includes the Olallie site (outlier), which was removed from Figure 6.3b for readability.

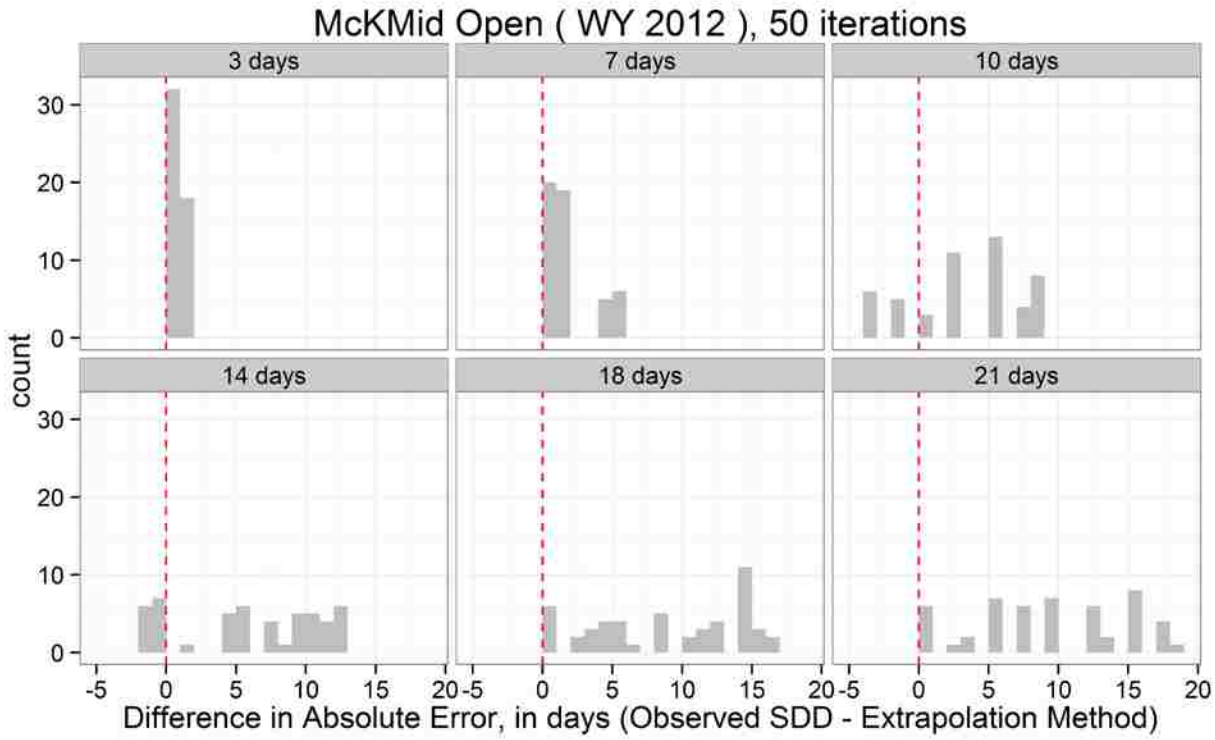

Figure 6.8 Histograms showing the frequency of difference (in days) in absolute error between using the observed SDD and using the extrapolated SDD method, for 50 iterations of a Monte Carlo approach used to resample the daily data at frequencies ranging from 3 to 21 days.

Chapter 7. Linking lidar-derived canopy metrics to the spatiotemporal variability of snow depth and snow duration in a maritime watershed

Susan E. Dickerson-Lange[1], Van R. Kane[2], Rolf F. Gersonde[3], and Jessica D. Lundquist[1]

[1]Civil and Environmental Engineering, University of Washington, Seattle, Washington, USA
[2]School of Environmental and Forest Sciences, University of Washington, Seattle, Washington, USA
[3]Seattle Public Utilities, Seattle, Washington, USA

Note: This chapter is in preparation for submission to *Ecohydrology.*

7.1 Abstract

Forests are a key influence on snow processes, and the increasing availability of airborne lidar data allows for high resolution quantification of forest structural characteristics over large areas. We assess linkages between forest metrics and four years of snow observations in a maritime mountain watershed in western Washington, USA, in order to inform process understanding and model development. We test the relationships between lidar-derived canopy predictor variables and snow observations that integrate forest effects on both snow accumulation and ablation processes, including the time series of snow depth observations through two years, and snow duration observations through four years. We find that 92% of the observed spatiotemporal variability of snow depth in a 1 km^2 area is approximated by two temporal modes determined from matrix decomposition, which represent snow accumulation and ablation. The spatial variance in the scaling of these modes is highly correlated ($r^2 > 0.7$) with several canopy variables in this even-aged forest stand, including mean canopy cover and mean canopy height. Multivariate models of snow duration across a 500 m elevation gradient, four years, and a range of forest types explain 52-72% of the variance in snow disappearance timing, and indicate a stepped response at two sites in which snow duration is longer where canopy cover is <60% and shorter where canopy cover is >80%. The difference in snow disappearance timing between open and forest is shown to be larger in higher snow years, and at lower elevations. Taken together, these results suggest that canopy openness directly overhead controls both accumulation and ablation processes, and subsequent snow disappearance timing. Furthermore, canopy edges drive the gradient of canopy cover in these even-aged stands, and delineating open versus forested area may be sufficient for approximating forest effects on snow in the maritime snow zone.

7.2 Introduction

The increasing availability of airborne lidar data allows for high resolution spatial characterization of forest attributes over large areas [*Harpold et al.*, 2015a]. In turn, this improved forest information holds large potential for advances in both process understanding and model representation of the interactions between forests and snow accumulation [*Trujillo et al.*, 2009; *Moeser et al.*, 2015] and ablation [*Broxton et al.*, 2015; *Musselman et al.*, 2015]. Canopy metrics derived from lidar are available at higher spatial resolutions (e.g. 5 m) than traditionally-used bulk metrics, such as canopy cover or leaf area index (e.g., 30 m data from the National Landcover Database), and can explicitly resolve the spatial arrangement of forest canopy features, such as the size and density of forest gaps, and the positions of edges between forests and openings.

Although the general ways in which forests modify snow processes are well established (e.g., [*Connaughton*, 1935; *Hedstrom and Pomeroy*, 1998; *Storck et al.*, 2002; *Geddes et al.*, 2005; *Essery et al.*, 2008; *Musselman et al.*, 2008; *Veatch et al.*, 2009; *Ellis et al.*, 2011; *Seyednasrollah et al.*, 2013]), there is substantial spatiotemporal variability in the magnitude and direction of forest effects on snow. Empirical studies have demonstrated that snow accumulation generally decreases with increasing forest density because the forest canopy intercepts snow and reduces under-canopy snowpack [*Varhola et al.*, 2010a], but the amount of interception and subsequent loss depends on climate conditions [*Kobayashi*, 1987; *Hedstrom and Pomeroy*, 1998; *Storck et al.*, 2002]. Snow ablation rates generally decrease with increasing forest density due to shading from sunlight and sheltering from wind [*Varhola et al.*, 2010a; *Ellis et al.*, 2011; *Seyednasrollah et al.*, 2013]. However, the amount of decrease varies with topographic position [*Strasser et al.*, 2011; *Ellis et al.*, 2013] and forest attributes [*Kittredge*, 1953; *Woods et al.*,

2006; *Gleason et al.*, 2013]. Alternatively, the presence of forest can increase ablation rates due to enhanced incoming longwave radiation from the forest canopy as compared to the atmosphere [*Essery et al.*, 2008; *Pomeroy et al.*, 2009; *Lundquist et al.*, 2013]. Snow accumulation and ablation rates are also spatially variable within and across diverse forest canopy types, such as forest stands subject to spatially variable thinning [*Woods et al.*, 2006; *Jost et al.*, 2007]. Previous work at the aggregated scale of a plot or silvicultural treatment unit has indicated that bulk representation of forest characteristics may miss important local variations in forest-snow processes (Dickerson-Lange *et al.*, 2015b).

Thus, implementing high resolution forest data in empirical and physically-based models has potential to improve representation of the spatiotemporal variability of snow processes [*Musselman et al.*, 2015; *Zheng et al.*, 2016]. Enhanced understanding of the relations between silvicultural actions, and the resulting lidar data and snow quantities is also of potential use to land and water managers who consider the contribution of snow storage to forest health, aquatic habitat, and water resources [*Grant et al.*, 2013; *Wigmosta et al.*, 2015]. Distributed hydrology modeling is critical for simulating future impacts of forest change, but is limited by the quality of parameterizations of forest-snow processes [*Essery et al.*, 2009; *Rutter et al.*, 2009; *Clark et al.*, 2015].

Several recent studies have begun to address the question of how to utilize lidar to improve representation of forest effects on snow. Strategies generally fall into two categories: those which utilize the three-dimensional lidar point cloud and those that compress the information into a two-dimensional forest metric. The former has been successfully used for small spatial-scale applications, such as explicit ray tracing of solar radiation through a forest canopy [*Musselman et al.*, 2015], but is computationally intensive. The latter seeks to develop a grid-based framework

to represent the forest, which can be readily implemented into grid-based models or compared with other gridded data.

This investigation focuses on the usage of gridded lidar metrics to explain observed snow quantities. Most previous work has focused on using forest metrics to explain snow metrics, such as peak snow magnitude, intercepted snow magnitude, and ablation rates. Peak snow water equivalent (SWE) and snow ablation rate in interior British Columbia, Canada, were shown to correlate with the percent of canopy cover, a lidar-derived ratio of the number of lidar returns from the canopy (i.e., > 2m above ground surface) to the total number of lidar returns for a given spatial domain [*Varhola et al.*, 2010b, 2014]. In an application of lidar metrics across a 2150 m elevation gradient in the Sierra Nevada, California, USA, Zheng et al. (2016) determined that lidar-derived canopy cover explained 14% of the variance in peak snow depth values, whereas elevation explained 43%. [*Moeser et al.*, 2015] linked lidar-derived forest metrics that describe gap size and position relative to gap edges to observations of the amount of intercepted snow from individual storm events in Switzerland, and developed a model for canopy snow interception. Additional previous studies have also demonstrated the importance of position relative to canopy edge, which is readily quantifiable from lidar data, for explaining the spatial variation of snow mass and energy fluxes [*Veatch et al.*, 2009; *Broxton et al.*, 2015].

This investigation assesses linkages between lidar forest metrics and snow observations that integrate forest effects on both snow accumulation and ablation processes in western Washington, USA. In this forested maritime snow zone, a relatively warm winter climate regime contributes to multiple episodes of accumulation and melt throughout a single winter. Whereas previous studies have focused heavily on individual snow metrics, such as peak snow depth [*Varhola et al.*, 2010b, 2014] or amount of intercepted snow from a single event [*Moeser et al.*,

2015], multiple peak values of snow depth interspersed by periods of substantial mid-winter melt are common in the maritime Pacific Northwest, USA [*Storck et al.*, 2002; *Dickerson-Lange et al.*, 2015a; *Wayand et al.*, 2015a].

Since forest modifications of snow processes are different depending on the process and conditions, the link between forest and snow is this climate is complex. For example, canopy density directly overhead may be the primary control on snow depth at the first peak value in a season, but if a warm, sunny period follows that first peak, the second peak value will be a function of both canopy density overhead, which controls interception, and canopy density to the south, which controls incoming solar radiation. Lidar data allow for consideration of both the size and shape of the spatial extent of forest characteristics that influence snow processes.

Thus, we consider snow observations that integrate the spatiotemporal variability of forest modifications of snow processes, including time series of snow depth observations and snow duration metrics. In particular, we utilize spatially distributed observations of snow depth (2 years) and snow duration (4 years) collected on the forested western slope of the Cascade Mountains, Washington, USA, to address the following overarching questions:

1. Which lidar-derived metrics are most predictive of the observed spatiotemporal variability in snow depth and snow duration under a range of forest canopy densities?
2. How do forest characteristics influence different modes of temporal variance in snow depth, and can this help us understand the influence of forest on different snow processes?
3. What are the relative importance and influence of canopy characteristics in controlling snow duration across a range of forest and topographic attributes?

Assessment of the relations between forest metrics and snow quantities will inform future development of both physically-based and empirical models that integrate lidar data to represent forest-snow interactions. Additionally, we aim to further elucidate the roles of forests in

modifying snow accumulation and ablation processes in the maritime snow zone. Previous studies illustrate that the magnitude and direction of forest-snow processes vary considerably with climate [*Lundquist et al.*, 2013; *Dickerson-Lange et al.*, 2016b]. Improved understanding of these interactions in the warm and wet maritime snow zone may support improved prediction of the combined effects of forest and climate change across models that are intended to be applied worldwide.

7.3 Methods

7.3.1 Study site and snow observations

Observations of snow magnitude and snow duration were collected from WY 2011 through WY 2014 in the upper Cedar River Municipal Watershed, approximately 50 km east of Seattle, Washington, USA (Figure 7.1). The watershed is situated on the western slope of the Cascade Range and is subject to a maritime climate, with heavy winter precipitation and winter temperatures that fluctuate around the freezing point. Data were collected at 5 study sites, ranging from 620 m to 1165 m in elevation, and ranging in forest characteristics. Peak SWE values at the study sites were highest in WY 2012 (63-151 cm) and lowest in WY 2014 (28-85 cm, Table 7.1).

The site characteristics and data collected are described only briefly here because the experimental design and physiography of the study area are detailed in [*Dickerson-Lange et al.*, 2015b]. The entire observational dataset and related metadata are publicly available. Snow observations at all sites were designed to robustly sample 40 × 40 m experimental plots that represent a single forest type or silvicultural treatment. The present study uses snow observations at individual locations, but we reference the membership in different types of experimental plots to describe forest type and to link to previous work. Experimental plots at the Bear Creek (elevation 620-640 m, BC on Figure 7.1a) site and Mount Gardner (elevation 860-900 m, MG on Figure 7.1a) site include dense second-growth forest with closed canopy, thinned second-growth forest, and plots with 20 m diameter canopy gaps located in the middle (e.g., Figure 7.1b). Mount Gardner additionally includes an old-growth forest plot, and the City Cabin (elevation 775-780 m, CC on Figure 7.1a) site consists of a single old-growth forest plot. The higher Tinkham Creek (elevation 910-930 m, TC on Figure 7.1a) and Rex River (elevation 1160-1165 m, RR on Figure

7.1a) sites each include a sparsely-forested plot previously subjected to multiple episodes of silvicultural thinning. Tinkham Creek additionally includes a dense, second-growth forest plot. National Resource Conservation Service Snow Telemetry (SNOTEL) stations are co-located with the Mount Gardner, Tinkham Creek, and Rex River sites. We additionally collected sub-daily snow depth data with an acoustic snow depth sensor at the Clearing Meteorological station (CM on Figure 7.1a).

Biweekly manual snow depth transects were performed at Bear Creek in WY 2011 and 2012, and distributed ground temperature data were collected in WY 2011-2014 at Bear Creek, Mount Gardner, and City Cabin, and in WY 2013-2014 at Tinkham Creek and Rex River (see Figure 7.1b for an example of sample locations). Hourly ground temperature data from individual iButton temperature sensors (Maxim DS 1922L thermochrons) buried approximately 2 cm below the ground surface were used to infer daily snow presence and annual snow duration at each sample location following the methods detailed in [*Dickerson-Lange et al.*, 2015a].

7.3.2 Snow metrics

Individual observations of snow depth from manual snow courses were spaced approximately 1 m apart along two perpendicular 20-m transects in each 40 × 40 m experimental plot. Snow depth at 15 plots was measured consistently in WY 2011 on a weekly to bi-weekly frequency. In WY 2012, snow courses were consistently performed at 5 plots on a bi-weekly to monthly frequency. These observations are spatially auto-correlated and vary in precise location from snow course to snow course. The minimum spacing for independent samples of snow duration (i.e., the range on a semi-variogram) was previously shown to be 4-8 m at this site [*Dickerson-Lange et al.*, 2015a]. Thus, to reduce redundancy from autocorrelation and noise

from imprecise geolocation, we use a nearest neighbor approach to aggregate observations by taking the mean along 5 m sections of the transect, at 5 positions in each plot. Thus, the snow depth dataset is aggregated to five observations at each experimental plot, representing the center of the plot and the 5m at both ends of each perpendicular transect. In total, we analyze snow depth at 75 and 24 aggregated locations in WY 2011 and 2012, respectively.

Snow duration is computed from daily snow presence as the relative number of snow covered days (RSCD) since the final peak snow depth value for the site. This metric of snow duration was previously shown to be more representative than snow disappearance date (SDD) of forest-snow interactions at the Bear Creek site because of intermittent snow cover and late-season snow accumulation events [*Dickerson-Lange et al.*, 2015a]. For example, some locations that become snow-free early in the ablation season are then recovered during a spring snow storm, resulting in synchronous values for SDD across many sites that do not reflect the differences in forest-snow processes at those locations.

Furthermore, in order to assess forest influences on snow duration across multiple sites and years, we use a relative metric of ΔRSCD as the difference in relative number of snow covered days between a reference open location and the sample location. The reference open values are derived from snow depth sensors at the Mount Gardner, Tinkham Creek, and Rex River SNOTEL stations, and at the Clearing Meteorological station for comparison to the Bear Creek and City Cabin sample locations. Thus, the ΔRSCD metric essentially normalizes for sites and years where snow disappears earlier or later as a function of differences in the amount of snow accumulation or the conditions during the ablation season. Since maximum snow duration tends to occur in the center of gaps, as in all of the open reference stations, all values of ΔRSCD are

negative. Higher (lower) values of ΔRSCD indicate that snow duration is longer (shorter), and that there is less (more) difference between the sample location and the reference open station.

7.3.3 Lidar data and forest metrics

Airborne lidar data were acquired over the study sites in 2012 by the National Center for Airborne Laser Mapping (NCALM, see Acknowledgments). The survey was performed with an Optech Gemini on 31 August 2012 and 1 September 2012 (i.e., leaf on), with an average pulse density of 7.5 m^2 and up to four returns per pulse.

The 3-dimensional point clouds are processed in the open-source FUSION software (http://forsys.cfr.washington.edu/fusion/fusion_overview.html) to produce gridded 1 m bare earth and canopy surface models, and 5 m canopy cover and canopy height metrics. The height (m) of the top of the canopy is interpolated in every 1 m grid based on the canopy surface model (CSM). Canopy cover (%) is computed as the ratio of lidar returns from greater than 2 m above the ground surface (represented by the bare earth model) in a given 5 m grid cell to the total number of returns in that grid cell.

We compute gridded metrics over a range of size, shapes, and summary statistics (i.e., mean and standard deviation) to empirically test the strength of relationships between canopy cover, canopy height, and snow observations. By testing a range of spatial domains, we aim to elucidate the most relevant spatial scale and the directionality of forest influences on snow processes. Since forest effects on incoming solar radiation are directional, we hypothesize that forest metrics based on the forest directly overhead may have a different influence on snow observations than forest metrics to the south of the sample location. Thus, we test gridded canopy cover (5 m) in aggregated 15, 25, and 35 m square domains (Figure 7.2a) and 15 and 25

m wedge-shaped domains, for which the apex of the wedge was oriented toward north to reflect influences from trees to the south (Figure 7.2c). We also test gridded canopy height (1 m) in aggregated 3, 5, 9, 15, 25, and 35 m square domains and 15 and 25 m wedge-shaped domains.

For all spatial domains greater than the base data (i.e., 5 m for canopy cover and 1 m for canopy height), we aggregate via focal mean and standard deviation, where the summary statistics are computed based on the distribution of gridded values in the defined neighborhood, and the summary value (e.g., mean) is assigned to the pre-defined neighborhood kernel (e.g., often the center pixel in a square neighborhood, Figure 7.2a). Focal metrics control the position of the point of interest in the domain (e.g., the snow sample location), in contrast to extracting point values from an aggregated domain, which results in a wide variety of point positions relative to the grid cell (e.g., Figure 7.2b).

We also test the use of the 1 m canopy height values to quantify the percent open area in a domain. Since the canopy surface model relies only upon first lidar returns rather than the ratio of canopy returns to ground returns, the canopy surface model can be more robust in very dense forests where ground returns are sparse. Thus, metrics from canopy height could be a useful alternative to canopy cover in some locations. We therefore classify each 1 m pixel as under canopy or open based on a threshold canopy height of 2 m and compute percent open area, within the same size and shape focal domains as discussed above.

From the bare earth digital elevation model, we extract focal mean values for topographic metrics in 10 m and 30 m square domains. Topographic quantities include elevation, surface curvature, slope and aspect. Surface curvature is represented by a topographic position index (TPI, after [*Weiss*, 2001]). TPI values range from -1 to 1, with low values representing concavities, have values representing convexities, and 0 values indicative of constant slope.

Slope and aspect are combined into a single 'northness' metric, after [*Molotch et al.*, 2005], which is computed as the product of the cosine of the aspect and the sine of the slope. Values range from -1 to 1, with low values indicative of southern exposure and high values indicative of northern exposure.

7.3.4 Data Analysis

7.3.4.1 Singular Value Decomposition of Snow Depth at Bear Creek

We apply singular value decomposition (SVD) to quantify the spatiotemporal variability in the entire dataset of spatially aggregated (i.e., 5 m nearest neighbor, see section 2.2) snow depth observations through time at Bear Creek in WY 2011 and 2012. Since the snow depth observations were all collected in one < 1 km^2, relatively flat location, the spatial variability in snow depth is expected to be primarily due to forest canopy influences. We analyze each WY of snow depth separately, after removing the mean snow depth for the entire WY from all individual observations so that the mean of the WY dataset equals zero.

SVD is a matrix decomposition method for reducing dimensionality and redundancy in a dataset. The decomposition empirically determines new orthogonal bases for data transformation that maximize the variance explained. In essence, SVD analysis of these datasets results in ranked time modes and the corresponding multipliers for each time mode at each location in space. Thus, the complete observed pattern of snow depth through time at any location is approximated by the linear combination of the most important temporal modes multiplied by the corresponding coefficients at that location in space and the singular values (which are proportional to the amount of variance explained by the mode).

We then assess the correlation between the spatial coefficients related to each of the dominant temporal modes and the lidar-derived spatial predictors, including canopy and topographic metrics. The spatial coefficients reflect the variability in the response through the entire season of observations, rather than on a single day, as in linear correlation. We regress the spatial coefficients against the predictors and use the correlation coefficient (r^2) and p-values to quantify the strength of the correlation.

7.3.4.2 Random Forest Models of Snow Duration Across Years and Sites

We apply a random forest approach to empirically build optimal multivariate models to predict snow duration across multiple years and sites. Random forest is a non-parametric classification and regression tree (CART, Breiman et al., 1984) approach that empirically selects a multivariate predictor set that explains the most variance in the response variable [*Breiman*, 2001; *Cutler et al.*, 2007]. The algorithm is implemented in the randomForest package [*Liaw and Wiener*, 2002] for the R statistical program (release 3.1.0) [*R Core Development Team*, 2014]. Random forest uses an iterative approach to build and combine hundreds of binary regression trees (i.e., a forest of regression trees, typically 500). By building each tree from a randomly selected subset of predictors at each node, the model avoids over-emphasizing a single, dominant predictor variable. In addition, the algorithm assesses the relative contribution of correlated predictors through quantifying the additional variance explained. In the case of highly correlated forest canopy metrics, for example, if canopy height is chosen as the best predictor then canopy density will be included only insofar as it explains additional variance in the data. Furthermore, by taking the average across hundreds of trees the model averages out the tendency of a single iteration to over-fit to the data and reduces the need for post-construction pruning of the tree.

Since the four-year dataset of snow duration includes sites and experimental plots that were added or subtracted through time, we subset the dataset to build four models. We build a 1-site model based on snow duration at Bear Creek over WY2011-2014 to assess the influence of canopy across multiple water years in a single, topographically similar site. We build 2-site models to additionally investigate the relative influence of elevation; the Mount Gardner site is approximately 250 m higher than Bear Creek, has generally lower canopy heights but similarly dense forest canopy (see Table 4.1 and Figure 7.8 in the supporting materials). Two 2-site models are assessed: (1) based on snow duration observations collected at gap, thinned, and control forest plots at Bear Creek and Mount Gardner in WY 2011 and 2012, and (2) based on snow duration observations collected at gap, thinned, and control forest plots at Bear Creek and at thinned and control forest plots at Mount Gardner in WY 2011-2014. Observations collected in the gap plot at Mount Gardner during WY 2011 and 2012, and at the old growth plot at Mount Gardner in WY 2013 and 2014 were excluded from the second model. These subsets of data were used because observations from the Mount Gardner gap in WY 2011 and 2012 represent canopy values that are more open (i.e., from an additional gap plot) and are less well-represented in the dataset (e.g., distribution of canopy cover values presented in the supporting section, Figure 7.8), but the gap plot was not sampled in WY 2013 and 2014. Similarly, the Mount Gardner old growth plot was only sampled in WY 2013 and 2014. Mixing data from these plots when assessing inter-annual forest-snow dynamics could influence the results.

Lastly, we build a 5-site model from observations collected during WY 2013-2014 at five sites, which span an elevation range of 620 – 1165 m and diverse forest types (see Table 4.1). In addition to the control second growth forest, thinned forest, and gap plots at Bear Creek and Mount Gardner, the observations sampled old growth forest at Mount Gardner and City Cabin,

dense second growth at Tinkham Creek, and plots subject to multiple episodes of thinning at Tinkham Creek and Rex River. Thus, the 5-site model reflects the predictability of snow duration in diverse forest and topographic conditions.

For each of these models, the random forest approach selects the optimal predictor set and quantifies the relative importance of each predictor variable in the optimal set. This 'importance' metric is computed from the decrease in mean squared error associated with iteratively including each predictor variable in the model. Although the random forest algorithm inherently accounts for dependent predictor datasets, parsimonious predictor inputs can simplify model construction and improve interpretability [*Kane et al.*, 2015]. Thus, we cycled through several options for predictor inputs, ranging from using all predictors to constraining predictors to one type of canopy variable (i.e., canopy cover versus canopy height) or one spatial domain (i.e., 15 versus 25 m).

7.4 Results

7.4.1 Spatiotemporal variability of snow depth

7.4.1.1 Dominant modes of variability

Observations of snow depth through time at one site (Bear Creek) demonstrate that values in a single year follow a similar temporal pattern, indicating multiple peak snow depth values through a single winter (Figure 7.3). Both the magnitude and amplitude of variation are similar at all control forest locations, with more variance between all locations in the thinned forest and open locations (not shown).

SVD was applied to the time versus space matrix of all snow depth values for each water year, and the decomposition demonstrates that in WY 2011 and 2012 the majority of the temporal variability is approximated by 3 modes, with 52% (WY 2011) and 57% (WY 2012) of the variance explained in the 1st mode, 35% (WY 2011) and 40% (WY 2012) in the 2nd mode, and 3% (WY 2011) and 4% (WY 2012) explained in the 3rd mode. The first mode scales the local maxima of snow depth (Figure 7.4a), and the spatial coefficients for the first mode are all positive (Figure 7.4b), indicating a temporal mode that is in-phase, but is different in magnitude and slope at all locations. In other words, snow depth at all locations rises and falls together but to variable maxima and minima, which is illustrated for four example locations by multiplying the temporal mode by the singular value (i.e., the variance explained) and spatial coefficient for each location (Figure 7.5). The largest variance in the first temporal mode occurs at times that coincide with peak snow depth observations. Spatial coefficients are highest at the sites with less canopy cover, such as in the center of a gap, and lowest within dense canopy, indicating above average snow magnitudes at open locations with higher spatial coefficients (Figure 7.4b and Figure 7.5).

The second temporal mode displays the largest variance at times between or following peak values in snow depth observations. The signs of the spatial coefficients are mixed, such that the second temporal mode displays diverging trends through time depending on location (Figure 7.4b and Figure 7.5). In particular, many locations in gaps are described by a negative coefficient, such that the second mode indicates above average snow depth between and following days of peak snow depth. In contrast, locations in dense forest are described by positive coefficients, indicating below average snow depth between and following days of peak snow depth.

The third temporal mode represents a much smaller portion of the variance in the dataset, but improves the low-dimensional approximation of late season snow depth at many locations. The mode modifies the amount of snow depth for one or two days of observations in April of both WY2011 and 2012, affecting the magnitude of the final peak snow observation and the subsequent rate of ablation.

7.4.1.2 Correlation analysis on spatial coefficients

The spatial coefficient for each sample location reflects the local conditions that scale the snow variability through time in both direction and magnitude. Thus, the spatial pattern of coefficients reflects local attributes. The spatial coefficients therefore correlate strongly with some metrics of the lidar-derived predictor dataset (Figure 7.6, Table 7.2). The predictors that correlate most strongly (r^2: 0.68-0.74) with the spatial coefficients for the first and second modes of snow depth variability are mean canopy cover and mean canopy height in 15 and 25 m square domains. The standard deviation of canopy cover and the percent open area (based on the 1m canopy surface model) also correlate highly with the spatial coefficients for the first mode, and

have slightly lower correlation coefficient for the second mode. None of the topographic metrics derived from lidar, including northness or TPI, correlate strongly with any of the top modes.

Notably, the strength of correlation between canopy predictors and the SVD spatial coefficients are similar between the first and second modes for each predictor (Figure 7.6,Table 7.2). None of the spatial predictors correlate strongly with the third mode, with a maximum correlation coefficient of < 0.3 (Figure 7.6).

7.4.2 Multivariate models of snow duration

7.4.2.1 One-site model: Bear Creek, WY 2011-2014

The random forest binary regression tree model of snow duration at a single site (Bear Creek) over WY 2011-2014 explains 74% of the variance with a RMSE of 4.4 days. The top three predictor variables are mean canopy cover in a 15 m square (33% of the importance), WY (19% of the importance), and mean canopy cover in a 15 m wedge (14% of importance) (Figure 7.7a). Models that are constructed using both canopy cover and canopy height predictors achieve similar amounts of variance explained (i.e., r^2), and the importance is divided into similar amounts between mean canopy height and mean canopy cover. Similarly, in a model constructed from only canopy height predictors, rather than canopy cover predictors, the same types of variables are selected as for the model fit to the canopy cover predictors, and the functional relationships are similar in shape (Figure 7.9 in the supporting materials).

Partial plots illustrate the snow duration response of an individual predictor variable in the fitted model across the range of predictor values, with all other predictors held constant at their mean values (Figure 7.7). The snow duration response to canopy cover at Bear Creek mimics a step function, for which snow duration is longer (i.e. higher values of ΔRSCD) where mean

canopy cover is 0-60%, and snow duration is shorter (i.e. lower values of ΔRSCD) where canopy cover is greater than 80% (Figure 7.7a). The response of snow duration to WY indicates that there was less difference between sample locations and the reference open location (i.e., Clearing Meteorological station) in WY 2011 and 2012, and more difference in WY 2013 and 2014. The response of snow duration to the remaining canopy predictors indicates that snow lasts longer where canopy cover both immediately overhead and to the south is lower (low values of mean canopy cover in a wedge). The variable snow duration response across the range of elevation values likely reflects the spatial arrangement of experimental plots rather than a true elevation effect.

7.4.2.2 Two-site models: Bear Creek and Mount Gardner, WY 2011-2014

The first two-site model is built from snow duration data from the gap, thinned, and control forest plots at Bear Creek and Mount Gardner in WY 2011 and 2012. The model demonstrates less predictive value ($r^2 = 0.52$) overall, but the results are similar to the Bear Creek model in that canopy cover is the dominant predictor (importance metric of 25%; Figure 7.7b). Snow duration demonstrates a stepped response to canopy cover that is similar to the response in the one-site model (previous section). The inclusion of data from the Mount Gardner gap and thinned plots results in slightly higher frequencies of mid-range canopy values than in the one-site model, illustrated by the comparison of histograms in Figure 7.7a and Figure 7.7b. Elevation and the standard deviation of canopy cover emerge as the second most important variables (23 and 22%). The frequency of elevation values is bimodal, reflecting observations collected at two sites that are separated by approximately 250 m elevation. The snow duration response to elevation indicates that there is more difference between the sample locations and the reference open location at Bear Creek than at Mount Gardner. The response to standard deviation of canopy

cover is also stepped: longer snow duration where canopy variance is higher. Water year is not an important predictor variable for this dataset from WY 2011 and 2012, with a flat snow duration response between the different years (not shown).

The second two-site model explains a higher percent of the variance in the data ($r^2 = 0.74$), and also selects canopy cover as a dominant variable along with elevation (25% importance each) across two sites and four WY of snow duration data (Figure 7.7c). Canopy cover in a wedge is the third predictor (14% importance), and WY is the fourth (12% importance). Similar to the first two-site model, the response of snow duration to elevation is stepped, with more difference between snow duration at a sample location and at a reference open location at the Bear Creek site. In contrast to the first two-site model (WY 2011 and 2012), the second two-site model (WY 2011-2014) demonstrates a clear dependence on WY as a predictor, with less difference between sample locations and their open reference locations in WY 2011 and 2012 and more difference in WY 2013 and 2014.

7.4.2.3 Five-site model: All Sites, WY 2013-2014

The Random Forest model explains 60% of the variance of the dataset, with the two top predictors capturing site differences characterized by elevation (30% importance) and northness (19% importance, Figure 7.7d). The third and fourth predictors are mean canopy cover in a 15 m square and in a 15 m wedge (tied at 17% importance each): the overall trend is toward longer snow duration in locations with less canopy cover directly overhead and to the south, but the response is variable, particularly in the range of 40-80% canopy cover. Notably, the importance of WY is less than 1% for this dataset that spans WY 2013-2014.

7.5 Discussion

7.5.1 Relating SVD modes to forest-snow processes

Singular value decomposition of snow depth through time distills the temporal and spatial variance at one site (Bear Creek) through an entire snow season, rather than representing a single moment in time. As such, the dominant modes of temporal variance, and the spatial coefficients at each location, reflect the integration of key snow processes and how they are modified by the spatial attributes at each location. Since the dataset is constrained to observations collected within a < 1 km^2, relatively flat site, observed snow variability is likely to be linked to local attributes related to the forest canopy (or lack thereof) or local topographic features (i.e., curvature), rather than reflecting larger spatial scale differences in snow processes that could be attributed, for example, to orographic effects on precipitation.

The dominant mode of temporal snow depth variability reflects the amplitude of peak values throughout the snow season. From a process perspective, this scaling is primarily related to forest modification of snow accumulation via canopy snow interception. Where dense canopy is present, snow is intercepted, and the under-canopy snow accumulation is reduced, resulting in lower peak values. At this site, the snow depth peaks are highest in the gap center and lowest in the control forest (Figure 7.5, row 1).

The second mode of variability scales snow depth in between or following peak values, and is related to ablation processes. In particular, snow depth during periods of ablation is higher at the gap sites and lower at the control sites (Figure 7.5, row 2). Mathematically, some of the scaling is related to over (or under) representation of the ablation curve resulting from fitting the first mode to the amplitude of peak values and therefore affecting both the minima and maxima. However, the adjustments made by the second mode (i.e., since the scaled modes are summed to

approximate snow depth at a single site) are larger in magnitude than the over (or under) estimations of snow depth minima in the first mode. Thus, the mode may represent higher ablation rates in the forest versus the gaps at some locations and in some events.

Both the first and second temporal modes, which broadly represent accumulation and ablation processes, are correlated approximately equally to the same canopy predictor variables (Figure 7.6 and Table 7.2). This finding supports previous analysis in the Pacific Northwest that suggested diminished importance of the role of forest in shading the snowpack from sunlight in the net effect of forest on snow duration [*Dickerson-Lange et al.*, 2016b]. If forest shading from sunlight were important to under-canopy ablation, we would expect to find that canopy metrics that describe canopy density or openness to the south of a sample location to be more strongly correlated with the second mode than canopy metrics that represent the canopy directly overhead. That both modes are most strongly related to canopy density directly overhead suggests that the amount of snow present from accumulation processes, or the differential longwave radiation contribution from overhead forest versus sky are more likely to contribute to the temporal variability in snow depth following a peak value.

The third mode of variability represents much less variance explained (3%), but is interesting because it mainly modifies snow depth in the late season, April and May, in both WY 2011 (Figure 7.6, row 3) and 2012 (not shown). In contrast to the first two modes, the spatial coefficients of the third modes are not robustly explained by any of the canopy or topographic predictor variables (Figure 7.7). We speculate that the third mode reflects whether the overlying canopy completely attenuates the snow accumulation signal during small, late-season events when intercepted snow is likely to be completely lost to the under-canopy snowpack via melt driven by high energy inputs. In particular, we hypothesize that a different metric that better

reflects the total longwave radiation input from both the overlying canopy and the multi-directional tree stem inputs, such as distance from a tree stem, may be more predictive of the variability in snow depth response to these late-season snow storms.

7.5.2 Multivariate modeling of snow duration

Random Forest modeling of snow duration allows for estimation of the contribution of individual predictor values to the overall multivariate explanation of snow duration across sites and years. For a single densely forested site, Bear Creek, canopy cover is the most important predictor variable, even over four winters of data collection (Figure 7.7a). Similarly, canopy cover is one of the top two predictors for both 2-site models (Figure 7.7b and Figure 7.7c). The trend of the response indicates that snow duration is longer where canopy cover is lower (i.e., more open), and the shape suggests a threshold value of canopy density at which snow duration shifts from longer in a more open site (canopy cover < 60%) to shorter snow duration in a densely forested site (canopy cover > 70%). This stepped result is influenced to some extent by the distribution of canopy values that were sampled, since snow duration observations were sparsely collected where canopy cover is < 70% (Figure 7.7a, histogram of canopy cover). However, the stepped response is consistent when adding more locations in the 2-site model, which includes slightly higher frequencies of mid-range canopy cover values (Figure 7.7b, histogram of canopy cover). The consistent result supports the robustness of a stepped response. A threshold response to snow duration at this location is also supported by previous analysis of the distribution of snow duration observations at the Bear Creek and Mount Gardner sites, in which snow duration at the 40 × 40 m plot-scale was statistically indistinguishable between the thinned and control second-growth forest [*Dickerson-Lange et al.*, 2015a]. The basal area of the

thinned plots was reduced by approximately 30%, which resulted in a 10-16% decrease in canopy cover (derived from lidar).

The ranked importance of predictor variables in the 1-site and 2-site models further indicates that canopy cover is more important for predicting relative snow duration than inter-annual variability, and equally or more important than elevation, at the Bear Creek and Mount Gardner sites. The response of relative snow duration to WY suggests more difference between forested and open sites in lower snow years. Peak SWE at the nearby meteorological stations (Clearing Meteorological station and Mount Gardner SNOTEL) was slightly less than WY 2013 than in WY 2011, and approximately 50% less in WY 2014 than in 2011 (Table 7.1). Elevation is the second most important predictor in the 2-site model, indicating less difference in snow duration between forested and open locations at the higher Mount Gardner site than at Bear Creek. Similar to the finding that there is less difference during high snow years, the larger amounts of snow accumulation at Mount Gardner likely overwhelm the canopy snow storage capacity and thus reduce the difference in under-canopy versus open snowpack accumulation. Recent observations of forest snowpack at nearby sites at the crest of the Cascade range in Washington also show very large differences in snow duration between open and forested locations during the anomalously low snow year of WY 2015 [*Dickerson-Lange et al.*, 2016b].

7.5.3 Implications for linking canopy metrics to snow

Mean canopy height and mean canopy cover have similar explanatory value for distributed snow depth at Bear Creek and snow duration at Bear Creek and Mount Gardner (Table 7.2, Figure 7.7 and Figure 7.9). Percent open area, derived from the canopy height model also is highly correlated with the spatiotemporal variability of snow depth at Bear Creek. These results

reflect the forest structure at both sites: dense, even-aged stands of second growth interspersed with open forest gaps. Thus, the canopy height metric describes the position of the sample location relative to an edge, since a mid-range canopy height value is the results of averaging spatially consistent canopy height values with adjacent zero values where there is a gap. Previous work and the stepped response of snow duration to canopy cover at these two sites (Figure 7.7) indicate that silvicultural thinning to the extent completed at this site has little to no effect on snow duration, despite resulting decreases in canopy cover values relative to the control second-growth forest (Figure 7.8). Rather, the presence or absence of a canopy opening appears to be the driver of snow variability and, ultimately, snow duration.

Canopy height functions differently as a predictor in the 5-site model. The inclusion of canopy height improves the 5-site model, likely because canopy height correlates with elevation and helps to distinguish the sites (Figure 7.8). This relationship relates to tree physiology and growth rates as a function of elevation, as well as the forest management history that resulted in a patchwork of mostly even-aged stands where the canopy height is spatially homogeneous except where there are gaps or open areas [*Kane et al.*, 2011].

Therefore, in even-aged stands, particularly where canopy cover is dense, simply distinguishing whether a location is in the forest or in the open may be as useful for prediction of relative snow duration as a higher resolution canopy metric derived from lidar. Many previous studies across climate regimes and forest types have also showed that the relative amount and position of canopy edges and openings strongly influence both accumulation and ablation processes [*Musselman et al.*, 2008; *Veatch et al.*, 2009; *Harpold et al.*, 2015b; *Moeser et al.*, 2015]. Previous work by Veatch et al. (2009) found than an edgeness metric to quantify the direction and gradient of canopy cover change improved a statistical model of peak SWE, but

their metric utilized 30 m canopy cover data, and we did not find that such a metric based on higher resolution canopy height or cover provided strong explanatory value for snow depth or duration. Regardless, these findings support the importance of edges and of open areas in determining the magnitude and duration of snow storage. Canopy gaps, which can include openings resulting from natural disturbance, silviculture, or forest harvest patch cuts and skid tracks may be the key structure that contributes to the spatial heterogeneity of snow and ultimately to the duration of stand-scale snow storage. We note, however, that this study is limited to the effects of small canopy gaps on snow, and does not account for decreasing shading and sheltering in larger gaps [*Seyednasrollah and Kumar*, 2014; *Musselman et al.*, 2015].

Quantification of the presence, size, and density of these gaps could be accomplished by estimating focal mean and variance of canopy attributes from gridded data in predominantly even-aged stands, as demonstrated in this study. Other, more computationally intensive approaches such as vector tracing have been successfully implemented to quantify gap density in previous work [*Moeser et al.*, 2015]. However, at the Cedar River Municipal Watershed in particular, and perhaps for much of the western Pacific Northwest region, mapping open or forested from aerial photography could possibly provide a robust first order approximation of spatially distributed snow duration based on sparse observations. Automated edge detection (e.g., [*Liu and Jezek*, 2004]) from photography or from gridded products like a lidar-derived canopy surface model has potential to quantify canopy edges and openings over large areas for use in forest-snow modeling.

7.6 Conclusion

Since forest effects on snow processes vary in magnitude and direction, predicting the effect of forest characteristics on snow storage is an ongoing research challenge. Particularly in the maritime snow zone where forest modifications of both snow accumulation and ablation processes are integrated throughout a winter season, linking forest metrics to snow observations is complex. Thus, we utilize two data analysis strategies to help understand the link between the full time series of snow depth and canopy metrics, and between snow duration and canopy, climate, and topographic drivers.

We find that lidar-derived canopy metrics that describe the canopy openness directly overhead correlate equally well with the temporal variability associated with accumulation processes as with ablation processes. Canopy openness also drives the snow duration response over four years, particularly at two densely forested sites; a stepped snow duration response to canopy cover indicates that snow duration is longer where canopy cover is < 60%. Together, these results indicate that representing the presence, size, and density of canopy gaps is critical for predicting snow duration over a landscape. Furthermore, the delineation of canopy edges in even-aged stands is not limited to canopy cover, but can be derived from a canopy surface model or aerial photography.

7.7 Acknowledgements

Primary support for this project was provided by the Department of the Interior Northwest Climate Science Center (NW CSC) through Cooperative Agreement GS297A from the United States Geological Survey (USGS). Lidar data collection and processing was provided by the National Center for Airborne Laser Mapping (NCALM, http://ncalm.cive.uh.edu/) via a seed grant to S. Dickerson-Lange. We thank the many researchers and technicians who contributed to field data collection at the Cedar River Municipal Watershed, and are grateful to Seattle Public Utilities for allowing watershed access and providing field equipment. We thank Paul Sampson for useful suggestions and guidance related to spatiotemporal data analysis. All data described herein are publicly available via the University of Washington (http://hdl.handle.net/1773/33268), the CUAHSI Water Data Center (https://dx.doi.org/10.4211/his-data-cedarriverforestsnow) and NSF Open Topography (http://www.opentopography.org/).

7.8 Tables

Table 7.1 Peak snow metrics from sub-daily snow depth sensors located in forest gaps during the four years of data collection, provided here to illustrate the inter-annual variability in snow conditions.

Site	2011		2012		2013		2014	
	SWE (cm)	*Depth (cm)*	*SWE (cm)*	*Depth (cm)*	*SWE (cm)*	*Depth (cm)*	*SWE (cm)*	*Depth (cm)*
Clearing Meteorological		166		204		151		110
Mount Gardner	51	147	63	198	48	150	28	102
Tinkham Creek	87	216	106	297	79	224	59	188
Rex River	132	277	151	343	121	290	85	239

Table 7.2 Linear correlation coefficients (r^2) for canopy predictor variables with the spatial coefficients associated with the first and second dominant modes of temporal variability (Mode 1 and Mode 2, respectively) from the SVD analysis of snow depth through time at Bear Creek in WY 2011.

Predictor	Size (m)	Shape	Mode1	Mode2
Mean canopy cover (%)	15	Focal square	0.74	0.73
Mean canopy cover (%)	25	Focal square	0.72	0.70
Mean canopy height (m)	15	Focal square	0.70	0.69
Mean canopy height (m)	25	Focal square	0.68	0.68
Percent open (from 1 m CSM)	15	Focal square	0.67	0.67
Standard deviation of canopy cover (%)	25	Focal square	0.67	0.63
Canopy cover (%)	5	Gridded square	0.65	0.65
Standard deviation of canopy cover (%)	35	Focal square	0.65	0.62
Mean canopy height (m)	9	Focal square	0.65	0.65
Mean canopy height (m)	15	Focal square	0.65	0.66
Percent open (from 1 m CSM)	9	Focal square	0.63	0.63
Mean canopy height (m)	35	Focal square	0.63	0.62
Mean canopy cover (%)	10	Focal N-pointed wedge	0.62	0.55
Percent open (from 1 m CSM)	5	Focal square	0.58	0.60

7.9 Figures

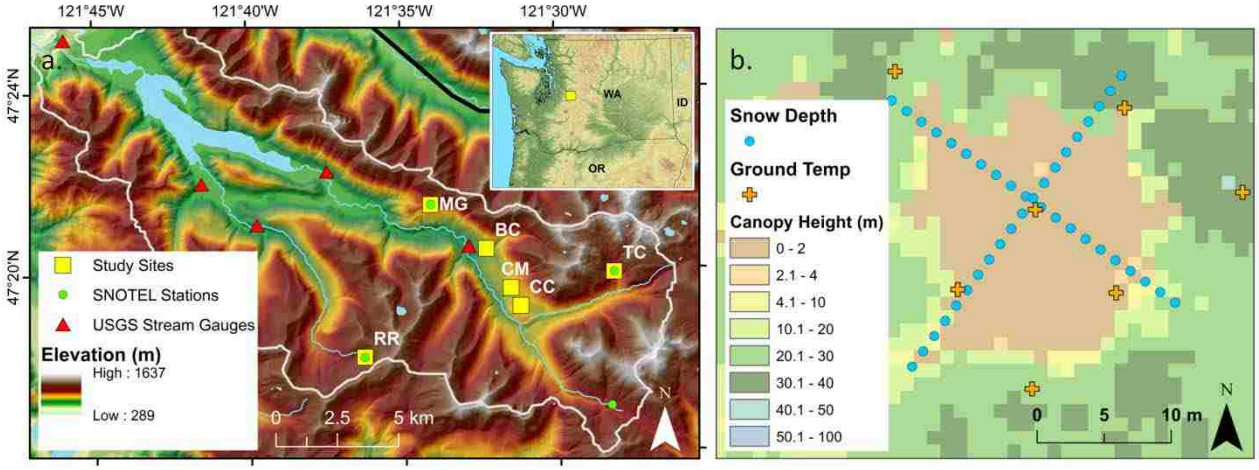

Figure 7.1 (a) Map of the Cedar River Municipal Watershed (inset shows region) with data collection sites indicated (adapted from (Dickerson-Lange et al., 2015a)). (b) Lidar-derived 1-m canopy surface model (i.e., canopy height) over one experimental forest gap plot at the Bear Creek (BC on (a)) site, with positions of snow observations indicated.

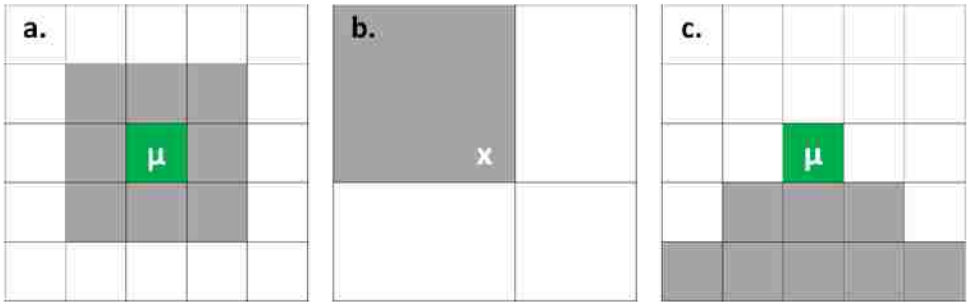

Figure 7.2 Cartoon illustrating different methods for computing gridded metrics. (a) Focal mean of a 3 × 3 square domain, with mean value assigned to kernel (in green). (b) Extraction of value for the point x based on the inclusion of x in the 3 × 3 domain. (c) Focal mean of a north-pointed wedge-shaped domain that is 3 pixels high, with mean value assigned to kernel (in green).

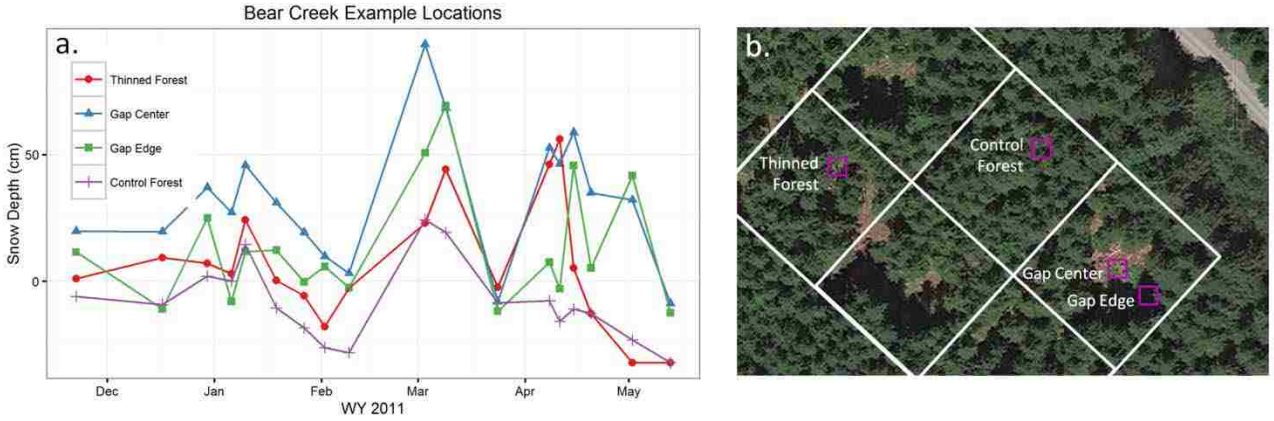

Figure 7.3 (a) Normalized snow depth observations (i.e., mean snow depth for all locations has been removed) during WY 2011 at four example locations at Bear Creek. (b) Aerial photograph of a portion of the Bear Creek site, with locations of the four examples in (a) noted by purple boxes and labels. Photograph courtesy of Google Earth Imagery, © 2016 Google, with the additional data from Landsat.

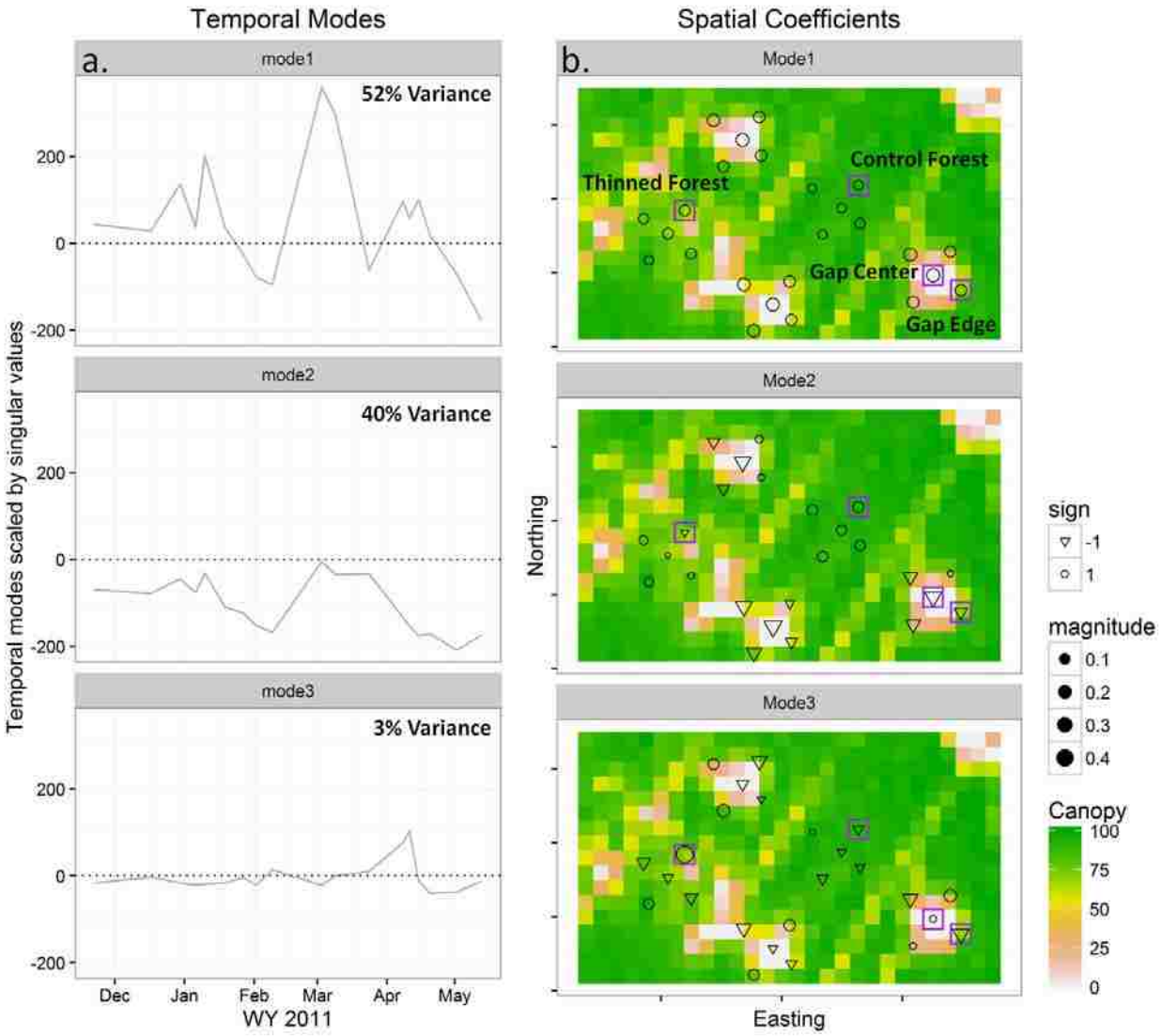

Figure 7.4 (a) Top three temporal modes, scaled by their singular values, for snow depth observations at Bear Creek from WY 2011. (b) Spatial coefficients for the top three temporal modes, plotted on gridded 5-m canopy cover (%) for a subset of sampling locations. Purple boxes indicate example locations shown in Figure 7.3 and Figure 7.5.

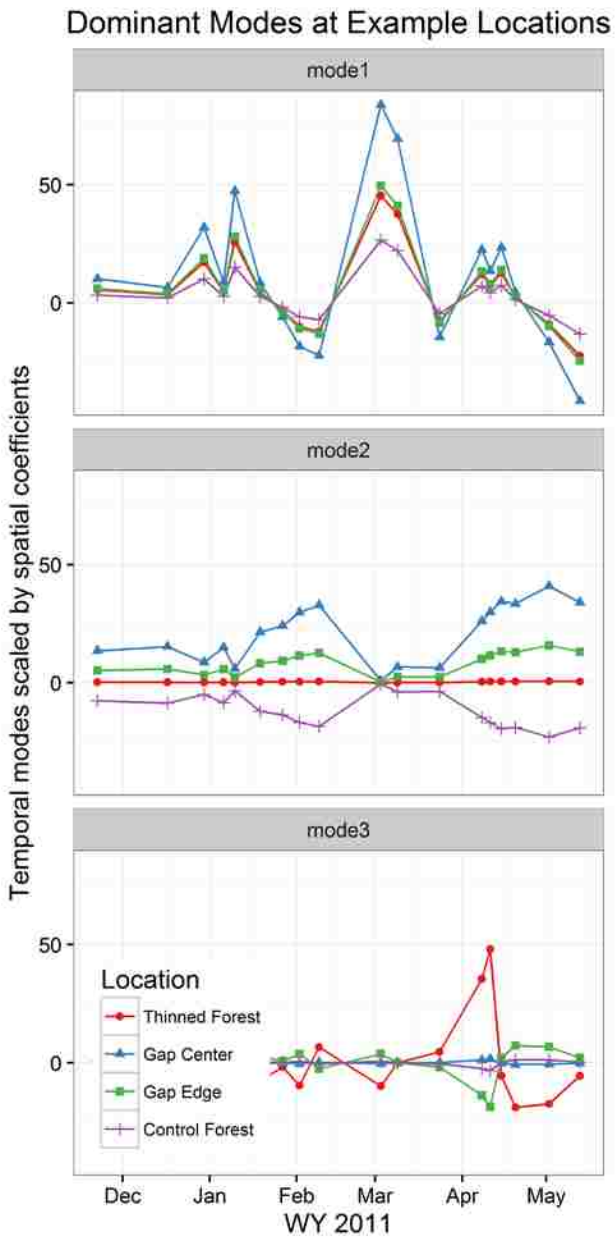

Figure 7.5 Dominant temporal modes for snow depth observations at Bear Creek from WY 2011, scaled by their singular values and by the spatial coefficients at four example locations, indicating the dominant patterns of snow depth variability through time at these locations.

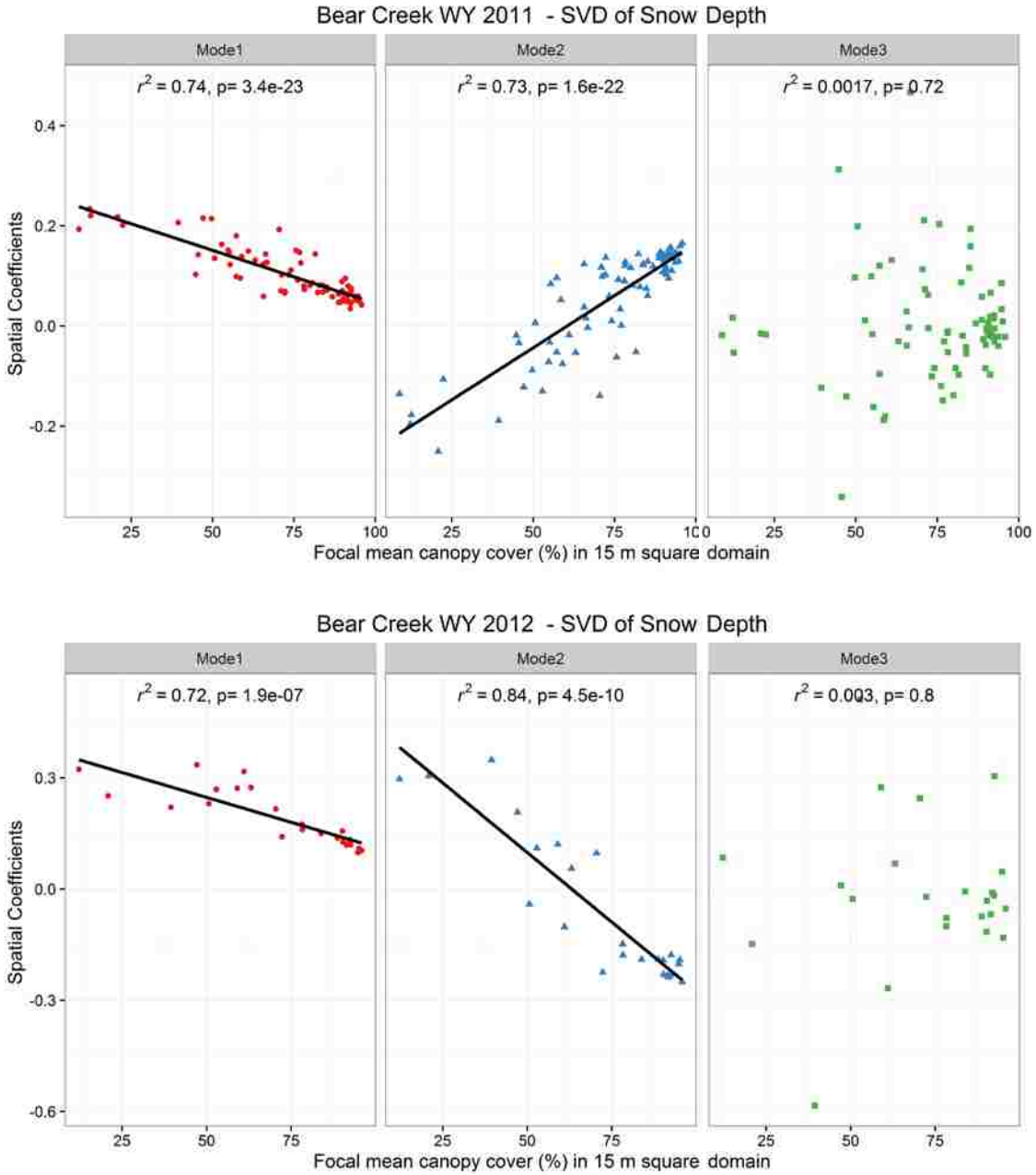

Figure 7.6 Scatterplots of spatial coefficients as a function of one lidar-derived canopy metric, mean canopy cover (%) in a 15 m square domain, and correlation statistics, for the top three modes of temporal variability in snow depth observations at Bear Creek for both WY 2011 and 2012.

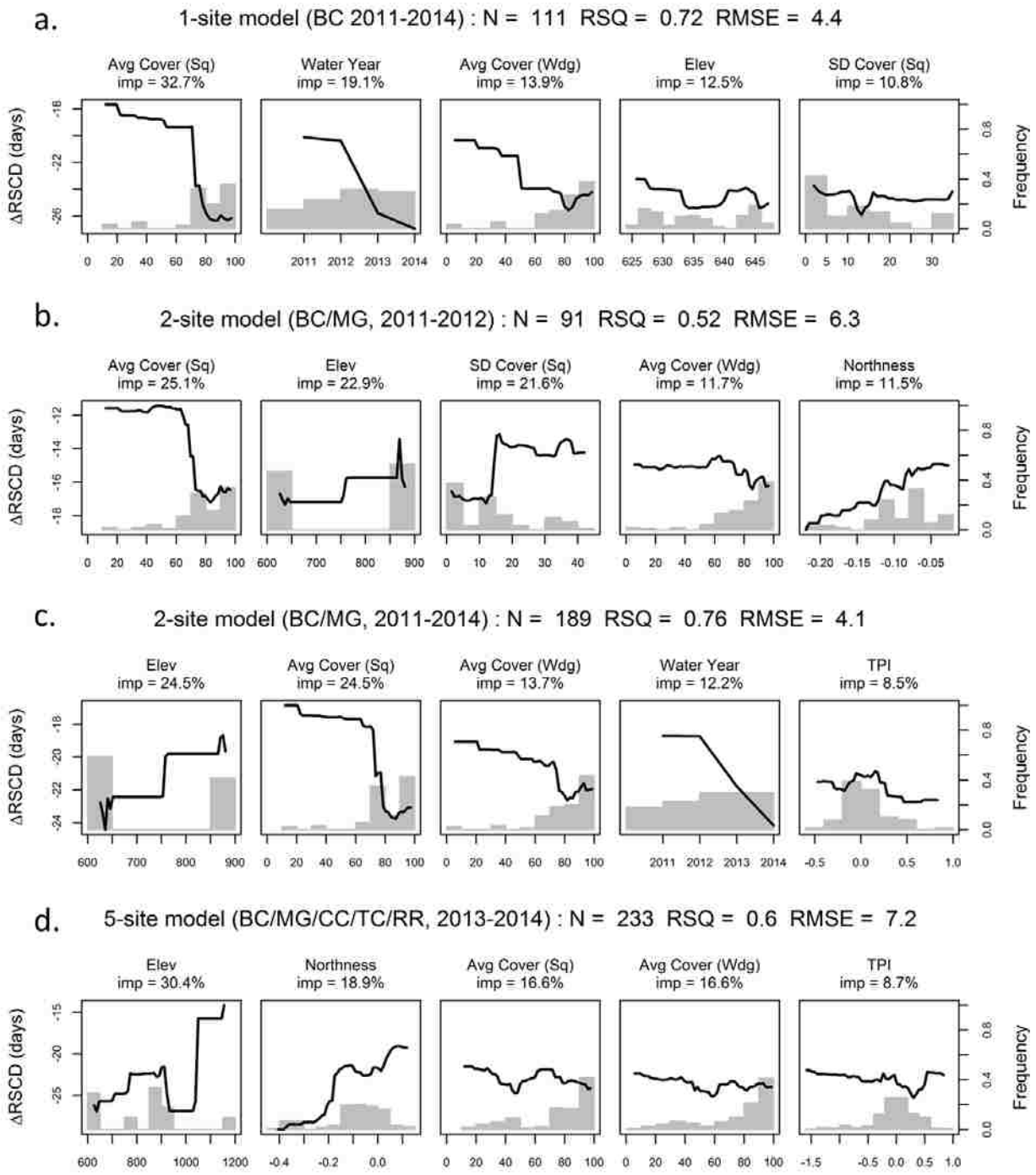

Figure 7.7 Partial plots from Random Forest model fitted to a suite of canopy and topographic predictor variables for snow duration observations (ΔRSCD, computed as snow duration in a reference open location minus snow duration at a sample location), where the black line shows the snow duration response to an individual predictor variable across the range of predictor values with all other predictors held constant at their mean values. The gray histogram indicates the frequency distribution of predictor values in the dataset. The subplots display the results for

models based on four subsets of snow data: (a) a 1-site model based on observations from Bear Creek (BC) in WY 2011-2014, (b) a 2-site model based on observations from BC and Mount Gardner (MG) in WY 2011-2012, and (c) in WY 2011-2014 (with all data from the MG gap and old growth plots excluded due to temporal inconsistency), and (d) a 5-site model based on observations from BC, MG, City Cabin (CC), Tinkham Creek (TC), and Rex River (RR) in WY 2013-2014.

7.10 Supporting Figures

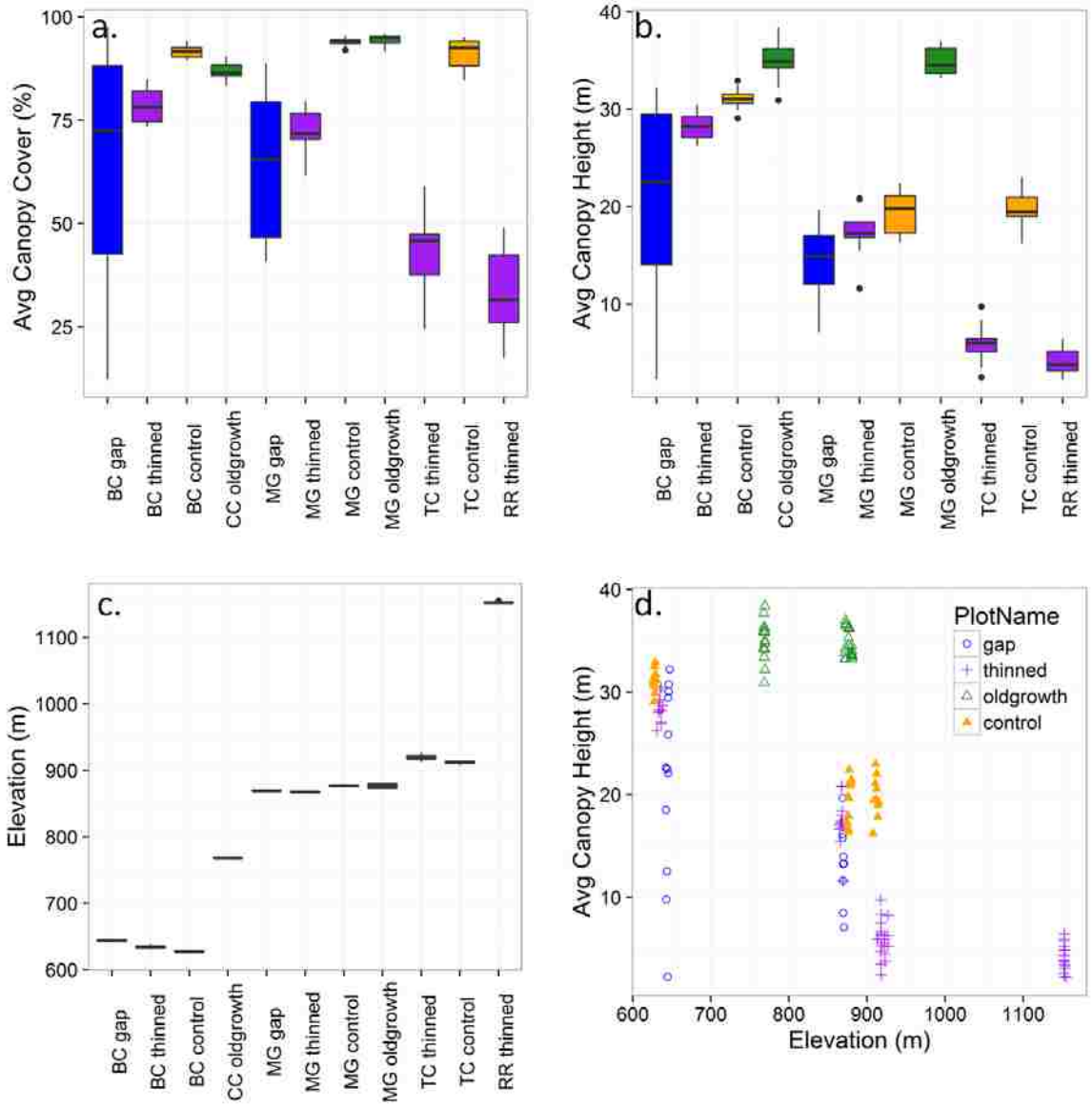

Figure 7.8 Meta-analysis of the variability of spatial predictor values with sites and with elevation. (a –c) Distributions of lidar-derived (a) canopy cover (%) and (b) canopy height (m) and (c) elevation (m) over snow duration sample locations at all experimental plots included in the 5-site snow duration model. Both canopy metrics are given as the focal mean values of 15 m square domains. (d) Lidar-derived canopy height as a function of elevation, with color and shape of symbols indicating experimental plot membership.

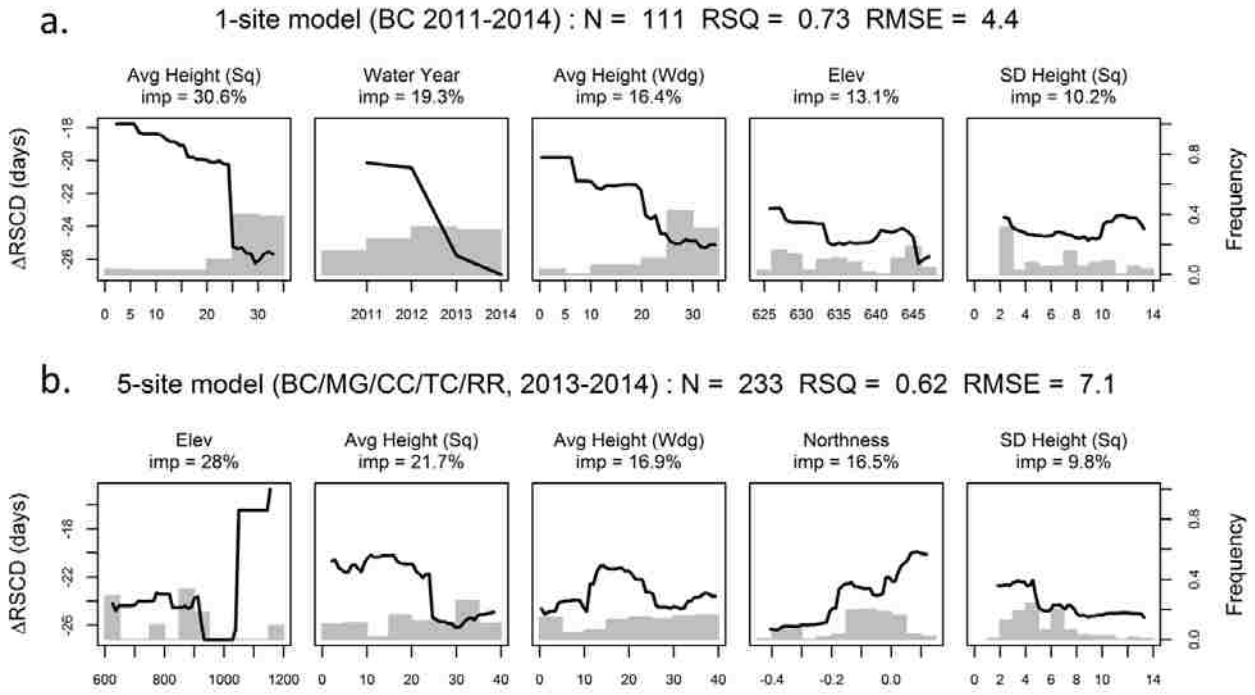

Figure 7.9 Partial plots from Random Forest model as presented in Figure 7.7a and Figure 7.7d, but showing the equivalent models built from canopy height rather than canopy cover metrics.

Chapter 8. References

Adam, J. C., A. F. Hamlet, and D. P. Lettenmaier (2009), Implications of global climate change for snowmelt hydrology in the twenty-first century, *Hydrol. Process.*, *23*(7), 962–972, doi:10.1002/hyp.7201.

Anderton, S. P., S. M. White, and B. Alvera (2004), Evaluation of spatial variability in snow water equivalent for a high mountain catchment, *Hydrol. Process.*, *18*(3), 435–453, doi:10.1002/hyp.1319.

Andreadis, K. M., P. Storck, and D. P. Lettenmaier (2009), Modeling snow accumulation and ablation processes in forested environments, *Water Resour. Res.*, *45*(5), 1–13, doi:10.1029/2008WR007042.

Bales, R. C., J. W. Hopmans, A. T. O'Geen, M. Meadows, P. C. Hartsough, P. Kirchner, C. T. Hunsaker, and D. Beaudette (2011), Soil Moisture Response to Snowmelt and Rainfall in a Sierra Nevada Mixed-Conifer Forest, *Vadose Zo. J.*, *10*(3), 786, doi:10.2136/vzj2011.0001.

Barbero, R., J. T. Abatzoglou, N. K. Larkin, C. A. Kolden, and B. Stocks (2015), Climate change presents increased potential for very large fires in the contiguous United States, *Int. J. Wildl. Fire*, A–H, doi:10.1071/WF15083.

Bingaman, D., and K. B. Eitel (2010), Boulder Creek Study: Fifth graders tackle a local environmental problem through an inquiry-based project, *Sci. Child.*, *47*(6), 52–56.

Blöschl, G. (1999), Scaling issues in snow hydrology, *Hydrol. Process.*, *13*(14-15), 2149–2175, doi:10.1002/(SICI)1099-1085(199910)13:14/15<2149::AID-HYP847>3.0.CO;2-8.

Bonney, R., C. B. Cooper, J. Dickinson, S. Kelling, T. Phillips, K. V. Rosenberg, and J. Shirk (2009), Citizen Science: A Developing Tool for Expanding Science Knowledge and Scientific Literacy, *Bioscience*, *59*(11), 977–984, doi:10.1525/bio.2009.59.11.9.

Bonney, R., J. L. Shirk, T. B. Phillips, A. Wiggins, H. L. Ballard, A. J. Miller-Rushing, and J. K. Parrish (2014), Citizen science. Next steps for citizen science., *Science*, *343*(6178), 1436–7, doi:10.1126/science.1251554.

Borden, R. J., K. S. Cline, T. Hussey, G. Longsworth, and I. Mancinelli (2007), A river runs through it: A college-community collaboration for watershed-based regional planning and education, *Hum. Ecol. Rev.*, *14*(1), 90–100.

Bosch, J., and J. Hewlett (1982), A review of catchment experiments to determine the effect of vegetation changes on water yield and evapotranspiration, *J. Hydrol.*, *55*, doi:http://dx.doi.org/10.1016/0022-1694(82)90117-2.

Breiman, L. (2001), Random Forests, *Mach. Learn.*, *45*(1), 5–32, doi:10.1023/A:1010933404324.

Brown, P. J., and A. T. DeGaetano (2011), A paradox of cooling winter soil surface temperatures in a warming northeastern United States, *Agric. For. Meteorol.*, *151*(7), 947–956, doi:10.1016/j.agrformet.2011.02.014.

Broxton, P. D., A. A. Harpold, J. A. Biederman, P. A. Troch, N. P. Molotch, and P. D. Brooks (2015), Quantifying the effects of vegetation structure on snow accumulation and ablation

in mixed-conifer forests, *Ecohydrology*, *8*(6), 1073–1094, doi:10.1002/eco.1565.

Burles, K., and S. Boon (2011), Snowmelt energy balance in a burned forest plot, Crowsnest Pass, Alberta, Canada, *Hydrol. Process.*, *25*(19), 3012–3029, doi:10.1002/hyp.8067.

Buytaert, W. et al. (2014), Citizen science in hydrology and water resources: opportunities for knowledge generation, ecosystem service management, and sustainable development, *Front. Hydrosph.*, *2*(October), 1–21, doi:10.3389/feart.2014.00026.

Carson, D. R. (2010), Quantification of snow pack mass and energy dyamics across a canopy discontinuity, University of Idaho.

Chen, J., J. F. Franklin, and T. a. Spies (1993), Contrasting microclimates among clearcut, edge, and interior of old-growth Douglas-fir forest, *Agric. For. Meteorol.*, *63*(3-4), 219–237, doi:10.1016/0168-1923(93)90061-L.

Cherkauer, K. A., and D. P. Lettenmaier (1999), Hydrologic effects of frozen soils in the upper Mississippi River basin, *J. Geophys. Res.*, *104*(D16), 19599–19610, doi:10.1029/1999JD900337.

Clark, M. P., A. G. Slater, A. P. Barrett, L. E. Hay, G. J. McCabe, B. Rajagopalan, and G. H. Leavesley (2006), Assimilation of snow covered area information into hydrologic and land-surface models, *Adv. Water Resour.*, *29*(8), 1209–1221, doi:10.1016/j.advwatres.2005.10.001.

Clark, M. P., J. Hendrikx, A. G. Slater, D. Kavetski, B. Anderson, N. J. Cullen, T. Kerr, E. Örn Hreinsson, and R. A. Woods (2011), Representing spatial variability of snow water equivalent in hydrologic and land-surface models: A review, *Water Resour. Res.*, *47*, W07539, doi:10.1029/2011WR010745.

Clark, M. P. et al. (2015), A unified approach for process-based hydrologic modeling: 2. Model implementation and case studies, *Water Resour. Res.*, *51*(4), 2515–2542, doi:10.1002/2015WR017200.

CoCoRaHS (2015), Community Collaborative Rain, Hail and Snow Network, Available from: http://www.cocorahs.org/ (Accessed 14 May 2015)

Connaughton, C. (1935), The accumulation and rate of melting of snow as influenced by vegetation, *J. For.*, *33*(6), 564–569.

Conrad, C. C., and K. G. Hilchey (2011), A review of citizen science and community-based environmental monitoring: Issues and opportunities, *Environ. Monit. Assess.*, *176*(1-4), 273–291, doi:10.1007/s10661-010-1582-5.

Cooper, C. B., J. Dickinson, T. Phillips, and R. Bonney (2007), Citizen science as a tool for conservation in residential ecosystems, *Ecol. Soc.*, *12*(2).

Cristea, N. C., J. D. Lundquist, S. P. Loheide, C. S. Lowry, and C. E. Moore (2014), Modelling how vegetation cover affects climate change impacts on streamflow timing and magnitude in the snowmelt-dominated upper Tuolumne Basin, Sierra Nevada, *Hydrol. Process.*, *28*(12), 3896–3918, doi:10.1002/hyp.9909.

Cutler, D. R., T. C. Edwards, K. H. Beard, A. Cutler, K. T. Hess, J. Gibson, and J. J. Lawler

(2007), Random forests for classification in ecology, *Ecology*, *88*(11), 2783–2792, doi:10.1890/07-0539.1.

Daly, C., M. Halbleib, J. I. Smith, W. P. Gibson, M. K. Doggett, G. H. Taylor, J. Curtis, and P. P. Pasteris (2008), Physiographically sensitive mapping of climatological temperature and precipitation across the conterminous United States, *Int. J. Climatol.*, *28*(15), 2031–2064, doi:10.1002/joc.1688.

Davis, R. E., J. P. Hardy, W. Ni, C. Woodcock, J. C. McKenzie, R. Jordan, and X. Li (1997), Variation of snow cover ablation in the boreal forest: A sensitivity study on the effects of conifer canopy, *J. Geophys. Res.*, *102*(D24), 29389–29395, doi:10.1029/97JD01335.

Deems, J. S., T. H. Painter, and D. C. Finnegan (2013), Lidar measurement of snow depth: a review, *J. Glaciol.*, *59*(215), 467–479, doi:10.3189/2013JoG12J154.

Deering, C. A., and J. M. Stoker (2014), Let's Agree on the Casing of Lidar, *LiDAR News Mag.*, *4*(6), 4–7.

Dickerson-Lange, S. E., J. A. Lutz, K. A. Martin, M. S. Raleigh, R. Gersonde, and J. D. Lundquist (2015a), Evaluating observational methods to quantify snow duration under diverse forest canopies, *Water Resour. Res.*, *15*(2), 1203–1224, doi:10.1002/2014WR015744.

Dickerson-Lange, S. E., J. A. Lutz, R. Gersonde, K. A. Martin, J. E. Forsyth, and J. D. Lundquist (2015b), Observations of distributed snow depth and snow duration within diverse forest structures in a maritime mountain watershed, *Water Resour. Res.*, *51*(11), 9353–9366, doi:10.1002/2015WR017873.

Dickerson-Lange, S. E., K. B. Eitel, L. Dorsey, T. E. Link, and J. D. Lundquist (2016a), Engaging citizen scientists to observe patterns of snow cover across the Pacific Northwest, *J. Sci. Commun.*, *15(01)*(A01).

Dickerson-Lange, S. E., R. F. Gersonde, J. A. Hubbart, T. E. Link, A. W. Nolin, G. H. Perry, T. R. Roth, N. E. Wayand, and J. D. Lundquist (2016b), Snow disappearance timing in warm winter climates is dominated by forest effects on snow accumulation, *Hydrol. Process.*, *In Review*.

Du, E., T. E. Link, J. A. Gravelle, and J. A. Hubbart (2013), Validation and sensitivity test of the distributed hydrology soil-vegetation model (DHSVM) in a forested mountain watershed, *Hydrol. Process.*, doi:10.1002/hyp.10110.

Du, E., T. E. Link, L. Wei, and J. D. Marshall (2016), Evaluating hydrologic effects of spatial and temporal patterns of forest canopy change using numerical modelling, *Hydrol. Process.*, *30*(2), 217–231, doi:10.1002/hyp.10591.

Durand, M., N. P. Molotch, and S. A. Margulis (2008), Merging complementary remote sensing datasets in the context of snow water equivalent reconstruction, *Remote Sens. Environ.*, *112*(3), 1212–1225, doi:10.1016/j.rse.2007.08.010.

Eick, C., B. Deutsch, J. Fuller, and F. Scott (2008), Making Science Relevant, *Sci. Teach.*, *75*(4), 26–29.

Elder, K., and D. Cline (2003), *CLPX-Ground: ISA Snow Depth Transects and Related Measurements*, Verson 2., edited by M. Parsons and M. Brodzik, Boulder, Colorado USA: NASA National Snow and Ice Data Center Distributed Active Archive Center.

Elder, K., W. Rosenthal, and R. E. Davis (1998), Estimating the spatial distribution of snow water equivalence in a montane watershed\r, *Hydrol. Process.*, *12*(AUGUST 1998), 1793–1808, doi:10.1002/(SICI)1099-1085(199808/09)12.

Elder, K., A. Goodbody, D. Cline, P. Houser, G. E. Liston, L. Mahrt, and N. Rutter (2009), NASA Cold Land Processes Experiment (CLPX 2002/03): Ground-Based and Near-Surface Meteorological Observations, *J. Hydrometeorol.*, *10*(1), 330–337, doi:10.1175/2008JHM877.1.

Ellis, C. R., J. W. Pomeroy, R. L. H. Essery, and T. E. Link (2011), Effects of needleleaf forest cover on radiation and snowmelt dynamics in the Canadian Rocky Mountains, *Can. J. For. Res.*, *41*(3), 608–620, doi:10.1139/X10-227.

Ellis, C. R., J. W. Pomeroy, and T. E. Link (2013), Modeling increases in snowmelt yield and desynchronization resulting from forest gap-thinning treatments in a northern mountain headwater basin, *Water Resour. Res.*, *49*(2), 936–949, doi:10.1002/wrcr.20089.

Elsner, M. M., L. Cuo, N. Voisin, J. S. Deems, A. F. Hamlet, J. A. Vano, K. E. B. Mickelson, S.-Y. Lee, and D. P. Lettenmaier (2010), Implications of 21st century climate change for the hydrology of Washington State, *Clim. Change*, *102*(1-2), 225–260, doi:10.1007/s10584-010-9855-0.

Essery, R., and J. Pomeroy (2004a), Implications of spatial distributions of snow mass and melt rate for snow-cover depletion: theoretical considerations, *Ann. Glaciol.*, *38*(1), 261–265, doi:10.3189/172756404781815275.

Essery, R., and J. Pomeroy (2004b), Vegetation and Topographic Control of Wind-Blown Snow Distributions in Distributed and Aggregated Simulations for an Arctic Tundra Basin, *J. Hydrometeorol.*, *5*(5), 735–744, doi:10.1175/1525-7541(2004)005<0735:VATCOW>2.0.CO;2.

Essery, R., J. Pomeroy, C. Ellis, and T. Link (2008), Modelling longwave radiation to snow beneath forest canopies using hemispherical photography or linear regression, *Hydrol. Process.*, *22*(15), 2788–2800, doi:10.1002/hyp.6930.

Essery, R., N. Rutter, J. Pomeroy, R. Baxter, M. Stähli, D. Gustafsson, A. Barr, P. Bartlett, and K. Elder (2009), SNOWMIP2: An Evaluation of Forest Snow Process Simulations, *Bull. Am. Meteorol. Soc.*, *90*(8), 1120–1135, doi:10.1175/2009BAMS2629.1.

Faria, D. A., J. W. Pomeroy, and R. L. H. Essery (2000), Effect of covariance between ablation and snow water equivalent on depletion of snow-covered area in a forest, *Hydrol. Process.*, *14*(15), 2683–2695, doi:10.1002/1099-1085(20001030)14:15<2683::AID-HYP86>3.0.CO;2-N.

Fassnacht, S. R., K. A. Dressler, and R. C. Bales (2003), Snow water equivalent interpolation for the Colorado River Basin from snow telemetry (SNOTEL) data, *Water Resour. Res.*, *39*(8), doi:10.1029/2002WR001512.

Fiala, A. C. S., S. L. Garman, and A. N. Gray (2006), Comparison of five canopy cover estimation techniques in the western Oregon Cascades, *For. Ecol. Manage.*, *232*(1-3), 188–197, doi:10.1016/j.foreco.2006.05.069.

Flint, A. L., L. E. Flint, and M. D. Dettinger (2008), Modeling soil moisture processes and recharge under a melting snowpack, *Vadose Zo. J.*, *7*(1), 350, doi:10.2136/vzj2006.0135.

Ford, K. R., A. K. Ettinger, J. D. Lundquist, M. S. Raleigh, and J. Hille Ris Lambers (2013), Spatial heterogeneity in ecologically important climate variables at coarse and fine scales in a high-snow mountain landscape., *PLoS One*, *8*(6), e65008, doi:10.1371/journal.pone.0065008.

Fortin, V., M. Jean, R. Brown, and S. Payette (2015), Predicting snow depth in a forest–tundra landscape using a conceptual model allowing for snow redistribution and constrained by observations from a digital camera, *Atmosphere-Ocean*, *53*(2), 200–211, doi:10.1080/07055900.2015.1022708.

Friesen, J., J. Lundquist, and J. T. Van Stan (2015), Evolution of forest precipitation water storage measurement methods, *Hydrol. Process.*, *29*(11), 2504–2520, doi:10.1002/hyp.10376.

Galloway, A., M. Tudor, and W. Haegen (2006), The reliability of citizen science: a case study of Oregon white oak stand surveys, *Wildl. Soc. Bull.*, *34*(5), 1425–1429, doi:10.2193/0091-7648(2006)34[1425:TROCSA]2.0.CO;2.

Garvelmann, J., S. Pohl, and M. Weiler (2013), From observation to the quantification of snow processes with a time-lapse camera network, *Hydrol. Earth Syst. Sci.*, *17*(4), 1415–1429, doi:10.5194/hess-17-1415-2013.

Gary, H. L. (1974), Snow accumulation and snowmelt as influenced by a small clearing in a lodgepole pine forest, *Water Resour. Res.*, *10*(2), 348–353, doi:10.1029/WR010i002p00348.

Gary, H. L., and C. A. Troendle (1982), Snow Accumulation and Melt Under Various Stand Densities in Lodgepole Pine in Wyoming and Colorado, *USDA For. Serv. Rock Mt. For. Range Exp. Stn.*, *RM-417*.

Geddes, C. A., D. G. Brown, and D. B. Fagre (2005), Topography and vegetation as predictors of snow water equivalent across the alpine treeline ecotone at Lee Ridge, Glacier National Park, Montana, U.S.A, *Arctic, Antarct. Alp. Res.*, *37*(2), 197–205, doi:10.1657/1523-0430(2005)037[0197:TAVAPO]2.0.CO;2.

Gelfan, A. N., J. W. Pomeroy, and L. S. Kuchment (2004), Modeling Forest Cover Influences on Snow Accumulation, Sublimation, and Melt, *J. Hydrometeorol.*, *5*(5), 785–803, doi:10.1175/1525-7541(2004)005<0785:MFCIOS>2.0.CO;2.

Gleason, K. E., A. W. Nolin, and T. R. Roth (2013), Charred forests increase snowmelt: Effects of burned woody debris and incoming solar radiation on snow ablation, *Geophys. Res. Lett.*, *40*(17), 4654–4661, doi:10.1002/grl.50896.

Golding, D. L., and R. H. Swanson (1986), Snow distribution patterns in clearings and adjacent forest, *Water Resour. Res.*, *22*(13), 1931–1940, doi:10.1029/WR022i013p01931.

Grant, G. E., C. L. Tague, and C. D. Allen (2013), Watering the forest for the trees: An emerging priority for managing water in forest landscapes, *Front. Ecol. Environ.*, *11*(6), 314–321, doi:10.1890/120209.

Gravelle, J. A., and T. E. Link (2007), Influence of timber harvesting on headwater peak stream temperatures in a northern Idaho Watershed, *For. Sci.*, *53*(2), 189–205.

Griffin, A. A. (1918), Influence of Forests upon the Melting of Snow in the Cascade Range, *Mon. Weather Rev.*, *46*(7), 324–327, doi:10.1175/1520-0493(1918)46<324:IOFUTM>2.0.CO;2.

Groffman, P. M., J. P. Hardy, C. T. Driscoll, and T. J. Fahey (2006), Snow depth, soil freezing, and fluxes of carbon dioxide, nitrous oxide and methane in a northern hardwood forest, *Glob. Chang. Biol.*, *12*(9), 1748–1760, doi:10.1111/j.1365-2486.2006.01194.x.

Guan, B., N. P. Molotch, D. E. Waliser, S. M. Jepsen, T. H. Painter, and J. Dozier (2013), Snow water equivalent in the Sierra Nevada: Blending snow sensor observations with snowmelt model simulations, *Water Resour. Res.*, *49*(8), 5029–5046, doi:10.1002/wrcr.20387.

Haklay, M. (2013), *Citizen Science and Volunteered Geographic Information: Overview and Typology of Participation*, edited by D. Z. Sui, S. Elwood, and M. F. Goodchild, Springer Netherlands.

Hamlet, A. F., and D. P. Lettenmaier (1999), Effects of climate change on hydrology and water resources in the Columbia River basin, *J. Am. Water Resour. Assoc.*, *35*(6), 1597–1623, doi:10.1111/j.1752-1688.1999.tb04240.x.

Hardy, J. P., R. Melloh, P. Robinson, and R. Jordan (2000), Incorporating effects of forest litter in a snow process model, *Hydrol. Process.*, *14*(18), 3227–3237, doi:10.1002/1099-1085(20001230)14:18<3227::AID-HYP198>3.0.CO;2-4.

Harpold, A. A. et al. (2015a), Laser vision: lidar as a transformative tool to advance critical zone science, *Hydrol. Earth Syst. Sci.*, *19*(6), 2881–2897, doi:10.5194/hess-19-2881-2015.

Harpold, A. A., N. P. Molotch, K. N. Musselman, R. C. Bales, P. B. Kirchner, M. Litvak, and P. D. Brooks (2015b), Soil moisture response to snowmelt timing in mixed-conifer subalpine forests, *Hydrol. Process.*, *29*(12), 2782–2798, doi:10.1002/hyp.10400.

Hedstrom, N. R., and J. W. Pomeroy (1998), Measurements and modelling of snow interception in the boreal forest, *Hydrol. Process.*, *12*(10-11), 1611–1625, doi:10.1002/(SICI)1099-1085(199808/09)12:10/11<1611::AID-HYP684>3.0.CO;2-4.

Hiemstra, C. A., G. E. Liston, and W. a Reiners (2002), Snow Redistribution by wind and interactions with vegetation at upper treeline in the Medicine Bow Mountains, Wyoming, U.S.A., *Arctic, Antarct. Alp. Res.*, *34*(3), 262, doi:10.2307/1552483.

Howe, J. (2006), The Rise of Crowdsourcing, *Wired Mag.*

Hubbart, J. A., T. E. Link, J. A. Gravelle, and W. Elliot (2007), Timber harvest impacts on water yield in the continental/maritime hydroclimatic region of the United States, *For. Sci.*, *53*(2), 169–180.

Hubbart, J. A., T. E. Link, and J. A. Gravelle (2015), Forest canopy reduction and snowpack

dynamics in a northern Idaho satershed of the continental-maritime region, United States, *For. Sci.*, *61*(5), 882–894, doi:10.5849/forsci.14-025.

Ide, R., and H. Oguma (2013), A cost-effective monitoring method using digital time-lapse cameras for detecting temporal and spatial variations of snowmelt and vegetation phenology in alpine ecosystems, *Ecol. Inform.*, *16*, 25–34, doi:10.1016/j.ecoinf.2013.04.003.

Jennings, S., N. Brown, and D. Sheil (1999), Assessing forest canopies and understorey illumination: canopy closure, canopy cover and other measures, *Forestry*, *72*(1), 59–74, doi:10.1093/forestry/72.1.59.

Jones, J. A. (2004), Seasonal and successional streamflow response to forest cutting and regrowth in the northwest and eastern United States, *Water Resour. Res.*, *40*(5), 1–19, doi:10.1029/2003WR002952.

Jost, G., M. Weiler, D. R. Gluns, and Y. Alila (2007), The influence of forest and topography on snow accumulation and melt at the watershed-scale, *J. Hydrol.*, *347*(1-2), 101–115, doi:10.1016/j.jhydrol.2007.09.006.

Kane, V. R., R. J. McGaughey, J. D. Bakker, R. F. Gersonde, J. A. Lutz, and J. F. Franklin (2010a), Comparisons between field- and LiDAR-based measures of stand structural complexity, *Can. J. For. Res.*, *40*(4), 761–773, doi:10.1139/X10-024.

Kane, V. R., J. D. Bakker, R. J. McGaughey, J. A. Lutz, R. F. Gersonde, and J. F. Franklin (2010b), Examining conifer canopy structural complexity across forest ages and elevations with LiDAR data, *Can. J. For. Res.*, *40*(4), 774–787, doi:10.1139/X10-064.

Kane, V. R., R. F. Gersonde, J. A. Lutz, R. J. McGaughey, J. D. Bakker, and J. F. Franklin (2011), Patch dynamics and the development of structural and spatial heterogeneity in Pacific Northwest forests, *Can. J. For. Res.*, *41*(12), 2276–2291, doi:10.1139/x11-128.

Kane, V. R., J. A. Lutz, C. Alina Cansler, N. A. Povak, D. J. Churchill, D. F. Smith, J. T. Kane, and M. P. North (2015), Water balance and topography predict fire and forest structure patterns, *For. Ecol. Manage.*, *338*, 1–13, doi:10.1016/j.foreco.2014.10.038.

Kerr, T., M. Clark, J. Hendrikx, and B. Anderson (2013), Snow distribution in a steep mid-latitude alpine catchment, *Adv. Water Resour.*, *55*, 17–24, doi:10.1016/j.advwatres.2012.12.010.

Kittredge, J. (1953), Influences of forests on snow in the Ponderosa, Sugar Pine, Fir zone of the central Sierra Nevada, *Hilgardia*, *22*, 1–96.

Klein, A. G., D. K. Hall, and G. A. Riggs (1998), Improving snow cover mapping in forests through the use of a canopy reflectance model, *Hydrol. Process.*, *12*(10-11), 1723–1744, doi:10.1002/(SICI)1099-1085(199808/09)12:10/11<1723::AID-HYP691>3.0.CO;2-2.

Kobayashi, D. (1987), Snow accumulation on a narrow board, *Cold Reg. Sci. Technol.*, *13*(3), 239–245, doi:10.1016/0165-232X(87)90005-X.

Koivusalo, H., and T. Kokkonen (2002), Snow processes in a forest clearing and in a coniferous forest, *J. Hydrol.*, *262*(1-4), 145–164, doi:10.1016/S0022-1694(02)00031-8.

Korhonen, L., K. Korhonen, M. Rautiainen, and P. Stenberg (2006), Estimation of forest canopy

cover: a comparison of field measurement techniques, *Silva Fenn.*, *40*(4), 577–588.

Landry, C. C., K. A. Buck, M. S. Raleigh, and M. P. Clark (2014), Mountain system monitoring at Senator Beck Basin, San Juan Mountains, Colorado: A new integrative data source to develop and evaluate models of snow and hydrologic processes, *Water Resour. Res.*, *50*(2), 1773–1788, doi:10.1002/2013WR013711.

Langan, S. J., L. Johnston, M. J. Donaghy, A. F. Youngson, D. W. Hay, and C. Soulsby (2001), Variation in river water temperatures in an upland stream over a 30-year period, *Sci. Total Environ.*, *265*(1-3), 195–207, doi:10.1016/S0048-9697(00)00659-8.

Lawler, R. R., and T. E. Link (2011), Quantification of incoming all-wave radiation in discontinuous forest canopies with application to snowmelt prediction, *Hydrol. Process.*, *25*(21), 3322–3331, doi:10.1002/hyp.8150.

Lawless, J. G., and B. N. Rock (1998), Student scientist partnerships and data quality, *J. Sci. Educ. Technol.*, *7*(1), 5–13, doi:10.2307/40188640.

Leach, J. A., and R. D. Moore (2014), Winter stream temperature in the rain-on-snow zone of the Pacific Northwest: Influences of hillslope runoff and transient snow cover, *Hydrol. Earth Syst. Sci.*, *18*(2), 819–838, doi:10.5194/hess-18-819-2014.

Li, L., and J. W. Pomeroy (1997), Estimates of threshold wind speeds for snow transport using meteorological data, *J. Appl. Meteorol.*, *36*(3), 205–213, doi:10.1175/1520-0450(1997)036<0205:EOTWSF>2.0.CO;2.

Liaw, A., and M. Wiener (2002), Classification and Regression by randomForest, *R News*, *2*(3), 18–22.

Link, T. E., D. Marks, and J. P. Hardy (2004), A deterministic method to characterize canopy radiative transfer properties, *Hydrol. Process.*, *18*(18), 3583–3594, doi:10.1002/hyp.5793.

Liston, G. (1999), Interrelationships among snow distribution, snowmelt, and snow cover depletion: Implications for atmospheric, hydrologic, and ecologic modeling, *J. Appl. Meteorol.*, *38*, 1474–1487, doi:10.1175/1520-0450(1999)038%25310.1175/1520-045 http://dx.doi.org/10.1175/1520-0450(1999)038<1474:IASDSA>2.0.CO;2.

Liston, G. E. (1995), Local Advection of Momentum, Heat, and Moisture during the Melt of Patchy Snow Covers, *J. Appl. Meteorol.*, *34*(7), 1705–1715, doi:10.1175/1520-0450-34.7.1705.

Liston, G. E. (2004), Representing Subgrid Snow Cover Heterogeneities in Regional and Global Models, *J. Clim.*, *17*(6), 1381–1397, doi:10.1175/1520-0442(2004)017<1381:RSSCHI>2.0.CO;2.

Liston, G. E., and K. Elder (2006), A meteorological distribution system for high-resolution terrestrial modeling (MicroMet), *J. Hydrometeorol.*, *7*(2), 217–234, doi:10.1175/JHM486.1.

Liston, G. E., C. J. Perham, R. T. Shideler, and A. N. Cheuvront (2016), Modeling snowdrift habitat for polar bear dens, *Ecol. Modell.*, *320*, 114–134, doi:10.1016/j.ecolmodel.2015.09.010.

Liu, H., and K. C. Jezek (2004), Automated extraction of coastline from satellite imagery by

integrating Canny edge detection and locally adaptive thresholding methods, *Int. J. Remote Sens.*, *25*(5), 937–958, doi:10.1080/0143116031000139890.

Liu, J., C. E. Woodcock, R. A. Melloh, R. E. Davis, C. McKenzie, and T. H. Painter (2008), Modeling the View Angle Dependence of Gap Fractions in Forest Canopies: Implications for Mapping Fractional Snow Cover Using Optical Remote Sensing, *J. Hydrometeorol.*, *9*(5), 1005–1019, doi:10.1175/2008JHM866.1.

López-Moreno, J. I., and J. Latron (2008), Influence of canopy density on snow distribution in a temperate mountain range, *Hydrol. Process.*, *22*(1), 117–126, doi:10.1002/hyp.6572.

López-Moreno, J. I., S. R. Fassnacht, J. T. Heath, K. N. Musselman, J. Revuelto, J. Latron, E. Morán-Tejeda, and T. Jonas (2013), Small scale spatial variability of snow density and depth over complex alpine terrain: Implications for estimating snow water equivalent, *Adv. Water Resour.*, *55*(2013), 40–52, doi:10.1016/j.advwatres.2012.08.010.

Lowry, C. S., and M. N. Fienen (2013), CrowdHydrology: Crowdsourcing hydrologic data and engaging citizen scientists, *GroundWater*, *51*(1), 151–156, doi:10.1111/j.1745-6584.2012.00956.x.

Luce, C. H., and D. G. Tarboton (2004), The application of depletion curves for parameterization of subgrid variability of snow, *Hydrol. Process.*, *18*(8), 1409–1422, doi:10.1002/hyp.1420.

Luce, C. H., D. G. Tarboton, and K. R. Cooley (1998), The influence of the spatial distribution of snow on basin-averaged snowmelt, *Hydrol. Process.*, *12*(10-11), 1671–1683, doi:10.1002/(SICI)1099-1085(199808/09)12:10/11<1671::AID-HYP688>3.0.CO;2-N.

Luce, C. H., D. G. Tarboton, and K. R. Cooley (1999), Sub-grid parameterization of snow distribution for an energy and mass balance snow cover model, *Hydrol. Process.*, *13*(1213), 1921–1933, doi:10.1002/(SICI)1099-1085(199909)13:12/13<1921::AID-HYP867>3.3.CO;2-J.

Lundquist, J. D., and B. Huggett (2010), Evergreen trees as inexpensive radiation shields for temperature sensors, *Water Resour. Res.*, *46*, W00D04, doi:10.1029/2008WR006979.

Lundquist, J. D., and F. Lott (2008), Using inexpensive temperature sensors to monitor the duration and heterogeneity of snow-covered areas, *Water Resour. Res.*, *44*(4), W00D16, doi:10.1029/2008WR007035.

Lundquist, J. D., M. D. Dettinger, and D. R. Cayan (2005), Snow-fed streamflow timing at different basin scales: Case study of the Tuolumne River above Hetch Hetchy, Yosemite, California, *Water Resour. Res.*, *41*(7), W07005, doi:10.1029/2004WR003933.

Lundquist, J. D., S. E. Dickerson-Lange, J. A. Lutz, and N. C. Cristea (2013), Lower forest density enhances snow retention in regions with warmer winters: A global framework developed from plot-scale observations and modeling, *Water Resour. Res.*, *49*(10), 6356–6370, doi:10.1002/wrcr.20504.

Lutz, J. A., J. W. van Wagtendonk, and J. F. Franklin (2010), Climatic water deficit, tree species ranges, and climate change in Yosemite National Park, *J. Biogeogr.*, *37*(5), 936–950, doi:10.1111/j.1365-2699.2009.02268.x.

Lutz, J. A., K. A. Martin, and J. D. Lundquist (2012), Using Fiber-Optic Distributed Temperature Sensing to Measure Ground Surface Temperature in Thinned and Unthinned Forests, *Northwest Sci.*, *86*(2), 108–121, doi:10.3955/046.086.0203.

Lyon, S. W., P. A. Troch, P. D. Broxton, N. P. Molotch, and P. D. Brooks (2008), Monitoring the timing of snowmelt and the initiation of streamflow using a distributed network of temperature/light sensors, *Ecohydrology*, *1*(3), 215–224, doi:10.1002/eco.18.

Mahat, V., and D. G. Tarboton (2012), Canopy radiation transmission for an energy balance snowmelt model, *Water Resour. Res.*, *48*(1), 1–16, doi:10.1029/2011WR010438.

Malek, E. (2008), The daily and annual effects of dew, frost, and snow on a non-ventilated net radiometer, *Atmos. Res.*, *89*(3), 243–251, doi:10.1016/j.atmosres.2008.02.006.

Marks, D., J. Kimball, D. Tingey, and T. Link (1998), The sensitivity of snowmelt processes to climate conditions and forest cover during rain-on-snow: a case study of the 1996 Pacific Northwest flood, *Hydrol. Process.*, *12*(10-11), 1569–1587, doi:10.1002/(SICI)1099-1085(199808/09)12:10/11<1569::AID-HYP682>3.0.CO;2-L.

Martin, K. A., J. T. Van Stan, S. E. Dickerson-Lange, J. A. Lutz, J. W. Berman, R. Gersonde, and J. D. Lundquist (2013), Development and testing of a snow interceptometer to quantify canopy water storage and interception processes in the rain/snow transition zone of the North Cascades, Washington, USA, *Water Resour. Res.*, *49*(6), 3243–3256, doi:10.1002/wrcr.20271.

Mass, C. (2008), *The weather of the Pacific Northwest*, Seattle: University of Washington Press.

Meromy, L., N. P. Molotch, T. E. Link, S. R. Fassnacht, and R. Rice (2013), Subgrid variability of snow water equivalent at operational snow stations in the western USA, *Hydrol. Process.*, *27*(17), 2383–2400, doi:10.1002/hyp.9355.

Miller, D. H. (1964), Interception processes during snowstorms, in *U.S. Forest Service Research Paper PSW – 18*, p. 24, Pacific Southwest Forest and Range Experiment Station, Berkeley, California.

Moeser, D., M. Stähli, and T. Jonas (2015), Improved snow interception modeling using canopy parameters derived from airborne LiDAR data, *Water Resour. Res.*, *51*(7), 5041–5059, doi:10.1002/2014WR016724.

Molotch, N. P., and R. C. Bales (2005), Scaling snow observations from the point to the grid element: Implications for observation network design, *Water Resour. Res.*, *41*(11), n/a–n/a, doi:10.1029/2005WR004229.

Molotch, N. P., M. T. Colee, R. C. Bales, and J. Dozier (2005), Estimating the spatial distribution of snow water equivalent in an alpine basin using binary regression tree models: The impact of digital elevation data and independent variable selection, *Hydrol. Process.*, *19*(7), 1459–1479, doi:10.1002/hyp.5586.

Molotch, N. P., P. D. Blanken, M. W. Williams, A. A. Turnipseed, R. K. Monson, and S. A. Margulis (2007), Estimating sublimation of intercepted and sub-canopy snow using eddy covariance systems, *Hydrol. Process.*, *21*(12), 1567–1575, doi:10.1002/hyp.6719.

Molotch, N. P., P. D. Brooks, S. P. Burns, M. Litvak, R. K. Monson, J. R. McConnell, and K. Musselman (2009), Ecohydrological controls on snowmelt partitioning in mixed-conifer sub-alpine forests, *Ecohydrology*, *2*(2), 129–142, doi:10.1002/eco.48.

Moore, R. D., D. L. Spittlehouse, and A. Story (2006), Riparian microclimate and stream temperature response to forest harvesting: A review, *J. Am. Water Resour. Assoc.*, *7*(4), 813–834, doi:10.1111/j.1752-1688.2005.tb04465.x.

Morin, S., Y. Lejeune, B. Lesaffre, J.-M. Panel, D. Poncet, P. David, and M. Sudul (2012), An 18-yr long (1993–2011) snow and meteorological dataset from a mid-altitude mountain site (Col de Porte, France, 1325 m alt.) for driving and evaluating snowpack models, *Earth Syst. Sci. Data*, *4*(1), 13–21, doi:10.5194/essd-4-13-2012.

Mote, P. W., A. F. Hamlet, M. P. Clark, and D. P. Lettenmaier (2005), Declining Mountain Snowpack in Western North America*, *Bull. Am. Meteorol. Soc.*, *86*(1), 39–49, doi:10.1175/BAMS-86-1-39.

Mott, R., D. Scipión, M. Schneebeli, N. Dawes, A. Berne, and M. Lehning (2014), Orographic effects on snow deposition patterns in mountainous terrain, *J. Geophys. Res. Atmos.*, *119*(3), 1419–1439, doi:10.1002/2013JD019880.

Murray, C., and J. Buttle (2003), Impacts of clearcut harvesting on snow accumulation and melt in a northern hardwood forest, *J. Hydrol.*, *271*(2003), 197–212.

Musselman, K. N., N. P. Molotch, and P. D. Brooks (2008), Effects of vegetation on snow accumulation and ablation in a mid-latitude sub-alpine forest, *Hydrol. Process.*, *22*(15), 2767–2776, doi:10.1002/hyp.7050.

Musselman, K. N., N. P. Molotch, S. A. Margulis, M. Lehning, and D. Gustafsson (2012), Improved snowmelt simulations with a canopy model forced with photo-derived direct beam canopy transmissivity, *Water Resour. Res.*, *48*(10), doi:10.1029/2012WR012285.

Musselman, K. N., S. A. Margulis, and N. P. Molotch (2013), Estimation of solar direct beam transmittance of conifer canopies from airborne LiDAR, *Remote Sens. Environ.*, *136*, 402–415, doi:10.1016/j.rse.2013.05.021.

Musselman, K. N., J. W. Pomeroy, and T. E. Link (2015), Variability in shortwave irradiance caused by forest gaps: Measurements, modelling, and implications for snow energetics, *Agric. For. Meteorol.*, *207*, 69–82, doi:10.1016/j.agrformet.2015.03.014.

Nolin, A. W., and C. Daly (2006), Mapping “at risk” snow in the Pacific Northwest, *J. Hydrometeorol.*, *7*(5), 1164–1171, doi:10.1175/JHM543.1.

OSU (2016), Willamette Water 2100, Available from: http://water.oregonstate.edu/ww2100/ (Accessed 18 March 2016)

Otsu, N. (1979), A Threshold Selection Method from Gray-Level Histograms, *IEEE Trans. Syst. MAN Cybern.*, *9*(1), 62–66.

Parajka, J., P. Haas, R. Kirnbauer, J. Jansa, and G. Blöschl (2012), Potential of time-lapse photography of snow for hydrological purposes at the small catchment scale, *Hydrol. Process.*, *26*(22), 3327–3337, doi:10.1002/hyp.8389.

Peckenham, J. M., and S. K. Peckenham (2014), Assessment of quality for middle level and high school student-generated water quality data, *JAWRA J. Am. Water Resour. Assoc.*, *50*(6), 1477–1487, doi:10.1111/jawr.12213.

Pfister, R., and M. Schneebeli (1999), Snow accumulation on boards of different sizes and shapes, *Hydrol. Process.*, *13*(14-15), 2345–2355, doi:10.1002/(SICI)1099-1085(199910)13:14/15<2345::AID-HYP873>3.0.CO;2-N.

Pohl, S., J. Garvelmann, J. Wawerla, and M. Weiler (2014), Potential of a low-cost sensor network to understand the spatial and temporal dynamics of a mountain snow cover, *Water Resour. Res.*, doi:10.1002/2013WR014594.

Pomeroy, J. W., D. M. Gray, K. R. Shook, B. Toth, R. L. H. Essery, A. Pietroniro, and N. Hedstrom (1998a), An evaluation of snow accumulation and ablation processes for land surface modelling, *Hydrol. Process.*, *12*(15), 2339–2367, doi:10.1002/(SICI)1099-1085(199812)12:15<2339::AID-HYP800>3.0.CO;2-L.

Pomeroy, J. W., J. Parviainen, N. Hedstrom, and D. M. Gray (1998b), Coupled modelling of forest snow interception and sublimation, *Hydrol. Process.*, *12*(15), 2317–2337, doi:10.1002/(SICI)1099-1085(199812)12:15<2317::AID-HYP799>3.0.CO;2-X.

Pomeroy, J. W., D. M. Gray, N. R. Hedstrom, and J. R. Janowicz (2002), Prediction of seasonal snow accumulation in cold climate forests, *Hydrol. Process.*, *16*(18), 3543–3558, doi:10.1002/hyp.1228.

Pomeroy, J. W., D. Marks, T. Link, C. Ellis, J. Hardy, A. Rowlands, and R. Granger (2009), The impact of coniferous forest temperature on incoming longwave radiation to melting snow, *Hydrol. Process.*, *23*(17), 2513–2525, doi:10.1002/hyp.7325.

PRISM Climate Group (2012), PRISM Climate Group, *Oregon State Univ.* Available from: http://prism.oregonstate.edu

Pueschel, P., H. Buddenbaum, and J. Hill (2012), An efficient approach to standardizing the processing of hemispherical images for the estimation of forest structural attributes, *Agric. For. Meteorol.*, *160*(2012), 1–13, doi:10.1016/j.agrformet.2012.02.007.

Pugh, E., and E. Small (2012), The impact of pine beetle infestation on snow accumulation and melt in the headwaters of the colorado river, *Ecohydrology*, *5*(4), 467–477, doi:10.1002/eco.239.

Qiu, H., D. R. Huggins, J. Q. Wu, M. E. Barber, D. K. McCool, and S. Dun (2011), Residue Management Impacts on Field-Scale Snow Distribution and Soil Water Storage, *Trans. ASABE*, *54*(5), 1639–1647, doi:10.13031/2013.39852.

R Core Development Team (2014), R: A language and environment for statistical computing, Available from: http://www.r-project.org/

Raleigh, M. S., K. Rittger, C. E. Moore, B. Henn, J. A. Lutz, and J. D. Lundquist (2013), Ground-based testing of MODIS fractional snow cover in subalpine meadows and forests of the Sierra Nevada, *Remote Sens. Environ.*, *128*, 44–57, doi:10.1016/j.rse.2012.09.016.

Raman, C. V., and K. S. Krishnan (1928), A New Type of Secondary Radiation, *Nature*,

121(3048), 501–502, doi:10.1038/121501c0.

Reba, M. L., D. Marks, M. Seyfried, A. Winstral, M. Kumar, and G. Flerchinger (2011), A long-term data set for hydrologic modeling in a snow-dominated mountain catchment, *Water Resour. Res.*, *47*(7), n/a–n/a, doi:10.1029/2010WR010030.

Reba, M. L., J. Pomeroy, D. Marks, and T. E. Link (2012), Estimating surface sublimation losses from snowpacks in a mountain catchment using eddy covariance and turbulent transfer calculations, *Hydrol. Process.*, *26*(24), 3699–3711, doi:10.1002/hyp.8372.

Revuelto, J., J. I. López-Moreno, C. Azorin-Molina, and S. M. Vicente-Serrano (2015), Canopy influence on snow depth distribution in a pine stand determined from terrestrial laser data, *Water Resour. Res.*, *51*(5), 3476–3489, doi:10.1002/2014WR016496.

Rice, R., and R. C. Bales (2010), Embedded-sensor network design for snow cover measurements around snow pillow and snow course sites in the Sierra Nevada of California, *Water Resour. Res.*, *46*(3), W03537, doi:10.1029/2008WR007318.

Rice, R., R. C. Bales, T. H. Painter, and J. Dozier (2011), Snow water equivalent along elevation gradients in the Merced and Tuolumne River basins of the Sierra Nevada, *Water Resour. Res.*, *47*(8), W08515, doi:10.1029/2010WR009278.

Richards, W. H., R. Koeck, R. Gersonde, G. Kuschnig, W. Fleck, and E. Hochbichler (2012), Landscape-Scale Forest Management in the Municipal Watersheds of Vienna, Austria, and Seattle, USA: Commonalities Despite Disparate Ecology and History, *Nat. Areas J.*, *32*(2), 199–207, doi:10.3375/043.032.0209.

Riesch, H., C. Potter, and L. Davies (2013), Combining citizen science and public engagement: The open airlaboratories programme, *J. Sci. Commun.*, *12*(3).

Rock, B. N., and G. N. Lauten (1996), K-12th grade students as active contributors to research investigations, *J. Sci. Educ. Technol.*, *5*(4), 255–266, doi:10.1007/BF01677123.

Rodell, M., and P. R. Houser (2004), Updating a Land Surface Model with MODIS-Derived Snow Cover, *J. Hydrometeorol.*, *5*(6), 1064–1075, doi:10.1175/JHM-395.1.

Roesch, A., M. Wild, H. Gilgen, and A. Ohmura (2001), A new snow cover fraction parameterization for the ECHAM4 GCM, *Clim. Dyn.*, *17*(12), 933–946, doi:10.1007/s003820100153.

Rosenberg, K. V., R. S. Hames, R. W. Rohrbaugh, Jr., S. B. Swarthout, J. D. Lowe, and A. A. Dhondt (2003), *Improving Habitat for Forest Thrushes*, Cornell Lab of Ornithology.

Rothacher, J. (1970), Increases in water yield following clear-cut logging in the pacific northwest, *Water Resour. Res.*, *6*(2), 653–658, doi:10.1029/WR006i002p00653.

Rutter, N. et al. (2009), Evaluation of forest snow processes models (SnowMIP2), *J. Geophys. Res.*, *114*(D6), doi:10.1029/2008JD011063.

Ryan, W. A., N. J. Doesken, and S. R. Fassnacht (2008), Evaluation of ultrasonic snow depth sensors for U.S. snow measurements, *J. Atmos. Ocean. Technol.*, *25*(5), 667–684, doi:10.1175/2007JTECHA947.1.

Schmidt, R. . (1991), Sublimation of snow intercepted by an artificial conifer, *Agric. For.*

Meteorol., *54*(1), 1–27, doi:10.1016/0168-1923(91)90038-R.

Schmidt, R. A., and D. R. Gluns (1991), Snowfall interception on branches of three conifer species, *Can. J. For. Res.*, *21*(8), 1262–1269, doi:10.1139/x91-176.

Schon, J. A., K. B. Eitel, D. Bingaman, and B. G. Miller (2014), Big project, small leaders, *Sci. Child.*, *51*(9), 48–54.

Seattle (2000), *Cedar River Watershed Habitat Conservation Plan*.

Selker, J. S., L. Thévenaz, H. Huwald, A. Mallet, W. Luxemburg, N. van de Giesen, M. Stejskal, J. Zeman, M. Westhoff, and M. B. Parlange (2006), Distributed fiber-optic temperature sensing for hydrologic systems, *Water Resour. Res.*, *42*(12), 1–8, doi:10.1029/2006WR005326.

Seyednasrollah, B., and M. Kumar (2014), Net radiation in a snow-covered discontinuous forest gap for a range of gap sizes and topographic configurations, *J. Geophys. Res. Atmos.*, *119*(17), 10,323–10,342, doi:10.1002/2014JD021809.

Seyednasrollah, B., M. Kumar, and T. E. Link (2013), On the role of vegetation density on net snow cover radiation at the forest floor, *J. Geophys. Res. Atmos.*, *118*(15), 8359–8374, doi:10.1002/jgrd.50575.

Shidei, T., T. Takahashi, K. Takahashi, and K. Kataoka (1952), Study of the fallen snow on the forest trees, *Bull. Gov. For. Exp. Stn.*, 115–164. (in Japanese with English abstract).

Sicart, J. E., R. L. H. Essery, J. W. Pomeroy, J. Hardy, T. Link, and D. Marks (2004), A sensitivity study of daytime net radiation during snowmelt to forest canopy and atmospheric conditions, *J. Hydrometeorol.*, *5*(5), 774–784, doi:10.1175/1525-7541(2004)005<0774:ASSODN>2.0.CO;2.

Silvertown, J. (2009), A new dawn for citizen science, *Trends Ecol. Evol.*, *24*(9), 467–471, doi:10.1016/j.tree.2009.03.017.

Slater, A. G. et al. (2001), The Representation of Snow in Land Surface Schemes: Results from PILPS 2(d), *J. Hydrometeorol.*, *2*(1), 7–25, doi:10.1175/1525-7541(2001)002<0007:TROSIL>2.0.CO;2.

Spies, T. A., and J. F. Franklin (1991), The structure of natural young, mature, and old-growth Douglas-fir forests in Oregon and Washington, in *Wildlife and vegetation of unmanaged Douglas-fir forests, USDA Forest Service General Technical Report PNW-GTR-285*, pp. 91–111, Portland, USA. Pacific Northwest Research Station, Portland, OR.

Sproles, E. A., A. W. Nolin, K. Rittger, and T. H. Painter (2013), Climate change impacts on maritime mountain snowpack in the Oregon Cascades, *Hydrol. Earth Syst. Sci.*, *17*(7), 2581–2597, doi:10.5194/hess-17-2581-2013.

Sprugel, D. G., K. G. Rascher, R. Gersonde, M. Dovčiak, J. A. Lutz, and C. B. Halpern (2009), Spatially explicit modeling of overstory manipulations in young forests: Effects on stand structure and light, *Ecol. Modell.*, *220*(24), 3565–3575, doi:10.1016/j.ecolmodel.2009.07.029.

Stednick, J. D. (1996), Monitoring the effects of timber harvest on annual water yield, *J. Hydrol.*,

176(1-4), 79–95, doi:10.1016/0022-1694(95)02780-7.

Storck, P. (2000), Trees, snow and flooding: An investigation of forest canopy effects of snow accumulation and melt at the plot and watershed scales in the Pacific Northwest, University of Washington.

Storck, P., D. P. Lettenmaier, and S. M. Bolton (2002), Measurement of snow interception and canopy effects on snow accumulation and melt in a mountainous maritime climate, Oregon, United States, *Water Resour. Res.*, *38*(11), 1123, doi:10.1029/2002WR001281.

Strasser, U., M. Warscher, and G. E. Liston (2011), Modeling snow–canopy processes on an idealized mountain, *J. Hydrometeorol.*, *12*(4), 663–677, doi:10.1175/2011JHM1344.1.

Sturm, M., J. Holmgren, and G. Liston (1995), A seasonal snow cover classification system for local to global applications, *J. Clim.*, doi:10.1175/1520-0442(1995)0082.0.CO;2.

Sturm, M., B. Taras, G. E. Liston, C. Derksen, T. Jonas, and J. Lea (2010), Estimating Snow Water Equivalent Using Snow Depth Data and Climate Classes, *J. Hydrometeorol.*, *11*(6), 1380–1394, doi:10.1175/2010JHM1202.1.

Tabler, R. D. (1975), Predicting profiles of snowdrifts in topographic catchments, *Proc. West. snow Conf. 43rd Annu. Meet.*, (Proceedings of the western snow conference 43rd annual meeting), 87–97.

Thyer, M., J. Beckers, D. Spittlehouse, Y. Alila, and R. Winkler (2004), Diagnosing a distributed hydrologic model for two high-elevation forested catchments based on detailed stand- and basin-scale data, *Water Resour. Res.*, *40*(1), n/a–n/a, doi:10.1029/2003WR002414.

Trujillo, E., J. A. Ramírez, and K. J. Elder (2009), Scaling properties and spatial organization of snow depth fields in sub-alpine forest and alpine tundra, *Hydrol. Process.*, *23*(11), 1575–1590, doi:10.1002/hyp.7270.

Trumbull, D. J., R. Bonney, D. Bascom, and A. Cabral (2000), Thinking scientifically during participation in a citizen-science project, *Sci. Educ.*, *84*(2), 265–275, doi:10.1002/(sici)1098-237x(200003)84:2<265::aid-sce7>3.0.co;2-5.

Tyler, S. W., S. A. Burak, J. P. McNamara, A. Lamontagne, J. S. Selker, and J. Dozier (2008), Spatially distributed temperatures at the base of two mountain snowpacks measured with fiber-optic sensors, *J. Glaciol.*, *54*(187), 673–679, doi:10.3189/002214308786570827.

Tyler, S. W., J. S. Selker, M. B. Hausner, C. E. Hatch, T. Torgersen, C. E. Thodal, and S. G. Schladow (2009), Environmental temperature sensing using Raman spectra DTS fiber-optic methods, *Water Resour. Res.*, *45*, W00D23, doi:10.1029/2008WR007052.

U.S. Army Corps of Engineers (1956), *Snow hydrology. Summary report of the snow investigations of the North Pacific Division*, Portland, OR.

Varhola, A., and N. C. Coops (2013), Estimation of watershed-level distributed forest structure metrics relevant to hydrologic modeling using LiDAR and Landsat, *J. Hydrol.*, *487*(2013), 70–86, doi:10.1016/j.jhydrol.2013.02.032.

Varhola, A., N. C. Coops, M. Weiler, and R. D. Moore (2010a), Forest canopy effects on snow accumulation and ablation: An integrative review of empirical results, *J. Hydrol.*, *392*(3-4),

219–233, doi:10.1016/j.jhydrol.2010.08.009.

Varhola, A., N. C. Coops, C. W. Bater, P. Teti, S. Boon, and M. Weiler (2010b), The influence of ground- and lidar-derived forest structure metrics on snow accumulation and ablation in disturbed forests, *Can. J. For. Res.*, *40*(4), 812–821, doi:10.1139/X10-008.

Varhola, A., G. W. Frazer, P. Teti, and N. C. Coops (2012), Estimation of forest structure metrics relevant to hydrologic modelling using coordinate transformation of airborne laser scanning data, *Hydrol. Earth Syst. Sci.*, *16*(10), 3749–3766, doi:10.5194/hess-16-3749-2012.

Varhola, A., N. C. Coops, Y. Alila, and M. Weiler (2014), Exploration of remotely sensed forest structure and ultrasonic range sensor metrics to improve empirical snow models, *Hydrol. Process.*, *28*(15), 4433–4448, doi:10.1002/hyp.9952.

Veatch, W., P. Brooks, J. Gustafson, and N. Molotch (2009), Quantifying the effects of forest canopy cover on net snow accumulation at a continental, mid-latitude site, *Ecohydrology*, *2*(2), 115–128, doi:10.1002/eco.

Wayand, N. E., A. Massmann, C. Butler, E. Keenan, J. Stimberis, and J. D. Lundquist (2015a), A meteorological and snow observational data set from Snoqualmie Pass (921 m), Washington Cascades, USA, *Water Resour. Res.*, *51*(12), 10092–10103, doi:10.1002/2015WR017773.

Wayand, N. E., J. D. Lundquist, and M. P. Clark (2015b), Modeling the influence of hypsometry, vegetation, and storm energy on snowmelt contributions to basins during rain-on-snow floods, *Water Resour. Res.*, n/a–n/a, doi:10.1002/2014WR016576.

Weiss, A. (2001), Topographic position and landforms analysis, in *ESRI User Conference*, San Diego, CA.

Welch, C. M., P. C. Stoy, F. A. Rains, A. V. Johnson, and B. L. McGlynn (2015), The impacts of mountain pine beetle disturbance on the energy balance of snow during the melt period, *Hydrol. Process.*, n/a–n/a, doi:10.1002/hyp.10638.

Westerling, A. L. (2006), Warming and earlier spring increase western U.S. forest wildfire activity, edited by Intergovernmental Panel on Climate Change, *Science (80-.).*, *313*(5789), 940–943, doi:10.1126/science.1128834.

Whitaker, A., Y. Alila, J. Beckers, and D. Toews (2003), Application of the distributed hydrology soil vegetation model to Redfish Creek, British Columbia: model evaluation using internal catchment data, *Hydrol. Process.*, *17*(2), 199–224, doi:10.1002/hyp.1119.

Whitaker, A. C., and H. Sugiyama (2005), Seasonal snowpack dynamics and runoff in a cool temperate forest: lysimeter experiment in Niigata, Japan, *Hydrol. Process.*, *19*(20), 4179–4200, doi:10.1002/hyp.6059.

Wigmosta, M., Z. Duan, A. Coleman, and R. Skaggs (2015), *Development of a distributed hydrology model for use in a forest restoration decision support tool to increase snowpack in the upper Columbia*.

Wilm, H., and E. Dunford (1948), Effect of timber cutting on water available for stream flow from a lodgepole pine forest, *USDA Tech. Bull., No. 968*, 1–43.

Wilson, A. A., K. Bacher, I. Breckheimer, J. Lundquist, R. Rochefort, L. Whiteaker, and J. HilleRisLambers (2015), Monitoring Wildflower Phenology using Traditional Science, Citizen Science, and Crowd Sourcing, *Park Sci., In Review*.

Wimberly, M. C., and Z. Liu (2014), Interactions of climate, fire, and management in future forests of the Pacific Northwest, *For. Ecol. Manage.*, *327*, 270–279, doi:10.1016/j.foreco.2013.09.043.

Winkler, R. D., D. L. Spittlehouse, and D. L. Golding (2005), Measured differences in snow accumulation and melt among clearcut, juvenile, and mature forests in southern British Columbia, *Hydrol. Process.*, *19*(1), 51–62, doi:10.1002/hyp.5757.

Winstral, A., and D. Marks (2002), Simulating wind fields and snow redistribution using terrain-based parameters to model snow accumulation and melt over a semi-arid mountain catchment, *Hydrol. Process.*, *16*(18), 3585–3603, doi:10.1002/hyp.1238.

Winstral, A., and D. Marks (2014), Long-term snow distribution observations in a mountain catchment: Assessing variability, time stability, and the representativeness of an index site, *Water Resour. Res.*, *50*(1), 293–305, doi:10.1002/2012WR013038.

Woods, S. W., R. Ahl, J. Sappington, and W. McCaughey (2006), Snow accumulation in thinned lodgepole pine stands, Montana, USA, *For. Ecol. Manage.*, *235*(1-3), 202–211, doi:10.1016/j.foreco.2006.08.013.

Work, R. A., H. J. Stockwell, T. G. Freeman, and R. T. Beaumont (1965), *Accuracy of field snow surveys, western United States, including Alaska*, No. TR-163., Cold Regions Research and Engineering Lab, Hanover, NH.

Xin, Q., C. E. Woodcock, J. Liu, B. Tan, R. a. Melloh, and R. E. Davis (2012), View angle effects on MODIS snow mapping in forests, *Remote Sens. Environ.*, *118*, 50–59, doi:10.1016/j.rse.2011.10.029.

Yatheendradas, S. et al. (2012), Distributed assimilation of satellite-based snow extent for improving simulated streamflow in mountainous, dense forests: An example over the DMIP2 western basins, *Water Resour. Res.*, *48*(9), W09557, doi:10.1029/2011WR011347.

Zheng, Z., P. B. Kirchner, and R. C. Bales (2016), Topographic and vegetation effects on snow accumulation in the southern Sierra Nevada: a statistical summary from lidar data, *Cryosph.*, *10*(1), 257–269, doi:10.5194/tc-10-257-2016.